

Imaging of the Equine Neck

With a Focus on Vertebral Variation and
the Intervertebral Disc

Stefanie Veraa



Imaging of the Equine Neck

With a Focus on Vertebral Variation and the Intervertebral Disc

Stefanie Veraa

Imaging of the Equine Neck

With a Focus on Vertebral Variation and the Intervertebral Disc

Stefanie Veraa

PhD thesis, Utrecht University, Faculty of Veterinary Medicine, The Netherlands

ISBN: 978-90-393-7237-1

Cover: Proefschrift-AIO and Stefanie Veraa

Layout and print: Proefschrift-AIO.

Copyright (c) 2019 Stefanie Veraa. All rights reserved. No part of this thesis may be reproduced, stored in a retrieval system of any nature or transmitted in any form or by any means, without prior written consent of the author. The copyright of the articles that have been published has been transferred to the respective journals.

Imaging of the Equine Neck

With a Focus on Vertebral Variation and the Intervertebral Disc

Beeldvorming van de paardenhals

**Met een focus op wervelvariatie en de tussenwervelschijf
(met een samenvatting in het Nederlands)**

Proefschrift

ter verkrijging van de graad van doctor aan de Universiteit Utrecht
op gezag van de rector magnificus, prof. dr. H.R.B.M. Kummeling,
ingevolge het besluit van het college voor promoties
in het openbaar te verdedigen op
donderdag 9 januari 2020 des ochtends te 10.30 uur

door

Stefanie Veraa

geboren op 24 november 1979 te Krefeld, Duitsland

Promotoren: Prof. dr. P.R. van Weeren

Prof. dr. J.W. Hesselink

Copromotor: Dr. A.J.M. van den Belt

Content

Chapter 1 General Introduction	P. 9	Chapter 4 Caudal Cervical Vertebral Variation is Not Associated with Clinical Signs in Warmblood Horses	P. 67
Chapter 2 Domesticated Animals as a Translational Model for Vertebral Congenital Malformations. A Literature Review.	P. 31	Chapter 5 Equine Cervical Intervertebral Disc Degeneration is Associated with Location and MRI Features	P. 85
Chapter 3 Ex Vivo Computed Tomographic Evaluation of Morphologic Variations in Equine Cervical Vertebrae	P. 51		



Chapter 6
Cervical Disc Height Index in Young
Dutch Warmblood Horses; Intra- and
Interobserver Agreement

P. 107

Chapter 7
Intervertebral Disc Degeneration in
Warmblood Horses: Morphology, Grading
and Distribution of Lesions

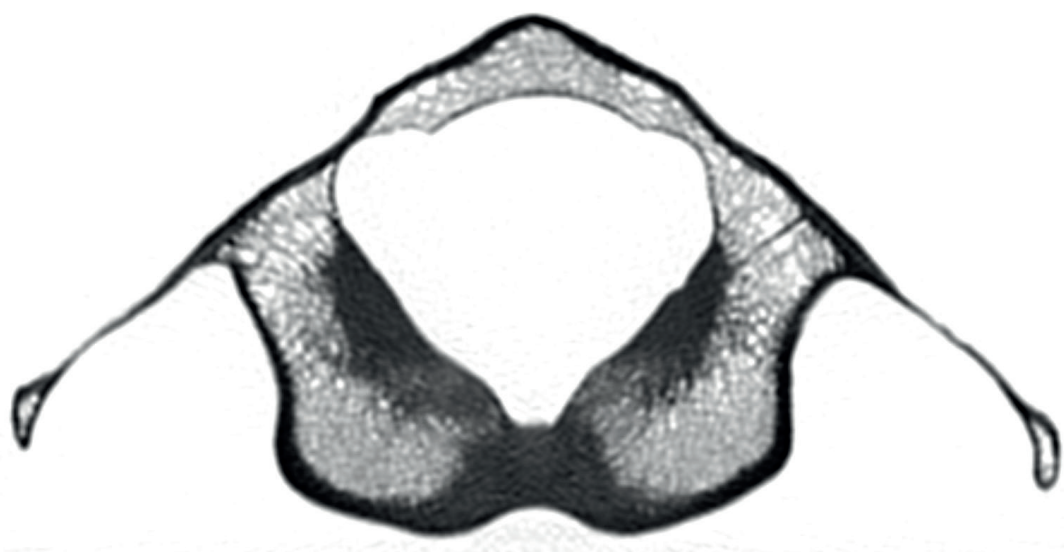
P. 127

Chapter 8
General Discussion

P. 147

P. 159
Summary -Samenvatting
Dankwoord
Curriculum Vitae





1

General Introduction

INTRODUCTION

The cervical spine in horses is increasingly recognized as a region of clinical importance certainly from the perspective of equestrian sports. A variety of pathological conditions can lead to a multitude of clinical symptoms hindering adequate functioning of the horse. Simultaneously, an ongoing debate on animal welfare during maximum flexion of head and neck (Rollkur) is focusing on clinical symptoms related to extreme postures.

Due to the continuing development of advanced imaging options and improved utilization of the conventional imaging modalities, it is nowadays possible to improve the accuracy of the diagnosis of these disorders. So far, little is known about the possibilities that imaging modalities such as CT and MRI can offer in diagnostics of the equine neck. The studies in this thesis are intended to fill this knowledge gap, with a focus on vertebral variation and the intervertebral disc. In this introductory chapter, anatomy and embryology, diseases and pathology, clinical features and diagnostic imaging of the equine neck are discussed. Finally, the scope and aims of this thesis are described.

Anatomy and embryology

The cervical vertebral column of the horse consists of seven vertebrae as in almost all mammalian species (the rule of seven) (fig. 1) [1-3]. The first and second vertebra (atlas and axis) are of a different shape and allow head movement [3]. The vertebrae are connected by synovial articular process joints dorsally and a fibrocartilaginous intervertebral disc ventrally in between the vertebral bodies [3]. In between these structures an opening, called intervertebral foramen, is present through which the spinal nerves can leave the vertebral canal [3].

The vertebrae are formed out of paraxial mesoderm that condenses into somites via a process called somitogenesis that is visible from day 19 in the equine embryo [4-6]. The somites split into a dorsolateral dermomyotome and a ventromedial sclerotome, the latter giving rise to the vertebral elements and ribs [4, 5]. Vertebral ossification starts around day 54 of the embryo [6]. Vertebrae consist of an axial part including the vertebral body, lamina, pedicle and articular process thereby encircling the vertebral canal, and an abaxial or lateral part including the transverse process in which the transverse foramen forms the passage for the exiting vertebral nerve, artery and vein [3]. The lateral end of the transverse process gives rise to a dorsal and ventral tubercle, the latter forming a plate-like extension caudo-ventrally at C6 [3]. This part of the transverse process forms one of the attachment sites of the longus colli muscle, which

functions as a neck stabilizing and flexor muscle and counteracts the weight of the head [7]. The string of vertebrae along the vertebral column, including the occiput, cervical, thoracic, lumbar, sacral and caudal series, are determined by a cranio-caudal gradient of the homeobox genes (Hox), and these genes determine the final shape of each vertebra [8, 9]. This division in series is also known as axial patterning of the vertebral column [9].

The intervertebral disc consists of a peripheral fibrous ring described as the annulus fibrosus and a small central pulpy fibrocartilaginous part named the nucleus pulposus [3]. The intervertebral disc is formed embryonically out of the central somite and forms the division between the cranial and caudal half of a sclerotome (von Ebner's fissure) which will give rise to the caudal half and cranial half of two adjacent vertebrae respectively [10]. The somites and sclerotomes form around a dense area of mesoderm called notochord [10]. The nucleus pulposus derives directly from a local perseverance of the notochord while the rest will disappear [10].

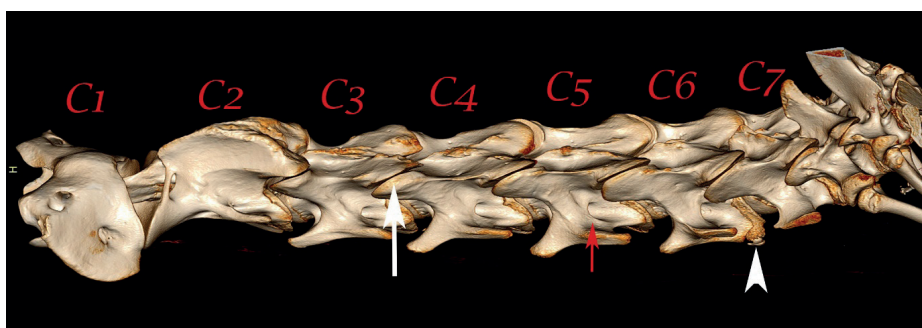


Fig. 1. Lateral oblique computed tomographic 3D reconstruction of the cervical vertebral column of a horse. The seven cervical vertebrae (C1 to C7) are visible, with the dorsal process joints (white arrow), the transverse foramen at the base of the transverse process (red arrow) and the plate-like extension of the caudal tubercle of the transverse process of C6 (arrowhead).

Diseases and Pathology

Cervical vertebral compressive myelopathy (CVCM)

Cervical vertebral malformation-malarticulation with secondary compressive myelopathy is the most common developmental pathology in the equine cervical spine [11]. It occurs most frequently at C3-C4 in young, fast growing male horses where the Thoroughbred is the breed in which it occurs most frequently [11]. The affected horses can have a variety of pathologic changes that can lead to stenosis of the

vertebral canal and intervertebral foramina, including vertebral subluxation, flaring of the caudal vertebral body, articular process arthrosis, but also soft tissue changes such as ligamentum flavum hypertrophy, synovial proliferation or synovial cyst formation [11, 12]. A dynamic compression is created when the horse bends its neck, therefore surgical stabilization of the vertebral column by application of washer-screws, pedicle screw-rods and plates has been attempted with varying success [13-16]. Although some of the less affected Thoroughbred horses diagnosed with CVCM can race, most of them cannot [17]. An optimal performance is not possible due to the lack of adequate treatment available [17]. Recently, the application of intrathecal allogeneic mesenchymal stem cells has been assessed for treatment of these compressive spinal cord lesions [18]. The stem cells did spread best through the cerebrospinal fluid when they were injected with an occipito-atlantal approach, but were not found in higher concentrations at the site of compressive myelopathy [18]. In older horses, cervical vertebral compressive myelopathy usually consists of a static stenosis of the vertebral column and intervertebral foramina caused by degenerative joint disease of the articular process joints with secondary articular process enlargement and synovial joint effusion or cyst formation [11].

Articular process joint disease

Articular process joint arthrosis or degenerative joint disease is the second most reported pathologic disorder. It can, as described above, be considered as a chronic condition caused by cervical vertebral malformation [11, 12]. Synovitis and enlargement of the joint due to new bone formation can lead to narrowing of the vertebral canal or intervertebral foramen. This may, but does not necessarily, cause spinal cord or nerve compression [19]. Causes underlying degenerative joint disease such as trauma or infections must be considered and evaluated before treatment is started [20]. Osteochondrosis of the articular process joints is also a predisposing factor for development of arthrosis. The condition has been reported at all levels of the cervical vertebral column including the occipital condyles and articular process joints, and even at the cranial articular surface of C2 [21-23]. Horses with osteochondrosis at other locations throughout the body are at increased risk of osteochondrosis of the articular process joints, as osteochondrosis should be considered as a systemic developmental disorder that manifest itself in different locations. A link between osteochondrosis and CVCM has been made in Thoroughbreds [11, 12, 22, 24, 25]. Although horses with secondary compressive myelopathy tend to have larger osteochondral fragments, the prevalence of the disorder is similar in horses not showing compressive myelopathy [22].

C6 and C7 congenital cervical vertebral variation

The first report of an abnormal cervical vertebra due to congenital vertebral variation at C6 and C7 dates from almost a century ago [26]. This type of variation consists of a shift of the caudal tubercle of C6 to C7 with associated anatomical variation of the longus colli muscle. The condition has received increased interest the last decade, as being a possible cause of fore limb lameness or neck pain due to altered biomechanical forces [27-30]. This anomaly are mostly seen in Thoroughbreds and warmblood horses [27-30]. A widening of the intervertebral disc space of C6-C7 together with a longer C7 vertebral body has also been noted in association with this vertebral variation [30]. A significant number of these horses did have an intra-vertebral sagittal ratio of <0.5 at C6, a feature that might be indicative of CVCM and stenosis of the vertebral canal [30].

Intervertebral disc disease

The intervertebral disc in horses has a different composition than in humans and dogs. It has a much smaller, integrated and fibrocartilaginous nucleus pulposus, which is therefore less prone to disc extrusion [31]. Equine cervical intervertebral disc disease has been documented less frequently than in other species and can consist of (a combination of) age-related changes [32], disc herniation [33-37], fibrocartilaginous embolism [38-40] or discospondylitis (traumatic or infectious) [34, 41, 42].

Meningomyelitis

Infectious meningomyelitis in horses has been reported to be viral (e.g. Herpes, West-Nile), bacterial, parasitic or fungal in origin. It occurs most frequently after trauma to head or neck, or as a sequel to septicemia, but can also be a result of systemic viral or fungal disease [43-48]. Nonspecific clinical symptoms, such as spinal ataxia and neurologic lameness, are noted that can be similar to those seen in other cervical pathologic conditions [45]. Prognosis is highly dependent on the infectious agent and the outcome can vary between a complete recovery and death [43].

Miscellaneous

Occipito-atlantal malformation in horses has been described in multiple breeds but has a genetic familial trait in Arabian horses, with documented changes near *HoxD3*, one of the genes responsible for determining the junction between and the morphology of occiput, C1 and C2 [8, 49-54].

Fractures of the cervical vertebrae in horses do occur, but no reliable data exist on their prevalence, possibly due to underreporting because of limited treatment options [55-58]. Atlanto-axial subluxation with odontoid fractures are the most reported traumatic fractures and in foals or ponies surgery may be considered [59-62].

Cervical vertebral neoplasia with secondary spinal cord compression seldomly occurs in horses, but cases of vertebral hemangiosarcoma, lymphoma, and giant granular cell neurofibroma have been described (fig. 2) [63-66].

There are several case reports on cervical vertebral epidural hematomas. They are considered of traumatic origin and manifest with acute neurological signs such as severe spinal ataxia [67-69]. In one of these cases fibrocartilaginous tissue was found in the epidural thrombus, focally occluding the ventral vertebral plexus and believed to derive from the cartilaginous tissue of the vertebral body growth plate [69].

There are single case reports of horses displaying neurological symptoms related to the cervical spine caused by rare conditions, such as an arachnoid diverticulum located at C6 to Th1 [32], cervical vertebral osteomyelitis in a warmblood foal [70], and physeal necrosis with secondary metaphyseal and diaphyseal dysplasia of C3 in a young Quarter horse [71].

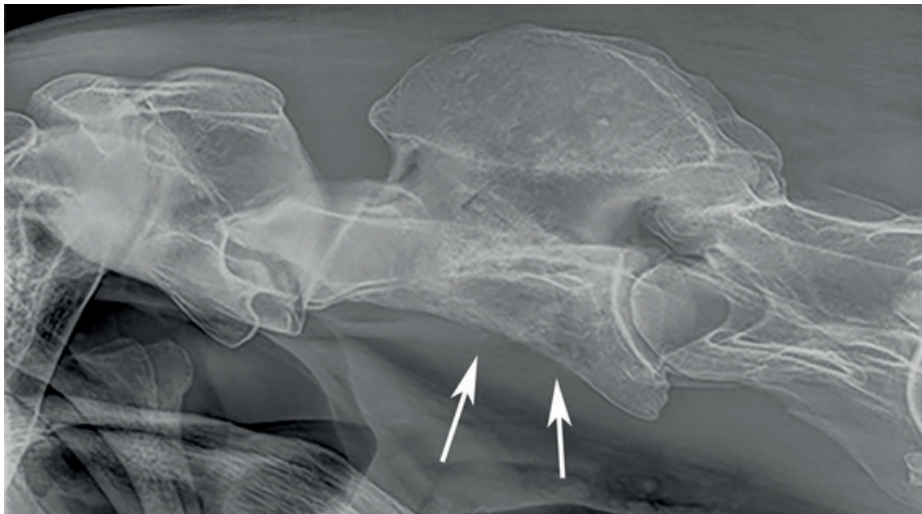


Fig. 2. Lateral radiographic view of the cranial cervical vertebral column of a warmblood horse. Note the diffuse moth-eaten osteolytic aspect of the vertebral body (arrows) and laminae of C2. Histopathological diagnosis was lymphoma.

Clinical symptoms

Clinical symptoms seen in horses with cervical pathology can include spinal ataxia, hypermetria, pain on palpation or during movement, muscle atrophy, and front limb lameness.

Spinal ataxia is one of the most common clinical features of neck pathology and has been described as a lack of voluntary coordination of muscle movement caused by a combination of upper motor neuron (UMN) and general proprioceptive (GP) tract dysfunction [11]. Incoordination and spasticity can be observed as a disorderly gait and faults or anomalies in hind limb movement. However, these signs can be misinterpreted as musculoskeletal lameness [11, 72]. At the same time, one should keep in mind that muscle weakness can also be caused by generalized neurological pathology, like equine lower motor neuron disease (EMND) or grass sickness [73].

Pain on palpation can be of help in localizing vertebral or articular pathology but can also be a result of muscle pain and tension [11, 74]. Abnormal movement of the head and neck, such as head shaking or a low position of the head, can also be caused by pain in the neck or fore limbs, or by mechanical restrictions [11, 73, 74]. Disuse or denervation muscle atrophy can occur secondarily [73].

Lameness of the fore limbs that does not respond to local anesthesia of the limbs may be caused by cervical lesions in the region of the brachial plexus, which originates at the caudal cervical and cranial thoracic spine [73, 74].

Clinical examination

Patient history and clinical signs may be indicative of a cervical lesion. The above described clinical symptoms related to the cervical spine are dependent on the location of the lesion and certain pathologies are more common in certain horse breeds [11, 73]. For example, cervical vertebral malformation at C3-C4 is one of the most common pathologies in younger Thoroughbred horses. This less the case in warmbloods and Tennessee Walking horses whereas vertebral morphologic variation at C6 and C7 has been described in around one third of the Thoroughbred and warmblood population [11, 29, 30, 75, 76]. Making a correct diagnosis of these varying pathologies of the cervical spine of horses can be challenging and such a diagnosis is always based on a thorough clinical examination in conjunction with diagnostic imaging [11, 73, 74]. A detailed clinical examination of the neck region includes inspection in rest while evaluating conformation and posture of both head and neck, palpation of the musculature to evaluate shape, volume and tension, passive manual and active flexion

of the neck laterally and up-and-down. Then moving in hand over a straight line and in circles, walking on or off a slope, on the lunge and possibly ridden for evaluation of posture and lameness, and pulling the horse's tail or mane to a side to assess balance and correction of movement [11, 73, 74].

The use of electromyography (EMG) and motor-evoked potentials (MEP) may be considered as an extended part of the clinical examination in horses with spinal ataxia [77, 78].

Diagnostic Imaging of the equine cervical spine

Imaging is one of the keystones in the work-up of the equine patient with clinical symptoms related to the cervical spine [74]. Imaging of the cervical vertebral column has long been restricted to radiography and ultrasonography [74]. These are still the most used imaging modalities in equine practice because of patient size, practical applicability, availability and cost-effectiveness [1, 79, 80]. The use of advanced imaging modalities as computed tomography and magnetic resonance imaging is also gaining ground because these techniques are becoming increasingly applicable in horses [80, 81].

Radiography

Radiography is by far the most used imaging technique of the cervical vertebral column in the work-up of equine patients but also in pre-purchase examinations. Positioning of the cervical vertebral column during radiographic examinations can vary, amongst others depending on breed, technique and sedation. A latero-lateral direction is considered the standard projection whereas ventro-dorsally directed radiographs can be challenging due to patient size and associated influence of soft tissues [1]. During the last decade, oblique projections of the neck highlighting the articular process joints have gained importance and are now deemed to belong to the standard set of cervical radiographs if arthrosis of the articular process joints is suspected [82].

Myelography is used to evaluate sites of compression by means of radiographic contrast columns in the subarachnoid space and allows differentiation between extradural lesions, intradural extramedullary lesions, and intradural intramedullary lesions, the latter due to spinal cord swelling or opacification in cases of myelomalacia [83]. The use of myelography in ataxic horses and CVCM has for long been described as the gold standard for identification of the site of compression [75, 84-88]. Injection of the contrast medium in the subarachnoid space at the level of the occipito-atlantal junction can be guided by ultrasound, making the procedure less traumatic and

risky [89, 90]. Even myelography in the standing horse has been proposed, thereby extending the possibilities of the radiographic examination in the awake horse [91]. Adverse reactions to the injection of contrast medium under general anesthesia have been reported but are in most cases mild and self-limiting, although a case of pleuropneumonia has been documented [92, 93]. In only 2% of cases, severe neurologic reactions required euthanasia. These may have been the result of a combination of an adverse reaction to the contrast medium and complications related to general anesthesia [92]. Lately, the variations in contrast column thickness and the subjectivity of this technique have cast doubts on its suitability as a gold standard [76, 94]. This might be partially explained by the fact that dynamic narrowing during flexion of the vertebral canal occurs at dorsolateral or ventrolateral locations, whereas radiographic projections are mostly made in latero-lateral direction during myelography [95]. Cervical vertebral canal endoscopy has therefore been proposed as an alternative for better localization of the site of compression [96].

Extensive anatomic radiographic description of the neck region is essential for correct radiographic interpretation of radiographic images [82]. The detailed description of the development of the growth plates of atlas and axis over time is an example hereof, as fractures of the odontoid process of the dens with associated atlanto-axial subluxation occur and are most often diagnosed by radiography [97]. Differentiation between fracture versus growth plate is essential for diagnosis, prognosis and eventual pre-operative planning [59-62]. Also, familiarity with the possible vertebral morphologic variations and hence with the differences in radiographic appearance is important, as misinterpretation might lead to erroneous identification of C6, C7 or Th1 in some horses [27, 30].

The structures of the equine cervical vertebral column that are routinely radiographically evaluated include the vertebrae with their articular process joints and the intervertebral disc space. A grading scheme for articular process joint size and arthrosis has been investigated [98, 99]. Also, stenosis of the intervertebral foramen due to the presence of new bone formation may occur. However, positional changes of the neck during radiographic examinations may affect the size of these foramina and a standardized positioning has been proposed [100].

Multiple radiographic measurements of the cervical vertebral column have been developed and are used as diagnostic tools in the work-up of for example suspected CVCM and articular process arthrosis [25, 98, 101, 102]. These measurements often include the intravertebral and intervertebral sagittal ratio [99, 102-105]. Variation of

the neck position (flexion or extension) does not influence most of these measurements [106].

Ultrasonography

Ultrasound of the neck in horses includes assessment of soft tissues, bony surfaces and articular process joints and is increasingly being used [79]. Ultrasound guided injection of the articular process joints with corticosteroids to relief pain associated with synovitis has proven to be an accurate and reliable technique that now can be regarded common practice [107-109]. Three-dimensionally printed training models have recently been developed and evaluated to assess their usability to improve this injection technique in Thoroughbreds [110].

Ultrasound can also be used as a non-invasive way to evaluate several structures or perform ultrasound-guided centesis of the vertebral canal via the occipito-atlantal window [89, 90, 111]. Evaluation of the spinal cord and artery at this location in neonatal foals with maladjustment syndrome (NMS) has proven to be valuable [112]. With this, new diagnostic approaches are being developed with help of a non-invasive and practically applicable imaging technique.

Computed tomography

The use of computed tomography (CT) has long been limited by the size of the horse's neck but the development of equipment with a larger bore diameter has overcome this problem and scanning of the neck up to Th2 in live horses has been documented [80, 81].

Computed tomographic anatomy of the cervical vertebral column has been reported in several Quarter horses [113, 114]. Intervertebral foraminal size can vary in different head and neck positions and can, together with articular process joint arthrosis, be a reason for stenosis and secondary spinal cord or nerve compression [100, 115]. Due to the transverse nature of the CT images and possibility of three-dimensional reconstruction and reformatting, excellent visualization of articular process joint anatomy, articular process joint extent and relation to the spinal cord or nerves is possible with CT, which is a major advantage compared to radiography [19]. The use of contrast-enhanced CT and myelography was described as early as the 1990's to evaluate locations of compression in CVCM [81, 88]. It has also been used in Thoroughbred foals with signs of CVCM [116]. Computed tomography has also been used for pre-operative cervical vertebral fracture treatment planning, like it is, more commonly, used in the distal limbs of horses [58]. With the establishment of new CT equipment in equine

veterinary centers, more possibilities of applying this technique for an advanced work-up of the equine cervical patient will become available [80].

Magnetic Resonance Imaging

For MRI, only in vivo imaging of the cranial cervical vertebral column or ex vivo imaging is feasible at the moment due to technical limitations such as bore size [114, 117-119]. The comparison of MRI findings with radiographic findings in CVCM has proven to be very valuable [118] and further evaluation of these findings with histology has strengthened the evidence for the hypothesis that developmental pathology in combination with biomechanical forces contribute to CVCM [24]. True bone cysts in the articular processes have been found in horses with CVCM, together with osteochondrosis and fibrous tissue replacement of bone and osteosclerosis [24]. Secondary compressive myelopathy can be seen as T2 hyperintensity, however compression sites on MR images do not always reflect histologic compressive lesions of the spinal cord, as can be explained by the dynamic character of compression in horses with CVCM [119]. As the bore is too small to perform a dynamic MRI study, including neutral, flexed and extended positioning of the head and neck, only static compression can be visualized in MR images of the equine neck [119].

SCOPE OF THE THESIS

The cervical vertebral column in horses has increasingly been recognized as a region of clinical importance with its pathologies leading to clinical symptoms such as spinal ataxia or weakness in the hind limbs, intermittent lameness, abnormal neck posture, pain on palpation, patchy sweating, hypermetria and poor performance, amongst others [73, 74].

The equine neck contributes to balancing and translating sensory input from visual, vestibular and proprioceptive nature to movement [120]. Biomechanical function is supported by a synergy of the vertebrae, ligaments, tendons and muscles of the neck with transmission to the trunk and limbs [120]. Variation of vertebrae at C6 and C7, together with a variation in anatomy of the longus colli musculature have been proposed to change biomechanical function of this region [27-30]. Changes in the biomechanical function have been proposed to be related with the development of clinical symptoms [29, 30]. Elongation of the vertebral body of C7, a smaller intravertebral sagittal ratio at C6 and widening of the C6-C7 intervertebral disc space have been suggested to be a part of the developmental and congenital cervical vertebral malformation complex and to possibly lead to similar pathology as seen in CVCM [30].

AIMS OF THE THESIS

The first aim of this thesis was to increase the knowledge of cervical vertebral patterning variations in horses and its clinical effects, focusing on the morphological features of these variations and the prevalence in an equine population consisting of various, but predominantly warmblood breeds.

The second aim of this thesis was to evaluate the development and degeneration of the cervical intervertebral disc in foals and adult horses keeping in mind the effects vertebral variation might have on the intervertebral disc, as regional anatomy and biomechanical forces might have changed in these horses.

The specific aims per chapter are described below.

In **Chapter 2** the embryonic development of the vertebral column and the variation or malformation of the vertebral conformation in domesticated animals is reviewed and their potential translational value for human medicine is discussed.

In **Chapter 3** the computed tomographic (CT) features of morphology variations of the equine cervical vertebral column from occiput to Th1 and the frequency of these findings in a population of different horse breeds is presented. The possible association of the presence of vertebral morphologic variations with clinical symptoms is assessed.

In **Chapter 4** the possible association of clinical symptoms with radiographically detected caudal cervical vertebral variations at C6 and C7 is investigated in a case-control study of warmblood horses.

MRI features of the non-degenerated and degenerated intervertebral disc of the cervical spine as well as the association with factors such as location and intervertebral disc protrusion detected by MRI, are described in **Chapter 5**.

Chapter 6 highlights the radiographic development of the cervical intervertebral disc in a population of horses varying from one to 18 months old. The disc is evaluated by the disc height index (DHI) as a new parameter for evaluating the intervertebral disc space width. Inter- and intra-observer agreement for the DHI is determined and reference values are proposed.

Chapter 7 describes the morphology, grading and distribution of intervertebral disc degeneration in a population of warmblood horses.

In **Chapter 8** the findings of the previous chapters are discussed.

REFERENCES

1. Butler, J.A., Colles, C.M., Dyson, S.J., Kold, S.E., and Poulos, P.W. (2011) The Spine. In: *Clinical Radiology of the Horse*, 3rd edn., Eds J.A. Butler, C.M. Colles, S.J. Dyson, S.E. Kold and P.W. Poulos. Wiley-Blackwell, Chichester. pp 505.
2. Galis, F. (1999) Why do almost all mammals have seven cervical vertebrae? Developmental constraints, Hox genes, and cancer. *J. Exp. Zool.* **285**, 19-26.
3. König, H.E. and Liebich, H.G. (2009) Vertebral column or spine (columna vertebralis). In: *Veterinary Anatomy of Domestic Mammals*, 4th edn., Eds H.E. König and H.G. Liebich. Schattauer GmbH, Stuttgart. pp 86.
4. Gilbert, S.C. and Barresi, M.J. (2017) Paraxial mesoderm; The Somites and Their Derivatives. In: *Developmental Biology*. 11th edn., Eds. Gilbert S.C., Barresi M.J. Oxford University Press Inc.
5. Scaal, M. (2016) Early development of the vertebral column. *Semin. Cell Dev. Biol.* **49**, 83-91.
6. Francioli, A.L., Cordeiro, B.M., da Fonseca, E.T., Rodrigues, M.N., Sarmiento, C.A., Ambrosio, C.E., de Carvalho, A.F., Miglino, M.A. and Silva, L.A. (2011) Characteristics of the equine embryo and fetus from days 15 to 107 of pregnancy. *Theriogenology*. **76**, 819-832.
7. Rombach, N., Stubbs, N.C. and Clayton, H.M. (2014) Gross anatomy of the deep perivertebral musculature in horses. *Am. J. Vet. Res.* **75**, 433-440.
8. Bordbari, M.H., Penedo, M.C.T., Aleman, M., Valberg, S.J., Mickelson, J. and Finno, C.J. (2017) Deletion of 2.7 kb near HOXD3 in an Arabian horse with occipitoatlantoaxial malformation. *Anim. Genet.* **48**, 287-294.
9. Buchholtz, E.A. and Stepien, C.C. (2009) Anatomical transformation in mammals: developmental origin of aberrant cervical anatomy in tree sloths. *Evol. Dev.* **11**, 69-79.
10. Cox, M.K. and Serra, A. (2014) Development of the Intervertebral Disc. In: *The Intervertebral Disc*. Eds I. Shapiro and M. Risbud. Springer, Vienna
11. Van Biervliet, J. (2007) An evidence-based approach to clinical questions in the practice of equine neurology. *Vet. Clin. North Am. Equine Pract.* **23**, 317-328.
12. Trostle, S.S., Dubielzig, R.R. and Beck, K.A. (1993) Examination of frozen cross sections of cervical spinal intersegments in nine horses with cervical vertebral malformation: lesions associated with spinal cord compression. *J. Vet. Diagn. Invest.* **5**, 423-431.
13. Aldrich, E., Nout-Lomas, Y., Seim, H.B., 3rd and Easley, J.T. (2018) Cervical stabilization with polyaxial pedicle screw and rod construct in horses: A proof of concept study. *Vet. Surg.* **47**, 932-941.
14. Kuhnle, C., Furst, A.E., Ranninger, E., Suarez Sanchez-Andrade, J. and Kummerle, J.M. (2018) Outcome of Ventral Fusion of Two or Three Cervical Vertebrae with a Locking Compression Plate for the Treatment of Cervical Stenotic Myelopathy in Eight Horses. *Vet. Comp. Orthop. Traumatol.* **31**, 356-363.
15. Reardon, R.J., Bailey, R., Walmsley, J.P., Heller, J. and Lischer, C. (2010) An in vitro biomechanical comparison of a locking compression plate fixation and kerf cut cylinder fixation for ventral arthrodesis of the fourth and the fifth equine cervical vertebrae. *Vet. Surg.* **39**, 980-990.
16. Pezzanite, L. and Easley, J. (2019) Update on Surgical Treatment of Wobblers. *Vet. Clin. North Am. Equine Pract.* **35**, 299-309.
17. Hoffman, C.J. and Clark, C.K. (2013) Prognosis for racing with conservative management of cervical vertebral malformation in thoroughbreds: 103 cases (2002-2010). *J. Vet. Intern. Med.* **27**, 317-323.
18. Barberini, D.J., Aleman, M., Aristizabal, F., Spriet, M., Clark, K.C., Walker, N.J., Galuppo, L.D., Amorim, R.M., Woolard, K.D. and Borjesson, D.L. (2018) Safety and tracking of intrathecal allogeneic mesenchymal stem cell transplantation in healthy and diseased horses. *Stem Cell. Res. Ther.* **9**, 96-018-0849-6.

19. Claridge, H.A., Piercy, R.J., Parry, A. and Weller, R. (2010) The 3D anatomy of the cervical articular process joints in the horse and their topographical relationship to the spinal cord. *Equine Vet. J.* **42**, 726-731.
20. Hestvik, G., Ekman, S. and Lindberg, R. (2006) Onchocercosis of an intervertebral joint capsule causing cervical vertebral stenotic myelopathy in a horse. *J. Vet. Diagn. Invest.* **18**, 307-310.
21. Lim, C.K., Hawkins, J.F., Vanderpool, A.L., Heng, H.G., Gillespie Harmon, C.C. and Lenz, S.D. (2017) Osteochondritis dissecans-like lesions of the occipital condyle and cervical articular process joints in a Saddlebred colt horse. *Acta Vet. Scand.* **59**, 76. <https://doi.org/10.1186/s13028-017-0345-5>
22. Stewart, R.H., Reed, S.M. and Weisbrode, S.E. (1991) Frequency and severity of osteochondrosis in horses with cervical stenotic myelopathy. *Am. J. Vet. Res.* **52**, 873-879.
23. Beck, C., Middleton, D., Maclean, A. and Lavelle, R. (2002) Osteochondrosis of the second cervical vertebra of a horse. *Equine Vet. J.* **34**, 210-212.
24. Janes, J.G., Garrett, K.S., McQuerry, K.J., Waddell, S., Voor, M.J., Reed, S.M., Williams, N.M. and MacLeod, J.N. (2015) Cervical Vertebral Lesions in Equine Stenotic Myelopathy. *Vet. Pathol.* **52**, 919-927.
25. Tomizawa, N., Nishimura, R., Sasaki, N., Hayashi, Y., Senba, H., Hara, S., Kadosawa, T. and Takeuchi, A. (1994) Morphological analysis of cervical vertebrae in ataxic foals. *J. Vet. Med. Sci.* **56**, 1081-1085.
26. Gorton, B. (1923) Abnormal Cervical Vertebra of a Horse. *J. Anat.* **57**, 380-381.
27. Santinelli, I., Beccati, F., Arcelli, R. and Pepe, M. (2014) Anatomical variation of the spinous and transverse processes in the caudal cervical vertebrae and the first thoracic vertebra in horses. *Equine Vet. J.* **48**, 45-49.
28. May-Davis, S. and Walker, C. (2015) Variations and Implications of the Gross Morphology in the *Longus colli* Muscle in Thoroughbred and Thoroughbred Derivative Horses Presenting With a Congenital Malformation of the Sixth and Seventh Cervical Vertebrae. *J. Equine Vet. Sci.* **35**, 560-568.
29. May-Davis, S. (2014) The Occurrence of a Congenital Malformation in the Sixth and Seventh Cervical Vertebrae Predominantly Observed in Thoroughbred Horses. *J. Equine Vet. Sci.* **34**, 1313-1317.
30. DeRouen, A., Spriet, M. and Aleman, M. (2016) Prevalence of Anatomical Variation of the Sixth Cervical Vertebra and Association with Vertebral Canal Stenosis and Articular Process Osteoarthritis in the Horse. *Vet. Radiol. Ultrasound.* **57**, 253-258.
31. Yovich, J.V., Powers, B.E. and Stashak, T.S. (1985) Morphologic features of the cervical intervertebral disks and adjacent vertebral bodies of horses. *Am. J. Vet. Res.* **46**, 2372-2377.
32. Allison, N. and Moeller, R.B., Jr. (2000) Spinal ataxia in a horse caused by an arachnoid diverticulum (cyst). *J. Vet. Diagn. Invest.* **12**, 279-281.
33. Foss, R.R., Genetzky, R.M., Riedesel, E.A. and Graham, C. (1983) Cervical intervertebral disc protrusion in two horses. *Can. Vet. J.* **24**, 188-191.
34. Furr, M.O., Anver, M. and Wise, M. (1991) Intervertebral disk prolapse and diskospondylitis in a horse. *J. Am. Vet. Med. Assoc.* **198**, 2095-2096.
35. Jansson, N. (2001) What is your diagnosis? Multiple cervical intervertebral disk prolapses. *J. Am. Vet. Med. Assoc.* **219**, 1681-1682.
36. Nixon, A.J., Stashak, T., S., Ingram J. T., Norrdin R.W. and Park R.D. (1984) Cervical intervertebral disc protrusion in a horse. *Vet. Surg.* **13**, 154-158.
37. Stadler, P., van den Berg, S.S. and Tustin, R.C. (1988) Cervical intervertebral disk prolapse in a horse. *J. S. Afr. Vet. Assoc.* **59**, 31-32.
38. Taylor, H.W., Vandeveld, M. and Firth, E.C. (1977) Ischemic myelopathy caused by fibrocartilaginous emboli in a horse. *Vet. Pathol.* **14**, 479-481.

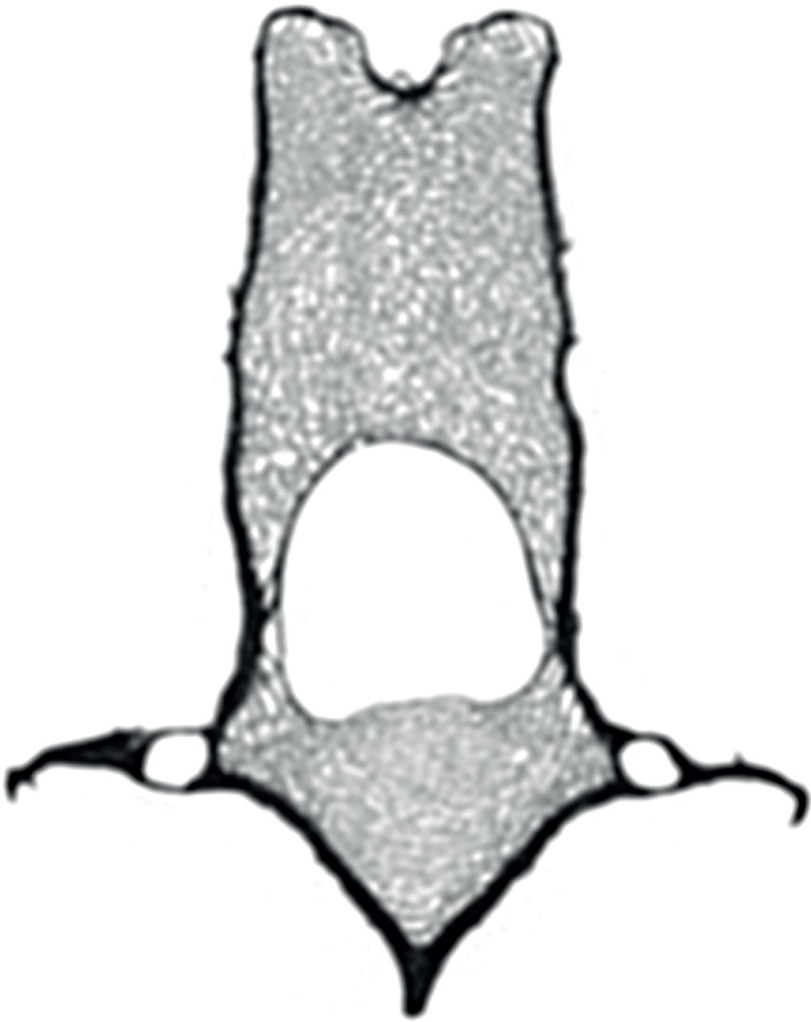
39. Sebastian, M.M. and Giles, R.C. (2004) Fibrocartilaginous embolic myelopathy in a horse. *J. Vet. Med. A Physiol. Pathol. Clin. Med.* **51**, 341-343.
40. Fuentealba, I.C., Weeks, B.R., Martin, M.T., Joyce, J.R. and Wease, G.S. (1991) Spinal cord ischemic necrosis due to fibrocartilaginous embolism in a horse. *J. Vet. Diagn. Invest.* **3**, 176-179.
41. Sweers, L. and Carstens, A. (2006) Imaging features of discospondylitis in two horses. *Vet. Radiol. Ultrasound.* **47**, 159-164.
42. Hillyer, M.H., Innes, J.F., Patteson, M.W. and Barr, A.R. (1996) Discospondylitis in an adult horse. *Vet. Rec.* **139**, 519-521.
43. Toth, B., Aleman, M., Nogradi, N. and Madigan, J.E. (2012) Meningitis and meningoencephalomyelitis in horses: 28 cases (1985-2010). *J. Am. Vet. Med. Assoc.* **240**, 580-587.
44. Mittelman, N.S., Divers, T.J., Engiles, J.B., Gerhold, R., Ness, S., Scrivani, P.V., Southard, T. and Johnson, A.L. (2017) Parelaphostrongylus tenuis Cerebrospinal Nematodiasis in a Horse with Cervical Scoliosis and Meningomyelitis. *J. Vet. Intern. Med.* **31**, 890-893.
45. Bryan, L.K., Hamer, S.A., Shaw, S., Curtis-Robles, R., Auckland, L.D., Hodo, C.L., Chaffin, K. and Rech, R.R. (2016) Chagas disease in a Texan horse with neurologic deficits. *Vet. Parasitol.* **216**, 13-17.
46. Meyer, E.E., Morris, P.G., Elcock, L.H. and Weil, J. (1986) Hindlimb hyperesthesia associated with rabies in two horses. *J. Am. Vet. Med. Assoc.* **188**, 629-632.
47. Rodrigues, A., Figuera, R.A., Souza, T.M., Schild, A.L. and Barros, C.S. (2009) Neuropathology of naturally occurring Trypanosoma evansi infection of horses. *Vet. Pathol.* **46**, 251-258.
48. Henninger, R.W., Reed, S.M., Saville, W.J., Allen, G.P., Hass, G.F., Kohn, C.W. and Sofaly, C. (2007) Outbreak of neurologic disease caused by equine herpesvirus-1 at a university equestrian center. *J. Vet. Intern. Med.* **21**, 157-165.
49. Watson, A.G. and Mayhew, I.G. (1986) Familial congenital occipitoatlantoaxial malformation (OAAM) in the Arabian horse. *Spine (Phila Pa. 1976).* **11**, 334-339.
50. Bell, S., Detweiler, D., Benak, J. and Pusterla, N. (2007) What is your diagnosis? Occipitoatlantoaxial malformation. *J. Am. Vet. Med. Assoc.* **231**, 1033-1034.
51. Rosenstein, D.S., Schott, H.C., 2nd and Stickle, R.L. (2000) Imaging diagnosis--occipitoatlantoaxial malformation in a miniature horse foal. *Vet. Radiol. Ultrasound.* **41**, 218-219.
52. de Lahunta, A., Hatfield, C. and Dietz, A. (1989) Occipitoatlantoaxial malformation with duplication of the atlas and axis in a half Arabian foal. *Cornell Vet.* **79**, 185-193.
53. Mayhew, I.G., Watson, A.G. and Heissan, J.A. (1978) Congenital occipitoatlantoaxial malformations in the horse. *Equine Vet. J.* **10**, 103-113.
54. Cole, R., Taintor, J. and Hanson, R. (2017) Atlanto-axial malformation in an adult Quarter horse gelding. *Can. Vet. J.* **58**, 923-925.
55. Rossignol, F., Brandenberger, O. and Mespoulhes-Riviere, C. (2016) Internal Fixation of Cervical Fractures in Three Horses. *Vet. Surg.* **45**, 104-109.
56. Scheffer, C.J., Blaauw, G., Dik, K.J. and Sloet van Oldruitenborgh-Oosterbaan, M.M. (2001) Ataxia and pruritus in a pony due to a cervical vertebral fracture. *Tijdschr. Diergeneesk.* **126**, 419-422.
57. Sysel, A.M., Moll, H.D., Carrig, C.B. and Newton, T.J. (1998) What is your diagnosis? Oblique fracture of the caudal half of the transverse process of the fourth cervical vertebra. *J. Am. Vet. Med. Assoc.* **213**, 607-608.
58. Barnes, H.G., Tucker, R.L., Grant, B.D., Roberts, G.D. and Prades, M. (1995) Lag screw stabilization of a cervical vertebral fracture by use of computed tomography in a horse. *J. Am. Vet. Med. Assoc.* **206**, 221-223.
59. Cillan-Garcia, E., Taylor, S.E., Townsend, N. and Licka, T. (2011) Partial ostectomy of the dens to correct atlantoaxial subluxation in a pony. *Vet. Surg.* **40**, 596-600.

60. McCoy, D.J., Shires, P.K. and Beadle, R. (1984) Ventral approach for stabilization of atlantoaxial subluxation secondary to odontoid fracture in a foal. *J. Am. Vet. Med. Assoc.* **185**, 545-549.
61. Vos, N.J., Pollock, P.J., Harty, M., Brennan, T., de Blaauw, S. and McAllister, H. (2008) Fractures of the cervical vertebral odontoid in four horses and one pony. *Vet. Rec.* **162**, 116-119.
62. Slone, D.E., Bergfeld, W.A. and Walker, T.L. (1979) Surgical decompression for traumatic atlantoaxial subluxation in a weanling filly. *J. Am. Vet. Med. Assoc.* **174**, 1234-1236.
63. Berry, S. (1999) Spinal cord compression secondary to hemangiosarcoma in a saddlebred stallion. *Can. Vet. J.* **40**, 886-887.
64. Civello, A.N.E., Dunkel, B., Summers, B.A. and Martineau, H.M. (2017) Spinal Cord Compression in a Horse due to a Granular Cell Variant of Neurofibroma. *J. Comp. Pathol.* **157**, 303-307.
65. Hirsch, J.E., Grant, B.D., Linovitz, R., Peppers, T.A. and Rantanen, N.W. (2010) Diagnosis and surgical treatment of epidural neoplasm in two ataxic horses. *Equine Vet. Educ.* **11**, 564-568.
66. Newton-Clarke, M.J., Guffoy, M.R., Dykes, N.L. and Divers, T.J. (1994) Ataxia due to a vertebral haemangiosarcoma in a horse. *Vet. Rec.* **135**, 182-184.
67. Gold, J.R., Divers, T.J., Miller, A.J., Scrivani, P.V., Perkins, G.A., VanBierliet, J. and de LaHunta, A. (2008) Cervical vertebral spinal hematomas in 4 horses. *J. Vet. Intern. Med.* **22**, 481-485.
68. Bolz, W. (1966) Epidural hematomas in the cervical spinal cord in horses. *Dtsch. Tierarztl. Wochenschr.* **73**, 585-588.
69. Dorner, C., Uzal, F., Carvallo, F. and Palmero, J. (2015) Compressive myelopathy caused by epidural haematoma associated with fibrocartilaginous embolism in a horse. *Equine Vet. Educ.* **8**, 405-409.
70. Boswinkel, M., van der Lugt, J.J. and Sloet van Oldruitenborgh-Oosterbaan, M.M. (2006) Vertebral osteomyelitis caused by *Rhodococcus equi* in a three-and-half-month-old Dutch Warmblood foal. *Tijdschr. Diergeneeskd.* **131**, 612-616.
71. Yang, C., Weisbrode, S., Yardley, J., Schroeder, E. and Premanandan, C. (2018) Metaphyseal and Diaphyseal Dysplasia of the Third Cervical Vertebra Secondary to Physeal Necrosis in a Quarter Horse Foal. *J. Comp. Pathol.* **163**, 38-41.
72. Ishihara, A., Reed, S.M., Rajala-Schultz, P.J., Robertson, J.T. and Bertone, A.L. (2009) Use of kinetic gait analysis for detection, quantification, and differentiation of hind limb lameness and spinal ataxia in horses. *J. Am. Vet. Med. Assoc.* **234**, 644-651.
73. Wijnberg, I.D., Bergmann, W. and Veraa, S. (2015) Diagnose und prognose neurologischer Erkrankungen der Halswirbelsäule beim pferd. *Praktischer Tierarzt.* **96**, 150-158.
74. Dyson, S.J. (2011) Lesions of the equine neck resulting in lameness or poor performance. *Vet. Clin. North Am. Equine Pract.* **27**, 417-437.
75. Levine, J.M., Scrivani, P.V., Divers, T.J., Furr, M., Mayhew, I.J., Reed, S., Levine, G.J., Foreman, J.H., Boudreau, C., Credille, B.C., Tennent-Brown, B. and Cohen, N.D. (2010) Multicenter case-control study of signalment, diagnostic features, and outcome associated with cervical vertebral malformation-malarticulation in horses. *J. Am. Vet. Med. Assoc.* **237**, 812-822.
76. Szklarz, M., Lipinska, A., Slowikowska, M., Niedzwiedz, A., Marycz, K. and Janeczek, M. (2019) Comparison of the clinical and radiographic appearance of the cervical vertebrae with histological and anatomical findings in an eight-month old warmblood stallion suffering from cervical vertebral stenotic myelopathy (CVSM). *BMC Vet. Res.* **15**, 296. <https://doi.org/10.1186/s12917-019-2047-x>
77. Wijnberg, I.D. and Franssen, H. (2016) The potential and limitations of quantitative electromyography in equine medicine. *Vet. J.* **209**, 23-31.
78. Nollet, H., Deprez, P., Van Ham, L., Verschooten, F. and Vanderstraeten, G. (2002) The use of magnetic motor evoked potentials in horses with cervical spinal cord disease. *Equine Vet. J.* **34**, 156-163.

79. Berg, L.C., Nielsen, J.V., Thoenner, M.B. and Thomsen, P.D. (2003) Ultrasonography of the equine cervical region: a descriptive study in eight horses. *Equine Vet. J.* **35**, 647-655.
80. Pease, A., Mair, T. and Spriet, M. (2017) Imaging the equine head and spine. *Equine Vet. J.* **49**, 13-14.
81. Kristoffersen, M., Pulchalski, S., Skog, S. and Lindegaard, C. (2014) Cervical computed tomography (CT) and CT myelography in live horses; 16 cases. *Equine Vet. J.* **46**, 11.
82. Withers, J.M., Voute, L.C., Hammond, G. and Lischer, C.J. (2009) Radiographic anatomy of the articular process joints of the caudal cervical vertebrae in the horse on lateral and oblique projections. *Equine Vet. J.* **41**, 895-902.
83. Roberts, R.E. and Selcer, B.A. (1993) Myelography and epidurography. *Vet. Clin. North Am. Small Anim. Pract.* **23**, 307-329.
84. Papageorges, M., Gavin, P.R., Sande, R.D., Barbee, D.D. and Grant, B.D. (1987) Radiographic and myelographic examination of the cervical vertebral column in 306 Ataxic horses. *Vet. Radiol.* **28**, 53-59.
85. Nappert, G., Vrins, A., Breton, L. and Beauregard, M. (1989) A retrospective study of nineteen ataxic horses. *Can. Vet. J.* **30**, 802-806.
86. Oswald, J., Love, S., Parkin, T.D. and Hughes, K.J. (2010) Prevalence of cervical vertebral stenotic myelopathy in a population of thoroughbred horses. *Vet. Rec.* **166**, 82-83.
87. van Biervliet, J., Scrivani, P.V., Divers, T.J., Erb, H.N., de Lahunta, A. and Nixon, A. (2004) Evaluation of decision criteria for detection of spinal cord compression based on cervical myelography in horses: 38 cases (1981-2001). *Equine Vet. J.* **36**, 14-20.
88. Moore, B.R., Holbrook, T.C., Stefanacci, J.D., Reed, S.M., Tate, L.P. and Menard, M.C. (1992) Contrast-enhanced computed tomography and myelography in six horses with cervical stenotic myelopathy. *Equine Vet. J.* **24**, 197-202.
89. Audigie, F., Tapprest, J., Didierlaurent, D. and Denoix, J.M. (2004) Ultrasound-guided atlanto-occipital puncture for myelography in the horse. *Vet. Radiol. Ultrasound.* **45**, 340-344.
90. Pease, A., Behan, A. and Bohart, G. (2012) Ultrasound-guided cervical centesis to obtain cerebrospinal fluid in the standing horse. *Vet. Radiol. Ultrasound.* **53**, 92-95.
91. Rose, P.L., Abutarbush, S.M. and Duckett, W. (2007) Standing myelography in the horse using a nonionic contrast agent. *Vet. Radiol. Ultrasound.* **48**, 535-538.
92. Mullen, K.R., Furness, M.C., Johnson, A.L., Norman, T.E., Hart, K.A., Burton, A.J., Bichalo, R.C., Ainsworth, D.M., Thompson, M.S. and Scrivani, P.V. (2015) Adverse reactions in horses that underwent general anesthesia and cervical myelography. *J. Vet. Intern. Med.* **29**, 954-960.
93. Rainger, J.E., Hughes, K.J., Kessell, A. and Dart, C.M. (2006) Pleuropneumonia as a sequela of myelography and general anaesthesia in a Thoroughbred colt. *Aust. Vet. J.* **84**, 138-140.
94. Estell, K., Spriet, M., Phillips, K.L., Aleman, M. and Finno, C.J. (2018) Current dorsal myelographic column and dural diameter reduction rules do not apply at the cervicothoracic junction in horses. *Vet. Radiol. Ultrasound.* **59**, 662-666.
95. Schmidburg, I., Pagger, H., Zsoldos, R.R., Mehnen, J., Peham, C. and Licka, T.F. (2012) Movement associated reduction of spatial capacity of the equine cervical vertebral canal. *Vet. J.* **192**, 525-528.
96. Prange, T., Carr, E.A., Stick, J.A., Garcia-Pereira, F.L., Patterson, J.S. and Derksen, F.J. (2012) Cervical vertebral canal endoscopy in a horse with cervical vertebral stenotic myelopathy. *Equine Vet. J.* **44**, 116-119.
97. Maierl, J., Zechmeister, R., Schill, W., Gerhards, H. and Liebich, H.G. (1998) Radiologic description of the growth plates of the atlas and axis in foals. *Tierarztl. Prax. Ausg. G. Grosstiere Nutztiere.* **26**, 341-345.
98. Down, S.S. and Henson, F.M. (2009) Radiographic retrospective study of the caudal cervical articular process joints in the horse. *Equine Vet. J.* **41**, 518-524.

99. Hett, A.R., Busato, A. and Ueltschi, G. (2006) Radiologische Messungen an der arthrotisch veränderten Halswirbelsäule des Pferdes – eine retrospektive, statistische Studie. *Pferdeheilkunde*. **22**, 241-249.
100. Berner, D., Brehn, W. and Gerlach, K. (2012) The influence of head and neck position on radiographic examination of the intervertebral foramina of the neck of horses at latero-lateral projection. *Pferdeheilkunde*. **28**, 39-45.
101. Moore, B.R., Reed, S.M., Biller, D.S., Kohn, C.W. and Weisbrode, S.E. (1994) Assessment of vertebral canal diameter and bony malformations of the cervical part of the spine in horses with cervical stenotic myelopathy. *Am. J. Vet. Res.* **55**, 5-13.
102. Hahn, C.N., Handel, I., Green, S.L., Bronsvort, M.B. and Mayhew, I.G. (2008) Assessment of the utility of using intra- and intervertebral minimum sagittal diameter ratios in the diagnosis of cervical vertebral malformation in horses. *Vet. Radiol. Ultrasound*. **49**, 1-6.
103. Scrivani, P.V., Levine, J.M., Holmes, N.L., Furr, M., Divers, T.J. and Cohen, N.D. (2011) Observer agreement study of cervical-vertebral ratios in horses. *Equine Vet. J.* **43**, 399-403.
104. Hughes, K.J., Laidlaw, E.H., Reed, S.M., Keen, J., Abbott, J.B., Trevail, T., Hammond, G., Parkin, T.D. and Love, S. (2014) Repeatability and intra- and inter-observer agreement of cervical vertebral sagittal diameter ratios in horses with neurological disease. *J. Vet. Intern. Med.* **28**, 1860-1870.
105. Lischer, C.J., Withers, J.M. and Parkin, T. (2010) Accuracy of radiographic measurements of the cervical articular process joints of the horse. *Pferdeheilkunde*. **26**, 553-558.
106. Beccati, F., Santinelli, I., Nannarone, S. and Pepe, M. (2018) Influence of neck position on commonly performed radiographic measurements of the cervical vertebral region in horses. *Am. J. Vet. Res.* **79**, 1044-1049.
107. Mattoon, J.S., Drost, W.T., Grguric, M.R., Auld, D.M. and Reed, S.M. (2004) Technique for equine cervical articular process joint injection. *Vet. Radiol. Ultrasound*. **45**, 238-240.
108. Nielsen, J.V., Berg, L.C., Thoenfert, M.B. and Thomsen, P.D. (2003) Accuracy of ultrasound-guided intra-articular injection of cervical facet joints in horses: a cadaveric study. *Equine Vet. J.* **35**, 657-661.
109. Purefoy Johnson, J., Stack, J.D., Rowan, C., Handel, I. and O'Leary, J.M. (2017) Ultrasound-guided approach to the cervical articular process joints in horses: a validation of the technique in cadavers. *Vet. Comp. Orthop. Traumatol.* **30**, 165-171.
110. Beaulieu, A., Linden, A.Z., Phillips, J., Arroyo, L.G., Koenig, J. and Monteith, G. (2019) Various 3D printed materials mimic bone ultrasonographically: 3D printed models of the equine cervical articular process joints as a simulator for ultrasound guided intra-articular injections. *PLoS One*. **14**, e0220332.
111. Sgorbini, M., Marmorini, P., Rota, A., Briganti, A. and Corazza, M. (2011) Ultrasound measurements of the dorsal subarachnoid space depth in healthy trotter foal during the first week of life. *J. Equine Vet. Sci.* **31**, 41-43.
112. Mackenzie, C.J., Haggett, E.F., Pinchbeck, G.L. and Marr, C.M. (2017) Ultrasonographic assessment of the atlanto-occipital space in healthy Thoroughbred foals and Thoroughbred foals with neonatal maladjustment syndrome. *Vet. J.* **223**, 55-59.
113. Zafrá, R., Carrascosa, C., Rivero, M., Pená, S., Fernández, T., Suarez-Bonnet, A. and Jaber, J.R. (2012) Analysis of equine cervical spine using three-dimensional computed tomographic reconstruction. *J. Applied Anim. Res.* **40**, 108-111.
114. Sleutjens, J., Cooley, A.J., Sampson, S.N., Wijnberg, I.D., Back, W., van der Kolk, J.H. and Swiderski, C.E. (2014) The equine cervical spine: comparing MRI and contrast-enhanced CT images with anatomic slices in the sagittal, dorsal, and transverse plane. *Vet. Q.* **34**, 74-84.
115. Sleutjens, J., Voorhout, G., Van Der Kolk, J.H., Wijnberg, I.D. and Back, W. (2010) The effect of ex vivo flexion and extension on intervertebral foramina dimensions in the equine cervical spine. *Equine Vet. J.* **38**, 425-430

116. Yamada, K., Sato, F., Hada, T., Horiuchi, N., Ikeda, H., Nishihara, K., Sasaki, N., Kobayashi, Y. and Nambo, Y. (2016) Quantitative evaluation of cervical cord compression by computed tomographic myelography in Thoroughbred foals. *J. Equine Sci.* **27**, 143-148.
117. Gutierrez-Crespo, B., Kircher, P.R. and Carrera, I. (2014) 3 Tesla Magnetic Resonance Imaging of the Occipitoatlantoaxial Region in the Normal Horse. *Vet. Radiol. Ultrasound.* **55**, 278-285.
118. Janes, J.G., Garrett, K.S., McQuerry, K.J., Pease, A.P., Williams, N.M., Reed, S.M. and MacLeod, J.N. (2014) Comparison of magnetic resonance imaging with standing cervical radiographs for evaluation of vertebral canal stenosis in equine cervical stenotic myelopathy. *Equine Vet. J.* **46**, 681-686.
119. Mitchell, C.W., Nykamp, S.G., Foster, R., Cruz, R. and Montieth, G. (2012) The use of Magnetic Resonance Imaging in Evaluating Horses with Spinal Ataxia. *Vet. Radiol. Ultrasound.* **53**, 613-620
120. Zsoldos, R.R. and Licka, T.F. (2015) The equine neck and its function during movement and locomotion. *Zoology (Jena).* **118**, 364-376.



2

Domesticated Animals as a Translational Model for Vertebral Congenital Malformations. A Literature Review.

Stefanie Veraa

Division of Diagnostic Imaging, Faculty of Veterinary Medicine, Utrecht University,
Yalelaan 108, NL-3584 CM, Utrecht, The Netherlands

In preparation of submission.

ABSTRACT

Congenital vertebral malformations occur in most domesticated animals and can be one of the hallmarks of a more complex congenital syndrome with multiple organ involvement. Clinically relevant features such as scoliosis and kyphosis, short neck, dwarfism, thoracic outlet syndrome and intervertebral disc disease can be related to these malformations necessitating thorough understanding of the etiology, genetic background and clinical impact. The aim of this study was to provide an overview of available data on these vertebral malformations in domestic animals, focusing on the translational aspects in relation to the same condition in humans.

Vertebral malformations have been described in all parts of the vertebral column in humans, livestock, companion animals and horses. They are considered to be secondary to a failure in segmentation with secondary fusion of vertebrae such as bars or block vertebrae. Failure in formation of parts of the vertebra can result in for example hemivertebrae, wedge-shaped vertebrae or butterfly vertebrae. Failure in segmentation of the lateral part of the vertebral column, creates transitional vertebrae with aberrant positioning of ribs or transverse processes. This results in shortening or elongation of vertebral series but seldom leading to a change in total vertebral count. With it, conditions such as intervertebral disc extrusion, due to adjacent segment syndrome, or degenerative lumbosacral stenosis causing clinical symptoms have been identified in both companion animals and humans. Some of these malformations have a similar genetic background such as Robinow syndrome in humans and screw-tailed dog breeds.

It can be concluded that congenital vertebral malformations exist in many forms in domestic animals and are in shape, genetic and clinical features very similar to the same phenomena in humans. Therefore, the use of domestic animals as translational models for vertebral congenital malformations can be beneficial for both human and veterinary patients.

INTRODUCTION

Vertebral congenital morphologic malformations that cause scoliosis, including in humans, represent a failure in vertebral segmentation or formation, or are due to abnormal vertebral development with changes in shape and size [1, 2]. These malformations can be an isolated anomaly, or part of a complex syndrome with varying clinical impact [1-3]. For instance in up to 61% of human scoliosis patients abnormalities have been recorded in other organs [1] and the presence of a rib at the last cervical vertebra has been shown to increase changes of stillbirth in the human fetus or development of cancer later in life [3].

Vertebral congenital morphologic malformations in domestic animals are well-recognized and are reported to affect health [4-6], economic status [7, 8] as well as athletic performance [9] or esthetic appearance [10-13]. Public awareness of the existence of spinal variations is expanding in social media together with changes in animal welfare legislation and with it the need to become familiar with the extent and possible impact on domestic animals [14-16]. Translation of findings associated with congenital vertebral malformations from veterinary to human patients can be valuable in light of the rapidly increasing possibilities of genetic screening as well as treatment options, as has already been recognized in intervertebral disc disease related research [17]. Also, potential ethical and breeding benefits for the veterinary patient populations warrant further exploration in this research field; for example, thoracolumbar hemivertebrae are more common in screw-tail breeds that have recently been diagnosed as being genetically affected by the same defect causing a type of dwarfism in humans [13, 17]. Some of these malformations lead to directly (e.g. stenosis of the vertebral canal) and indirectly related clinical signs if part of a syndrome [4, 5] and might even be a reason for loss of purpose (e.g. sales, competition performance) and secondary euthanasia in horses [14]. Therefore, the aim of this review is to provide an overview of available data on vertebral malformations in domesticated animals that could possibly serve as translational models for vertebral congenital malformations in humans. The vertebral malformations are explored in two ways: first thematical explanation against the background of the normal embryonic development of the vertebral column (formation of vertebrae, segmentation of vertebrae, and vertebral patterning), then more in detail species-related (livestock, companion animals, horses).

Embryonic development of the vertebral column

Vertebral development

The early embryonic development of the vertebral column in mammals comprises the process of somitogenesis and with it creation of bilateral symmetric areas of paraxial mesoderm defined as somites [18, 19]. These somites are formed along the anterior-posterior axis, budding longitudinally from anterior to posterior like the beads on a pearl-string. Development occurs along the notochord, a dense rod of mesoderm along this body axis and the embryonic origin of the intervertebral disc, and neural tube where presomitic mesoderm, otherwise referred to as the segmental plate, expands towards the tail bud [18].

As the somites have been formed, division into a smaller dorsolateral dermomyotome and a larger ventromedial sclerotome occurs under the expression of the paired-box transcription factor 1 (*Pax1*) amongst others [19]. Sequential segmentation of the sclerotome follows and these segments will give rise to the vertebrae, ribs and the dorsal part of the aortic wall. As such, the caudo-central part of the sclerotomes becomes a mesenchymal area that will develop into the ventral part of the vertebral pedicle, transverse processes and proximal ribs [18, 19]. At this moment the vertebral sub-unit is being formed from a caudal and cranial adjacent part of the adjacent sclerotomes as the outwardly expanding nerves split the initial sclerotomes in two halves, forming von Ebner's cleft. The intervertebral disc will form at this location. Chondrification and thereafter ossification of the early vertebral components will commence after downregulation of *Pax1* and activation of other factors such as *chondroitin-6-sulphate* [19].

As the vertebral sub-units are formed in tetrapods, divisional differentiation in cranio-caudal direction starts with the expression of the Homeobox genes (*Hox*) [20, 21]. Cervical, thoracic, lumbar, sacral and caudal series are defined by junctions that are the result of gradients of *Hox* genes expression along the cranio-caudal axis [20, 21]. For example, the *Hox3* gene complex regulates the occipito-atlanto-axial junction whereas the cervico-thoracic junction is regulated by the *Hox5* gene and *Hox6* gene complex [20, 22, 23]. This is otherwise defined as axial patterning of the vertebral column or patterning along the axis by the *Hox*-code and mutations can lead to variation in vertebral identity [21, 23]. The occiput is a derivative of the first 4 to 5 somites and therefore can be considered as part of the cervical series of the vertebral column [19].

Interestingly, close alignment of lateral element patterning including the ribs and transverse processes, otherwise referred to as abaxial patterning, and limb positioning is defined in the lateral plate mesoderm by the same *Hox* genes [21]. As such, *Hox6* has been

defined as a regulator of the cervicothoracic junction and thoracic limb bud origination [20]. *Hox6* is specifically expressed at the last somitic segment that contributes a spinal nerve to the brachial plexus, being the first thoracic vertebra [20].

Intervertebral disc development

Development of the intervertebral disc occurs in the same time frame as vertebral body formation and both are derivatives from ventral sclerotome that creates a mesenchymal perinotochordal sheath [19]. The annulus fibrosus and vertebral bodies are created from a metameric pattern or series of similar dense, highly proliferative cell population areas and loose less proliferative cell population areas respectively [19]. The annulus fibrosus is a derivative of the central somite and forms the border between the cranial and caudal half of the sclerotome (von Ebner's fissure) as described above [24]. Progression in a fibrocartilaginous structure consisting of collagen II with aggrecan occurs under the influence of TGF- β amongst others [24]. The nucleus pulposus is formed by perseverance of a small part of the central notochord in between the developing vertebral subunits under influence of Sonic hedgehog (*Shh*) and hypoxia inducible factor 2-alpha (*HIF-1 α*) [19, 24]. The rest of the notochord undergoes degeneration and will disappear during further embryonic development [19].

Vertebral Patterning in Domesticated mammals

Vertebral axial patterning can be described as development along the cranial-caudal axis. This patterning in cervical, thoracic, lumbar, sacral and caudal series with a fixed number of vertebrae per series occurs in most animal species, however 4 types of divergence have been described (homologous, axial homeotic, meristic, associational) [26]. Homologous variation alters the shape or size of a vertebra after serial junctions have been set, whereas homeotic variation alters the number of vertebra in one serie with preservation of total vertebral count [26]. In meristic variation the total number of vertebrae changes and in associational variation complete vertebral series can be lost, added or associated with other series [26]. Divergence in vertebral axial patterning in domesticated animals is a wide-spread phenomenon in the thoracic and lumbar area but less so in the cervical area [5, 25, 27-33]. In livestock these homeotic vertebral variations have health and economic implications such as an increase in musculature [33, 34] whereas in horses vertebral morphologic variations might also affect athletic performance [35]. In companion animals variations are recorded to have health implications such as intervertebral disc disease [4-6] but also influence esthetic appearance such as a short back and presence of a screw-tail [10, 11]. All the vertebral column elements are derivatives of the same notochord, somites and sclerotomes and therefore developmental alterations in one of the areas of the axial skeleton can lead to

alterations in an adjacent area [24]. Vertebral patterning and morphology aberrations are a reflection of this and need to be seen in light of the evolution of species [23, 25].

Companion animals (dogs and cats)

Both vertebral patterning variations and vertebral malformations have been frequently reported in certain dog and cat breeds and with it possible health as well as esthetic issues arise [31, 36].

Cranio-cervical junction abnormalities have been mainly identified in toy breeds and Cavalier King Charles, including Chiari-like malformations, atlanto-occipital overlap, dorsal constriction at C1-C2 and atlanto-axial instability [37]. These abnormalities reflect embryonic variation in the somitogenesis, recalling that the occiput is also formed by the first 4 to 5 somite pairs [19]. Other more rarely reported cervical vertebral abnormalities include atlantal hypoplasia, Klippel-Feil syndrome like changes, block-vertebrae and cervical ribs (fig. 1) [10, 38, 39]. Varying clinical symptoms such as neck pain, lameness, scratching or scoliosis are associated with these conditions of which Chiari-like malformation, that has been found to be similar to Chiari-type I malformation in humans, has been most well documented [36, 37]. The screening of dogs for the presence of Chiari-like malformations and associated syringomyelia has been applied to overcome the complex genetic basis of the cranio-cervical junction abnormalities [37, 40].

Screw-tailed brachycephalic dog breeds such as pugs and, English and French bulldogs are known to have a very high (up to 80%) incidence of thoracolumbar vertebral homologous and homeotic malformations [5, 41]. These include hemivertebrae and wedge-shaped, block or butterfly vertebrae that can vary in severity and that may or may not be incarcerated or segmented (fig. 2) [2, 42, 43]. Although most of these dogs do not show neurological signs, the dorsal and dorsolateral hemivertebrae were most frequently identified in a small group of dogs with relevant clinical signs [43]. A recent publication reported that the presence of thoracic vertebral malformations in conjunction with kyphosis in French Bulldogs was thought to increase the risk of intervertebral disc extrusion [44]. That being said, neurologically normal pugs seem more likely to have kyphosis of the thoracolumbar spine than neurologically normal English or French Bulldogs [41] and no consensus has yet been reached about the clinical relevance of thoracic vertebral malformations in pugs [5, 45]. An English population of Pugs has recently been recorded to have a high number of cervical ribs (of up to 46%), a homeotic variation of the cervico-thoracic junction in combination with a significantly higher frequency of thoraco-lumbar transitional vertebrae and

a pre-sacral count of 26 vertebrae [10]. Moreover, bulldogs and related screw-tailed dog breeds are described to have a genetic frame shift mutation that is similar to the Robinow-like syndrome in humans [13]. This syndrome is characterized by mesomelic-limbed dwarfism, a broad nasal root and forehead, thoracic vertebral fusion and hemivertebrae [46].

Apart from changes in the ventral part of the vertebra, clinically relevant malformations in the dorsal part of the vertebra (such as articular process absence) have been recognized in screw-tailed dogs [47, 48]. These can be considered to represent posterior element anatomic variations that also include lamina fusion, pedicle absence and bifid areas [1].

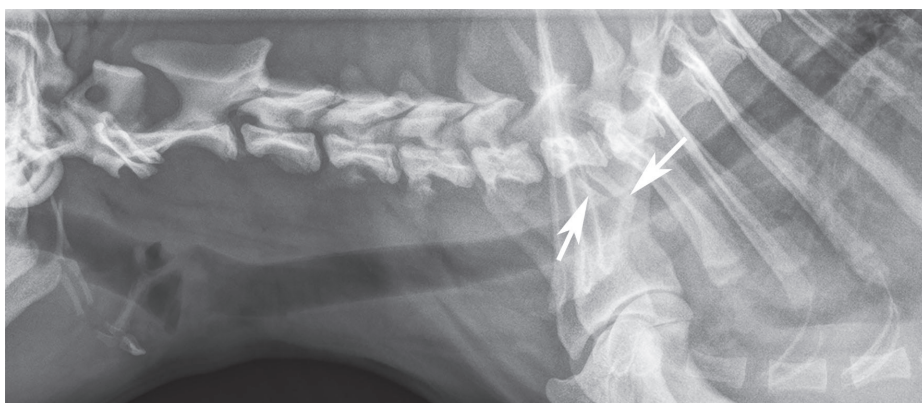


Fig. 1. Lateral radiographic view of the cervical vertebral column of a Pug dog. Note the cervical ribs ventral to C7 (white arrows).

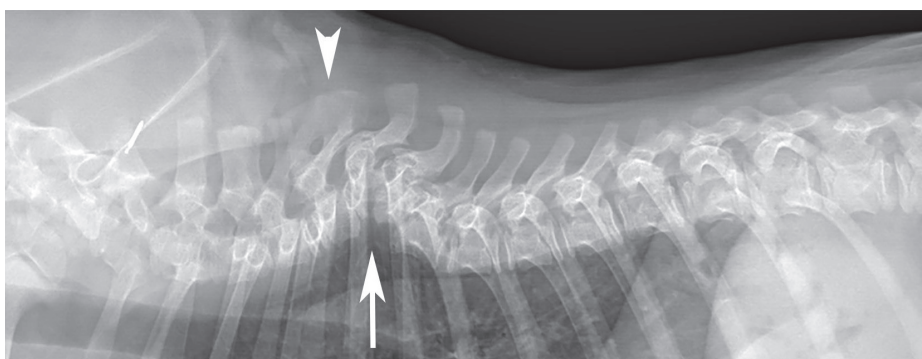


Fig. 2. Lateral radiographic view of the thoracolumbar vertebral column of a puppy. Hemivertebrae causing kyphosis midthoracic (arrow) and fusion of two spinous processes (arrowhead).

Lumbosacral transitional vertebrae in dogs have been classified [49] and an associated increased risk for developing degenerative lumbosacral stenosis and asymmetrical hip development was noted (fig.3) [6, 50]. Only recently, lumbar transitional vertebra have been related to degenerative joint disease and degenerative lumbosacral stenosis in humans [51, 52]. Another feature that has been described is the fact that maximal vertebral canal diameter shifts at a different pace than cauda equina location in dogs with thoracic or lumbar transitional vertebrae [53]. A more cranial localization of the maximal diameter is noted with a decreasing number of presacral vertebrae and a more caudal localization with an increasing number of presacral vertebrae [53]. Lumbosacral transitional vertebral features (e.g. unilateral, bilateral, shape) in offspring were directly related to the parental features in a breeding colony of dogs and therefore implying the result of a major gene effect [54].

Screening of the vertebral column to assess the presence of congenital vertebral malformations in dogs has been applied due to the genetic basis of some of these conditions and the clinical relevant implications of these malformations [5, 41, 54]. While, radiographic screening is a straightforward way of evaluating both number and shape of cervical, thoracic, lumbar and caudal vertebrae [43, 55, 56], computed tomography appears more sensitive in identifying shape variations and possibly clinically relevant congenital vertebral variations [57].

Although not so extensively documented, congenital vertebral malformations and abnormal vertebral patterning have also been described in cats; most of these, however, do not appear to have associated clinical symptoms (fig. 4) [4, 11, 28, 31, 58]. Occipito-atlantoaxial malformation has been described once in a cat with spinal ataxia and abnormal behavior that normalized after surgical stabilization [59]. Transient ataxia in a young kitten due to abnormal development with delayed fusion and vertebral canal stenosis of C2 and C3 has only recently been reported [60]. Lumbosacral spondylosis and lumbosacral stenosis due to intervertebral disc degeneration seem to coincide with lumbosacral transitional vertebrae in cats as was described in dogs and humans [4, 61]. Tail-less Manx cats have a higher incidence of spina bifida, urinary and faecal incontinence and pelvic limb locomotion abnormalities [58].

Livestock

Aberrations in vertebral patterning can have an economic impact in livestock as they can leave their mark on individuals, such as impaired health, but can also have economic impact on a breeding population as carcass characteristics can be altered [7, 33, 62].

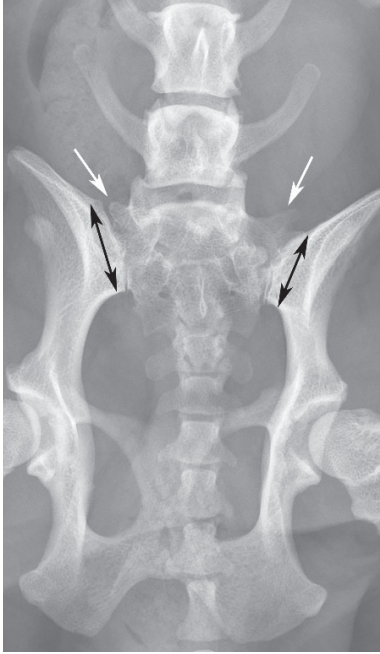


Fig. 3. Vento-dorsal radiographic view of the lumbosacral junction and pelvis. Note the asymmetrical shaped cranial aspect of the sacral wings or transverse processes of the first sacral vertebra (white arrows). Secondary asymmetry of the sacro-iliac joint length is present (black double arrows).

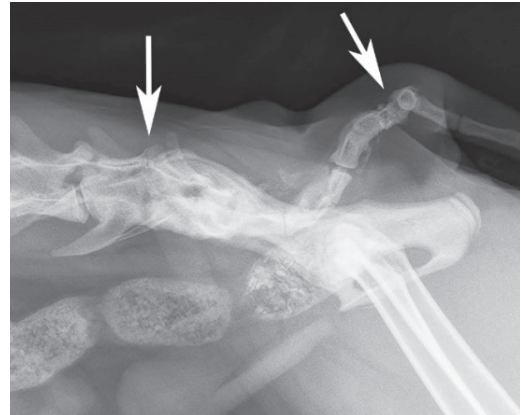
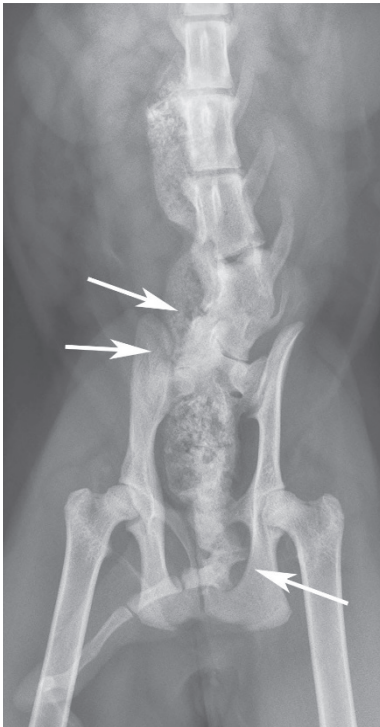


Fig. 4. A) Vento-dorsal (left) and B) lateral (above) radiographic views of the lumbosacral vertebral column of a domestic shorthair cat. Note the hemivertebrae at several locations (white arrows) with bar formation and partial fusion of L6 to S1.

In commercial pig breeds an increase in numbers of thoracic or lumbar vertebrae (so called multi-vertebrae) has been recognized as a trait affecting carcass weight, growth, fatness, muscularity and meat quality [7, 33]. Associated important genetic characteristics influencing meat quantity have been identified and with it the gateway to change morphometry in pigs [7, 34].

In several sheep breeds variation in numbers of the thoracic and lumbar spine has been recorded to range between 12 to 14 thoracic and 4 to 8 lumbar vertebrae, with the total number of thoracolumbar vertebrae varying between 17 to 21 [32]. Interestingly, increased thoracolumbar spine length, and therefore increase in carcass meat quantity, not only arose from a greater number of shorter vertebrae but also resulted from a smaller number of longer vertebrae [32].

In Holstein cattle, a hereditary congenital vertebral malformation complex including vertebral and spinal dysplasia has been found to severely affect thoracic and lumbar vertebral shape, but also to cause brachygnathia and abnormal internal organ development with fetal or early life death and therefore economical loss [62, 63]. A similar destructive, but not hereditary, effect has been noted following a Schmallenberg virus infection in small ruminants and cows, featuring secondary severe deformities of the vertebral column and other body structures, if not fetal death [64].

Horses

Vertebral malformations in horses have been documented in cervical, thoracic and lumbar series and serial junctions. The cranio-cervical [65-68] and cervico-thoracic [67, 69, 70] junctions in horses can be affected by morphologic variations or malformations of varying clinical impact. Occipito-atlantoaxial malformation (OAAM) in Arabian horses has been found to be a familial trait and a variation in the *Hoxd3* gene, a member of the Hox family that is involved in the embryonic divisional differentiation of the vertebrae in cranio-caudal direction (Hox-code) as mentioned earlier, has been described [22, 71]. Although not of hereditary origin, OAAM has also been found in other breeds including warmbloods, Quarter horses, Friesian, Standardbred, Morgan horse and even a Miniature horse [66-68, 71]. The presence of rudimentary ribs on the first thoracic vertebra and therefore cervicalisation or an anterior shift of the axial vertebral pattern has been recognized as early as a century ago [72]. Only recently, shape changes of the first rib have been suggested to be associated with clinical signs including fore limb lameness [69, 70]. Changes to the lateral elements of the first thoracic vertebra seem to coincide with variations in shape of the transverse processes of C6 and C7 (Fig. 5) [35, 67]. Together with *Longus colli* muscle attachment variations

and first thoracic rib variations in shape, these changes have been suggested a possible cause for biomechanical dysfunction of the cervico-thoracic boundary and thoracic limb in thoroughbred horses [69, 73, 74]. However, more recently it was reported that in Warmblood horses there was no association between the presence of C6 and C7 variations and the development of related clinical signs [75].

Transitional vertebrae exhibiting features of two adjacent vertebral series have been described in the thoracolumbar and lumbosacral area of horses although the clinical importance is unknown [29, 30, 76]. Most variation in lumbar numbers was seen in Przewalski horses with half of the examined horses having 5 instead of 6 lumbar vertebrae [30]. It has been found that horses originating from *Equus caballus pumPELLI* (consisting of Barber, Mustang, Sorraia, Arabian, Turkmene horses) vary in lumbar and not thoracic vertebral numbers as well [77]. In thoroughbred horses, a high incidence of variation in thoracolumbar vertebral count has been recognized with only 22% of horses having the expected vertebral count and shape [29].

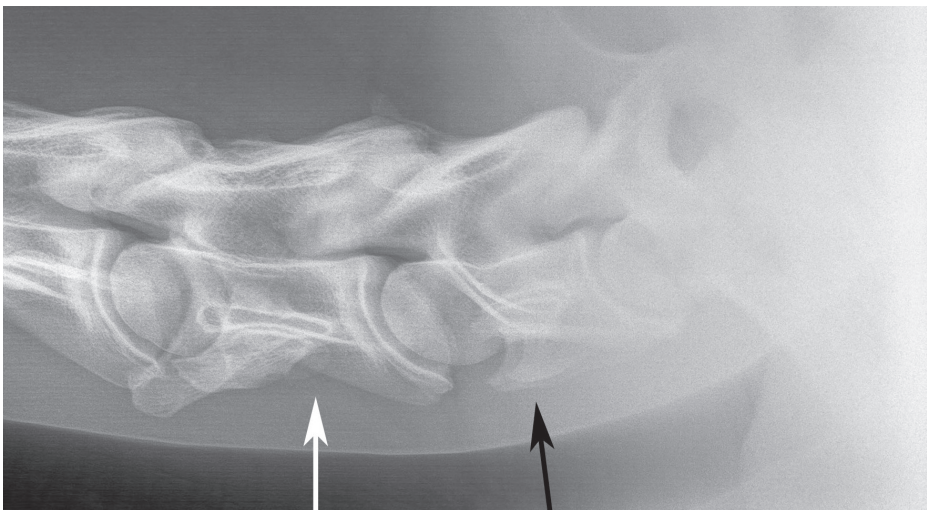


Fig. 5. Lateral radiographic view of the cervical vertebral column of a warmblood horse. There is a bilateral shift of the plate-like extension of the caudal tubercle of C6 (absent at white arrows) to the transverse processes of C7 (black arrow).

DISCUSSION

Vertebral column homeotic and homologous variations consisting in variation of number or shape in domestic animals are a frequent phenomenon and have been documented to be of clinical importance in some cases. Spinal development is a highly dynamic process that is subject to a landscape of genetic factors [18, 19]. Failure of one of these factors can lead to defects or abnormal development in other organ systems as well, such as positioning of the diaphragm positioning and limb bud positioning, neuronal problems, tumorigenesis or even still births [3, 26, 78, 79]. Evolutionary constraints tend to minimize vertebral variations and deviation from seven cervical vertebrae in most mammals, with the exception of sloths, manatees and dugongs [3, 26, 80, 81].

In domestic animals, evolution has taken a different path as strong population selection has influenced genetic diversity for commercial causes (such as meat production in pigs and competing capabilities in companion animals and horses) [7-9], and with the drive to manipulate esthetic appearance as breed characteristics [12, 13]. The strong selection in horses has resulted in a considerable drop of 16% in genetic diversity and individual heterozygosity during the last 200 years [8]. Reshaping of the horse phenotype in modern studbooks for locomotion, speed and morpho-anatomy plays a major role in this and has resulted in a high frequency (one-third of the population) of vertebral variations in the caudal cervical spine in warmbloods and thoroughbreds [8, 35, 67]. The clinical impact of these equine caudal cervical vertebral variations [75], or for that matter thoracolumbar vertebral variations in screw-tailed dogs [5, 45] is not evident. Recordings of possible associated side-effects on body conformation plan and life expectancy barely exist in horses or companion animals [10]. However, biomechanical alterations and possible associated degenerative disc disease have been mentioned [35, 44, 73, 74].

Only recently lumbar transitional vertebrae have been related to degenerative joint disease and degenerative lumbosacral stenosis in humans [51, 52], whereas in dogs that relationship had been recognized for over a decade [6]. This example highlights the role translational value of veterinary data on vertebral congenital malformations in domestic animals for human medicine.

In conclusion, vertebral patterning in domestic animals is subject to a high diversity in some breeds, except for the cervical region where severe evolutionary constraints set the rule of seven vertebrae. At present, limited knowledge hampers unravelling of

the in-depth effects of vertebral variation and malformation due to current breeding practices in domesticated animals and further research is hence warranted. There is potential translational value of findings on the subject in the veterinary patient to the human patient with respect to progress in diagnosis, treatment and discovering the genetic background.

REFERENCES

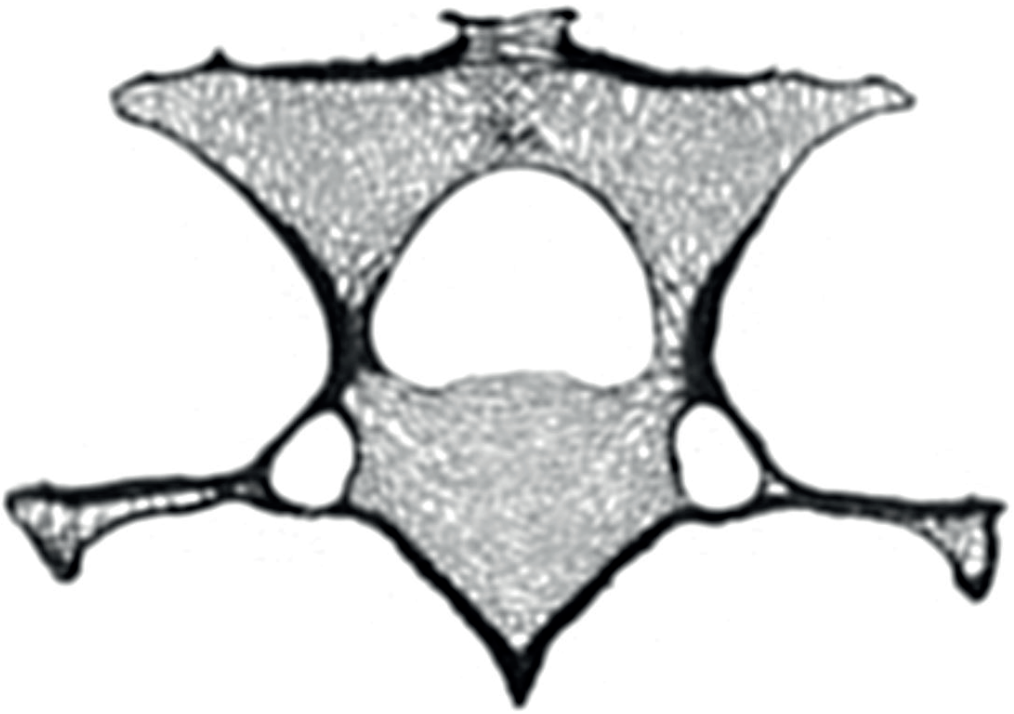
1. Hedequist, D. and Emans, J. (2004) Congenital scoliosis. *J. Am. Acad. Orthop. Surg.* **12**, 266-275.
2. Chaturvedi, A., Klionsky, N.B., Nadarajah, U., Chaturvedi, A. and Meyers, S.P. (2018) Malformed vertebrae: a clinical and imaging review. *Insights Imaging.* **9**, 343-355.
3. Galis, F. (1999) Why do almost all mammals have seven cervical vertebrae? Developmental constraints, Hox genes, and cancer. *J. Exp. Zool.* **285**, 19-26.
4. Newitt, A.L., German, A.J. and Barr, F.J. (2009) Lumbosacral transitional vertebrae in cats and their effects on morphology of adjacent joints. *J. Feline Med. Surg.* **11**, 941-947.
5. Ryan, R., Gutierrez-Quintana, R., Ter Haar, G. and De Decker, S. (2017) Prevalence of thoracic vertebral malformations in French bulldogs, Pugs and English bulldogs with and without associated neurological deficits. *Vet. J.* **221**, 25-29.
6. Fluckiger, M.A., Damur-Djuric, N., Hassig, M., Morgan, J.P. and Steffen, F. (2006) A lumbosacral transitional vertebra in the dog predisposes to cauda equina syndrome. *Vet. Radiol. Ultrasound.* **47**, 39-44.
7. Huang, J., Zhang, M., Ye, R., Ma, Y. and Lei, C. (2017) Effects of increased vertebral number on carcass weight in PIC pigs. *Anim. Sci. J.* **88**, 2057-2062.
8. Fages, A., Hanghoj, K., Khan, N., Gaunitz, C., Seguin-Orlando, A., et.al. (2019) Tracking Five Millennia of Horse Management with Extensive Ancient Genome Time Series. *Cell.* **177**, 1419-1435.e31.
9. Asadollahpour Nanaei, H., Ayatollahi Mehrgardi, A. and Esmailzadeh, A. (2019) Comparative population genomics unveils candidate genes for athletic performance in Hanoverians. *Genome.* **62**, 279-285.
10. Brocal, J., De Decker, S., Jose-Lopez, R., Manzanilla, E.G., Penderis, J., Stalin, C., Bertram, S., Schoenebeck, J.J., Rusbridge, C., Fitzpatrick, N. and Gutierrez-Quintana, R. (2018) C7 vertebra homeotic transformation in domestic dogs - are Pug dogs breaking mammalian evolutionary constraints? *J. Anat.* **233**, 255-265.
11. Pollard, R.E., Koehne, A.L., Peterson, C.B. and Lyons, L.A. (2015) Japanese Bobtail: vertebral morphology and genetic characterization of an established cat breed. *J. Feline Med. Surg.* **17**, 719-726.
12. Metzger, J., Rau, J., Naccache, F., Bas Conn, L., Lindgren, G. and Distl, O. (2018) Genome data uncover four synergistic key regulators for extremely small body size in horses. *BMC Genomics.* **19**, 492-018-4877-5.
13. Mansour, T.A., Lucot, K., Konopelski, S.E., Dickinson, P.J., Sturges, B.K., et.al. (2018) Whole genome variant association across 100 dogs identifies a frame shift mutation in DISHEVELLED 2 which contributes to Robinow-like syndrome in Bulldogs and related screw tail dog breeds. *PLoS Genet.* <https://doi.org/10.1371/journal.pgen.1007850>
14. Clothier, J. (2016) All you need to know about the hidden C6-C7 malformation that is bringing horses down. <http://TheHorsesBack.com> at **02-07-2019**,
15. Godfrey, R. and Godfrey, D. (2011) French Bulldog- Hemivertebrae. *Genetic Welfare Problems of Companion Animals An information resource for prospective pet owners.* **2019**, <https://www.ufaw.org.uk/dogs/french-bulldog-hemivertebrae>.
16. Milne, E.G. (2018) Time to stop accepting 'normal for the breed'. *Vet. Rec.* **183**, 630.
17. Thompson, K., Moore, S., Tang, S., Wiet, M. and Purmessur, D. (2018) The chondrodystrophic dog: A clinically relevant intermediate-sized animal model for the study of intervertebral disc-associated spinal pain. *JOR Spine.* Doi: 10.1002/jsp2.1011
18. Gilbert, S.C. and Barresi, M.J. (2017) Paraxial mesoderm; The Somites and Their Derivatives. In: *Developmental Biology.* 11th edn., Anonymous Oxford University Press Inc.
19. Scaal, M. (2016) Early development of the vertebral column. *Semin. Cell Dev. Biol.* **49**, 83-91.

20. Burke, A.C. (2000) Hox genes and the global patterning of the somitic mesoderm. *Curr. Top. Dev. Biol.* **47**, 155-181.
21. Nowicki, J.L. and Burke, A.C. (2000) Hox genes and morphological identity: axial versus lateral patterning in the vertebrate mesoderm. *Development.* **127**, 4265-4275.
22. Bordbari, M.H., Penedo, M.C.T., Aleman, M., Valberg, S.J., Mickelson, J. and Finno, C.J. (2017) Deletion of 2.7 kb near HOXD3 in an Arabian horse with occipitoatlantoaxial malformation. *Anim. Genet.* **48**, 287-294.
23. Chen, J.W., Zahid, S., Shilts, M.H., Weaver, S.J., Leskowitz, R.M., Habbsa, S., Aronowitz, D., Rokins, K.P., Chang, Y., Pinnella, Z., Holloway, L. and Mansfield, J.H. (2013) Hoxa-5 acts in segmented somites to regulate cervical vertebral morphology. *Mech. Dev.* **130**, 226-240.
24. Cox, M.K. and Serra, A. (2014) Development of the Intervertebral Disc. In: *The Intervertebral Disc*. Eds I. Shapiro and M. Risbud. Springer, Vienna
25. Narita, Y. and Kuratani, S. (2005) Evolution of the vertebral formulae in mammals: a perspective on developmental constraints. *J. Exp. Zool. B. Mol. Dev. Evol.* **304**, 91-106.
26. Buchholtz, E.A. and Stepien, C.C. (2009) Anatomical transformation in mammals: developmental origin of aberrant cervical anatomy in tree sloths. *Evol. Dev.* **11**, 69-79.
27. Proks, P., Stehlik, L., Paninarova, M., Irova, K., Hauptman, K. and Jekl, V. (2014) Congenital Abnormalities of the Vertebral Column in Ferrets. *Vet. Radiol. Ultrasound.* **56**, 117-123
28. Newitt, A., German, A.J. and Barr, F.J. (2008) Congenital abnormalities of the feline vertebral column. *Vet. Radiol. Ultrasound.* **49**, 35-41.
29. Haussler, K.K., Stover, S.M. and Willits, N.H. (1997) Developmental variation in lumbosacropelvic anatomy of thoroughbred racehorses. *Am. J. Vet. Res.* **58**, 1083-1091.
30. Stecher, R.M. (1962) Anatomical Variations of the Spine in the Horse. *J. Mamm.* **43**, 205-219.
31. Westworth, D.R. and Sturges, B.K. (2010) Congenital spinal malformations in small animals. *Vet. Clin. North Am. Small Anim. Pract.* **40**, 951-981.
32. Donaldson, C.L., Lambe, N.R., Maltin, C.A., Knott, S. and Bunger, L. (2013) Between- and within-breed variations of spine characteristics in sheep. *J. Anim. Sci.* **91**, 995-1004.
33. Borchers, N., Reinsch, N. and Kalm, E. (2004) The number of ribs and vertebrae in a Piétrain cross: Variation, heritability and effects on performance traits. *J. Anim. Breed. Gen.* **121**, 392-403.
34. Zhang, X., Li, C., Li, X., Liu, Z., Ni, W., Hazi, W., Cao, Y., Yao, Y., Wang, D., Hou, X. and Hu, S. (2018) Expression profiles of MicroRNAs from multiple lumbar spine in sheep. *Gene.* **678**, 105-114.
35. May-Davis, S. (2014) The Occurrence of a Congenital Malformation in the Sixth and Seventh Cervical Vertebrae Predominantly Observed in Thoroughbred Horses. *Journal of Equine Veterinary Science.* **34**, 1313-1317.
36. Rusbridge, C., McFadyen, A.K. and Knowler, S.P. (2019) Behavioral and clinical signs of Chiari-like malformation-associated pain and syringomyelia in Cavalier King Charles spaniels. *J. Vet. Intern. Med.* doi.org/10.1111/jvim.15552
37. Dewey, C.W., Marino, D.J. and Loughin, C.A. (2013) Craniocervical junction abnormalities in dogs. *N. Z. Vet. J.* **61**, 202-211.
38. Fernandes, R., Fitzpatrick, N., Rusbridge, C., Rose, J. and Driver, C.J. (2019) Cervical vertebral malformations in 9 dogs: radiological findings, treatment options and outcomes. *Ir. Vet. J.* **72**, 2-019-0141-9. eCollection 2019.
39. Cantalamessa, A., Martin, S., Marchegiani, A., Fruganti, A., Dini, F. and Tambella, A.M. (2017) Bilateral cervical ribs in a mixed breed dog. *J. Vet. Med. Sci.* **79**, 1120-1124.

40. Wijnrocx, K., Van Bruggen, L.W.L., Eggelmeijer, W., Noorman, E., Jacques, A., Buys, N., Janssens, S. and Mandigers, P.J.J. (2017) Twelve years of chiari-like malformation and syringomyelia scanning in Cavalier King Charles Spaniels in the Netherlands: Towards a more precise phenotype. *PLoS One*. **12**, e0184893.
41. Ryan, R., Gutierrez-Quintana, R., Haar, G.T. and De Decker, S. (2019) Relationship between breed, hemivertebra subtype, and kyphosis in apparently neurologically normal French Bulldogs, English Bulldogs, and Pugs. *Am. J. Vet. Res.* **80**, 189-194.
42. Besalti, O., Ozak, A., Pekcan, Z. and Eminaga, S. (2005) Nasca classification of hemivertebra in five dogs. *Ir. Vet. J.* **58**, 688-690.
43. Gutierrez-Quintana, R., Guevar, J., Stalin, C., Faller, K., Yeaman, C. and Penderis, J. (2014) A proposed radiographic classification scheme for congenital thoracic vertebral malformations in brachycephalic "screw-tailed" dog breeds. *Vet. Radiol. Ultrasound*. **55**, 585-591.
44. Inglez de Souza, M.C.C.M., Ryan, R., Ter Haar, G., Packer, R.M.A., Volk, H.A. and De Decker, S. (2018) Evaluation of the influence of kyphosis and scoliosis on intervertebral disc extrusion in French bulldogs. *BMC Vet. Res.* **14**, 5-017-1316-9.
45. Rohdin, C., Haggstrom, J., Ljungvall, I., Nyman Lee, H., De Decker, S., Bertram, S., Lindblad-Toh, K. and Hultin Jaderlund, K. (2018) Presence of thoracic and lumbar vertebral malformations in pugs with and without chronic neurological deficits. *Vet. J.* **241**, 24-30.
46. Patton, M.A. and Afzal, A.R. (2002) Robinow syndrome. *J. Med. Genet.* **39**, 305-310.
47. Bertram, S., Ter Haar, G. and De Decker, S. (2018) Caudal articular process dysplasia of thoracic vertebrae in neurologically normal French bulldogs, English bulldogs, and Pugs: Prevalence and characteristics. *Vet. Radiol. Ultrasound*. **59**, 396-404.
48. Driver, C.J., Rose, J., Tauro, A., Fernandes, R. and Rusbridge, C. (2019) Magnetic resonance image findings in pug dogs with thoracolumbar myelopathy and concurrent caudal articular process dysplasia. *BMC Vet. Res.* **15**, 182-019-1866-0.
49. Damur-Djuric, N., Steffen, F., Hassig, M., Morgan, J.P. and Fluckiger, M.A. (2006) Lumbosacral transitional vertebrae in dogs: classification, prevalence, and association with sacroiliac morphology. *Vet. Radiol. Ultrasound*. **47**, 32-38.
50. Fluckiger, M.A., Steffen, F., Hassig, M. and Morgan, J.P. (2017) Asymmetrical lumbosacral transitional vertebrae in dogs may promote asymmetrical hip joint development. *Vet. Comp. Orthop. Traumatol.* **30**, 137-142.
51. Abbas, J., Peled, N., Hershkovitz, I. and Hamoud, K. (2019) Is Lumbosacral Transitional Vertebra Associated with Degenerative Lumbar Spinal Stenosis? *Biomed. Res. Int.* **2019**, 3871819.
52. Tucker, B.J., Weinberg, D.S. and Liu, R.W. (2019) Lumbosacral Transitional Vertebrae: A Cadaveric Investigation of Prevalence and Relation to Lumbar Degenerative Disease. *Clin. Spine Surg.* **32**, 330-334
53. Breit, S. and Kunzel, W. (2002) The diameter of the vertebral canal in dogs in cases of lumbosacral transitional vertebrae or numerical vertebral variations. *Anat. Embryol. (Berl)*. **205**, 125-133.
54. Moeser, C.F. and Wade, C.M. (2017) Relationship between transitional lumbosacral vertebrae and eight lumbar vertebrae in a breeding colony of Labrador Retrievers and Labrador Crosses. *Aust. Vet. J.* **95**, 33-36.
55. Baines, E.A., Grandage, J., Herrtage, M.E. and Baines, S.J. (2009) Radiographic definition of the anticlinal vertebra in the dog. *Vet. Radiol. Ultrasound*. **50**, 69-73.
56. Paninarova, M., Stehlik, L., Proks, P. and Vignoli, M. (2016) Congenital and acquired anomalies of the caudal vertebrae in dogs: Radiographic classification and prevalence evaluation. *Acta Vet. Hung.* **64**, 330-339.
57. Brocal, J., De Decker, S., Jose-Lopez, R., Guevar, J., Ortega, M., Parkin, T., Ter Haar, G. and Gutierrez-Quintana, R. (2018) Evaluation of radiography as a screening method for detection and characterisation of congenital vertebral malformations in dogs. *Vet. Rec.* **182**, 573.

58. Deforest, M.E. and Basrur, P.K. (1979) Malformations and the Manx syndrome in cats. *Can. Vet. J.* **20**, 304-314.
59. Jaggy, A., Hutto, V.L., Roberts, R.E. and Oliver, J.E. (1991) Occipitoatlantoaxial malformation with atlantoaxial subluxation in a cat. *Journal Small Anim. Pract.* **7**, 366-372.
60. Dean, B.L., Smith, C., Liebel, F.X. and Warren-Smith, C. (2019) Multiple Cervical Vertebral Malformations in a 21-week-old Kitten. *Journal of the American Animal Hospital Association.* **55 (5)**, 256-260.
61. Harris, G., Ball, J. and De Decker, S. (2019) Lumbosacral transitional vertebrae in cats and its relationship to lumbosacral vertebral canal stenosis. *J. Feline Med. Surg.* **21**, 286-292.
62. Kromik, A., Kusenda, M., Tipold, A., Stein, V.M., Rehage, J., Weikard, R. and Kuhn, C. (2015) Vertebral and spinal dysplasia: A novel dominantly inherited congenital defect in Holstein cattle. *Vet. J.* **204**, 287-292.
63. Agerholm, J.S., Bendixen, C., Arnbjerg, J. and Andersen, O. (2004) Morphological variation of "complex vertebral malformation" in Holstein calves. *J. Vet. Diagn. Invest.* **16**, 548-553.
64. Peperkamp, N.H., Luttkiholt, S.J., Dijkman, R., Vos, J.H., Junker, K., Greijdenus, S., Roumen, M.P., van Garderen, E., Meertens, N., van Maanen, C., Lievaart, K., van Wuyckhuise, L. and Wouda, W. (2015) Ovine and Bovine Congenital Abnormalities Associated With Intrauterine Infection With Schmallenberg Virus. *Vet. Pathol.* **52**, 1057-1066.
65. Watson, A.G. and Mayhew, I.G. (1986) Familial congenital occipitoatlantoaxial malformation (OAM) in the Arabian horse. *Spine (Phila Pa. 1976).* **11**, 334-339.
66. Bell, S., Detweiler, D., Benak, J. and Pusterla, N. (2007) What is your diagnosis? Occipitoatlantoaxial malformation. *J. Am. Vet. Med. Assoc.* **231**, 1033-1034.
67. Veraa, S., Bergmann, W., van den Belt, A.J., Wijnberg, I. and Back, W. (2016) Ex Vivo Computed Tomographic Evaluation of Morphology Variations in Equine Cervical Vertebrae. *Vet. Radiol. Ultrasound.* **57**, 482-488.
68. Brünisholz, H.P., Wildhaber, N., Hoey, S., Ruetten, M., Boos, A. and Kümmerle, J.M. (2019) Congenital occipitoatlantoaxial malformation in a Warmblood mare. *Equine Vet. Ed.* **31 (5)**, 242-247.
69. May-Davis, S. (2017) Congenital Malformations of the First Sternal Rib. *J. Eq. Vet. Sci.* **49**, 92-100.
70. Audigie, F., Rovel, T., Coudry, V., Bertoni, L., Jacquet, S., Danjon, C. and Denoix, J.M. (2017) Malformations of the first ribs in equine sports and racehorses. *Vet. Radiol. Ultrasound.* **57**, 711-712.
71. Mayhew, I.G., Watson, A.G. and Heissan, J.A. (1978) Congenital occipitoatlantoaxial malformations in the horse. *Equine Vet. J.* **10**, 103-113.
72. Bradley, O.C. (1901) On a case of rudimentary first thoracic rib in a horse. *J Anat Physiol.* **36**, 54-62.
73. May-Davis, S. and Walker, C. (2015) Variations and Implications of the Gross Morphology in the *Longus colli* Muscle in Thoroughbred and Thoroughbred Derivative Horses Presenting With a Congenital Malformation of the Sixth and Seventh Cervical Vertebrae. *J. Eq. Vet. Sci.* **35**, 560-568.
74. DeRouen, A., Spriet, M. and Aleman, M. (2016) Prevalence of Anatomical Variation of the Sixth Cervical Vertebra and Association with Vertebral Canal Stenosis and Articular Process Osteoarthritis in the Horse. *Vet. Radiol. Ultrasound.* **57**, 253-258.
75. Veraa, S., de Graaf, K., Wijnberg, I.D., Back, W., Vernooij, H., Nielen, M. and van den Belt, A.M. (2019) Caudal cervical vertebral morphological variation is not associated with clinical signs in Warmblood horses. *Equine Vet. J.* doi.org/10.1111/evj.13140
76. Gorgas, D., Kircher, P., Doherr, M.G., Ueltschi, G. and Lang, J. (2007) Radiographic technique and anatomy of the equine sacroiliac region. *Vet. Radiol. Ultrasound.* **48**, 501-506.
77. Bennett, D.K. and Hoffmann, R.S. (1999) *Equus caballus*. *Mammalian Species.* **628**, 1-14.
78. Schumacher, R., Mai, A. and Gutjahr, P. (1992) Association of rib anomalies and malignancy in childhood. *Eur. J. Pediatr.* **151**, 432-434.

79. Reumer, J.W., Ten Broek, C.M. and Galis, F. (2014) Extraordinary incidence of cervical ribs indicates vulnerable condition in Late Pleistocene mammoths. *PeerJ.* **2**, e318.
80. Galis, F. (1999) On the homology of structures and Hox genes: the vertebral column. *Novartis Found. Symp.* **222**, 80-94.
81. Galis, F., Van Dooren, T.J., Feuth, J.D., Metz, J.A., Witkam, A., Ruinard, S., Steigenga, M.J. and Wijnaendts, L.C. (2006) Extreme selection in humans against homeotic transformations of cervical vertebrae. *Evolution.* **60**, 2643-2654.



3

Ex Vivo Computed Tomographic Evaluation of Morphology Variations in Equine Cervical Vertebrae.

Stefanie Veraa^a, Wilhelmina Bergmann^b, Antoon-Jan M. van den Belt^a, Inge D. Wijnberg^c, Willem Back^{c,e}

^a Division of Diagnostic Imaging, Faculty of Veterinary Medicine, Utrecht University, Yalelaan 110, NL-3584 CM Utrecht, The Netherlands.

^bDepartment of Pathobiology, Faculty of Veterinary Medicine, Utrecht University, Yalelaan 1, NL-3584 CL, The Netherlands

^c Department of Equine Sciences, Faculty of Veterinary Medicine, Utrecht University, Yalelaan 114, NL-3584 CM Utrecht, The Netherlands

^d Department of Farm Animal Health, Yalelaan 7, NL-3584 CL, The Netherlands

^e Department of Surgery and Anaesthesiology of Domestic Animals, Faculty of Veterinary Medicine, Ghent University, Salisburylaan 133, B-9820 Merelbeke, Belgium

Veterinary Radiology and Ultrasound, 2016, 57 (5), 482-8

ABSTRACT

Diagnostic imaging is one of the pillars in the clinical workup of horses with clinical signs of cervical spinal disease. An improved awareness of morphologic variations in equine cervical vertebrae would be helpful for interpreting findings. The aim of this anatomic study was to describe CT variations in left–right symmetry and morphology of the cervical and cervicothoracic vertebrae in a sample of horses. Postmortem CT examinations of the cervical spine for horses without congenital growth disorders were prospectively and retrospectively recruited. A total of 78 horses (27 foals, 51 mature horses) were evaluated. Twenty-six horses (33.3%) had homologous changes in which a transposition of the caudal part of the transverse process (caudal ventral tubercle) of C6 toward the ventral aspect of the transverse process of C7 was present ($n = 10$ bilateral, $n = 12$ unilateral left-sided, $n = 4$ unilateral right-sided). There was one horse with occipito-atlantal malformation, two horses with rudimentary first ribs bilaterally, and one horse with bilateral transverse processes at Th1, representing homeotic (transitional) vertebral changes. Chi-square tests identified no significant differences in the number of conformational variations between the group of mature horses with or without clinical signs ($P = 0.81$) or between the group of mature horses and the group of foals ($P = 0.72$). Findings indicated that, in this sample of horses, the most frequently identified variations were homologous variations (transposition of the caudal part of the transverse process of C6–C7) in the caudal equine cervical vertebral column. Homeotic (transitional) variations at the cervicothoracic vertebral column were less common.

Keywords: cervical vertebral column, homeotic, homologous, horse, transitional vertebra

INTRODUCTION

Diagnostic imaging is an essential tool in the clinical workup of horses with signs that may be related to the cervical spine such as spinal ataxia, decreased mobility, and lameness [1-4]. It is therefore important to appreciate the possibility of anatomic vertebral variations when interpreting diagnostic images of horses. The deviation from traditional vertebral patterning can be a change in numbers in one section with preservation of total vertebral count (*homeotic variation*) such as seen in transitional vertebrae, but may also consist of a change in the total number of vertebrae (*meristic variations*). Changes in merely one subunit with preservation of the traditional number and identity of the vertebrae can occur when only size and/or shape of vertebrae are altered (*homologous variations*), [5] an example is the transposition of the caudal part of C6–C7 in horses [6]. Anatomical variations of the equine cervical vertebral column have been reported in the early 1900s [7,8]. The prevalence of cervical anatomical variations in larger populations has recently been described in the literature [6, 9, 10]. There is one retrospective study based on radiographic examinations in which anatomical variations of the spinous and transverse processes in the caudal cervical vertebrae and the first thoracic vertebrae were found in, respectively, 24.9% and 13.3% of the horses [10]. An incidence of 38% of congenital malformations of the sixth and seventh vertebrae was recorded during dissection in a thoroughbred-based population of horses in another study [6] and associated variations in longus colli muscle attachment at this level [11]. A prevalence of 24% anomalous C6 was recorded in a recent study with a predilection for Warmblood breeds as these accounted for almost 80% of the affected and included horses [12]. Advanced imaging modalities such as computed tomography (CT) [13-15] and magnetic resonance imaging (MRI) [13-17] are increasingly being applied in the evaluation of horses with suspected cervical spinal disease. However, little published information is currently available on CT and MRI characteristics of equine cervical vertebral morphologic variations. The purpose of the present study was to assess the presence and the morphological appearance of anatomical variations of the cervical vertebral column and cervicothoracic junction using *ex vivo* CT in a group of horses. We hypothesized that, given the reported prevalence of 13.3% using radiography and 38% in dissected thoroughbreds, the prevalence of these vertebral variations in the equine vertebral column as diagnosed by CT would be between 13% and 38% with the anatomy generally being as described in the classic anatomical references [18,19]. We also hypothesized that the prevalence of anatomical variations would be equal in the groups of horses with and without clinical signs related to the cervical column.

MATERIAL AND METHODS

Horses

The study was an anatomic design. Equine cadaver necks were prospectively collected for CT examination after owner consent or retrospectively retrieved from horse cadavers included in a different study [20]. All available ex vivo CT examinations of the cervical vertebral column during the period of January 2009 to July 2014 in the Picture Archiving and Communication System (PACS) of the Division of Diagnostic Imaging, Faculty of Veterinary Medicine of Utrecht University were considered for inclusion. Horses were excluded if they had a known congenital growth disorder or if there was incomplete evaluation of the cervical vertebral column in the scan. Medical records for included horses were retrieved and available clinical data (breed, age, clinical signs) were recorded.

Specimen Collection and CT Scanning Techniques

The cervical vertebral column was disarticulated at the level of thoracic vertebrae (Th) 2–3, the head disarticulated (when possible) at the occipito-atlantal junction and a large part of the soft tissues surrounding the vertebral column was removed in horses before CT examination at the Department of Pathobiology of the Faculty of Veterinary Medicine, Utrecht University by a board-certified pathologist (W.B.). Dissection was not performed in eight foals. In one horse, dissection was not possible at the occipito-atlantal junction and the head remained attached. Computed tomography scans were made from the first cervical vertebra (C1) to the second thoracic vertebra (Th2). All CT examinations were performed with a single slice CT scanner (Philips Secura, Eindhoven, The Netherlands) using the following scanning protocol: scanning parameters 100 kVp, 220 mA, 0.7 s tube rotation time and 2- to 3-mm thick contiguous slices. A bone algorithm was applied. A standard matrix of 512 × 512 pixels was used. The field of view (FOV) varied between the examinations depending on the size of the cadaver neck.

Data Analysis

The CT images of the cervical vertebrae were evaluated by a board-certified veterinary radiologist (S.V.), who was not aware of the in vivo clinical status of the horse at that time. Images were retrieved from the available PACS system (Impax, version 6.5.2.657, Agfa Healthcare N.V., Mortsels, Belgium). Multiplanar reconstruction (MPR) and 3D volume rendering of the vertebrae were performed. Left-right symmetry and anatomy (such as vertebral body, lamina, pedicles, transverse processes, spinous process, and presence of intervertebral disc space) of the cervical vertebrae were evaluated. The

vertebral shape and conformation were compared to the images and descriptions of the standard anatomical reference works [18,19]. Variations were considered homeotic if they were positioned only at a section junction (head-cervical and cervical-thoracic) and the vertebra had the characteristics of a transitional vertebra. Variations were considered homologous if the changes were not positioned at a section junction and merely changed the shape of the vertebra without true characteristics of a transitional vertebra.

The horses were assigned to two groups according to the recorded clinical status: without clinical signs or with clinical signs related to the cervical vertebral column. Clinical signs related to the cervical vertebral column recorded were, among others, pain, reduced motion, or spinal ataxia. Clinical examinations were performed by a board-certified veterinary surgeon (W.B.) or board-certified veterinary internist (I.W.). Prevalences of anatomical variations in the groups of mature horses with vs. without clinical signs and the groups of mature horses vs. foals were compared using a chi-square test (IBM SPSS Statistics version 22, IBM, New York). Statistical analyses were completed by the first author (S.V.) and significance was determined using $P < 0.05$.

RESULTS

Horses

Included in this study were 78 horses (65 Dutch Warmblood horses, two Friesians, two Zangersheide Studbook horses, two cross-breed horses, two Westfaler, one Arabian, one Oldenburger, one Trotter, one New Forest Pony, one Appaloosa) including 29 mares, 17 stallions, and 32 geldings; 51 mature horses (median age 6.9 years, range 2.2– 22 years); and 27 foals (median age 7 days, range 0–150 days). Thirty mature horses had clinical signs related to cervical vertebral column pathology (such as spinal ataxia or pain) and 21 died of or were euthanized for reasons unrelated to cervical vertebral column pathology (such as lameness due to tendinitis or joint pathology of the limbs). The 27 foals died of or were euthanized for reasons unrelated to cervical vertebral column pathology (such as respiratory distress, viral or bacterial septicemia, and gastric rupture).

The cervical vertebral column of all equine cadavers was examined within 24 h after death. The cervical vertebral columns of 51 of the 78 horses in this study were considered symmetric and conformed to the description in the anatomical references (Figs. 1A, 2A, and 3A). In 27 horses, asymmetry and/or variations of the standard anatomy were detected (Table 1).

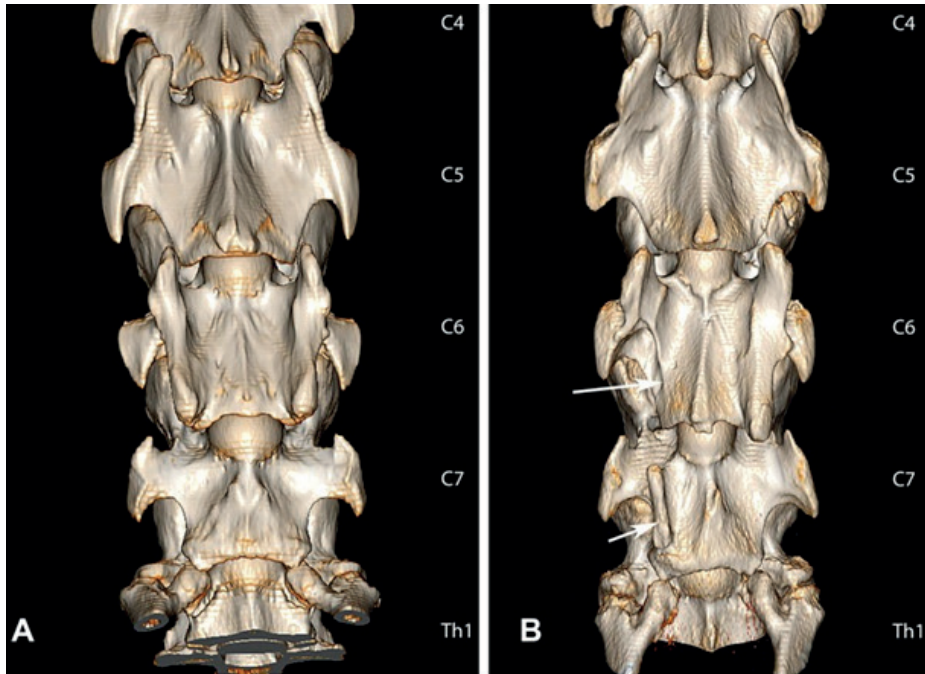


Fig. 1. 3D computed tomography (CT) reconstructions of the caudal cervical vertebral column, ventral aspect. (A) Normal vertebral anatomy, (B) unilateral right-sided homologous vertebral changes at the level of C6 and C7. The ventral part of the transverse process of C6 is not present (long arrow), however, a ventral protuberance is present at the ventral aspect of the transverse process of C7 (short arrow).

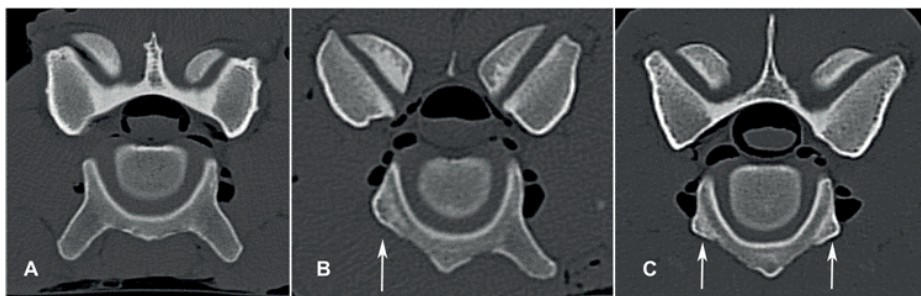


Fig. 2. Transverse CT images at the caudal aspect of C6; right side is at the left side of the image, dorsal is at the top of the image. (A) Normal vertebral anatomy (arrow); (B) unilateral right-sided absence of the ventral part of the transverse process; (C) bilateral absence of the ventral part of the transverse process (arrows).

Table 1. Numbers of Foals and Mature Horses with Normal and Abnormal Cervical

	Foals		Mature horses	
	Normal anatomy	Aberrant anatomy	Normal anatomy	Aberrant anatomy
Total	19	8	32	19
Breeds	14 DW*, 2 ZS†, 1 Westfaler, 1 Arabian, 1 Cross-breed	8 DW*	29 DW*, 1 Friesian, 1 New Forest Pony, 1 Appaloosa,	14 DW*, 1 Oldenburger, 1 Westfalen, 1 Trotter, 1 Friesian, 1 Cross-breed
Occipito-atlantal fusion		0		1
Bilateral changes C6-7		2		8
Unilateral left-sided changes C6-C7		6		6
Unilateral right-sided changes C6-C7		0		4
Bilateral vertebral foramen C7		1		2
Unilateral left-sided vertebral foramen C7		4		4
Unilateral right-sided vertebral foramen C7		0		3
Rudimentary ribs bilaterally Th1		0		2
Transverse processes bilaterally Th1		0		1
Absent fovea costalis		0		7

*DW= Dutch Warmblood; †ZS=Zangersheide Studbook

Homeotic or Transitional Variations

Homeotic or transitional vertebral variations were seen in four horses. Asymmetric occipito-atlantal fusion, without changes in shape and/or position of the axis, was seen in one (Dutch Warmblood) horse. The presence of bilateral rudimentary ribs at the level of Th1 was noted in two (Dutch Warmblood) horses with concurrent unilateral right-sided and bilateral transverse process changes in C6 and C7, respectively (Fig. 4A and B). In one (Dutch Warmblood) horse, ribs were absent at Th1 and replaced by transverse processes with a shallow split-like indentation in the lateral aspect (Fig. 4C). This horse also had bilateral changes at C6 and C7. No fusion of vertebrae with concurrent loss of intervertebral disc space was seen in any of the horses.

Homologous Variations

In 26 horses (21 Dutch Warmbloods, one Oldenburger, one Westfaler, one Trotter, one Friesian, and one cross-breed) homologous variations were seen. The caudoventral part of the transverse process (caudal-ventral tubercle) was partially ($n = 2$) or completely ($n = 24$) absent unilaterally ($n = 12$, left-sided; $n = 4$, right-sided) or bilaterally ($n = 10$; Figs. 1B and 2B and C). Absence of the ventral part of the transverse process of C6 was associated in all horses with a protuberance at the ventral aspect of the transverse process of C7. Therefore, a unilateral ($n = 12$, left-sided; $n = 4$, right-sided) or bilateral ($n = 10$) protuberance was present (Figs. 1B and 3B and C). A vertebral foramen was present in the base of four left-sided and six bilateral C7 transverse process ventral protuberances (Fig. 3B).

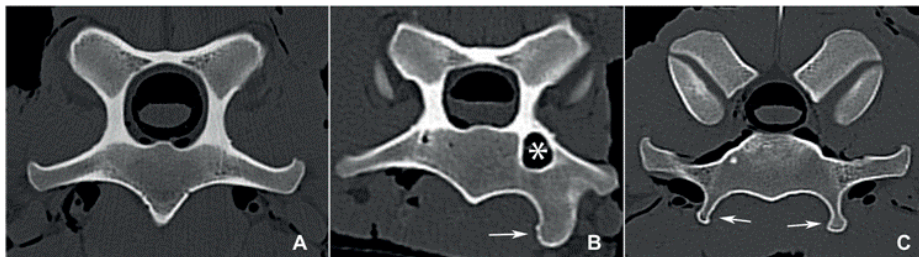


Fig. 3. Transverse CT images at the level of C7; right side is at the left side of the image, dorsal is at the top of the image. (A) Normal vertebral anatomy; (B) unilateral left-sided presence of a ventral protuberance at the transverse process of C7 (arrow) in concurrence with a vertebral foramen at the base of the transverse process (asterisk); (C) bilateral presence of a ventral protuberance at the transverse process of C7 (arrows). This image is slightly more caudally positioned than the images (A) and (B) to allow optimal visualization of the protuberances.

The absence of a proper fovea costalis in the caudo-ventral endplate of C7 (Fig. 5) was detected bilaterally in seven horses, which all had bilateral transverse process changes in C6 and C7. Presence of a spinous process at C7 was seen in all adult horses and in 24 foals. In three foals (0 days of age) no spinous process could be seen yet. The spinous processes were ranging in height from 23.6 to 54.8 mm with a median height of 40 mm.

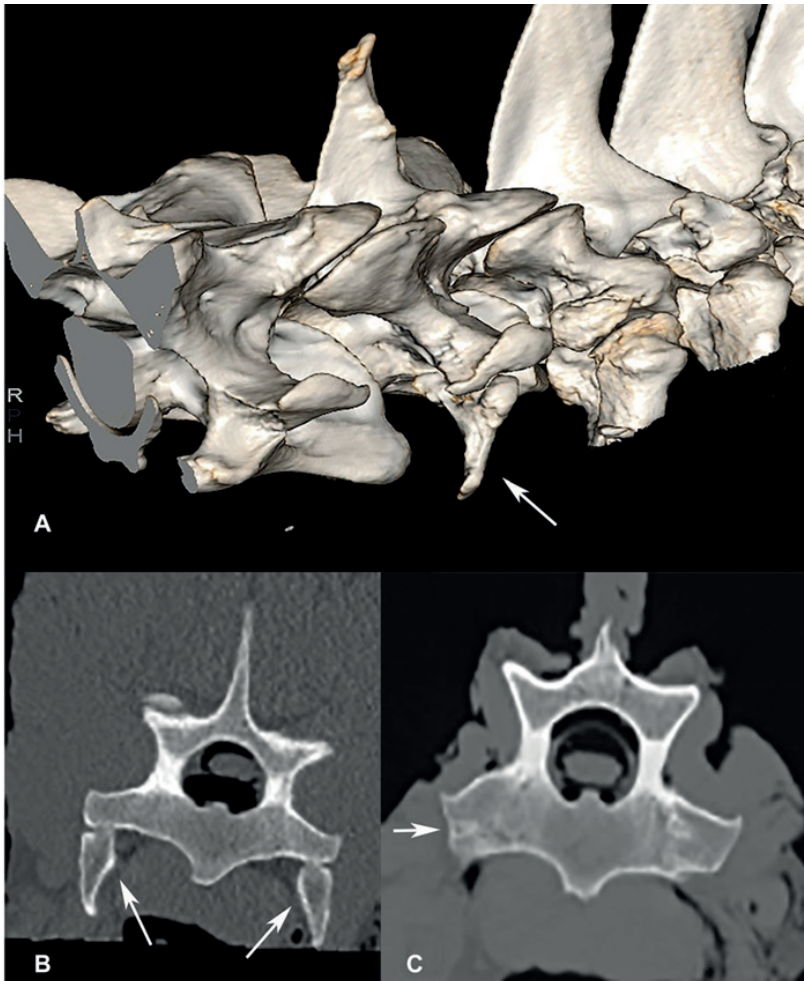


Fig. 4. (A) 3D CT reconstruction of the caudal cervical vertebral column, left craniolateral view. Note the presence of a very short and small first (rudimentary) rib at the ventral aspect of the first thoracic vertebra. (B) Transverse CT image at the level of Th1. Right side is at the left side of the image, dorsal is at the top of the image. Rudimentary ribs are present bilaterally. (C) Transversely reconstructed CT image at the level of Th1. Right side is at the left side of the image; dorsal is at the top of the image. No ribs are present; bilateral transverse processes with a small slit-like opening are visible.

The conformational variations in the caudal cervical vertebral column were seen in 18 of 51 mature horses (35.3%), 11 of 30 (36.7%) mature horses with clinical signs related to the cervical vertebral column and in seven of 21 mature horses (33.3%) without clinical signs related to the cervical vertebral column. The changes were bilateral in six, left-sided in three and right-sided in two of the 11 mature horses that were presented

with clinical signs related to the cervical vertebral column. No significant difference in number of conformational variations was noted between the group of mature horses with or without clinical signs (chi-square test, $P=0.81$).

Eight of 27 foals (29.6%) had conformational variations. No significant difference in number of conformational variations was noted between the group of mature horses and the group of foals (chi-square test, $P=0.72$).

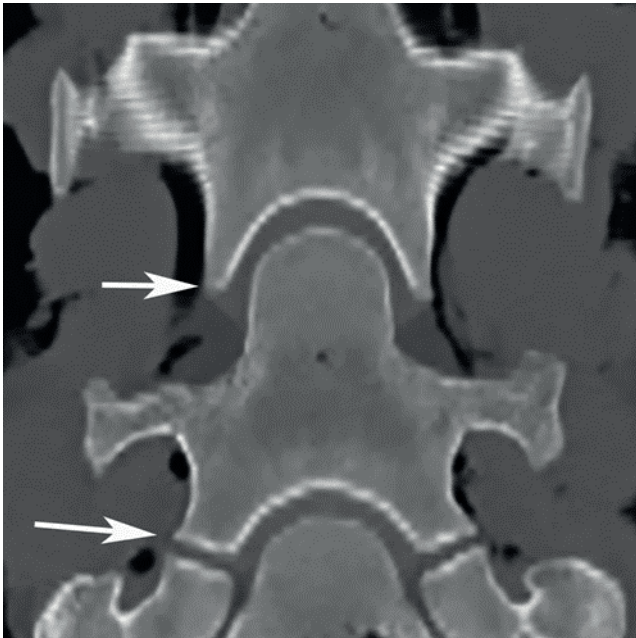


Fig. 5. Dorsal plane reconstructed CT image at the level of C7–Th1 and Th1–Th2, right side is at the left side; cranial is at the top of the image. No proper fovea costalis is present at the caudo-ventral aspect of the vertebral body of C7 due to the absence of ribs at Th1 (arrow). Note the appearance of a fovea costalis at the caudo-ventral aspect of Th1 bilaterally (arrow).

DISCUSSION

In the present study, homeotic and/or homologous variations of the cervical vertebral column were found in 34.6% (27 of 78) horses, of which 5% (four of 78) had homeotic and 33.3% (26 of 78) had homologous changes. Prevalence of homologous variations was close to 38% and within groups not statistically different, which confirms our hypotheses.

Homeotic vertebral patterning variations (transitional vertebra) were described before in other animals as the presence of occipito-atlantal fusion/occipitalization of the atlas, rudimentary (small or undeveloped) ribs at the first thoracic vertebra, or cervical ribs (small ribs at C7)⁵ and detected in four horses of this study. In one horse occipito-atlantal fusion was found without malformation of the axis or clinical signs. Clinical consequences of occipito-atlanto-axial malformation (OAAM) have been identified in horses and humans depending on the severity of vertebral changes and involvement of the axis [21–23]. There were two mature horses with rudimentary ribs at Th1 and one mature horse in which there were no ribs but transverse processes at Th1, features of homeotic variation and therefore transitional vertebrae. Only one case report on the existence of a rudimentary first rib in a horse was found in literature [7]. In some sloths and human fetuses, the existence of rudimentary or no ribs at the first thoracic vertebra (“posterior” patterning) has been described without known clinical relevance [5,24]. The lack of literature regarding this variation in equine patients might be explained by the inability of analog radiography to image the area of the first thoracic vertebra.

Presence of cervical ribs in humans has been correlated to a higher occurrence of malformations and neoplasia in childhood [24–26] and has been identified in humans with thoracic outlet syndrome (brachial plexus, subclavian artery, and vein compression) [27], a syndrome that has not been described or identified in horses. None of the horses in the present study had cervical ribs but 26 horses did present with a ventral protuberance, causing a change in position of the associated soft tissue structures and therefore possibly altered biomechanical function of this area [11].

Homologous changes refer to morphological changes of size or shape of individual vertebrae [5]. Twenty-six of 78 horses (33.3%) had morphologic changes restricted to the transverse processes of C6 and C7 (otherwise named lateral vertebral or costal elements), described before as transposition of the caudal ventral tubercle from C6 to C7 [6,9]. This is considerably more than the 13% or 24% prevalence described in

the studies using conventional radiography and more in line with the findings during dissection of the thoroughbred-based population [6,10]. This difference is probably due to the higher sensitivity of CT compared to plain radiography, but may also have to do with differences in breed composition of the study populations. The relatively high prevalence in the present group of horses seems to plead for a rather benign character of these conformational changes in terms of clinical relevance. Although a cross-sectional observational study like ours cannot provide evidence about causal relationships, the fact that there was no significant difference in frequency between the groups of mature horses presented with or without clinical signs related to the cervical vertebral column (36.7% compared to 33.3%, $P = 0.81$) and foals (35.3% compared to 29.6%, $P = 0.72$) supports this conjecture to some extent. To define possible causal relationships of these homologous changes with clinical signs, a different subset of horses and standardized clinical examinations would be necessary.

The mammalian number of seven cervical vertebrae seems to have a very high degree of conservation. However, while maintaining this number, a shift in function and therefore related features of the last cervical and first thoracic vertebra has been described in giraffes as adaptations to biomechanical strain [28]. The variation in features of the transverse processes in C6 and C7 in the 26 horses presented in our study may be interpreted as a shift of function and features from C6 to C7 with alteration of biomechanical strain [11]. The assumption was that C7 takes on some of the features of C6 or “transposition of a ventral process from C6 to C7” seems likely, especially when considering embryogenesis [6,9]. During gastrulation of the mammalian embryo, somites are formed around the notochord. Each vertebra is formed by a caudal part of a cranial somite and a cranial part of a caudal somite, forming a sclerotome [29]. *Hoxa-5* has been found to regulate the somites and thereafter sclerotomes in the cervical-thoracic transition area of chicken embryos [30]. *Hoxa-5* contributes first to the regional vertebral patterning (homeotic), as it is expressed highly in the somites of this region. Thereafter, *Hoxa-5* is expressed more specifically in the ventrolateral part of sclerotomes and plays a role in the formation of the lateral vertebral elements (costal elements) and the shaping of the morphology of the vertebra (homologous) after the determination of the vertebral pattern [30]. Although the vertebral patterning is predominantly maintained in the horses in our study, the lateral vertebral elements (transverse processes) were altered in 26 horses. A temporary and regional (lateroventral) deregulation of the *Hoxa-5* gene in one somite could cause the loss of this element in C6 and presence in C7, when dividing in a cranial and caudal part. Therefore, the described changes seem to represent homologous variations in shape of these distal cervical vertebrae. The rest of the vertebral column was not examined

in these horses and therefore no further differentiation can be made in axial homeotic or meristic variations.

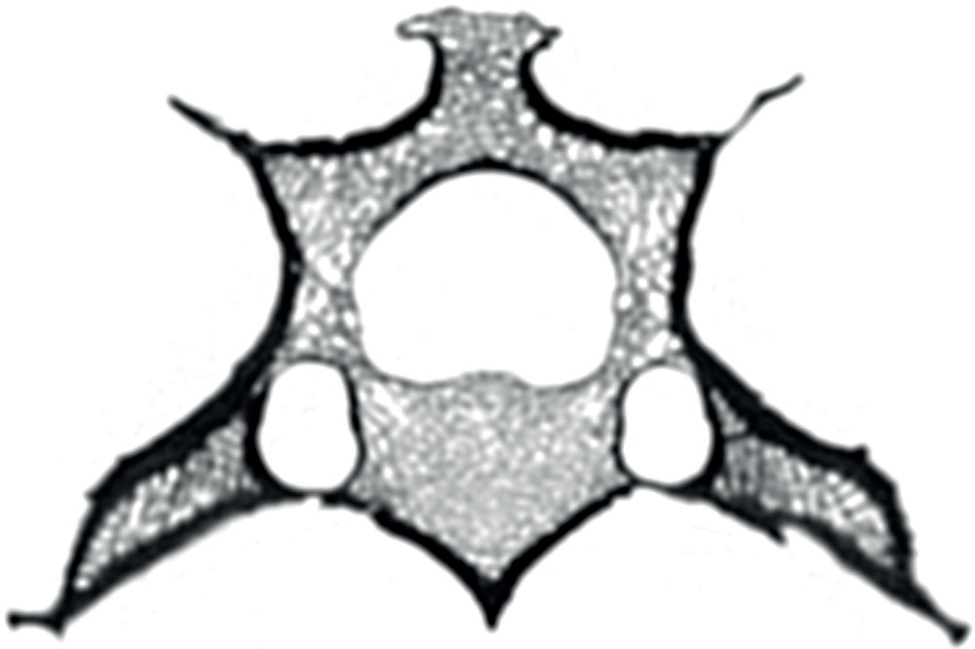
In conclusion, findings indicated that familiarity with equine cervical vertebral anatomical variations during CT examinations is important, as homologous changes in this group of horses seem rather common. Homeotic variations in the equine occipitocervical or cervicothoracic vertebral junction in this group of horses were seen less commonly, but have to be considered as well. Although CT examination of the complete cervical spine in living horses became only recently possible, the CT images provided in this study can form a basis and reference for future studies as well as guidance in recognizing vertebral variations in other imaging modalities. Further workup is warranted to identify the appearance and frequency of these changes in different imaging modalities such as radiography and ultrasonography. To identify possible clinical implications, different populations of horses with and without clinical signs attributable to this anatomic region, as identified with a standardized clinical examination, are needed.

Acknowledgements: The authors thank Professors G. Voorhout and P. R. van Weeren for their help in preparing this manuscript.

REFERENCES

1. Down SS, Henson FM. (2009) Radiographic retrospective study of the caudal cervical articular process joints in the horse. *Equine Vet J.* **41**, 518–524.
2. Dyson SJ. (2011). Lesions of the equine neck resulting in lameness or poor performance. *Vet Clin N Am Equine Pract.* **27**, 417–437.
3. Withers JM, Voute LC, Hammond G, Lischer CJ. (2009) Radiographic anatomy of the articular process joints of the caudal cervical vertebrae in the horse on lateral and oblique projections. *Equine Vet J.* **41**, 895–902.
4. Berg LC, Nielsen JV, Thoenfer MB, Thomsen PD. (2003) Ultrasonography of the equine cervical region: a descriptive study in eight horses. *Equine Vet J.* **35**, 647–655.
5. Buchholtz EA, Stepien CC. (2009) Anatomical transformation in mammals: developmental origin of aberrant cervical anatomy in tree sloths. *Evol Dev.* **11**, 69–79.
6. May-Davis S. (2015) The occurrence of a congenital malformation in the sixth and seventh cervical vertebrae predominantly observed in thoroughbred horses. *J Equine Vet Sci.* **34**:1313–1317.
7. Bradley OC. (1901) On a case of rudimentary first thoracic rib in a horse. *J Anat Physiol.* **36**, 54–62.
8. Gorton B. (1923) Abnormal cervical vertebra of a horse. *J Anat.* **57**, 380–381.
9. Butler JA, Colles CM, Dyson SJ, Kold SE, Poulos PW (2011). The spine. In: Butler JA, Colles CM, Dyson SJ, et al., editors.: *Clinical radiology of the horse*. 3rd ed. Oxford, England: Wiley-Blackwell, p. 50.
10. Santinelli I, Beccati F, Arcelli R, Pepe M. (2015). Anatomical variation of the spinous and transverse processes in the caudal cervical vertebrae and the first thoracic vertebra in horses. *Equine Vet J.* **48**, 5–49.
11. May-Davis S, Walker C. (2015) Variations and implications of the gross morphology in the *longus colli* muscle in thoroughbred and thoroughbred derivative horses presenting with a congenital malformation of the sixth and seventh cervical vertebrae. *J Equine Vet Sci.* **35**, 560–568.
12. DeRouen A, Spriet M, Aleman M. (2016). Prevalence of anatomical variation of the sixth cervical vertebra and association with vertebral canal stenosis and articular process osteoarthritis in the horse. *Vet Radiol Ultrasound.* **57**, 253–258.
13. Sleutjens J, Cooley AJ, Sampson SN, et al. (2014). The equine cervical spine: comparing MRI and contrast-enhanced CT images with anatomic slices in the sagittal, dorsal, and transverse plane. *Vet Q* **34**, 74–84.
14. Zafra R, Carrascosa C, Rivero M, et al. (2012) Analysis of equine cervical spine using three-dimensional computed tomographic reconstruction. *J Appl Anim Res.* **40**, 108–111.
15. Claridge HA, Piercy RJ, Parry A, Weller R. (2010) The 3D anatomy of the cervical articular process joints in the horse and their topographical relationship to the spinal cord. *Equine Vet J.* **42**, 726–731.
16. Mitchell CW, Nykamp SG, Foster R, Cruz R, Montieth G. (2012) The use of magnetic resonance imaging in evaluating horses with spinal ataxia. *Vet Radiol Ultrasound.* **53**, 613–620.
17. Janes JG, Garrett KS, McQuerry KJ, et al. (2013) Comparison of magnetic resonance imaging with standing cervical radiographs for evaluation of vertebral canal stenosis in equine cervical stenotic myelopathy. *Equine Vet J.* **16**, 681–686.
18. König HE, Liebich HG. (2009) Vertebral column or spine (columna vertebralis). In: König HE, Liebich HG, editors.: *Veterinary anatomy of domestic mammals*, 4th ed. Stuttgart: Schattauer GmbH, p. 86.
19. Popesko P (ed). (1993) *Atlas der Topographischen Anatomie der Haustiere*. Stuttgart: Ferdinand Enke Verlag.
20. Sleutjens J, Voorhout G, Van Der Kolk JH, Wijnberg ID, Back W. (2010) The effect of ex vivo flexion and extension on intervertebral foramina dimensions in the equine cervical spine. *Equine Vet J.* **42** (Suppl 38), 425–430.

21. Watson AG, Mayhew IG.(1986) Familial congenital occipitoatlantoaxial malformation (OAAM) in the Arabian horse. *Spine (Phila Pa 1976)*. **11**, 334–339.
22. Mayhew IG, Watson AG, Heissan JA. (1978) Congenital occipitoatlantoaxial malformations in the horse. *Equine Vet J*. **10**, 103–113.
23. Smoker WR, Khanna G. (2008) Imaging the craniocervical junction. *Childs Nerv Syst*. **24**,1123–1145.
24. Ten Broek CM, Bakker AJ, Varela-Lasheras I, Bugiani M, Van Dongen S, Galis F.(2012) Evo-devo of the human vertebral column: on homeotic transformations, pathologies and prenatal selection. *Evol Biol*. **39**, 456–471.
25. Galis F.(1999) Why do almost all mammals have seven cervical vertebrae? Developmental constraints, hox genes, and cancer. *J Exp Zool*. **285**, 19–26.
26. Schumacher R, Mai A, Gutjahr P. (1992) Association of rib anomalies and malignancy in childhood. *Eur J Pediatr*. **151**, 432–434.
27. Weber AE, Criado E. (2014) Relevance of bone anomalies in patients with thoracic outlet syndrome. *Ann Vasc Surg*. **28**, 924–932.
28. van Sittert SJ, Skinner JD, Mitchell G. (2010) From fetus to adult—an allometric analysis of the giraffe vertebral column. *J Exp Zool B Mol Dev Evol*. **15**, 314:469–479.
29. Gilbert SC (1997) Chapter 9. Early vertebrate development: mesoderm and endoderm. In: Gilbert SC, editor. *Developmental biology*. 5th ed. Sunderland, MA: Sinauer Associates, Inc., p. 341.
30. Chen JW, Zahid S, Shilts MH, et al. (2013) Hoxa-5 acts in segmented somites to regulate cervical vertebral morphology. *Mech Dev*. **130**, 226–234



4

Caudal Cervical Vertebral Variation is Not Associated with Clinical Signs in Warmblood Horses

Stefanie Veraa^a, Kim M. de Graaf, Inge D. Wijnberg^c, Willem Back^{c,e}, Johannes C.M. Vernooij^d, Mirjam Nielen^d, Antoon-Jan M. van den Belt^a

^a Division of Diagnostic Imaging, Faculty of Veterinary Medicine, Utrecht University, Yalelaan 110, NL-3584 CM Utrecht, The Netherlands.

^b Equine Veterinary Clinic "Veterinair Centrum Someren", Slievenstraat 16, NL-5711 PK, Someren, The Netherlands

^c Department of Equine Sciences, Faculty of Veterinary Medicine, Utrecht University, Yalelaan 114, NL-3584 CM Utrecht, The Netherlands

^d Department of Farm Animal Health, Yalelaan 7, NL-3584 CL, The Netherlands

^e Department of Surgery and Anaesthesiology of Domestic Animals, Faculty of Veterinary Medicine, Ghent University, Salisburylaan 133, B-9820 Merelbeke, Belgium

Accepted for Publication in Equine Veterinary Journal

ABSTRACT

Background: Variation in equine caudal cervical spine morphology at C6 and C7 has high prevalence in Warmblood horses and is suspected to be associated with pain in a large mixed-breed group of horses. At present no data exist on the relationship between radiographic phenotype and clinical presentation in Warmblood horses in a case-control study.

Objectives: To establish the frequency of radiographically visible morphologic variation in a large group of Warmblood horses with clinical signs and compare this with a group without clinical signs. We hypothesised that occurrence of morphologic variation in the case group would not differ from the control group, indicating there is no association between clinical signs and morphologic variation.

Study design: Retrospective case-control.

Methods: Radiographic presence or absence of morphologic variation of cervical vertebrae C6 and C7 was recorded in case (n = 245) and control horses (n = 132). Case and control groups were compared by univariable Pearson's Chi-square and multivariable logistic regression for measurement variables age, sex, breed, degenerative joint disease and morphologic variation at C6 and C7. Odds ratio and confidence intervals were obtained. A $P \leq 0.05$ was considered statistically significant.

Results: Morphologic variation at C6 and C7 (n = 108/377 = 28.6%; Cases 58/245 = 23.7%; Control 50/132 = 38%) was less frequent in horses with clinical signs in univariable testing (OR 0.48, 95% CI 0.3–0.8, $P = 0.001$). Age, sex, breed and degenerative joint disease were not retained in the final multivariable logistic regression step whereas morphologic variation remained significantly less present in horses with clinical signs.

Main limitations: Possible demographic differences between equine clinics.

Conclusions: Morphologic variation in the caudal cervical spine was detected more frequently in horses without clinical signs. Therefore, radiographic presence of such variation does not necessarily implicate the presence of clinical signs.

Keywords: horse; anatomy; transitional vertebra; homologous

INTRODUCTION

The occurrence of vertebral morphologic variations in the equine cervico- thoracic vertebral column, such as rudimentary first ribs and shape variations of C7, has been described as early as the beginning of the 20th century, even before radiography was performed in horses [1,2]. At that time, it was believed that a decrease in the number of ribs was a sign of evolutionary progression whereas an increase would indicate evolutionary devolution [1].

About a century later, the role of the Hox-genes in defining cervical vertebral numbers and shape was established [3]. Variations in cervical vertebral numbers (homeotic changes) have been reported in horses as occipito-atlanto-axial malformation (OAAM) [4–6], and also as the presence of rudimentary or malformed ribs which seem to coincide in all cases with shape variations of C6 and C7 [7–9]. Existence of vertebral morphologic variation in the caudal cervical spine has been reported in one-third of both Thoroughbred and Warmblood populations [7,10]. This variation has been evaluated in more detail in radiographic studies in larger mixed groups of horses [11,12]. In their retrospective study DeRouen et al. [12] concluded that anomalous C6 vertebrae were more common in the Warmblood horses (n = 55, 79.2%), than in other breeds (n = 45, 47.4%) and possible relationships with cervical pain due to altered regional biomechanics were suggested. Vertebral morphologic variation has been reported as unilateral or bilateral and always in two consecutive (mostly C6 and C7) vertebrae [7,11,12].

Radiography remains the first and most important tool for screening and diagnosis of abnormalities of the equine cervical spine. It is important to assess the potential of this tool to distinguish between morphological variations that may or may not be associated with clinical signs. Therefore, the objectives of this retrospective case-control study were to 1) establish the frequency of morphologic variation in cervical vertebrae of adult Warmblood horses with and without clinical signs related to the neck, and 2) to determine a possible association between variation at C6 and C7 with the presence of clinical signs.

MATERIALS AND METHODS

Study data

Study data, including cervical radiographic examinations, breed, age, sex, electromyography, clinical signs, when applicable, were obtained from the Division of Diagnostic Imaging of the Faculty of Veterinary Medicine, Utrecht University and the private equine clinic of the Veterinary Centre Someren. Cervical radiographic examinations of all Warmblood horses (with and without clinical signs) performed between January 2011 and December 2013 ($n = 245$), were retrieved from the Picture Archiving and Communication System (Impax, version 6.6.1.5003)^a of the Division of Diagnostic Imaging of the Faculty of Veterinary Medicine, Utrecht University. Data of radiographic examinations of Warmblood horses without clinical signs, which had been performed during pre-purchase examinations between January 2009 and December 2012 ($n = 132$), were retrieved from the Picture Archiving and Communication System (EasyIMAGE, VetZ)^b of the equine clinic of the Veterinary Centre Someren. Radiographic examinations were excluded if only the cranial cervical spine was assessable.

The radiographic data were reviewed by one board certified radiologist (S.V.) who was not blinded to the clinical data for the presence (unilateral, bilateral) or absence of morphologic variation (absence of a ventral laminar part of the transverse process in combination with a ventral protuberance at another transverse process) and its anatomic location. Furthermore, presence or absence of degenerative joint disease of the articular facet joint of C6 and C7 was recorded. The clinical data of the above-mentioned horses were reviewed and considered to be relevant if classified in one of the following groups: spinal ataxia during neurologic examination, restricted (latero- or dorso-) flexion of the neck, cervical pain on palpation, abnormal behaviour (e.g. head shaking, bolting), cervical muscle atrophy, lameness and more specifically presumed thoracic neurological lameness, and hypermetric gait of fore- or hindlimbs. Presumed brachial plexus neurological lameness was defined as any lameness that did not alter after diagnostic anaesthesia and/or was diagnosed as such based on electromyography. Clinical examinations were performed by board certified surgeons and internal medicine specialists, as well as residents under their supervision.

Data analysis

Measurement variables were presented as categorical data and median and range were calculated for age of case and control groups. Age was classified as younger and older horses, defined as 0–10 years old and >10 years old. Sex was defined as female and male. Breed was divided into Dutch Warmblood and other Warmbloods.

Degenerative joint disease was defined as absent or present. Attribute: Morphologic variation was first defined as present or not present; thereafter unilateral or bilateral variation were separated.

The following case definitions of the case group were used: A1) all horses with at least one recorded clinical sign, A2) horses with spinal ataxia, A3) horses with cervical pain on palpation, A4) horses with lameness. Clinical signs in case definitions A2 to A4 were considered as inclusion criteria but not as limiting factors. Therefore, combinations of the above mentioned recorded clinical signs were possible as horses could have more than one clinical sign recorded (see Table 1). In case definitions A1 to A3 presumed brachial plexus neurological lameness could be one of the recorded clinical signs; in case definition A4 all lameness cases were included.

Associations between horse measurement variable (age, sex, breed and degenerative joint disease at C6 and C7), the attribute morphologic variation and groups (case-control) were tested in two stages. The first stage included univariable analysis of the case-control groups with each of the horse measurement variables and the attribute morphologic variations (yes/none, or unilateral/bilateral/none) by applying Pearson's chi-square test for all four case definitions. The odds ratios (OR) with 95% confidence interval were calculated, where the H_0 for the OR = 1. Secondly, multi- variable stepwise logistic regression analysis with backward elimination approach of the case-control groups was performed in a subset of the horse study population including only those under 16 years of age and being Dutch Warmbloods, as measurement variables "age" and "breed" were seen to be most related to case-control status during univariable analysis. Through this restriction, the case and control groups had a similar distribution for age and breed. Multivariable step-wise logistic regression, with backward elimination approach, was performed for the respective four case definitions including age, sex, degenerative joint disease as measurement variables and unilateral/bilateral/none shape variation as attribute. Inclusion of a measurement variable in the four case-control models depended on $P < 0.05$. An eliminated variable was considered a confounding factor if it altered the coefficient (b) of the remaining variables by $> 10\%$. The odds ratios (OR) with 95% confidence intervals were calculated with OR = 1 considered according to the stated lack of difference between the two groups. Statistical processing was carried out in SPSS (Version 24.0)^c (S.V.). A $P \leq 0.05$ was considered statistically significant.

RESULTS

Horses

Included were 377 horses with radiographic examinations of the equine cervical spine and clinical recordings that met the requirements of this study. The frequency distribution of clinical signs for all case definitions is given in Table 1. Evaluated were 245 case horses (median age of 8 years; range 1–27 years; 146 geldings, 11 stallions and 87 mares and one unknown; 210 Royal Dutch Sporthorse, 9 Dutch Riding Horse 4 Belgian Warmblood, 6 Hanoverian, 3 Oldenburg, 5 Westfalen, one Holstein, 4 Zangersheide, one Rheinlander, one Trakehner, one Warmblood cross) and 132 control horses (median age 7 years; range 2–13 years; 71 geldings, 21 stallions and 40 mares; 82 Royal Dutch Sporthorse, one Dutch Riding Horse, 11 Belgian Warmblood, 8 Hanoverian, 11 Oldenburg, 2 Westfalen, 5 Holstein, 2 Zangersheide, 3 Rheinlander, 3 Polish Warmblood, one Trakehner, one Selle Francais, one Swedish Warmblood, one Italian Warmblood) (see also Table 2).

Table 1: Distribution of clinical signs in absolute numbers and percentages for case groups ($n=245$, $n=123$, $n=106$) and the control group ($n=132$) with all horses included. Multiple clinical signs can be present per individual horse in a particular case group.

Clinical signs		All (A1)	Spinal ataxia (A2)	Pain Palpation (A3)	Lameness (A4)	Control
		($n=245$) n (%)	($n=123$) n (%)	($n=106$) n (%)	($n=116$) n (%)	($n=132$) n (%)
Spinal ataxia	Yes	123 (50.2)	123 (100.0)	61 (57.5)	40 (34.5)	0 (0)
	No	122 (49.8)	0 (0)	45 (42.5)	76 (65.5)	132 (100)
Restricted flexion of the neck	Yes	155 (63.3)	71 (57.7)	85 (80.2)	78 (67.2)	0 (0)
	No	90 (36.7)	52 (42.3)	21 (19.8)	38 (32.8)	132 (100)
Pain on palpation of the neck	Yes	106 (43.3)	61 (49.6)	106 (100.0)	51 (44.0)	0 (0)
	No	139 (56.7)	62 (50.4)	0 (0)	65 (56.0)	132 (100)
Abnormal behaviour (e.g. head shaking, bolting)	Yes	37 (15.1)	11 (8.9)	16 (15.1)	16 (13.8)	0 (0)
	No	208 (84.9)	112 (91.1)	90 (84.9)	100 (86.2)	132 (100)
Brachial plexus neurogenic lameness	Yes	27 (11.0)	12 (9.8)	15 (14.2)	27 (23.3)	0 (0)
	No	218 (89.0)	111 (90.2)	91 (85.8)	89 (76.7)	132 (100)
Muscular atrophy of the neck	Yes	46 (18.8)	24 (19.5)	22 (20.8)	19 (16.4)	0 (0)
	No	199 (81.2)	99 (80.5)	84 (79.2)	97 (83.6)	132 (100)
Hypermetria (fore- and/or hindlimbs)	Yes	32 (13.1)	22 (17.9)	15 (14.2)	14 (12.1)	0 (0)
	No	213 (86.9)	101 (82.1)	91 (85.8)	102 (87.9)	132 (100.0)

Note. The numbers in bold in case group A2 and A3, representing the case group selection criteria

Table 2: Frequency of variables in absolute numbers and percentages, odds ratio (OR), 95 % confidence interval (CI) and *p*-value of univariable Pearson's Chi-square test between all horses with (case; *n*=245) and without (control; *n*=132) clinical signs.

Variables	Categories	Case A1 (<i>n</i> =245) <i>n</i> (%)	Control (<i>n</i> =132) <i>n</i> (%)	OR A1	95% CI	<i>p</i> -value A1
Age	NA	3 (1.2)	1 (0.8)			
	0-10	189 (77.1)	113 (85.6)	0.6	0.3-1.02	0.06
	>10	53 (21.6)	18 (13.6)	Ref.		
Sex	NA	1 (0.4)	0 (0)			
	Female	87 (35.5)	40 (30.3)	1.3	0.8-2.0	0.295
	Male	157 (64.1)	92 (69.7)	Ref.		
Breed	Dutch WB	210 (85.7)	82 (62.1)	3.7	2.2-6.0	0.0001
	Other	35 (14.3)	50 (37.9)	Ref.		
Degenerative Joint Disease	Absent	206 (84.1)	109 (82.6)	Ref.		
	Present	39 (15.9)	23 (17.4)	1.1	0.6-1.96	0.71
Morphologic Variation C6-C7	None	190 (77.6)	82 (62.1)	Ref.		
	Yes	55 (22.4)	50 (37.9)	0.5	0.3-0.8	0.001
Morphologic Variation C6-C7	None	190 (77.6)	82 (62.1)	Ref.		
	Unilateral	26 (10.6)	22 (16.7)	0.5	0.2-0.95	0.03
	Bilateral	29 (11.8)	28 (21.2)	0.5	0.3-0.8	0.06

NA= not available and not included in statistical results, Ref.= reference group for odds ratio calculation, Dutch WB= Dutch Warmblood

Descriptive data analysis

Morphologic variation at C6 and C7 (case 58/245 = 23.7%, control 50/132 = 38.0%) consisted of absence of the ventral lamina part of the transverse process of C6 in combination with a ventral protuberance at the transverse process of C7 (Fig 1). This anomaly was seen unilaterally (*n* = 50) or bilaterally (*n* = 58). A single horse in the case group had a unilateral ventral protuberance at the transverse process of C5 with

absence of the ventral part of the transverse process of C6 and no visible changes of C7 (Fig 2). Location of lameness was recorded as follows: left front (n = 28), right front (n = 34), left hind (n = 3), right hind (n = 1), left front and right front (n = 39), left hind and right hind (n = 2), left front and right hind (n = 3), right front and left hind (n = 1), all limbs (n = 5). Degenerative joint disease was scored as absent in 314 horses (206 in the group with and 108 in the group without clinical signs) and present in 63 horses (39 in the group with and 24 in the group without clinical signs). Electromyography results were available and abnormal in 24 horses, including horses with a range of clinical signs, but most frequently showing signs of upper motor neuron involvement, e.g. signs of spinal ataxia (n = 8).

Case-control data analysis

Univariable analysis: A summary of the results of the univariable analysis with all horses included (i.e. A1) is shown in Table 2. For case definitions A2 to A4 and for a subset of horses <16 years old and Dutch Warmblood with case definitions A1 to A4, a summary of results is available in Supplementary Items 1 and 2.

When including horses of all ages and breeds, a higher age was noted in all case groups except for horses with spinal ataxia which were of similar age compared to the control group. There were more Dutch Warmblood horses in the case groups than the control group ($P < 0.05$). There were no differences related to sex or degenerative joint disease between the two groups. Presence of morphologic variation at C6 and C7 was statistically significantly more in the control group for all case definitions ($P < 0.05$). However, when divided in unilateral and bilateral morphologic variation compared to no variation, this was not true for all case definitions. The OR remained < 1 for case horses for all case definitions for bilateral morphologic variations and only in case definition A1 for unilateral morphologic variation. For case definitions A2 to A4, the upper limit of 95% CI was > 1 for cases.

Multivariable analysis: As variables age and breed were statistically different between case and control groups in univariable analysis, multivariable analysis was performed in a subset of horses <16 years old and Dutch Warmblood with case definitions A1 to A4. Decision making was based on the absence of horses older than 15 years of age in the control group and the overrepresentation of Dutch Warmblood horses in the case group. A summary of the results of multivariable analysis in the subset of horses being under 16 years old and Dutch Warmblood with spinal ataxia, is shown in Table 3. All results of other case definitions (all, pain on palpation, lameness) are included in Supplementary Item 3.

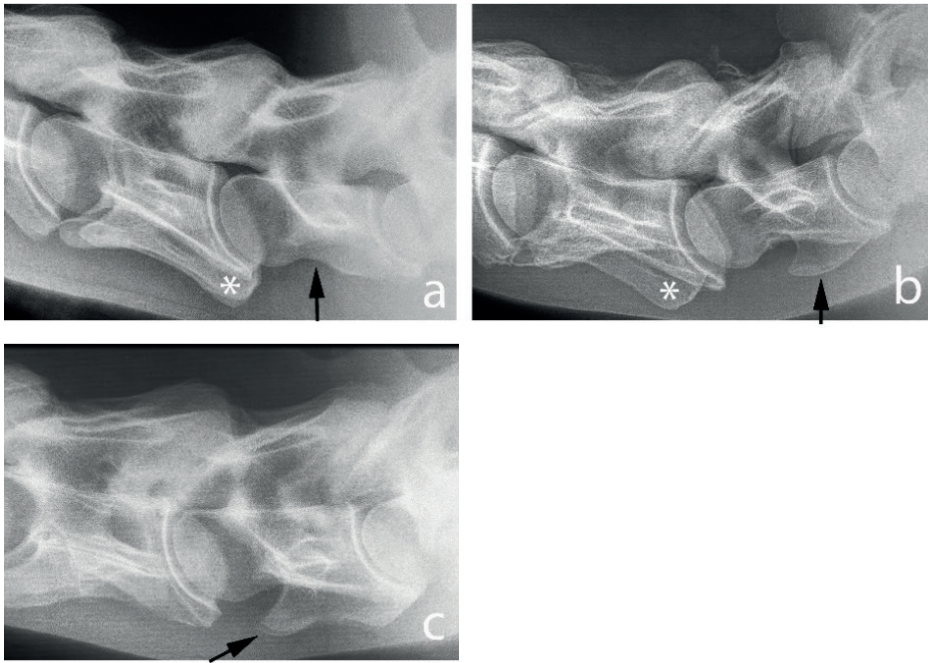


Fig. 1. Morphologic variation of the caudal cervical spine; white asterisk marks the ventral laminar part of the transverse process of C6 and the black arrow marks the transverse process of C7. (A) No variation is visible at C6 and C7 with a normal caudal part of the transverse process of C6 (asterisk) and horizontally oriented transverse processes of C7 (white arrow), (B) unilateral variation is visible with only one caudal part of a transverse process of C6 (asterisk) and a single ventrally oriented protuberance at C7 (white arrow), (C) bilateral variation is visible with no caudal part of the transverse process of C6 and two ventrally oriented protuberances at C7 (white arrow) as is arthrosis of the facet joints of C6-C7.

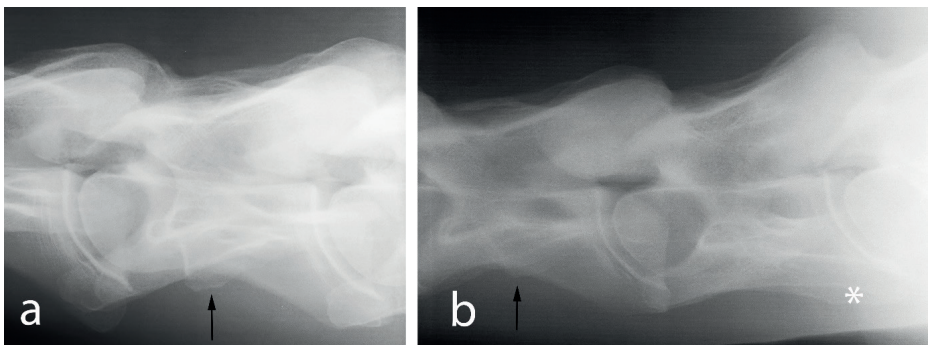


Fig. 2. Morphologic variation at C5 and C6 is present. Note the ventrally protruding part of the transverse process at C5 (white arrow) and the unilateral transverse process of C6 (black asterisk).

Stepwise logistic regression analysis with backward elimination approach in the above mentioned subset of horses and division of morphologic variation (none-yes) for all case definitions revealed that “morphologic variation” remained in the model but not the measurement variables sex, age and degenerative joint disease.

Morphologic variation at C6 and C7 was not related to the presence of clinical signs as most OR were <1 for case vs. control. In fact, more morphologic variations were present in the control horses in all cases (A1), spinal ataxia (A2), and in the group with pain on palpation (A3). Only, horses with any lameness (A4) did not differ in having a morphologic variation compared with control horses. The variable age did remain in the final step of case definition A4, leading to the conclusion that the lame horses in the case group were older than the control horses, which were pre-purchase horses.

Table 3. Results of multivariable stepwise logistic regression analysis with backward elimination approach in a subset of horses, (<16 years of age and Dutch Warmblood), with morphologic variation divided in categories none-unilateral-bilateral; for cases defined as horses with spinal ataxia (n=106) and the control group (n=82).

	Variable	p-values	OR	95% CI
Step 1 (Initial full model)	Age (>10, <10)	0.13	0.5	0.2-1.2
	Sex (male, female)	0.66	0.9	0.5-1.6
	Degenerative Joint Disease (Yes, No)	0.87	1.1	0.4-2.6
	Morphologic variation None e	0.036		
	Unilateral	0.025	0.4	0.2-0.9
	Bilateral	0.65	0.8	0.3-2.4
Step 2	Age	0.13	0.5	0.2-1.2
	Sex	0.65	0.9	0.5-1.6
	Morphologic variation None	0.035		
	Unilateral	0.022	0.4	0.2-0.9
	Bilateral	0.61	0.8	0.3-2.3
	..35			
Step 3	Age	0.13	0.5	0.2-1.2
	Morphologic variation None	0.036		
	Unilateral	0.023	0.4	0.2-0.9
	Bilateral	0.62	0.8	0.3-2.3
Step 4 (Final reduced model)	Morphologic variation None	0.054		
	Unilateral	0.038	0.4	0.2-0.95
	Bilateral	0.73	0.8	0.3-2.5

Note: OR= odds ratio; 95% CI= 95% confidence interval

DISCUSSION

This is the first case-control designed study investigating the possible associations of clinical signs with morphologic variation of the equine cervical vertebral column. The prevalence of morphologic variation at C6 and C7 (28.6%) was similar to a previous study in a more diverse, smaller population of horses [7]. Interestingly, these changes were more often seen in the group of Warmblood horses without clinical signs (control) than in the group with clinical signs (cases). Cases defined by lameness showed a similar presence of morphologic variations as control horses. All results suggest no positive relation between morphologic variations and clinical signs as defined in this study.

Homologous morphologic variations at C6 and C7 were found in almost a quarter of the cases and 38% of the controls resulting in an $OR > 1$ for cases vs. controls. The odds in these two populations for having a morphologic variation at C6 and C7 were therefore higher in the group without clinical signs. This is a somewhat unexpected and counter-intuitive finding, but these results seem to support the fact that caudal cervical vertebral morphologic variation might represent a favourable adaptation in Warmblood horses. However, selection bias of the study population could have influenced these results as horses were presented at different types of clinics (university vs. private equine clinic), for different reasons. The control horses were younger, and potentially more expensive as they were presented for pre-purchase radiography. This bias was partly controlled in the age and breed restricted analysis, but cannot be excluded entirely. That being said, the prevalence in other studies was close to our observations. A prevalence of 33.3% was recorded in a cross-sectional post-mortem CT study [7]. A radiographic study [11] found these morphologic variations in 13.3% of a random study population and in 15% (21/138) in a group of Warmblood horses with a higher prevalence in mares. Another cross-sectional radiographic study described a frequency of 33.5% (19/55) in Warmblood horses without sex association [12], which is again close to our observations. It is possible that geographic, demographic and breed-related differences can explain the minor differences in frequencies between studies.

Another reason for bias may have been that horses had a different clinical history and reason for presentation. Cases were horses that had been presented at the University clinic because of clinical signs that had been going on for some time. However, controls were pre-purchase horses without any clinical signs at the moment of examination at the private clinic. No follow-up data were available of the control horses, and therefore

it cannot be ruled out that they developed associated clinical signs later in life. The retrospective aspect of this study and therefore lack of a standardised diagnostic work-up might also have influenced the outcome. No radiographic association for presence of other vertebral pathologies such as arthrosis was found in cases nor controls, confirming a lack of association as previously reported [12]. The multivariable analysis was performed in a subset of horses to equalise groups as it was noted that the case group contained some older horses while the control group contained small numbers of different Warmblood breeds. However, with no plausible reason to be given at this stage, all findings indicated that horses that show clinical signs are less likely to have a congenital morphologic variation of the lower cervical spine, with the exception of cases with lameness. The latter groups were equally likely to show morphologic variation as controls.

Conclusions

Homologous morphologic variation is common in the caudal cervical spine of Warmbloods. This variation does not appear to be associated with clinical signs and in fact is less frequent in clinical cases than in control animals, perhaps suggesting some protective effect. The existence of such an effect can only be established if the results in this study would be confirmed by other independent prospective studies. These studies should include a standardised clinical work-up and a well-documented population of Warmblood horses that needs to be followed over time. The mechanism of any such possible protective effect remains entirely elusive at this stage. Thus radiographic presence of morphologic variation in the caudal cervical spine must be interpreted with care. There are no indications for any negative effect currently, but its clinical relevance has not yet been fully established and needs further investigation.

Manufacturers' addresses

^aAgfa Healthcare, Mortsel, Belgium.

^bVetZ GmbH, Isernhagen, Germany.

^cIBM SPSS Statistics for Windows, Armonk, New York, USA.

Acknowledgements

The authors would like to thank Prof Dr P. R. van Weeren, Prof Dr J.W. Hesselink and Prof Dr G. Voorhout for their help in preparing this manuscript.

REFERENCES

1. Bradley, O.C. (1901) On a case of rudimentary first thoracic rib in a horse. *J. Anat. Physiol.* 36, 54–62.
2. Gorton, B. (1923) Abnormal cervical vertebra of a horse. *J. Anat.* 57, 380–381.
3. Chen, J.W., Zahid, S., Shilts, M.H., Weaver, S.J., Leskowitz, R.M., Habbsa, S., Aronowitz, D., Rokins, K.P., Chang, Y., Pinnella, Z., Holloway, L. and Mansfield, J.H. (2013) Hoxa-5 acts in segmented somites to regulate cervical vertebral morphology. *Mech. Dev.* 130, 226–240.
4. de Lahunta, A., Hatfield, C. and Dietz, A. (1989) Occipitoatlantoaxial malformation with duplication of the atlas and axis in a half Arabian foal. *Cornell Vet.* 79, 185–193.
5. Mayhew, I.G., Watson, A.G. and Heissan, J.A. (1978) Congenital occipitoatlantoaxial malformations in the horse. *Equine Vet. J.* 10, 103–113.
6. Watson, A.G. and Mayhew, I.G. (1986) Familial congenital occipitoatlantoaxial malformation (OAAM) in the Arabian horse. *Spine (Phila. Pa. 1976)* 11, 334–339.
7. Veraa, S., Bergmann, W., van den Belt, A.J., Wijnberg, I. and Back, W. (2016) Ex Vivo Computed Tomographic Evaluation of Morphology Variations in Equine Cervical Vertebrae. *Vet. Radiol. Ultrasound.* 57, 482–488.
8. Audigie, F., Rovel, T., Coudry, V., Bertoni, L., Jacquet, S., Danjon, C. and Denoix, J.M. (2017) Malformations of the first ribs in equine sports and racehorses. *Vet. Radiol. Ultrasound.* 57, 711–712.
9. May-Davis, S. (2017) Congenital malformations of the first sternal rib. *J. Equine Vet. Sci.* 49, 92–100.
10. May-Davis, S. (2014) The occurrence of a congenital malformation in the sixth and seventh cervical vertebrae predominantly observed in thoroughbred horses. *J. Equine Vet. Sci.* 34, 1313–1317.
11. Santinelli, I., Beccati, F., Arcelli, R. and Pepe, M. (2014) Anatomical variation of the spinous and transverse processes in the caudal cervical vertebrae and the first thoracic vertebra in horses. *Equine Vet. J.* 48, 45–49.
12. DeRouen, A., Spriet, M. and Aleman, M. (2016) Prevalence of anatomical variation of the sixth cervical vertebra and association with vertebral canal stenosis and articular process osteoarthritis in the horse. *Vet. Radiol. Ultrasound* 57, 253–258.

Supplementary item 1. Univariable analysis in all available horses (n=377). Frequency of variables, odds ratio (OR), 95 % confidence interval (CI) and p-value of univariable Pearsons' Chi-square test between horses with clinical signs (case definitions A1: all, A2: spinal ataxia, A3: pain on palpation, A4: overall lameness) and without clinical signs (control). NA= not available and not included in statistical results, DJD= degenerative joint disease, DWB= Dutch Warmblood

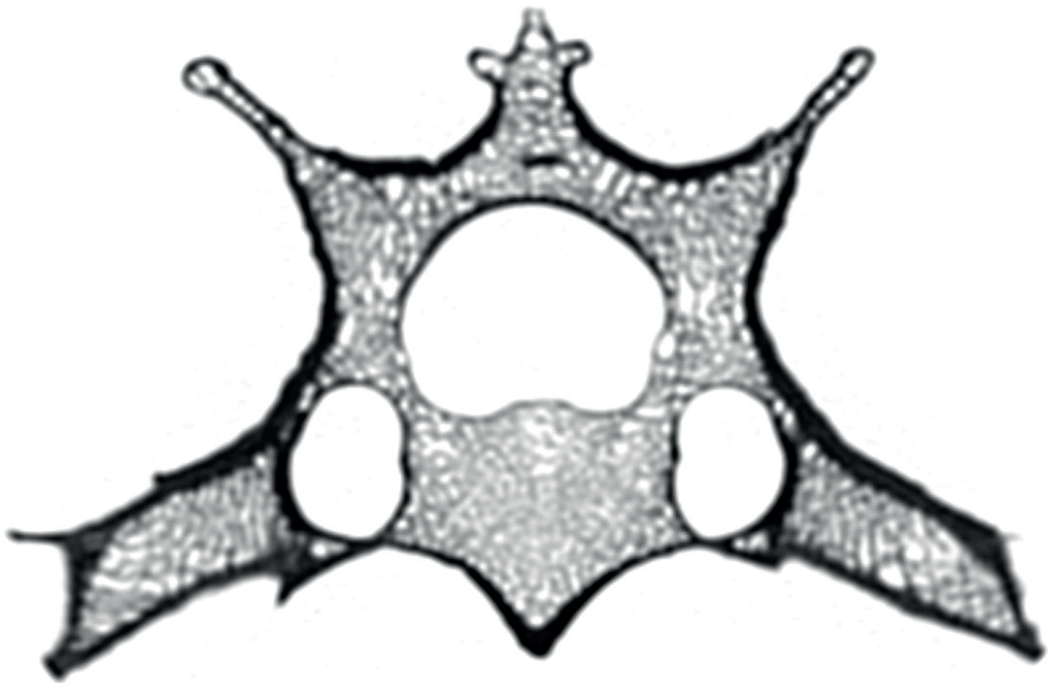
Variables	Categories	Case A1 All (n=245) n(%)	Case A2 Spinal ataxia (n=123) n(%)	Case A3 Pain (n=106) n(%)	Case A4 Lame (n=116) n(%)	Control (n=132) n(%)	OR A1 (95% CI)	OR A2 (95% CI)	OR A3 (95% CI)	OR A4 (95% CI)	p-value A1	p-value A2	p-value A3	p-value A4
Age	NA	3 (1.2)	1 (0.8)	0 (0)	2 (1.7)	1 (0.8)								
	0-10	189 (77.1)	107 (87.0)	80 (75.5)	80 (69.0)	113 (85.6)	0.6 (0.3-1.0)	1.1 (0.6-2.4)	0.5 (0.3-0.95)	0.4 (0.2-0.7)	0.055	0.733	0.034	0.002
	>10	53 (21.6)	15 (12.2)	26 (24.5)	34 (29.3)	18 (13.6)								
Sex	NA	1 (0.4)	1 (0.8)	1 (0.9)	0 (0)	0 (0)								
	Female	87 (35.5)	41 (33.3)	43 (40.6)	43 (37.1)	40 (30.3)	1.3 (0.8-2.0)	1.2 (0.7-1.97)	1.6 (0.9-2.7)	1.4 (0.8-2.3)	0.295	0.572	0.088	0.260
	Male	157 (64.1)	81 (67.9)	62 (57.5)	73 (62.9)	92 (69.7)								
Breed	DWB	210 (85.7)	106 (86.2)	93 (87.7)	101 (87.1)	82 (62.1)	3.7 (2.2-6.0)	3.8 (2.0-7.1)	4.4 (2.2-8.6)	4.1 (2.2-7.8)	0.0001	0.0001	0.0001	0.0001
	Other	35 (14.3)	17 (13.8)	13 (12.3)	15 (12.9)	50 (37.9)								
DJD	Present	39 (15.9)	17 (13.8)	18 (17.0)	18 (15.6)	23 (17.4)	0.9 (0.5-1.6)	0.8 (0.4-1.5)	0.97 (0.5-1.9)	0.9 (0.4-1.7)	0.71	0.43	0.93	0.69
	Absent	206 (84.1)	106 (86.2)	88 (83.0)	98 (84.4)	109 (82.6)								
Morph. Variation	Yes	55 (22.4)	26 (21.1)	23 (21.7)	30 (25.9)	50 (37.9)	0.5 (0.3-0.8)	0.4 (0.3-0.8)	0.5 (0.3-0.8)	0.6 (0.3-0.99)	0.001	0.003	0.007	0.043
	None	190 (77.6)	97 (78.9)	83 (78.3)	86 (74.1)	82 (62.1)								
	Unilateral	26 (10.6)	14 (11.4)	13 (12.3)	17 (14.7)	22 (16.7)	0.5 (0.2-0.95)	0.5 (0.3-1.1)	0.6 (0.3-1.2)	0.7 (0.4-1.5)	0.032	0.094	0.157	0.392
	Bilateral	29 (11.8)	12 (9.8)	10 (9.4)	13 (11.2)	28 (21.2)	0.5 (0.3-0.8)	0.4 (0.2-0.8)	0.4 (0.2-0.8)	0.4 (0.2-0.9)	0.06	0.06	0.07	0.025

Supplementary item 2. Univariable analysis in a subset of horses < 16 years old and being Dutch Warmblood (n=290). Frequency of variables, odds ratio (OR), 95 % confidence interval (CI) and p-value of univariable Pearsons' Chi-square test between horses with clinical signs (case definitions A1= all, A2: spinal ataxia, A3: pain on palpation, A4: overall lameness) and without clinical signs (control group). DWB= Dutch Warmblood

Variables	Categories	Case A1 all (n=207) n(%)	Case A2 spinal ataxia (n=107) n(%)	Case A3 pain (n=89) n(%)	Case A4 lame (n=99) n(%)	Control (n=83) n (%)	OR A1 (95% CI)	OR A2 (95% CI)	OR A3 (95% CI)	OR A4 (95% CI)	p-value A1	p-value A2	p-value A3	p-value A4
Age	0-10	167 (80.7)	97 (90.7)	71 (79.8)	70 (70.7)	72 (86.7)	0.6 (0.3-1.3)	1.5 (0.6-3.7)	0.6 (0.3-1.4)	0.4 (0.2-0.8)	0.220	0.394	0.222	0.009
	>10	40 (19.3)	10 (9.3)	18 (20.2)	29 (29.3)	11 (13.3)								
Sex	Female	76 (36.7)	37 (34.6)	37 (41.6)	37 (37.4)	27 (32.5)	1.2 (0.7-2.1)	1.1 (0.6-2.0)	1.5 (0.8-2.8)	1.2 (0.7-2.3)	0.501	0.767	0.220	0.495
	Male	131 (63.3)	70 (65.4)	52 (58.4)	62 (62.6)	56 (67.5)								
DJD	Absent	177 (85.5)	92 (86.0)	74 (83.1)	84 (84.9)	71 (85.6)								
	Present	30 (14.5)	15 (14.0)	15 (16.9)	15 (15.1)	12 (14.4)	1.0 (0.5-2.1)	0.97 (0.4-2.2)	1.2 (0.5-2.7)	1.1 (0.5-2.4)	0.994	0.931	0.666	0.896
Morph. Variation	Yes	49 (23.7)	24 (22.4)	22 (24.7)	25 (25.2)	31 (37.3)	0.5 (0.3-0.9)	0.5 (0.3-0.9)	0.6 (0.3-1.1)	0.6 (0.3-1.1)	0.018	0.025	0.073	0.078
	None	158 (76.3)	83 (77.6)	67 (75.3)	74 (74.8)	52 (62.7)								
	Unilateral	22 (10.7)	13 (12.1)	12 (13.5)	14 (14.1)	14 (16.9)	0.5 (0.3-1.1)	0.6 (0.3-1.3)	0.7 (0.3-1.6)	0.7 (0.3-1.6)	0.077	0.198	0.347	0.398
	Bilateral	27 (13.0)	11 (10.3)	10 (11.2)	11 (11.1)	17 (20.4)	0.5 (0.3-1.0)	0.4 (0.2-0.9)	0.5 (0.2-1.1)	0.455 (0.2-1.1)	0.060	0.031	0.070	0.061

Supplementary item 3. Final included variables of multivariable stepwise logistic regression analysis with backward elimination approach in a subset of horses, being <16 years of age and Dutch Warmblood, with shape variation divided in categories none=yes; for all cases ($n=245$) or cases defined as horses with pain on palpation ($n=89$) or lameness ($n=99$) and the control group ($n=83$); Sig. significance, S.E.= standard error, OR= odds ratio; 95% CI= 95% confidence interval.

	Variable	p-values (Sig.)	B (S.E.)	OR	95% CI
Case all- control	Morphologic Variation	0.019	-0.654 (0.28)	0.52	0.3-0.9
Case pain on palpation-control	Morphologic Variation	0.075	-0.596 (0.33)	0.6	0.3-1.1
Case lameness -control	Age	0.011	0.998 (0.39)	2.7	1.3-5.9



5

Equine Cervical Invertebral Disc Degeneration is Associated with Location and MRI Features

Stefanie Veraa^a, Wilhelmina Bergmann^b, Inge D. Wijnberg^c, Willem Back^{c,e}, Johannes C.M. Vernooij^d, Mirjam Nielen^d, Antoon-Jan M. van den Belt^a

^a Division of Diagnostic Imaging, Faculty of Veterinary Medicine, Utrecht University, Yalelaan 110, NL-3584 CM Utrecht, The Netherlands.

^b Department of Pathobiology, Faculty of Veterinary Medicine, Utrecht University, Yalelaan 1, NL-3584 CL, The Netherlands

^c Department of Equine Sciences, Faculty of Veterinary Medicine, Utrecht University, Yalelaan 114, NL-3584 CM Utrecht, The Netherlands

^d Department of Farm Animal Health, Yalelaan 7, NL-3584 CL, The Netherlands

^e Department of Surgery and Anaesthesiology of Domestic Animals, Faculty of Veterinary Medicine, Ghent University, Salisburylaan 133, B-9820 Merelbeke, Belgium

Veterinary Radiology and Ultrasound, 2019, 60(6), 696-706

ABSTRACT

Morphology of the equine cervical intervertebral disc is different from that in humans and small companion animals and published imaging data are scarcely available. The objectives of this exploratory, methods comparison study were (a) to describe MRI features of macroscopically non- degenerated and degenerated intervertebral discs (b) to test associations between spinal location and macroscopic degeneration or MRI-detected annular protrusion and between MRI-detected annular protrusion and macroscopic degeneration, and (c) to define MRI sequences for characterizing equine cervical intervertebral disc degeneration. Ex vivo MRI of intervertebral discs was performed in 11 horses with clinical signs related to the cervical region prior to macroscopic assessment. Mixed-effect logistic regression modeling included spinal location, MRI-detected annular protrusion, and presence of macroscopic degeneration with "horse" as random effect. Odds ratio and 95% confidence interval were determined. Reduced signal intensity in proton density turbo SE represented intervertebral disc degeneration. Signal voids due to presence of gas and/or hemorrhage were seen in gradient echo sequences. Presence of macroscopic intervertebral disc degeneration was significantly associated with spinal location with odds being higher in the caudal (C5 to T1) versus cranial (C2 to C5) part of the cervical vertebral column. Intervertebral discs with MRI-detected annular protrusion grades 2-4 did have higher odds than with grade 1 to have macroscopic degeneration. It was concluded that MRI findings corresponded well with gross macroscopic data. Magnetic resonance imaging of the equine cervical intervertebral disc seems to be a promising technique, but its potential clinical value for live horses needs to be explored further in a larger and more diverse population of horses.

Keywords: annulus fibrosus, disc disease, nucleus pulposus, spinal column

INTRODUCTION

Intervertebral disc disease is a well-known clinical entity in man and small companion animals and studies on normal anatomy, composition, and pathological conditions of the intervertebral disc are manifold [1–3]. In horses, the situation is different. The equine intervertebral disc has previously been described to have a different composition compared to that of most other mammals and to consist almost entirely of fibrous to fibrocartilaginous elements without a well-delineated nucleus pulposus [4,5]. However, new data do support the presence of a cartilaginous nucleus pulposus and fibrous annulus fibrosus similar to that in other mammals [6]. Intervertebral disc degeneration in the equine cervical spine has been characterized macroscopically by fibrillation, in severe cases accompanied by yellow discoloration and cleft formation and a gross degeneration grading scheme has been proposed [4,6]. Several case reports describe equine intervertebral disc degeneration, with a range of clinically potentially relevant consequences such as prolapse or herniation, [7–12] disruption of the annulus fibrosus by fibrocartilaginous nucleus pulposus material,⁵ and fibrocartilaginous embolism of the spinal cord with associated ischemic myelopathy [13–15]. Magnetic resonance imaging of the spine has become the method of choice in humans and small companion animals to evaluate intervertebral disc degeneration by applying a 1-5 MRI degeneration grading scale on T2-weighted images [16,17]. Also, sequences have been introduced to evaluate the biochemical composition of the nucleus pulposus [18]. Accompanying signal changes of the adjacent vertebral endplates and bodies have been evaluated with MRI and described as Modic changes type I (bone edema and inflammation), type II (conversion of the red hematopoietic bone marrow to yellow fat due to bone marrow ischemia), and type III (subchondral bone sclerosis) [19]. These changes have been shown to be related to low back pain in humans [20]. However, a recent systematic review has stated that associations between Modic changes and low back pain are inconsistent and studies may be biased in a positive associative direction [21].

Patient size in relation to gantry diameter has so far limited the use of MRI for examination of the lower equine cervical spine and published anatomical and pathological studies are mostly cadaver studies [22–25]. Given the fast development of technology and considering the fact that CT of the cervical spine is currently feasible [26], MRI of the cervical spine in live horses might not be too far off. Based on our review of the literature, neither magnetic resonance sequences that show equine intervertebral disc degeneration, nor MRI features of the non-degenerated and degenerated equine intervertebral disc have been reported in literature neither proof of concept. Furthermore, no comparison of these features to gross pathology findings has been reported thus far.

The aims of the present study were: (a) to describe the MRI features of non-degenerated and degenerated intervertebral discs in the horse that were macroscopically detectable, (b) to test associations between spinal location and macroscopic degeneration or MRI-detected annular protrusion and between MRI-detected annular protrusion and macroscopic degeneration, and (c) to define MRI sequences on which equine cervical intervertebral disc degeneration can be identified. It was hypothesized that MRI-detected annular protrusion would have a positive association with macroscopic intervertebral disc degeneration.

MATERIAL AND METHODS

Horses

Horses included in this exploratory methods comparison study were those that had shown clinical signs related to the neck region (such as spinal ataxia, neck pain). All horses were originally presented to the Utrecht University Equine Clinic and had been evaluated by a European College of Veterinary Surgeons-certified surgeon (W.B.) and/or European College of Equine Internal Medicine-certified internal medicine specialist (I.D.W.). Thereafter, these horses were included in an *ex vivo* study on the pathologic aspects of intervertebral disc degeneration published elsewhere.⁶ The current study included only those cases in which MRI scanning and dissection within 4 h of death could be realized. Decisions for subject inclusion or exclusion were made by a European College of Veterinary Diagnostic Imaging-certified veterinary radiologist (S.V.). Clinical records were reviewed for breed, age, sex, and clinical signs possibly related to the neck region. All horses were client-owned, owner-signed informed consent was obtained in accordance with Dutch legislation, and anonymity was preserved.

Data acquisition and interpretation

MRI

Postmortem MRI scans (1.5 T MRI system; Philips Ingenia, Eindhoven, the Netherlands) of the cervical vertebral column in right lateral recumbency were performed after separating the neck from the body between the second and third thoracic vertebrae within 1-3 h after euthanasia. Magnetic resonance imaging of the complete ($n = 9$) or partial ($n = 2$; occiput to C5 and C4 to T2) cervical spines was performed within 4 h following euthanasia. Magnetic resonance imaging scanning times were limited to 2 h as gross, histopathologic, and biochemical examination and sampling was performed afterward. Images were acquired (large anterior coil left lateral aspect, table posterior coil at the right lateral dependent side) mostly in the sagittal plane in

accordance with midsagittal dissection afterward. Sequences included sagittal two-dimensional T1-weighted turbo SE, two-dimensional T2-weighted turbo SE (with and without fat saturation), two-dimensional proton density turbo SE (with and without fat saturation), and transverse three-dimensional T1-weighted turbo field echo. The cartilage sensitive sagittal three-dimensional water selective cartilage (fast field echo, principle of selected excitation technique, three-dimensional T1 weighted) and fluid sensitive three-dimensional water selective fluid (fast field echo, principle of selected excitation technique) sequences were introduced in anticipation of the different intervertebral disc composition in the equine species (Table 1).

Table 1. A general overview of the applied MRI sequence details.

Manufacturer name	Generic name	TR (ms)	TE (ms)	Flip angle (degrees)	Slice thickness (mm)	Interslice (mm)	FOV (mm)	Matrix	Fat sat	NSA
T1W TSE	2D T1W TSE	583	8	90	2.5	-	420x190x50	600 x 215 (recm960)	-	3
T2W TSE (SPAIR)	2D T2W TSE	3048	124	90	2.5	-	420x190x50	600 x 208 (672)	- (ProSet)	2
PDW aTSE (SPIR)	2D PDW TSE	4500	30	90	2.27	-	420x190x50	1008x306 (1024)	- (Proset)	2
T1 TFE 3D	3D T1 TFE	8.1	4.6	25	1.2	-	240x202x155	200x 166 (432)	TFE 256	4
3D WATSc CLEAR	3D T1 FFE fat sat	20	7.6	25	2.5	-	420x190x50	620x238 (1024)	Proset Fat supp 1331	2
WATScf	3D FFE fat sat	20	8	50	3	-	420x187x75	852x380 (1024)	Proset Fat supp 1331	1

Notes: TR, Time of Repetition; TE, Time of Echo; FOV, Field of View; Fat Sat, Fat Saturation; NSA, Number of Signal Averages; T1W, T1 weighted; TSE, Turbo Spin Echo; SPAIR, Spectral Attenuated Inversion Recovery; SPIR, Spectral Presaturation with Inversion Recovery; FFE, Fast Field echo; TFE, Turbo Field Echo; WATSc, Water Selective cartilage; CLEAR, Constant Level Appearance; WATScf, Water Selective fluid; Fat supp, Fat suppression; Proset, Principle of Selected Excitation Technique

A European College of Veterinary Diagnostic Imaging-certified veterinary radiologist (S.V.) evaluated the MRI of the cervical intervertebral discs using the available picture archiving and communication system (Impax, AGFA Healthcare, Belgium) during a first evaluation session. During this session the MRI findings in the non-degenerated and degenerated intervertebral discs, as defined by macroscopic assessment, were defined. Sequences per horse were evaluated altogether, with the radiologist not blinded to macroscopic assessment results (non-degenerated or degenerated). Magnetic resonance imaging signal intensity compared to the adjacent muscle signal intensity, signal intensity distribution (dorsal, mid, ventral, rostral, caudal) in the different sequences, and

possible visibility of the nucleus pulposus (0, visible; 1, vaguely defined; 2, not visible), intervertebral disc endplate cartilage, vertebral endplate, epiphysis, physis, and spinal cord were descriptively evaluated for midsagittal images (Figure 1). Annular protrusion at C2 to T1 was graded as grade 1 = equal to dorsal aspect of vertebral body, grade 2 = minimal dorsal bulging with respect to vertebral body, grade 3 = moderate dorsal bulging without reaching the spinal cord, and grade 4 = severe dorsal bulging/extrusion of disc material with contact or deformation of the spinal cord (Figure 1). Image quality and detection of anatomic details or changes were evaluated to define MRI sequences that were able to depict equine intervertebral disc degeneration.

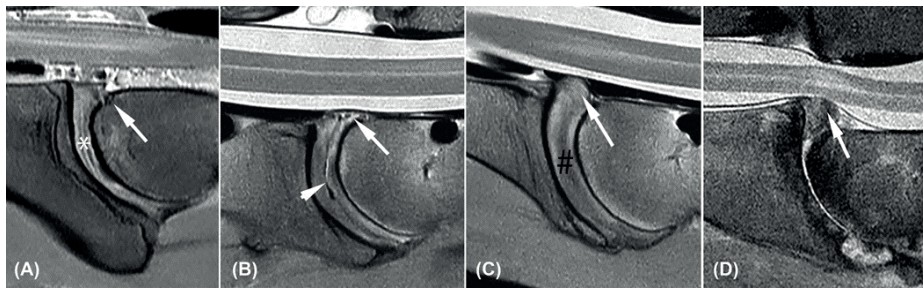


Fig. 1. Annular protrusion grading (white arrows) and visibility scoring of the nucleus pulposus; (A) Annulus protrusion grade 1, equal to dorsal aspect of vertebral body and visible nucleus pulposus (white asterisk); (B) annulus protrusion grade 2, minimal dorsal bulging with respect to vertebral body and gas in the central part of the discus (white arrowhead); (C) annulus protrusion grade 3, with moderate dorsal bulging without reaching the spinal cord, (black #); (D) severe dorsal bulging of disc material with contact and deformation of the spinal cord.

A second evaluation session of the MRI images was performed 1 year after the first evaluation. Degeneration status on MRI (non-degenerated = ND, degeneration = D) was scored by the same radiologist (S.V.), blinded for macroscopic assessment results and horse number. For this, all intervertebral discs per horse were evaluated at once using all available sequences, as would be the same for clinical situations. Criteria for decision-making were extrapolated from the first session and included (a) the presence of a hypointense signal area in the intervertebral disc in proton density turbo SE sequence, (b) vaguely defined or absent visibility of the nucleus pulposus, and/or (c) presence of a signal void in the intervertebral disc on gradient echo sequences.

Additional findings that were visible on the available MRI and that were potentially attributable to intervertebral disc degeneration were recorded including facet joint pathology (fragmentation or severe enlargement of articular facet), vertebral

morphologic variations, and spinal cord signal changes on MRI. Reviewing of available pre-mortem radiographic examinations for pathology including facet joint pathology and vertebral morphologic variations was performed.

Macroscopic assessment

Following MRI scanning the cadaver necks were dissected further and cut along the sagittal midline for macroscopic assessment of the intervertebral discs by a European College of Veterinary Pathologists- certified pathologist (W.B.), blinded to the MRI findings. The gross examination assessed presence or absence of fibrillation, cleft formation (with gas or associated hemorrhage) and discoloration of the annulus fibrosus and/or nucleus pulposus [6]. For the purpose of the current study, the intervertebral discs were scored as non-degenerated versus degenerated.

Statistical analysis

Descriptive statistics and statistical analysis were performed by a statistician (H.V.) using statistical analysis freeware (R version 3.4.4, Foundation for Statistical Computing, Vienna, Austria) [27].

Associations between factors spinal location (from C2-C3 to C7- Th1) and MRI-detected annulus protrusion (defined as grades 1 to 4), and outcome macroscopic assessment (defined as non-degenerated versus degenerated) were assessed with mixed-effect logistic regression model [28]. "Horse" (numbers 1-11) was considered a random effect. The number of observations was small and not all horses had complete data. Spinal location was combined for C2 to C5 versus C5 to T1 and annular protrusion grade 3 and 4 were grouped (grade 3+4) for analysis. Furthermore, annular protrusion grade 2 was also grouped with grade 3+4 (grade 2+3+4) for evaluation. Thereafter, odds ratio and 95% confidence interval were calculated.

RESULTS

Eleven horses were included (10 Dutch Warmbloods and one Appaloosa; median age: 9 years, range 9 months to 16 years, four mares, one stallion, and six geldings). Clinical recorded signs were spinal ataxia, (severe) neck pain, reduced range of neck motion, and lameness. Horse 10 was presented with an acute onset of severe spinal ataxia following a fall 1 week prior to presentation, but had a history of a minor degree of ataxia for many years (Supporting Information 1).

There were 65 intervertebral discs available for macroscopic evaluation (45 non-degenerated, 20 degenerated; see Table 3) and 60 intervertebral discs for MRI evaluation (42 non-degenerated, 18 degenerated). See Supporting Information 1-3 for all results per horse, intervertebral disc and for MRI-degeneration score, and nucleus pulposus visibility.

MRI sequences

The application of mainly sagittal sequences (comparable to midsagittal dissection and enclosing two to three intervertebral discs in one image) with the largest possible field-of-view necessitated three times (time consuming) repositioning of the coil and cadaver neck. This resulted in limitation of the imaging protocol to these sequences during this study.

All applied MRI sequences evaluated provided anatomic detail of the intervertebral disc and surrounding structures and all enabled grading of annular protrusion during the first evaluation session. Proton density sequence was essential for intervertebral disc degeneration detection, while T2-weighted-turbo SE was least informative due to low contrast resolution of the intervertebral disc structures and surrounding anatomy. Fat saturation proton density and T2-weighted sequences had both more artifacts and reduced detail. The gradient-recalled echo sequences (three-dimensional T1-turbo field echo, the three-dimensional water selective cartilage, and three-dimensional water selective fluid) did show small signal voids due to the presence of gas in clefts or hemorrhage in some intervertebral discs. The three-dimensional water selective cartilage provided high contrast images of the intervertebral disc and, more important, of the intervertebral disc cartilage endplate. Three-dimensional water selective fluid was not of additional value.

MRI assessment

MRI descriptive characteristics of macroscopically non-degenerated intervertebral discs (n = 42)

The annulus fibrosus was moderately homogeneous isointense compared to surrounding musculature in T1W images with small and vaguely defined hypointense areas in the dorsal and mid-caudal aspect (Figure 2). The annulus was irregularly and moderately hyperintense compared to musculature on T2-weighted and proton density (Figure 2A) images with minimally hypointense areas at the dorsal, mid-caudal, and ventral aspect, and slightly irregular hyperintense on water selective cartilage (Figure 2B). The nucleus pulposus presented as a very slim hyperintense core surrounded by a thin hypointense rim in the cranial mid-area of the intervertebral disc

space in T2- weighted and proton density images; this was slightly less distinct on water selective cartilage images. On T1-weighted images only a small hypointense line was visible at the caudal aspect of the nucleus pulposus. The cartilaginous endplates of the intervertebral disc were visible between the annulus fibrosus and vertebral endplates as a separate less than 1 mm thick hyperintense line compared to surrounding structures in water selective cartilage and T1-weighted images (Figure 2B). The vertebral endplates presented as well-defined hypointense lines of approximately 1.5-2 mm thickness in all sequences. They were slightly thinner in the ventral part of the cranial endplate. The epiphyseal areas showed varying degrees of hyperintensity on T1-weighted, T2-weighted, and proton density images and were hypointense on fat saturated images, which is consistent with the presence of fatty tissues.

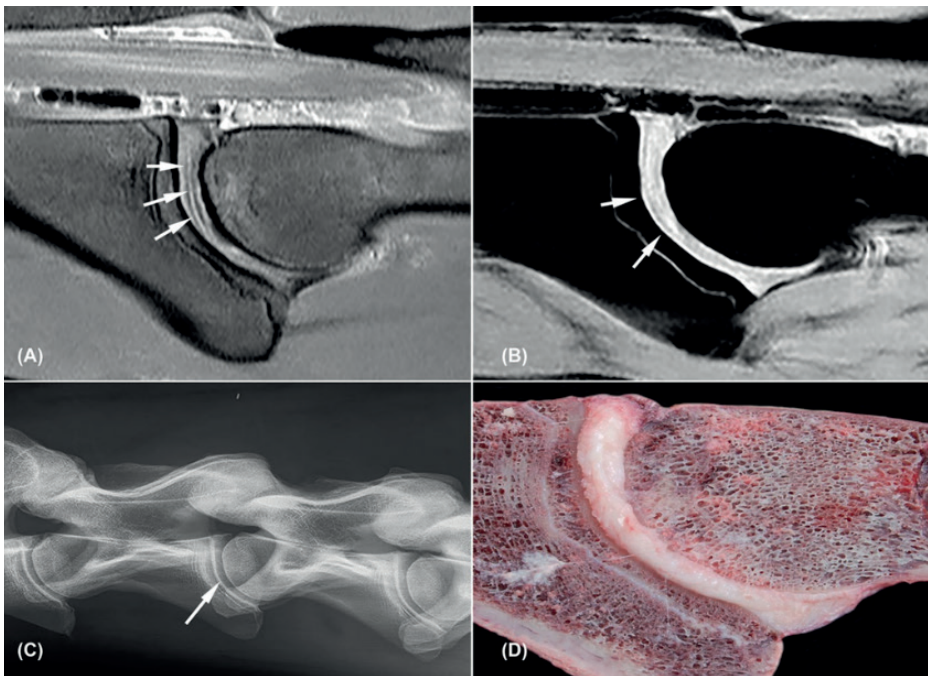


Fig. 2. Non-degenerated C3-C4 intervertebral disc (horse 2). All images are oriented with cranial to the left side of the image and dorsal to the topside of the image. A, Sagittal proton density weighted image; the nucleus pulposus is visible as a very slim hyperintense core surrounded by a thin hypointense rim (white arrows); B, sagittal water selective cartilage image, note the cartilaginous endplate visible as a thin hyperintense line parallel to the vertebral bone surface (white arrows); C, radiograph of C2 to C5 with centrally located intervertebral disc space C3-C4 (white arrow); D, macroscopic image.

MRI descriptive characteristics of macroscopically degenerated intervertebral discs (n = 18)

The annulus fibrosus contained moderately patchy to diffuse hypointense areas, which were subjectively most clearly defined in proton density images (Figures 3 and 4). These areas were more distinct and expanded further in dorsal and ventral directions compared to the above-described small and vaguely defined hypointense areas in the dorsal and mid-caudal aspect of the normal intervertebral discs. The delineation of the nucleus pulposus was irregular vaguely defined or completely absent (Supporting Information 2 and 3). Gradient-recalled echo sequence signal voids and/or susceptibility artifacts were seen mostly in the center of the intervertebral disc (at the level of the nucleus pulposus), consistent with bleeding and/or gas in a macroscopically ruptured intervertebral disc. Signal voids were seen in the dorsal aspect of the dorsal annulus toward the vertebral canal in one C6-C7 intervertebral disc (Figure 3b). The vertebral structures, intervertebral disc endplate cartilage, and spinal cord were comparable to the previously described non-degenerated intervertebral discs in all cases except one horse (horse 10; Figure 4). In this specific case, a complete collapse with associated dorsal extrusion and protrusion of disc material (annulus protrusion grade 4) and minimal vertebral subluxation due to tilting of the cranial aspect of C7 was noted. Severe shape and signal changes of the vertebral endplates and bodies were present showing as patchy hypointense signal on all sequences and varying from vaguely defined hyperintense areas in fat saturated proton density to more well-defined areas on Water selective cartilage images. The spinal cord dorsal to this intervertebral disc had an ill-defined hyperintense signal on T2-weighted and proton density images (Figures 4a and 4b). Gross pathological examination showed a complete collapse of the intervertebral disc space with severe remodeling of the vertebral endplates and bodies and greenish extruded disc material associated with hemorrhage in the vertebral canal (Figure 4d).

MRI annular protrusion grading

Annular protrusion (grade 2 to 4) was present in 26 of 30 caudal (C5 to T1) versus 13 of 31 cranial (C2 to C5) intervertebral discs. No (grade 1), minimal (grade 2), moderate (grade 3), and severe (grade 4) annulus protrusion was seen in 22, 29, nine, and one intervertebral discs, respectively (Table 2).

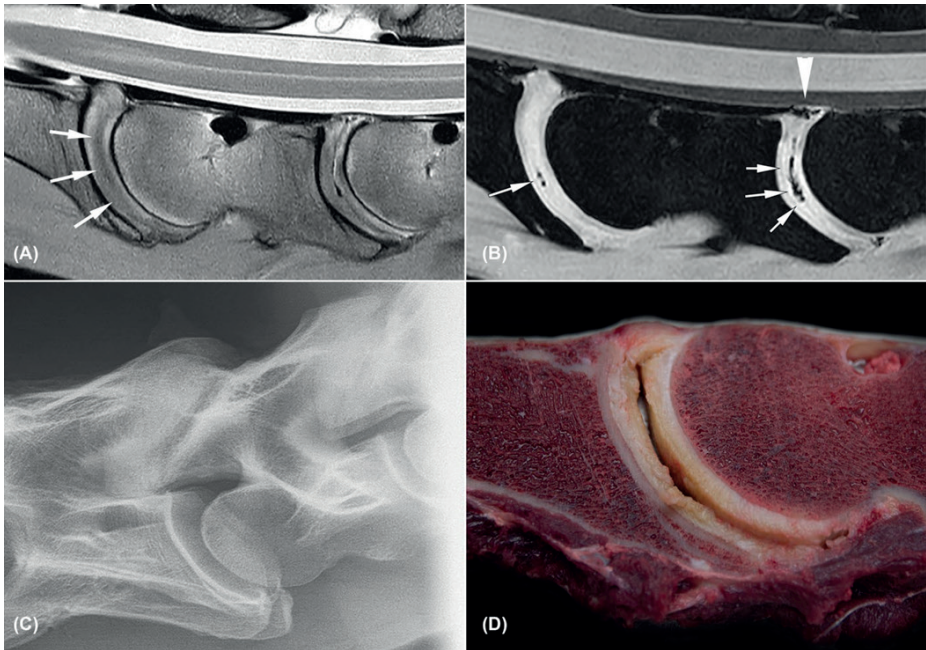


Fig. 3. Severely degenerated C5-C6 and C6-C7 intervertebral discs with cleft formation (horse 7). All images are oriented with cranial to the left side of the image and dorsal to the topside of the image. A, Sagittal proton density weighted image; diffuse hypointense areas are noted throughout the intervertebral discs with loss of definition of the nucleus (white arrows); B, sagittal water selective cartilage image; signal voids are noted in the clefts (white arrows) and dorsal aspect at the dorsal longitudinal ligament of C6-C7 (white arrow head); C, radiograph of C6-C7 depicts moderate degenerative joint disease but no changes at the intervertebral disc space; D, macroscopic image of C6-7 with a large cleft centrally, fibrillation, and yellow discoloration. The dorsal longitudinal ligament tear is not visible in this image.

Table 2. Frequency distribution of MRI-detected annulus protrusion grade (1-4) per spinal location (C2-C3 to C7-T1).

	MRI-annulus protrusion grade			
	1	2	3	4
All discs	21	29	9	1
C2-C3	7	3	0	0
C3-C4	6	2	2	0
C4-C5	4	5	1	0
C5-C6	1	8	1	0
C6-C7	0	6	3	1
C7-T1	3	5	2	0

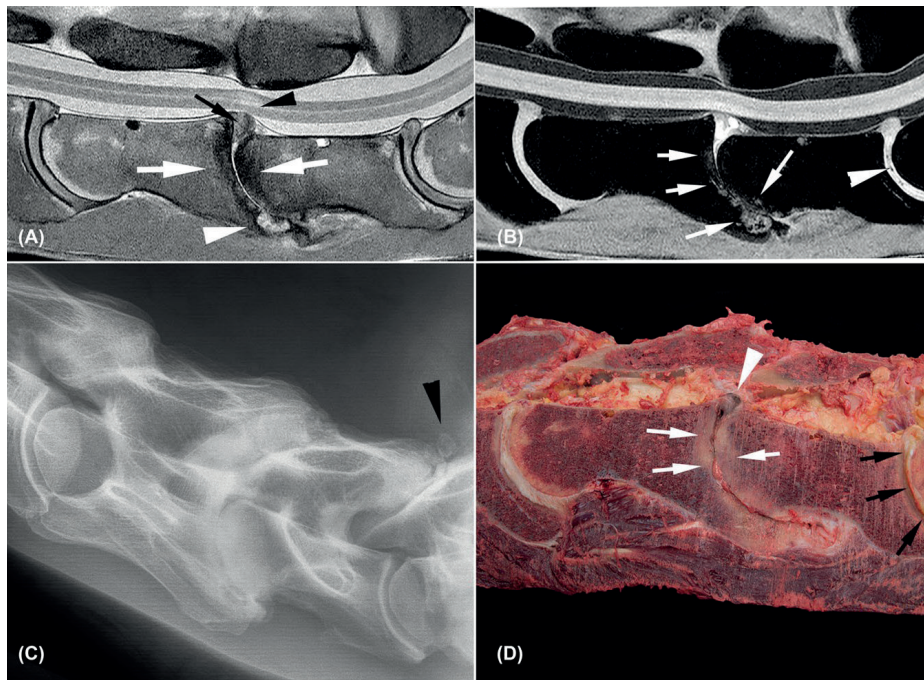


Fig. 4. Severely degenerated C6-C7 and C7-T1 intervertebral discs with complete collapse of C6-C7 (horse 10). All images are oriented with cranial to the left side of the image and dorsal to the topside of the image. A, Sagittal proton density weighted image; vertebral endplates of C6-C7 are diffusely hypointense (white arrows) with a hyperintense area ventrally (arrowhead) and grade 4 annulus protrusion of disc material (black arrow) with adjacent intra-medullary hyperintense signal (black arrowhead) and dorsal displacement of the spinal cord. C5-C6 and C7-T1 intervertebral discs show diffuse hypointense areas with grade 1 and grade 3 annulus protrusion. B, Sagittal water selective cartilage image; C6-C7 irregular hyperintense areas are seen in the vertebral endplates (white arrows) and hyperintense signal at the remaining disc material. Small signal voids are noted in the intervertebral disc of C7-T1 (white arrowhead); C, radiograph shows complete collapse with severe remodeling of the vertebral endplates at C6-C7 together with severe degenerative joint disease and mild ventral subluxation of C7. Separate mineralizations are noted dorsal to the facet joints of C7-T1 (black arrowhead) and the intervertebral disc space is slightly narrower compared to C5-C6 intervertebral disc space; D, macroscopic image; severe remodeling of the vertebral endplates (white arrows), dark discoloration of the dorsal protruding disc material at C6-C7 (white arrowhead). Severe cleft formation, fibrillation, and yellow discoloration of the C7-T1 intervertebral disc (black arrows)

MRI degeneration status grading

Degeneration grading performed during the second evaluation session resulted in 37 intervertebral discs being scored as non-degenerated and 24 intervertebral discs scored as degenerated (See Supporting Information 2 and 3). Discrepancy of the MRI

degeneration grading with macroscopic assessment was noted in 16 (MRI grade 11 degenerated, five non-degenerated) intervertebral discs of 60 evaluated discs.

Macroscopic assessment

Macroscopic assessment was performed in 65 discs (of which 60 intervertebral discs were also evaluated with MRI) and not possible in one C4-C5 intervertebral disc (Supporting Information 1), which was excluded from further statistical analysis. Of the discs evaluated with MRI, 42 intervertebral discs were judged as non-degenerated and 18 as degenerated, with most of the degenerated discs located at C6-C7 (5/18) and C7-T1 (5/18). It was remarkable that gross degeneration of all intervertebral discs was observed in one horse (horse 6), while in two other horses (horses 1 and 4) none of the intervertebral discs showed signs of gross degeneration. Intervertebral disc degeneration was detected in 13 of 30 caudal (C5 to T1) versus five of 30 cranial (C2 to C5) intervertebral discs. On gross pathological examination, hemorrhage and tearing of the dorsal longitudinal ligament was noted at a degenerated and torn intervertebral disc at C6-C7 in one Dutch Warmblood (horse 7) with a grade 3 annular protrusion without changes in shape or signal of the spinal cord, vertebral endplates, or intervertebral disc space width on MRI.

Additional MRI and radiographic findings

Radiography premortem was available in nine horses, with the following additional findings. Severe deformation of a right-sided C5-C6 facet joint due to osteochondrosis, bilaterally severely enlarged facet joints at C6-C7, and axially positioned rounded, focal, mineralized areas with enlargement of the left-sided facet joint of C7-T1 were found in one horse (horse 5). Intervertebral discs of C5-C6 to C7-T1 showed macroscopic signs of degeneration in this horse. A rounded, solitary area of dystrophic mineralization was present in the soft tissue axial to the first left rib head with severe intervertebral disc degeneration of C7-T1 in one horse (horse 7). Horse 10 that showed complete collapse of the intervertebral disc space had severe facet joint arthrosis at C6-7 and bilateral mineralisation in the soft tissue dorsal to C7-T1. Morphologic variations, more specifically a shift of the transverse process ventral lamina of C6 to C7, were seen on the sagittal MRI images in four Dutch Warmblood horses (36%); bilateral in two (horses 2 and 11) and unilateral in the other two (horses 4 and 6). Macroscopic intervertebral disc degeneration was found in these four horses and involved the intervertebral discs at C6-7 and C7-T1 in two and three horses, respectively.

Table 3. Odds ratio (95% CI) of the univariable mixed-effect logistic regression model for macroscopic degeneration status with MRI-detected annulus protrusion and spinal location in 11 horses.

	Macroscopy Normal	Macroscopy Degenerated	OR
	n (%)	n (%)	(95%CI)
Annulus (n=60)	42 (70.0)	18 (30.0)	
Grade 1 (Ref.)	19 (45.2)	2 (11.1)	1.0
Grade 2	19 (45.2)	10 (55.6)	6.5 (0.91-45.9)
Grade 3-4	4 (9.5)	6 (33.3)	40.6 (2.1-776.6)
Location (n=65)	45 (69.2)	20 (30.8)	
C2-C3 (Ref.)	10 (22.2)	1 (5.0)	1.0
C3-C4	10 (22.2)	1 (5.0)	1.0 (0.02-63.1)
C4-C5	7 (15.6)	3 (15.0)	10.6 (0.3-396.8)
C5-C6	10 (22.2)	1 (5.0)	1.0 (0.02-63.1)
C6-C7	4 (8.9)	7 (35.0)	143.8 (2.6-7869.1)
C7-T1	4 (8.9)	7 (35.0)	143.8 (2.6-7869.1)
Location (n= 65)	45 (69.2)	20 (30.8)	
C2-C5 (Ref.)	27 (60.0)	5 (25.0)	1.0
C5-T1	18 (40.0)	15 (75.0)	7.1 (1.6-30.8)

Note: OR= odds ratio, CI= confidence interval, Ref. = reference

Statistical analysis

Mixed-effect logistic regression modeling with “horse” as random effect was performed (Table 3). The odds to have macroscopic degeneration with annular protrusion grade 2 was higher than the odds to have annular protrusion grade 1 and for grade 3+4 even higher with a very wide confidence interval indicative for the small data set (Table 3). A statistically significant association between annular protrusion and macroscopic intervertebral disc degeneration was found by applying the mixed-effect model for annular protrusion grade 1 versus grade 2+3+4 (OR 8.1, 95% confidence interval, 1.3-50.5).

Macroscopic degeneration was found to be statistically significantly associated with spinal location (Table 3). Spinal location C4-C5, C6- C7, and C7-T1 showed an increased risk for macroscopic degeneration compared to C2-C3, although the confidence intervals are very wide. Location was thereafter recoded on cranial (C2 to C5) versus caudal (C5 to T1), resulting in higher odds to find macroscopic degeneration in the caudal than cranial cervical vertebral column (odds ratio 7.1, 95% confidence interval, 1.6-30.8). The model including both spinal location (C5-T1 vs C2-C5) and annular protrusion (3+4 vs 1 and 2) did not result in statistically significant associations with macroscopic degeneration (odds ratio = 3.1, 95% confidence interval 0.6-16.1 and odds ratio = 4.3, 95% confidence interval, 0.6-32.7, respectively).

DISCUSSION

Based on our review of the literature, this is the first published study to describe ex vivo MRI findings in non-degenerated and degenerated equine intervertebral discs. The study provides proof-of-concept of the potential for using MRI to depict macroscopically detectable equine intervertebral disc degeneration. Nucleus and annulus degeneration can be detected in proton density images; annulus protrusion and/or extrusion can be detected in all images. Cleft formation in the disc, within some instances the associated hemorrhage and/or gas collection, can be detected in gradient-recalled echo sequences such as water selective cartilage. Results from the second evaluation session demonstrate, however, some discrepancy in degeneration grading (non-degenerated vs degenerated) between MRI and macroscopic assessment in 16 of 60 intervertebral discs. Discrepancy was greatest for discs assessed as non-degenerated by macroscopy but degenerated with MRI, which can indicate a need to further specify MRI features of disc degeneration. From this study, it appeared that grade 2 and 3-4 of MRI-detected annular protrusion did have higher odds than grade 1 to have intervertebral disc degeneration on gross pathology. Macroscopic degeneration (n = 18) was statistically significantly associated with the spinal location with a wide confidence interval as described before.⁶ It should be realized that macroscopic degeneration was seen in 13 of 30 caudal (C5 to T1) versus five of 30 cranial (C2 to C5) intervertebral discs that were also evaluated by MRI.

The results of our study show that the nucleus pulposus dehydration-based T2 sequences as applied in humans and dogs [16,17] are most likely less suited for MRI evaluation of the equine intervertebral disc. This is probably due to the fact that the annular and nucleus part in this species consist of fibrous and cartilaginous tissues and were irregularly hypointense on T2 sequence while being more consistent in signal intensity in proton density images [6]. Visibility of the nucleus pulposus in proton density and T2 sequences was reduced in macroscopically degenerated intervertebral discs (Supporting Information 2 and 3). This might be caused by diffuse fibrillation and therefore structural changes of both fibrous as well as cartilaginous tissues as scored with macroscopy.

The current study used mainly routine (proton density, T2-weighted, and T1-weighted) MRI sequences in the sagittal plane. For further evaluation of adjacent anatomic structures such as exiting nerves, transverse or dorsal images should be included. However, these were considered outside the scope of this study and were not performed due to limited scanning time. It should however be considered that

other sequences in different planes perform better in detection of different aspects of equine disc degeneration, such as lateralized annular protrusion or early stage of degeneration. An in-depth MRI study of histopathological confirmed degenerated discs, using different sequences and imaging planes is needed to gain further insight. This being said, histopathology results of intervertebral disc degeneration have not been conclusive yet and the macroscopic appearance has been more discriminative so far [6]. Furthermore, both in dogs and humans histological scoring of intervertebral disc degeneration is validated by macroscopic grading among others [29]. This might also explain the discrepancies between the macroscopic and MRI assessments of intervertebral disc degeneration during the second evaluation session and may reflect the fact that MRI makes use of the biochemical composition of tissues for image formation.

The susceptibility of the gradient-recalled echo sequence as can be seen with cleft formation or tearing of the intervertebral disc proved to add useful information. The presence of gas due to vacuum phenomenon is well known in disc degeneration and can be helpful in identifying degenerated intervertebral discs [30]. Water selective cartilage sequence (brand-specific) is a less common MRI sequence that was previously reported to be excellent for cartilage evaluation [31]. Equivalent sequences exist in other high-field MRI systems and are known as fat saturated three-dimensional T1-weighted fast field echo, or fast-low angle shot. Water selective cartilage provided good means to evaluate the intervertebral disc cartilaginous endplate, a structure thought to play a crucial role in nutrient transport to the intervertebral disc [3].

Equine vertebral morphologic variations, vertebral pathology, and their clinical manifestations have previously been described [32],33 The small group of horses in this study presented varying clinical signs related to the cervical area. The severe spinal ataxia of the horse with the collapsed intervertebral disc (horse 10) and associated changes to the spinal cord were considered a direct consequence of the macroscopically visible intervertebral disc extrusion. The tear in the dorsal longitudinal ligament and hemorrhage in concurrence with a degenerated disc in the horse with low neck pain and ataxia (horse 7) were also considered causative. A low volume-high velocity disc extrusion with fibrocartilaginous embolism might have caused spinal cord damage in this horse [14]. Other relationships of the recorded MRI and macroscopic degenerative findings to the clinical signs are possible, but need further in-depth clinical studies. The clinical manifestation of low back pain in humans with lumbar intervertebral disc degeneration varies greatly between individuals [20]. In addition to intervertebral disc degeneration, pain also appears to correlate inconsistently with vertebral Modic

changes grade 1 (bone edema and inflammation) and discal endplate lesions [19–21]. In the current study, Modic changes or vertebral endplate lesions were not observed except in the horse with the completely collapsed intervertebral disc space at C6-C7 (horse 10). Early intervertebral disc degeneration in humans and small companion animals is mostly characterized by loss of proteoglycans and therefore loss of osmotic pressure and hydration in both nucleus pulposus and annulus fibrosis [34]. In a later stage, replacement of type II-collagen fibers with type I-collagen fibers occurs [34]. Both events provoke changes in mechanical and tensile properties, which can cause morphological changes such as decreased intervertebral disc width and protrusion and/or extrusion due to tearing of the annulus [34].

Annular protrusion detected with MRI shows an association with macroscopic intervertebral disc degeneration, even in this small group of horses. This is potentially of great clinical relevance, as focal disruption of the annulus fibers with fibro-cartilage has been described in horses as a possible cause of protrusion, fibrocartilaginous embolism, or intervertebral disc collapse with varying clinical complications [5,14]. Annulus protrusion and spinal cord diameter can be evaluated by the currently available in vivo imaging methods such as myelography or vertebral canal endoscopy [35,36]. However, these techniques are more invasive and will not provide additional information of changes in the intervertebral disc, spinal cord, nerve roots, and vertebrae. This study shows as proof-of-concept that MRI can offer an important additional benefit and that further application for the diagnosis of intervertebral disc degeneration in horses needs to be further investigated. To date, published reports on MRI of the equine cervical spine in live horses are very scarce due to the technical limitations, but it can be expected that these will be overcome in the future.

It is concluded that macroscopically confirmed degeneration in the equine cervical intervertebral disc can be detected with MRI and the best sequence to do so is the proton density turbo SE in combination with a gradient-recalled echo sequence. Furthermore, intervertebral disc degeneration was noted to be associated to caudal spinal location; annular protrusion on MRI had higher odds to have macroscopic degeneration of the equine cervical intervertebral disc. Magnetic resonance imaging of the equine cervical spine is a still scarcely available but promising technique. Further research is needed to improve practical feasibility and determine its full clinical potential in unraveling the cervical pathology in horses and hence the benefits of its clinical application.

Acknowledgements: The authors would like to thank Prof. Dr. P. R. van Weeren and Prof. Dr. J.W. Hesselink for their help in preparing this manuscript.

REFERENCES

1. Bergknut N, Grinwis G, Pickee E, et al. Reliability of macroscopic grading of intervertebral disk degeneration in dogs by use of the thompson system and comparison with low-field magnetic resonance imaging findings. *Am J Vet Res.* 2011;72(7):899-904.
2. Gopal D, Ho AL, Shah A, Chi JH. Molecular basis of intervertebral disc degeneration. *Adv Exp Med Biol.* 2012;760:114-133.
3. Tomaszewski KA, Adamek D, Konopka T, Tomaszewska R, Walocha JA. Endplate calcification and cervical intervertebral disc degeneration: The role of endplate marrow contact channel occlusion. *Folia Morphol.* 2015;74(1):84-92.
4. Bollwein A, Hanichen T. Age-related changes in the intervertebral disks of the cervical vertebrae of the horse. *Tierarztl Prax.* 1989;17(1):73-76.
5. Yovich JV, Powers BE, Stashak TS. Morphologic features of the cervical intervertebral disks and adjacent vertebral bodies of horses. *Am J Vet Res.* 1985;46(11):2372-2377.
6. Bergmann W, Bergknut N, Veraa S, et al. Intervertebral disc degeneration in warmblood horses: Morphology, grading, and distribution of lesions. *Vet Pathol.* 2018;55(30):442-452.
7. Foss RR, Genetzky RM, Riedesel EA, Graham C. Cervical intervertebral disc protrusion in two horses. *Can Vet J.* 1983;24(6):188-191.
8. Furr MO, Anver M, Wise M. Intervertebral disk prolapse and diskospondylitis in a horse. *J Am Vet Med Assoc.* 1991;198(12): 2095-2096.
9. Jansson N. What is your diagnosis? Multiple cervical intervertebral disk prolapses. *J Am Vet Med Assoc.* 2001;219(12):1681-1682.
10. Nixon AJ, Stashak TS, Ingram JT, Norrdin RW, Park RD. Cervical inter-vertebral disc protrusion in a horse. *Vet Surg.* 1984;13:154-158.
11. Speltz MC, Olson EJ, Hunt LM, Pool RR, Wilson JH, Carlson CS. Equine intervertebral disk disease: A case report. *J Equine Vet Sci.* 2006;26(9):413-419.
12. Stadler P, van den Berg SS, Tustin RC. Cervical intervertebral disk prolapse in a horse. *J S Afr Vet Assoc.* 1988;59(1):31-32.
13. Fuentealba IC, Weeks BR, Martin MT, Joyce JR, Wease GS. Spinal cord ischemic necrosis due to fibrocartilaginous embolism in a horse. *J Vet Diagn Invest.* 1991;3(2):176-179.
14. Sebastian MM, Giles RC. Fibrocartilaginous embolic myelopathy in a horse. *J Vet Med A Physiol Pathol Clin Med.* 2004;51(7-8): 341-343.
15. Taylor HW, Vandeveld M, Firth EC. Ischemic myelopathy caused by fibrocartilaginous emboli in a horse. *Vet Pathol.* 1977;14(5):479-481.
16. Pfirrmann CW, Metzendorf A, Zanetti M, Hodler J, Boos N. Magnetic resonance classification of lumbar intervertebral disc degeneration. *Spine (Phila Pa 1976).* 2001;26(17):1873-1878.
17. Bergknut N, Auriemma E, Wijsman S, et al. Evaluation of intervertebral disk degeneration in chondrodystrophic and nonchondrodystrophic dogs by use of pfirrmann grading of images obtained with low-field magnetic resonance imaging. *Am J Vet Res.* 2011;72(7):893-898.
18. Stelzeneder D, Trattnig S. Biochemical magnetic resonance imaging of intervertebral discs and facet joints. *Radiologe.* 2010;50(12): 1115-1119.
19. Modic MT, Steinberg PM, Ross JS, Masaryk TJ, Carter JR. Degenerative disk disease: Assessment of changes in vertebral body marrow with MR imaging. *Radiology.* 1988;166(1):193-199.

20. Luoma K, Vehmas T, Kerttula L, Gronblad M, Rinne E. Chronic low back pain in relation to Modic changes, bony endplate lesions, and disc degeneration in a prospective MRI study. *Eur Spine J.* 2016;25(9): 2873-2881.
21. Herlin C, Kjaer P, Espeland A, et al. Modic changes-their associations with low back pain and activity limitation: A systematic literature review and meta-analysis. *PLoS One.* 2018;13(8):e0200677.
22. Gutierrez-Crespo B, Kircher PR, Carrera I. 3 tesla magnetic resonance imaging of the occipitoatlantoaxial region in the normal horse. *Vet Radiol Ultrasound.* 2014;55(3):278-285.
23. Janes JG, Garrett KS, McQuerry KJ, et al. Comparison of magnetic resonance imaging with standing cervical radiographs for evaluation of vertebral canal stenosis in equine cervical stenotic myelopathy. *Equine Vet J.* 2014;46(6):681-686.
24. Mitchell CW, Nykamp SG, Foster R, Cruz R, Montieth G. The use of magnetic resonance imaging in evaluating horses with spinal ataxia. *Vet Radiol Ultrasound.* 2012;53(6):613-620.
25. Sleutjens J, Cooley AJ, Sampson SN, et al. The equine cervical spine: Comparing MRI and contrast-enhanced CT images with anatomic slices in the sagittal, dorsal, and transverse plane. *Vet Q.* 2014;34(2):74-84.
26. Kristoffersen M, Pulchalski S, Skog S, Lindegaard C. Cervical computed tomography (CT) and CT myelography in live horses; 16 cases. *Equine Vet J.* 2014;46(547):11.
27. R Core Team. *R: A Language and Environment for Statistical Computing.* Vienna, Austria: R Foundation for Statistical Computing; 2017.
28. Bates D, Maechler M, Bolker B, Walker S. Fitting linear mixed-effects models using lme4. *J Stat Softw.* 2015;67:1-48.
29. Bergknot N, Meij BP, Hagman R, et al. Intervertebral disc disease in dogs—part 1: A new histological grading scheme for classification of intervertebral disc degeneration in dogs. *Vet J.* 2013;195(2): 156-163.
30. Muller MK, Ludwig E, Oechtering G, Scholz M, Flegel T. The vacuum phenomenon in intervertebral disc disease of dogs based on computed tomography images. *J Small Anim Pract.* 2013;54(5):253-257.
31. Ruoff CM, Eichelberger BM, Pool RR, et al. The use of small field-of-view 3 Tesla magnetic resonance imaging for identification of articular cartilage defects in the canine stifle: An ex vivo cadaveric study. *Vet Radiol Ultrasound.* 2016;57(6):601-610.
32. Wijnberg ID, Bergmann W, Veraa S. Diagnose und prognose neurologischer erkrankungen der halswirbelsaule beim pferd. *Prakt Tierarzt.* 2015;96:150-158.
33. Veraa S, Bergmann W, van den Belt AJ, Wijnberg I, Back W. Ex vivo computed tomographic evaluation of morphology variations in equine cervical vertebrae. *Vet Radiol Ultrasound.* 2016;57(5):482-488.
34. Blumenkrantz G, Zuo J, Li X, Kornak J, Link TM, Majumdar S. In vivo 3.0-Tesla magnetic resonance T1rho and T2 relaxation mapping in subjects with intervertebral disc degeneration and clinical symptoms. *Magn Reson Med.* 2010;63(5):1193-1200.
35. van Biervliet J, Scrivani PV, Divers TJ, Erb HN, de Lahunta A, Nixon A. Evaluation of decision criteria for detection of spinal cord compression based on cervical myelography in horses: 38 cases (1981-2001). *Equine Vet J.* 2004;36(1):14-20.
36. Prange T, Derksen FJ, Stick JA, Garcia-Pereira FL, Carr EA. Cervical vertebral canal endoscopy in the horse: Intra- and post-operative observations. *Equine Vet J.* 2011;43(4):404-411.

Supplement 1. Tabular overview of the macroscopic evaluation and MRI-detected annulus protrusion grades (1-4) available per intervertebral disc, for all horses included in the study (n=11).

Horse	Age (yr)	Gender	Breed	Clinical signs	C2-C3		C3-C4		C4-C5		C5-C6		C6-7		C7-T1	
					m	a	m	a	m	a	m	a	m	a	m	a
1	0.8	Stallion	RDSH	Severe ataxia	ND	1	ND	1	N/A	1	ND	1	ND	2	ND	1
2	5	Mare	RDSH	Lameness, neck pain	ND	1	ND	2	ND	2	ND	2	D	2	ND	2
3	6	Gelding	RDSH	Ataxia	ND	1	ND	1	D	2	ND	2	ND	2	D	2
4	7	Mare	RDSH	Chronic lameness, stiff neck, tripping	ND	1	ND	1	ND	1	ND	2	ND	3	ND	2
5	9	Mare	RDSH	Stiff neck, neck pain, lameness	ND	1	ND	1	ND	1	ND	2	D	2	D	1
6	11	Gelding	RDSH	Ataxia	D	2	D	2	D	2	D	3	D	3	D	2
7	16	Gelding	RDSH	Lame, neck pain, ataxia	ND	1	ND	1	D	1	ND	2	D	2	ND	1
8	7	Gelding	RDSH	Lame, resistance, neck pain	ND	2	ND	3	ND	3	ND	2	ND	2	D	3
9	9	Mare	RDSH	Resistance, neck muscle atrophy, neck pain	ND	1	ND	1	ND	1	ND	2	D	3	D	2
10	11	Gelding	Appaloosa	Ataxia	ND	N/A	ND	N/A	ND	2	ND	2	D	4	D	3
11	15	Gelding	RDSH	Ataxia, neck pain	ND	2	ND	3	ND	2	ND	N/A	D	N/A	D	N/A

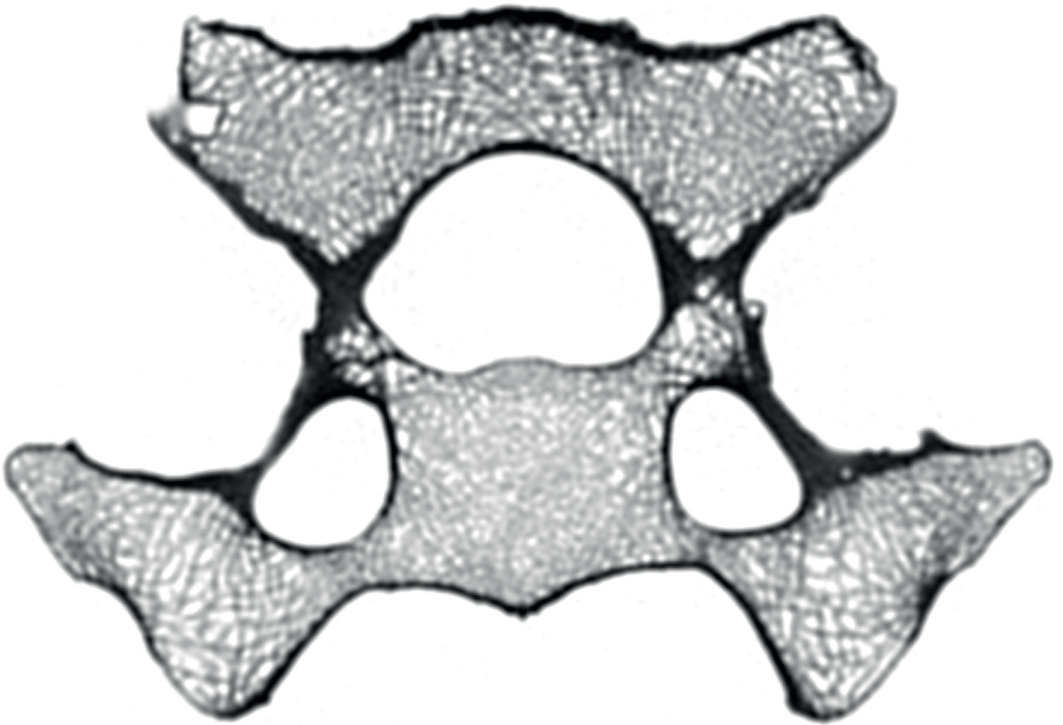
Supplement 2. Tabular overview of MRI nucleus pulposus visibility (n=0-2) and MRI degeneration scoring available per intervertebral disc, for all horses included in the study (n=11).

Horse	C2-C3			C3-C4			C4-C5			C5-C6			C6-7			C7-T1		
	m	n	d	m	n	d	m	n	d	m	n	d	m	n	d	m	n	d
1	ND	1	ND	ND	0	ND	N/A	0		ND	0	ND	ND	0	ND	ND	0	ND
2	ND	0	ND	ND	0	ND	ND	0	ND	ND	0	ND	D	2	D	ND	2	D
3	ND	0	ND	ND	0	ND	D	0	ND	ND	0	ND	ND	0	D	D	1	D
4	ND	0	ND	ND	0	ND	ND	0	ND	ND	0	ND	ND	0	ND	ND	0	ND
5	ND	0	D	ND	0	ND	ND	0	ND	ND	0	ND	D	1	D	D	1	ND
6	D	1	D	D	1	ND	D	1	ND	D	1	D	D	1	D	D	1	ND
7	ND	0	D	ND	0	D	D	0	D	ND	1	D	D	0	D	ND	1	D
8	ND	0	D	ND	0	ND	ND	0	ND	ND	0	ND	ND	2	D	D	1	D
9	ND	0	ND	ND	0	ND	ND	0	ND	ND	0	ND	D	1	D	D	2	D
10	ND			ND			ND	1	ND	ND	1	D	D	2	D	D	1	D
11	ND	0	ND	ND	0	D	ND	1	ND	ND			D			D		

Notes: m=macroscopic assessment (ND=non-degenerated, D=degenerated), n= MRI nucleus visibility (0=visible, 1=vaguely defined, 2=not visible) ; d= MRI degeneration scoring (ND= non-degenerated, D= degenerated)

Supplement 3. Tabular overview of macroscopic degeneration scoring (0-5) [6] versus MRI degeneration scoring (ND-D) and visibility of the nucleus pulposus scoring (0,1-2).

Macroscopic assessment degeneration score	MRI degeneration scoring (0-1)		MRI nucleus pulposus visibility scoring (0,1-2)		
	ND	D	0	1	2
1	13	3	13	2	1
2	18	8	21	4	1
3	0	1	0	1	0
4	5	6	2	8	1
5	0	6	1	3	2



6

Cervical Disc Height Index in Young Dutch Warmblood Horses; Intra- and Interobserver Agreement

Stefanie Veraa^a, Carmen J.W. Scheffer^b, Danielle H.M. Smeets^c, Renske B. de Bruin^c, Arie C. Hoogendoorn^b, Johannes C.M. Vernooij^d, Mirjam Nielen^d, Willem Back^{c,e}

^a Division of Diagnostic Imaging, Faculty of Veterinary Medicine, Utrecht University, Yalelaan 110, NL-3584 CM Utrecht, The Netherlands.

^b Equine Veterinary Clinic "De Watermolen", Watermolenweg 5, NL-7481 VL, Haaksbergen, The Netherlands

^c Department of Equine Sciences, Faculty of Veterinary Medicine, Utrecht University, Yalelaan 114, NL-3584 CM Utrecht, The Netherlands

^d Department of Farm Animal Health, Yalelaan 7, NL-3584 CL, The Netherlands

^e Department of Surgery and Anaesthesiology of Domestic Animals, Faculty of Veterinary Medicine, Ghent University, Salisburylaan 133, B-9820 Merelbeke, Belgium

Submitted to Veterinary Radiology and Ultrasound.

ABSTRACT

Intervertebral disc disease, as well as the associated alteration of the radiographic intervertebral disc space width, has been reported in horses. Disc height index (DHI) has proven to be a reliable parameter in other species but data related to this parameter are lacking in horses. Therefore, the aims of this retrospective longitudinal study were 1) to evaluate the reliability of measurements within and between observers of the DHI as parameter for radiographic equine cervical intervertebral disc space width, and 2) to evaluate the sequential development of the DHI in time. For this, DHI from C2-C3 to C7-Th1 was obtained in a group of 39 Dutch Warmblood horses at one, five and 18 months of age, by one radiologist and two veterinary students. Bland-Altman plots and ICC revealed a good intra- and interobserver agreement. A linear mixed-effect model did reveal that mean DHI increases towards the caudal cervical spine, but does not differ overall in time or between sexes. Spearman's rank test did show a correlation between vertebral alignment angle induced by different head-neck positions and a normalized DHI ($\rho= 0.33$, $P < 0.0001$). Student's t-test revealed that the presence of C6-C7 congenital malformation did not influence DHI significantly. It was concluded that DHI represents a reliable parameter the quantification of equine cervical radiographic intervertebral disc space width. Monitoring DHI over time in a group of adult horses with a controlled head-neck position would be a next step to take.

Keywords: disc degeneration, radiography, intervertebral disc space width, foal.

INTRODUCTION

Intervertebral disc disease such as disc protrusion, extrusion, discospondylitis or ischemic myelopathy due to a fibrocartilagenous spinal infarct, is common in dogs and humans [1, 2]. However, it appears to be uncommon in horses, as only incidental case descriptions have been published [3-9]. Although clinical signs such as pain, spasticity and spinal ataxia have been reported in these cases of intervertebral disc disease, the clinical impact of intervertebral disc degeneration in the aging horse has always been considered to be low [10]. However, in more recent years cervical vertebral column pathology is increasingly recognized clinically as a source of lameness or poor performance in horses [11, 12]. Degeneration of the cervical intervertebral disc has been described as disintegration of the discal fibrocartilagenous tissues with end stage cleft formation and a macroscopic degeneration, while recently a grading system has been developed [10, 13]. Intervertebral disc space narrowing can be a feature of intervertebral disc degeneration and herniation. Therefore, intervertebral disc space width has been defined and monitored by disc height calculation on lateral radiographs of the spine in humans and in research animal models [14-16].

Morphologic variations at C6 and C7 have a higher incidence in Warmblood horses [17, 18]. Along with these variations a significantly longer C7 and a wider intervertebral disc space between C6 and C7 have been described [17]. However, intra- and interobserver agreement for determination of the cervical intervertebral disc space width in horses has not been established yet.

Therefore, the aims of this study were: 1) to evaluate the reliability of measurements within and between observers of the disc height index (DHI) as parameter for the radiographic equine cervical intervertebral disc space width from C2 to Th1, and 2) to evaluate the natural development of the intervertebral disc space width in a group of young horses by sequential measurements at one, five and 18 months of age.

MATERIAL AND METHODS

Data collection

Radiographic studies of the cervical vertebral column were used that had been taken for breeding screening purposes of the foals born between February and June 2015 at the private equine veterinary clinic "De Watermolen". Selected were those foals that were radiographed when one-month old, at the time of weaning at 5 months and at

18 months when the young horses came in from the pasture. The group consisted of $n=39$ young Dutch Warmblood horses (Royal Dutch Sport Horses, $n=24$ colts and $n=15$ fillies). The young horses were sedated before the radiographic exams took place at 5 and 18 months with acepromazine (Neurotranq, Alfasan, Woerden, The Netherlands) (0.05 mg/kg bwt i.v.) and detomidine (Detogesic, Zoetis, Capelle a/d IJssel, The Netherlands) (0.01 mg/kg bwt). Right latero-lateral radiographs were obtained (Fujifilm PCCR with 24 x 30 cm cassettes Fujifilm Medical Systems France S.A.S., Steenberg, The Netherlands; Philips S80, Philips Healthcare, Eindhoven, The Netherlands) at settings of 55-60 kV, 15-20 mAs and a focus-film distance of 100 cm. The images were saved in DICOM format.

No intervertebral disc degeneration was presumed to be present because of the young age of the horses. During the 18-month period a daily check of the total group was performed and medical records were available for all young horses. None of the young horses had clinical signs related to the vertebral column, neither was any known to have suffered any form of trauma.

The radiographs were evaluated in a freeware DICOM viewer (RadiAnt DICOM viewer, Medixant, Poland) and measurements were made on latero-lateral radiographic views. During this reviewing and measuring, radiographs were only rejected if dorso-ventral or cranio-caudal obliquity deviated more than around 10 degrees from the latero-lateral view. The intervertebral disc space was only measured when clearly visible.

Data acquisition

The DHI was calculated after measuring the intervertebral disc width (D+E+F) and vertebral length (A+B+C) of the cranial vertebra on three levels and defined as follows: $DHI = (D+E+F)/(A+B+C)$ (Fig.1) [16]. For measurement of the intervertebral disc space width of C2-C3, the vertebral reference lines from C3 were used.

Measurements to calculate the DHI at one month were made twice with a two-week interval by a 5th year veterinary student (DS) and a European College of Veterinary Diagnostic Imaging (ECVDI) board-certified radiologist (SV). Measurements at five months were made once by a 4th year veterinary student (RdB) and the board-certified radiologist (SV), who also measured once at 18 months. The 4th year student (RdB) measured C2-C3, C3-C4 and C4-C5 a second time two weeks after the first measurement.

A possible effect of the vertebral column curvature representing the head-neck position (flexion, neutral or extension) was evaluated by measuring the vertebral alignment angle (VAA) at 18 months (Fig.1). For this purpose, an alternative calculation of DHI was introduced to create a normalized dorsal-ventral DHI as described by Schmidt et. al. [19]. This was defined as dorsal-ventral DHI= $((D/B)/(F/B))$, mean DHI being $((D/B)+(E/B)+(F/B)/3)$ and the normalized dorsal-ventral DHI= $((D/B)/(F/B))/$ mean DHI [19]. The central vertebral reference line (B) was used in all calculations to rule out any difference between dorsal-mid-ventral measurements, except dorsal-mid-ventral intervertebral disc space width.

The presence or absence of congenital vertebral morphologic variation at C6 and C7 was recorded only in the 18 month old horses.

Statistical analysis

Statistical analysis was performed by a board-certified radiologist (SV) using commercially available software SPSS (SPSS version 24.0, IBM Statistics for Windows, USA) and a statistician (JV) using freely available software R (R, version 3.4.3, R Foundation for Statistical Computing, Vienna, Austria).

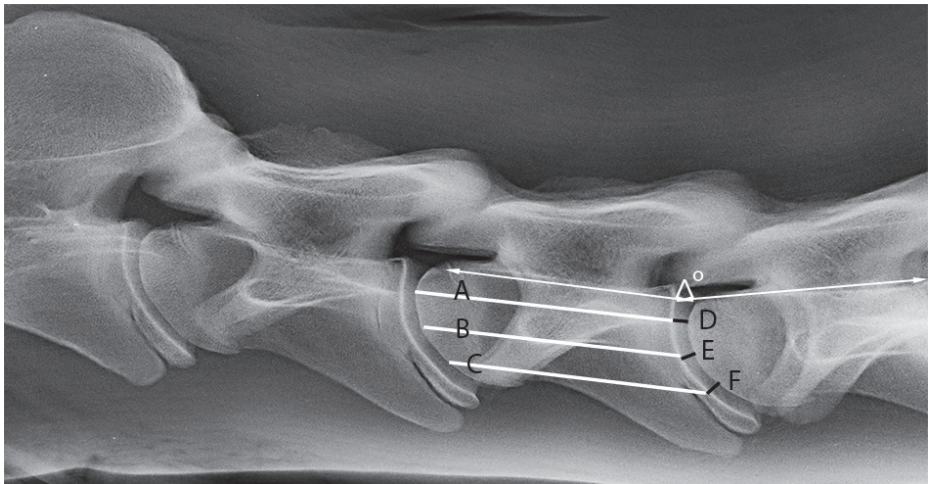


Fig. 1. Latero-lateral radiograph of the neck of an 18-month-old Dutch Warmblood horse. Disc height index (DHI)= $(D+E+F)/(A+B+C)$ (white lines at vertebral body and black lines at intervertebral disc space). The vertebral alignment angle (VAA) at C4-C5 is indicated by the white arrows.

The disc height index per intervertebral disc location was summarized as mean, standard deviation (sd) and range (min-max).

For assessing the repeatability of the disc height index determination, the inter-observer and intra-observer variability at one month of age and inter-observer variability at five months of age were evaluated by Bland-Altman plots and the calculation of the Intraclass Correlation Coefficient (ICC).

A linear mixed effect model [20] was used to analyze the association between the outcome of DHI (measured by the radiologist) and location, age and sex, and the interaction between location and age as explanatory factors. Horse was added to the model as random effect to take the correlation between repeated observations within horses into account. Age was also used as random slope to account for the correlation between observations at different ages. The model was adjusted by a variance function to account for different variability per location. The model was reparametrized to compare the change of DHI in course of time per location. The validity of the model was assessed by studying the residuals for normality and constant variance. The Akaike's Information Criterion was used to select the best model. [21]

A possible effect of angulation of the neck due to altering head-neck position on DHI was evaluated once at 18 months by applying Spearman correlation test between vertebral alignment angle at 18 months and the normalized dorsal-ventral DHI at that age for all discs.

Also a possible effect of the presence of C6-C7 congenital vertebral malformation on the DHI at C6-C7 was evaluated with an independent samples Student t-test.

A P-value of <0.05 was considered significant.

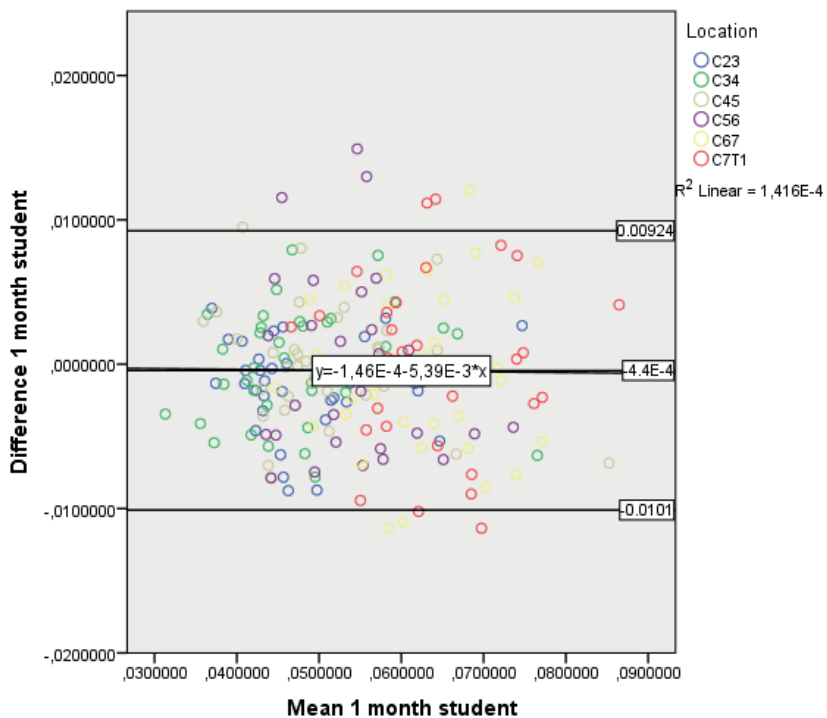
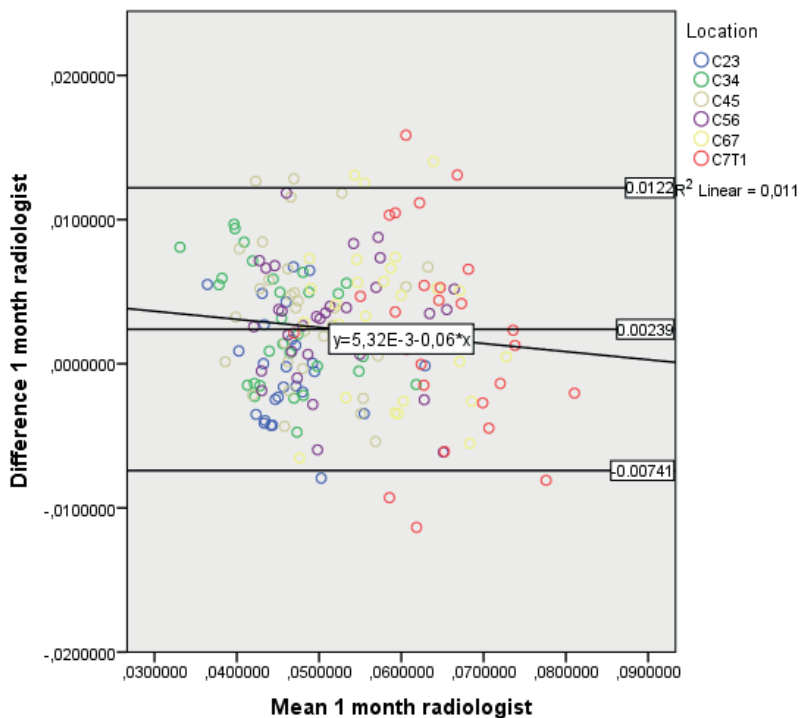
RESULTS

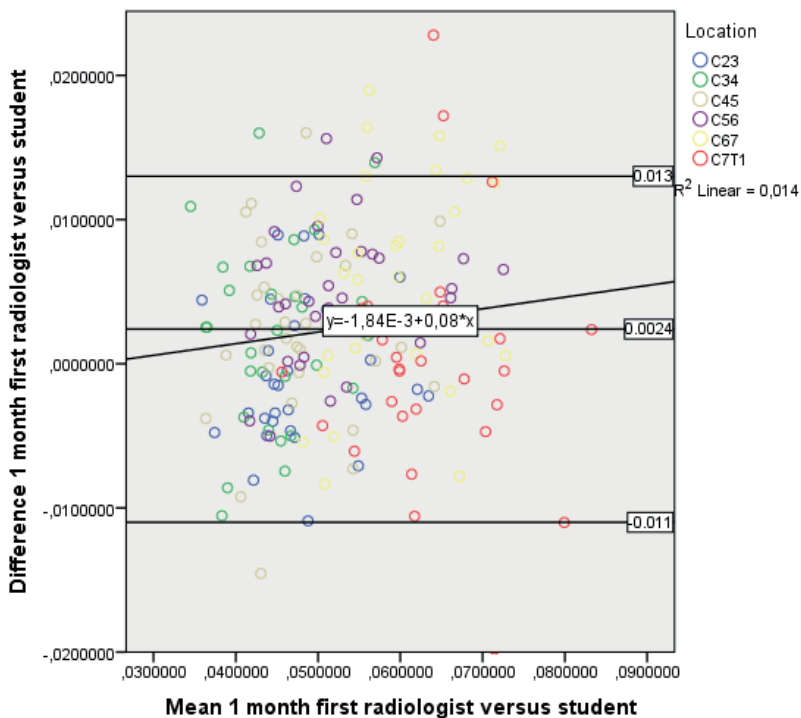
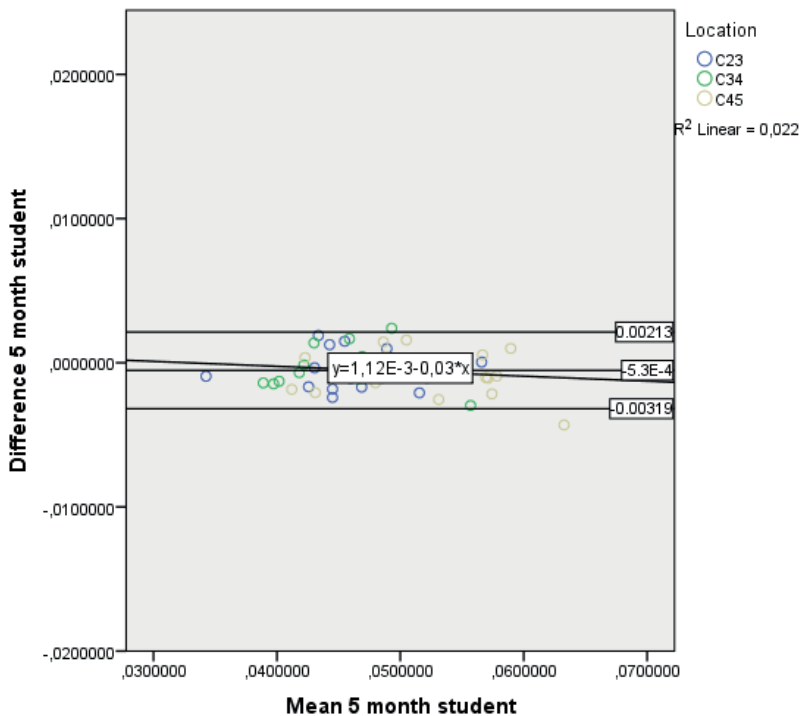
The latero-lateral views that were of sufficient quality varied between eight (mostly C7-Th1) and 35 foals at varying ages and locations and only these were included for further statistical analysis (Table 1). Measurements were mostly not possible at C7-Th1 due to a reduced visibility of the intervertebral disc space by superimposed musculature of the fore limbs.

The mean DHI over all horses increased from cranial to caudal at the consecutive intervertebral disc spaces with a wide range at certain locations (Table 1).

Table 1. Overview of the mean, standard deviation (sd) and range (min- max) of the DHI for radiologist at one, five and 18 months as well as for student A at one month and student B at five months.

Location	DHI Radiologist 1 month		DHI Radiologist 5 months		DHI radiologist 18 months		DHI Student DS 1 month		DHI Student RdB 5 months	
	Number	Mean (sd) (min-max)	Number	Mean (sd) (min-max)	Number	Mean (sd) (min-max)	Number	Mean (sd) (min-max)	Number	Mean (sd) (min-max)
Overall	191	0.052 (0.011)	164	0.058 (0.011)	150	0.052 (0.012)	205	0.055 (0.011)	165	0.056 (0.011)
C2-C3	31	0.029-0.084 0.048 (0.007)	28	0.037-0.0895 0.0498 (0.008)	29	0.032-0.088 0.042 (0.005)	35	0.033-0.089 0.049 (0.009)	30	0.033-0.086 0.047 (0.005)
C3-C4	31	0.034-0.065 0.045 (0.007)	29	0.039-0.075 0.050 (0.008)	29	0.033-0.053 0.043 (0.006)	35	0.035-0.073 0.048 (0.009)	30	0.034-0.061 0.048 (0.005)
C4-C5	33	0.029-0.063 0.047 (0.008)	29	0.039-0.075 0.054 (0.008)	29	0.032-0.058 0.049 (0.007)	35	0.033-0.079 0.051 (0.01)	31	0.038-0.058 0.053 (0.008)
C5-C6	34	0.036-0.065 0.050 (0.008)	29	0.037-0.067 0.058 (0.007)	28	0.037-0.062 0.058 (0.008)	35	0.034-0.089 0.055 (0.009)	32	0.033-0.065 0.058 (0.006)
C6-C7	32	0.039-0.069 0.057 (0.007)	30	0.042-0.073 0.067 (0.0098)	26	0.041-0.073 0.063 (0.011)	35	0.039-0.078 0.062 (0.009)	34	0.048-0.072 0.067 (0.009)
C7-Th1	30	0.045-0.073 0.064 (0.009)	19	0.045-0.081 0.072 (0.008)	9	0.034-0.088 0.068 (0.009)	30	0.046-0.079 0.064 (0.009)	8	0.05-0.084 0.073 (0.008)
		0.046-0.085		0.053-0.089		0.057-0.085		0.045-0.084		0.062-0.086





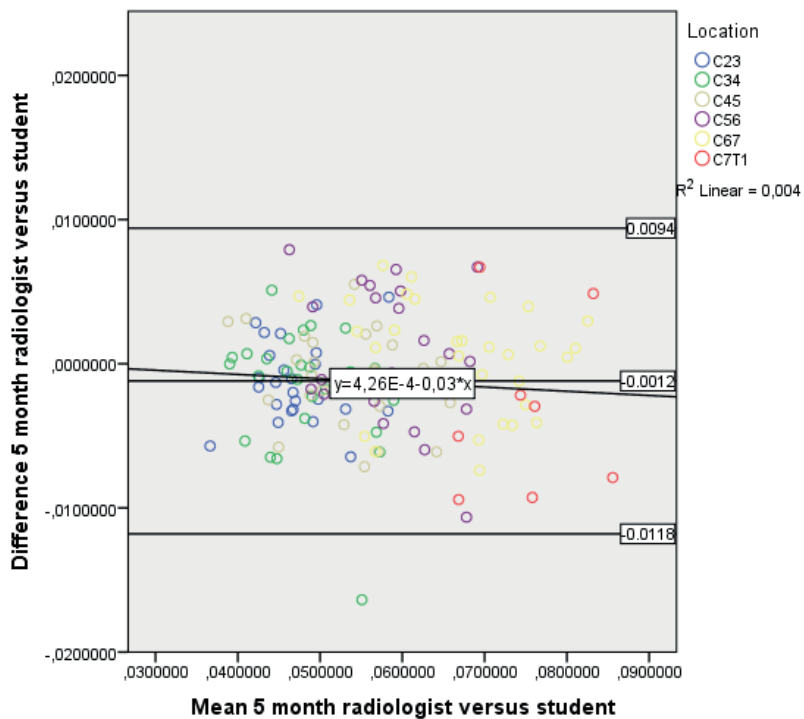
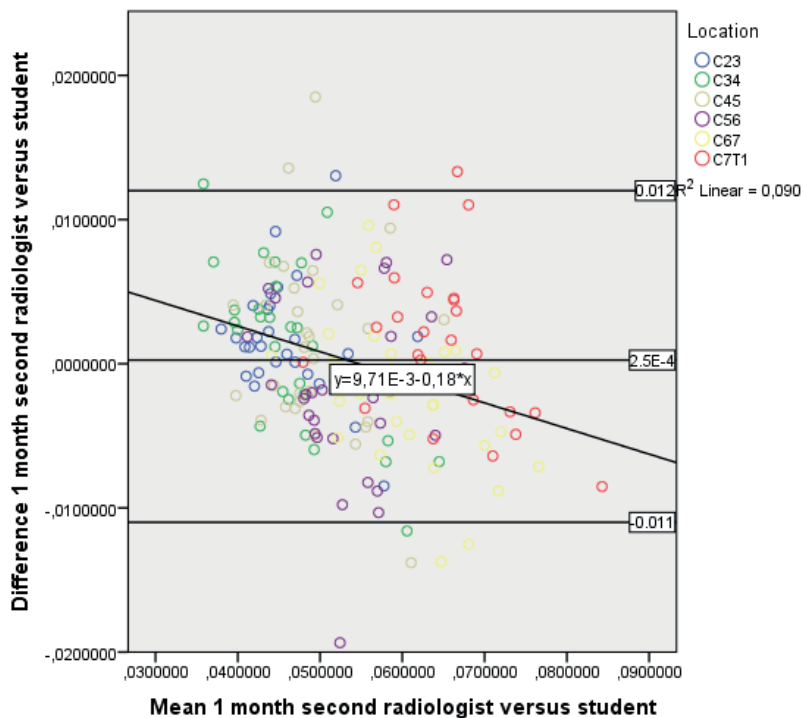


Fig. 2. Bland-Altman plots for intra-observer and inter-observer agreement. The mean \pm 2sd reference lines are provided as is the linear slope. Intra-observer a) for radiologist at one month (mean of difference 0.0024, standard deviation 0.005), b) for student DS at one month (mean of difference -0.0004, standard deviation 0.005), c) for student RdB at five months (mean of difference -0.0005, standard deviation 0.001); and interobserver d) for radiologist versus student DS at one month first measurement (mean of difference 0.0024, standard deviation 0.007), e) for radiologist versus student DS at one month second measurement (mean of difference 0.0003, standard deviation 0.006), f) for radiologist versus student RdB at five months (mean of difference -0.0012, standard deviation 0.005). Bland-Altman plots were created with the inclusion of limits of agreement (Figure 2).

The bias within observers at one month is 0.0024 for the radiologist and -0.0004 for the student. The bias between observers was 0.0024 for the first measurements of radiologist and student and was 0.00026 for second measurements. At five months the bias between measurements within observer (student) was -0.00053 and the bias between radiologist and student was -0.0012. The intra and interobserver limits of agreement varied approximately between -0.01 and +0.01 except for the student at five months. Limits of agreement were approximately between 0.002 and -0.003 within observer.

The ICC overall is 0.88 (Table 2) or even higher for both intra- and interobserver agreement regardless of location. ICC per location varies between 0.78 and 0.98 for intraobserver agreement and between 0.62 and 0.96 for interobserver agreement.

Interobserver agreement is slightly better at C6-C7 and C7-Th1 for the second measurement than for first at one month of age (Table 2).

Results of the analysis to assess the association of DHI with location in the neck and age are presented in Table 3. Sex was excluded for further analysis as Akaike's Information Criterion improved without this factor. At one month of age the mean DHI at location C34 was smaller than the mean DHI at C2-C3, and C6-C7 and C7-Th1 were larger than C2-C3. At 5 months mean DHI at all locations except C2-C3 were larger compared to one month of age. At 18 months mean DHI at C2-C3 was smaller, and C5-C6 and C6-C7 were larger compared to the mean DHI of the same location at one month.

The mean vertebral alignment angle at 18 months varied between 175 degrees at C5-C6 and 190 degrees at C2-C3 (sd : 9 degrees), while the normalized dorsal-ventral disc height index had an overall mean of 25.4 (sd : 7.2). A low but significant correlation was found between the vertebral alignment angle and normalized dorsal-ventral disc height index ($\rho= 0.33$, $P< 0.0001$) (Table 4).

Table 2. Overview of intra- and inter-observer intraclass correlation coefficient (ICC) at one and five months. CI= confidence interval, NA= not available.

Location	Intra-observer agreement				Inter-observer agreement			
	Radiologist 1 month	Student 1 month	Student 5 month		Radiologist-student DS, first measurement	Radiologist-student DS, second measurement	Radiologist-student RdB	
	number	ICC (95%CI)	number	ICC (95%CI)	number	ICC (95%CI)	number	ICC (95%CI)
Overall	177	0.91 (0.87-0.93)	205	0.95 (0.93-0.96)	56	0.95 (0.91-0.97)	186	0.88 (0.84-0.91)
C2-C3	28	0.89 (0.78-0.95)	35	0.96 (0.91-0.98)	19	0.98 (0.94-0.99)	31	0.86 (0.70-0.93)
C3-C4	29	0.85 (0.56-0.94)	35	0.96 (0.91-0.98)	19	0.98 (0.96-0.99)	31	0.78 (0.55-0.89)
C4-C5	32	0.78 (0.37-0.91)	35	0.96 (0.92-0.98)	18	0.89 (0.73-0.96)	32	0.79 (0.45-0.87)
C5-C6	31	0.89 (0.65-0.96)	35	0.86 (0.72-0.93)	NA	NA	33	0.82 (0.18-0.94)
C6-C7	30	0.81 (0.51-0.92)	35	0.89 (0.79-0.95)	NA	NA	31	0.66 (0.10-0.86)
C7-Th1	27	0.78 (0.52-0.89)	30	0.88 (0.75-0.94)	NA	NA	28	0.76 (0.47-0.89)
							178	0.91 (0.88-0.93)
							29	0.88 (0.72-0.94)
							30	0.84 (0.66-0.92)
							31	0.73 (0.45-0.87)
							31	0.78 (0.56-0.89)
							31	0.87 (0.73-0.94)
							26	0.87 (0.71-0.94)
							149	0.94 (0.92-0.96)
							27	0.62 (0.20-0.83)
							28	0.69 (0.34-0.85)
							28	0.95 (0.89-0.98)
							28	0.89 (0.75-0.95)
							30	0.96 (0.91-0.98)
							8	0.79 (0.10-0.96)

Table 3. Parameter estimates from the regression model for the differences in mean Disc Height Index per location in the neck for the foal in course of age (months).

Parameter	Estimate	95% Confidence interval	
Intercept C23:age 1 ¹	0.0487	0.0463	0.0512
Location C34:age 1 ²	-0.0038	-0.0063	-0.0013
Location C45:age 1 ²	-0.0013	-0.0038	0.0011
Location C56:age 1 ²	0.0014	-0.0010	0.0038
Location C67:age 1 ²	0.0079	0.0049	0.0110
Location C7Th1:age 1 ²	0.0149	0.0116	0.0182
Compared with age 1 month			
Location C23:age 5 ³	0.0011	-0.0015	0.0037
Location C34:age 5 ³	0.0050	0.0023	0.0077
Location C45:age 5 ³	0.0065	0.0039	0.0091
Location C56:age 5 ³	0.0079	0.0053	0.0105
Location C67:age 5 ³	0.0101	0.0064	0.0137
Location C7Th1:age 5 ³	0.0087	0.0040	0.0133
Compared with age 1 month			
Location C23:age 18 ³	-0.0067	-0.0098	-0.0035
Location C34:age 18 ³	-0.0016	-0.0049	0.0017
Location C45:age 18 ³	0.0014	-0.0019	0.0046
Location C56:age 18 ³	0.0077	0.0045	0.0109
Location C67:age 18 ³	0.0064	0.0021	0.0107
Location C7Th1:age 18 ³	0.0033	-0.0030	0.0096

¹ Estimated mean DHI at the reference location C23 at age 1 month.

² Estimated difference between mean DHI at specified location and mean DHI at C2-C3 at 1 month of age (= reference).

³ Estimated difference between mean DHI at specified location and age (5 or 18 months) and mean DHI at the same location at 1 month of age.

Table 4. Mean and range (min-max) of the vertebral alignment angle and normalized dorsal-ventral DHI.

	VAA (degrees)	Normalized DV-DHI
	Mean (min-max)	Mean (min-max)
Overall	180 (158-200)	25.4 (12.9-49.8)
C2-C3	190 (181-200)	33.7 (21.4-49.8)
C3-C4	186 (181-197)	24.3 (15.4-36.2)
C4-C5	178 (172-190)	23.9 (15.7-39.7)
C5-C6	175 (170-185)	21.4 (12.9-32.2)
C6-C7	168 (158-177)	23.2 (13.95-42.6)

VAA= vertebral alignment angle in degrees, DV-DHI= dorsal-ventral disc height index

There were 10 foals (10/28) that had recognizable congenital vertebral malformation at C6-C7 at 18 months. The DHI at 18 months between horses with or without congenital vertebral malformation did not differ significantly (Mean difference = -0.007, 95% confidence interval -0.024 - 0.01, P=0.78).

DISCUSSION

This study describes intra- and interobserver agreement for the evaluation of equine cervical intervertebral disc space width by means of calculation of the disc height index (DHI), as until now applied in other species than the horse. The outcome of this study might serve as a provider of initial reference values (mean \pm 2sd) for this new parameter in horses. It is based on measurements from a reasonable number of sound horses, using a parameter with a good to excellent intra- and interobserver agreement. Interobserver agreement became even slightly better for the second measurement at one month of age at C6-C7 and C7-Th1 between the radiologist and student A, possibly indicating a learning effect. [22] The number of available observations at C7-Th1 was much lower at the age of 18 months due to decreased visibility of the intervertebral disc as a result of superposition of soft tissues of the fore limbs. DHI was associated with a combination of the fixed factors 'location' and 'time', showing increase in mean DHI at all locations except C2-C3 between one and five months of age, but this increase disappeared at 18 months except for the locations C5-C6 and C6-C7. The vertebral alignment angle (VAA) also showed a low correlation with the normalized dorsal-ventral disc height index and these results suggest that a standardizing head- and neck position as well as sedating the horse may improve outcome when measuring the intervertebral disc space width, but further research is needed.

The composition of the cervical intervertebral disc in horses has been described as different from those in humans and companion animals [10, 13]. In horses, the annulus fibrosis comprises the largest part of the intervertebral disc, whereas the nucleus pulposus is much smaller than in other species [10]. Lately, a macroscopic degeneration scoring system was developed for the equine cervical intervertebral disc [13]. Narrowing of the intervertebral disc space due to the presence of C6-C7 congenital vertebral variations, degenerative herniation or even discospondylitis with severe clinical signs in these horses has been described [3-7, 17]. However, the intervertebral disc space width of horses without clinical signs has not been evaluated in these studies. Intervertebral disc degeneration is an ongoing process and has been described to start in humans during the first decade of life with molecular and

structural changes such as loss of lamellar arrangement of the annulus fibrosis [23, 24]. Radiographically determined DHI has proven to be a good parameter in human and animal studies presents a way to monitor the intervertebral space width during degeneration but also regeneration [14-16, 25, 26]. As the cervical vertebral spine of the horse has a different morphology, curvature and shape, a similar DHI approach had to be first evaluated before this technique could be recommended for routine clinical application. For this, one of the recorded DHI methods has been applied, with 3 reference lines in the cranial vertebral body and 3 measurements of the intervertebral disc space width [16]. This method was preferred over others, as the head-neck position has a large effect on the curvature and hence the intervertebral alignment of the long and flexible equine neck; there are no such effects on the far more rigid thoracolumbar column [14, 15, 25]. Determining the DHI approach seems to present a repeatable method to determine the intervertebral disc space width in young horses. The agreement interval was found to be moderately wide as limits between around - 0.01 and + 0.01. Therefore, some reservations are needed as criteria for what seems biological acceptable are not known in horses. Future establishment of DHI reference values for the adult non-degenerated and degenerated equine intervertebral disc would be of great interest. As the composition of the equine intervertebral disc is slightly different, degeneration has possibly a different effect on intervertebral disc space width compared to species with a less fibrous nucleus pulposus, like dogs and man. The macroscopic yellow discoloration, fibrillation and cleft formation as described in the horse [13] could be a pre-stage of collapse, as seen in end-stage discospondylitis [27]. Increased DHI due to widening of the radiographic intervertebral disc space has been reported as part of disc regeneration. [25] Widening of the dorsal part of the intervertebral disc space during flexion or ventral part of the intervertebral disc space in the equine neck during extension could alter DHI as well, keeping in mind that there was a significant association between vertebral alignment angle (VAA) and normalized dorsal-ventral DHI.

Limitations of this study include that measurements were performed in young horses up to 18 months of age but not in adult horses Besides, there was no standardized head and neck position and that the sample size was relatively small. However, most standard measurements in the equine cervical spine (such as minimal sagittal diameter, intravertebral sagittal diameter ratio and vertebral fossa angle) have been found to be equal or only minimally different in neutral versus low or high neck position [28]. Some margin in positioning horses for radiographs of the neck seems therefore acceptable.

In this study the assumption was made that foals or young horses are not prone to disc

degeneration yet, keeping in mind that a traumatic insult could not be fully excluded as the foals were kept in the fields as a group. None of the foals exhibited any clinical signs related to the vertebral column during the course of the study.

Conclusions

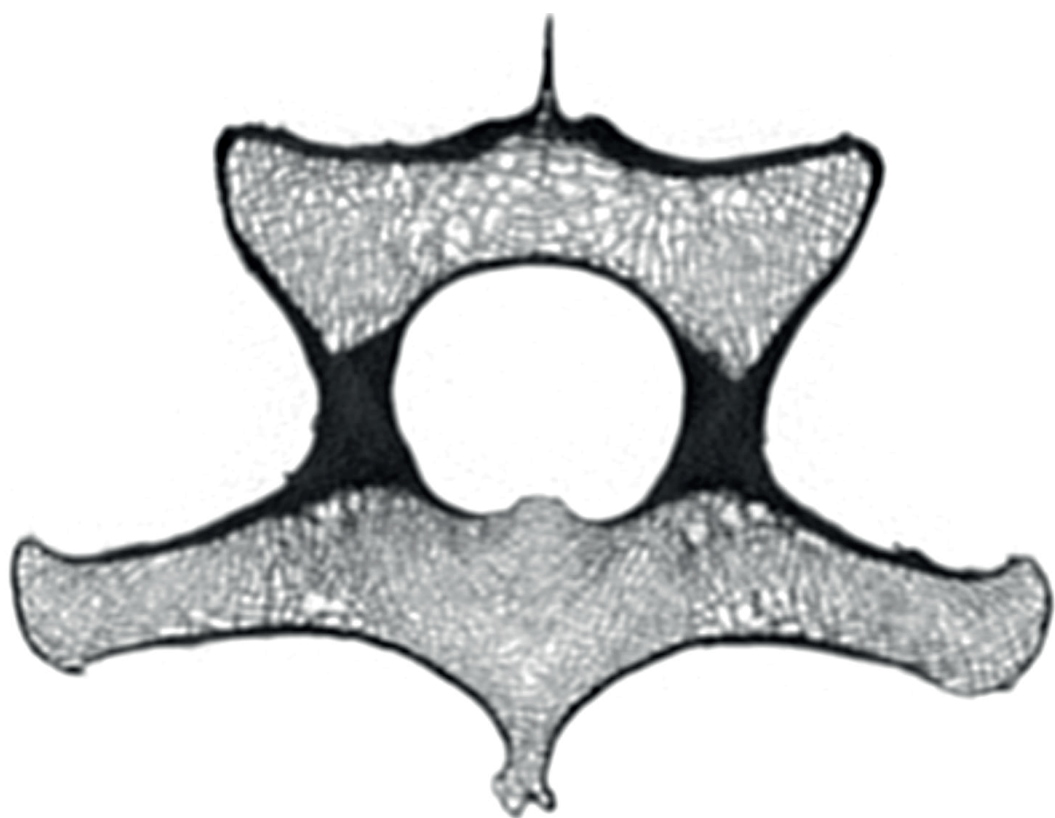
The DHI as presented in this study is a reliable and repeatable method to define the cervical intervertebral disc space width in young horses. The DHI does not alter significantly in time in young horses up to 18 months. Ideally, the head-neck position should become standardized when determining the DHI. As a next step, further evaluation of this method should be carried out in a larger population of adult warmblood horses with standardization of the head-neck position during radiography and with the concomitant degenerative status of the intervertebral discs known.

Acknowledgements: The authors would like to thank the personnel from the Equine Veterinary Clinic “De Watermolen” for their technical assistance, J. W. Greve, DVM, being the owner of “Equine Allround” for permission to use the data and Prof. Dr. J.W. Hesselink and Prof. Dr. P.R. van Weeren for their help in preparing this manuscript.

REFERENCES

1. Bergknut, N., Meij, B.P., Hagman, R., de Nies, K.S., Rutges, J.P., Smolders, L.A., Creemers, L.B., Lagerstedt, A.S., Hazewinkel, H.A. and Grinwis, G.C. (2013) Intervertebral disc disease in dogs - part 1: a new histological grading scheme for classification of intervertebral disc degeneration in dogs. *Vet. J.* **195**, 156-163.
2. Thompson, K., Moore, S., Tang, S., Wiet, M. and Purmessur, D. (2018) The chondrodystrophic dog: A clinically relevant intermediate-sized animal model for the study of intervertebral disc-associated spinal pain. *JOR Spine*. **1**, e1011. doi: 10.1002/jsp2.1011
3. Foss, R.R., Genetzky, R.M., Riedesel, E.A. and Graham, C. (1983) Cervical intervertebral disc protrusion in two horses. *Can. Vet. J.* **24**, 188-191.
4. Furr, M.O., Anver, M. and Wise, M. (1991) Intervertebral disk prolapse and diskospondylitis in a horse. *J. Am. Vet. Med. Assoc.* **198**, 2095-2096.
5. Nixon, A.J., Stashak, T., S., Ingram J. T., Norrdin R.W. and Park R.D. (1984) Cervical intervertebral disc protrusion in a horse. *Vet. Surg.* **13**, 154-158.
6. Stadler, P., van den Berg, S.S. and Tustin, R.C. (1988) Cervical intervertebral disk prolapse in a horse. *J. S. Afr. Vet. Assoc.* **59**, 31-32.
7. Sweers, L. and Carstens, A. (2006) Imaging features of discospondylitis in two horses. *Vet. Radiol. Ultrasound.* **47**, 159-164.
8. Fuentealba, I.C., Weeks, B.R., Martin, M.T., Joyce, J.R. and Wease, G.S. (1991) Spinal cord ischemic necrosis due to fibrocartilaginous embolism in a horse. *J. Vet. Diagn. Invest.* **3**, 176-179.
9. Taylor, H.W., Vandeveld, M. and Firth, E.C. (1977) Ischemic myelopathy caused by fibrocartilaginous emboli in a horse. *Vet. Pathol.* **14**, 479-481.
10. Bollwein, A. and Hanichen, T. (1989) Age-related changes in the intervertebral disks of the cervical vertebrae of the horse. *Tierarztl. Prax.* **17**, 73-76.
11. Dyson, S.J. (2011) Lesions of the equine neck resulting in lameness or poor performance. *Vet. Clin. North Am. Equine Pract.* **27**, 417-437.
12. Wijnberg, I.D., Bergmann, W. and Veraa, S. (2015) Diagnose und prognose neurologischer Erkrankungen der Halswirbelsäule beim pferd. *Praktischer Tierarzt.* **96**, 150-158.
13. Bergmann, W., Bergknut, N., Veraa, S., Grone, A., Vernooij, H., Wijnberg, I.D., Back, W. and Grinwis, G.C.M. (2018) Intervertebral Disc Degeneration in Warmblood Horses: Morphology, Grading, and Distribution of Lesions. *Vet. Pathol.* **55**, 442-452.
14. Lu, D.S., Shono, Y., Oda, I., Abumi, K. and Kaneda, K. (1997) Effects of chondroitinase ABC and chymopapain on spinal motion segment biomechanics. An in vivo biomechanical, radiologic, and histologic canine study. *Spine (Phila Pa. 1976)*. **22**, 1828-34; discussion 1834-5.
15. Hoogendoorn, R.J., Wuisman, P.I., Smit, T.H., Everts, V.E. and Helder, M.N. (2007) Experimental intervertebral disc degeneration induced by chondroitinase ABC in the goat. *Spine (Phila Pa. 1976)*. **32**, 1816-1825.
16. Wei, F., Zhong, R., Wang, L., Zhou, Z., Pan, X., Cui, S., Sun, H., Zou, X., Gao, M., Jiang, B., Chen, W., Zhuang, W., Sun, H. and Liu, S. (2015) Pingyangmycin-induced in vivo lumbar disc degeneration model of rhesus monkeys. *Spine (Phila Pa. 1976)*. **40**, E199-210.
17. DeRouen, A., Spriet, M. and Aleman, M. (2016) Prevalence of Anatomical Variation of the Sixth Cervical Vertebra and Association with Vertebral Canal Stenosis and Articular Process Osteoarthritis in the Horse. *Vet. Radiol. Ultrasound.* **57**, 253-258.

18. Santinelli, I., Beccati, F., Arcelli, R. and Pepe, M. (2014) Anatomical variation of the spinous and transverse processes in the caudal cervical vertebrae and the first thoracic vertebra in horses. *Equine Vet. J.* **48**, 45-49
19. Schmidt, H., Dreischarf, M., Strube, P. and Putzier, M. (2016) Preoperative Segmental Disc Geometry as a Possible Predictor for the Clinical Outcome of Lumbosacral Total Disc Replacement. *J. Spine.* **5**
20. Pinheiro, J.C., Bates, D.M., Debroy, S. and Deepayan, S. (2017) Linear and nonlinear mixed effects models. R package. R Foundation for Statistical Computing, Vienna, Austria URL <https://www.R-project.org/>.
21. R Core Team. (2017) R: A language and environment for statistical computing. R Foundation for Statistical Computing, Vienna, Austria URL <https://www.R-project.org/>.
22. Koo, T.K. and Li, M.Y. (2016) A Guideline of Selecting and Reporting Intraclass Correlation Coefficients for Reliability Research. *J. Chiropr Med.* **15**, 155-163.
23. Fontes, R.B., Baptista, J.S., Rabbani, S.R., Traynelis, V.C. and Liberti, E.A. (2015) Structural and Ultrastructural Analysis of the Cervical Discs of Young and Elderly Humans. *PLoS One.* **10**, e0139283. doi:10.1371/journal.pone.0139283.
24. Trout, J.J., Buckwalter, J.A., Moore, K.C. and Landas, S.K. (1982) Ultrastructure of the human intervertebral disc. I. Changes in notochordal cells with age. *Tissue Cell.* **14**, 359-369.
25. Masuda, K., Imai, Y., Okuma, M., Muehleman, C., Nakagawa, K., Akeda, K., Thonar, E., Andersson, G. and An, H.S. (2006) Osteogenic protein-1 injection into a degenerated disc induces the restoration of disc height and structural changes in the rabbit anular puncture model. *Spine (Phila Pa. 1976).* **31**, 742-754.
26. Masuda, K., Aota, Y., Muehleman, C., Imai, Y., Okuma, M., Thonar, E.J., Andersson, G.B. and An, H.S. (2005) A novel rabbit model of mild, reproducible disc degeneration by an anulus needle puncture: correlation between the degree of disc injury and radiological and histological appearances of disc degeneration. *Spine (Phila Pa. 1976).* **30**, 5-14.
27. Veraa, S., Bergmann, W., Wijnberg, I.D., Back, W., Vernooij, H., Nielen, M. and van den Belt, A.M. (2019) Equine cervical intervertebral disc degeneration is associated with location and MRI features. *Vet. Radiol. Ultrasound.* <https://doi.org/10.1111/vru.12794>
28. Beccati, F., Santinelli, I., Nannarone, S. and Pepe, M. (2018) Influence of neck position on commonly performed radiographic measurements of the cervical vertebral region in horses. *Am. J. Vet. Res.* **79**, 1044-1049.



7

Intervertebral Disc Degeneration in Warmblood Horses: Morphology, Grading and Distribution of Lesions

Wilhelmina Bergmann^a, Niklas Bergknut^b, Stefanie Veraa^c, Andrea Grone^a, Hans Vernooij^d, Inge D. Wijnberg^e, Willem Back^{e,f}, Guy C.M. Grinwis^a

^a Department of Pathobiology, Faculty of Veterinary Medicine, Utrecht University, Yalelaan 1, NL-3584 CL, The Netherlands

^b Evidensia verwijsklinik Hart van Brabant, Waalwijk, The Netherlands

^c Division of Diagnostic Imaging, Faculty of Veterinary Medicine, Utrecht, University, Yalelaan 108, NL-3584 CM, Utrecht, The Netherlands

^d Department of Farm Animal Health, Yalelaan 7, NL-3584 CL, The Netherlands

^e Department of Equine Sciences, Faculty of Veterinary Medicine, Utrecht University, Yalelaan 114, NL-3584 CM Utrecht, The Netherlands

^f Department of Surgery and Anaesthesiology of Domestic Animals, Faculty of Veterinary Medicine, Ghent University, Salisburylaan 133, B-9820 Merelbeke, Belgium

Veterinary Pathology, 2018, 55(3), 442-452

ABSTRACT

Equine intervertebral disc degeneration is thought to be rare and of limited clinical relevance, although research is lacking. To objectively assess pathological changes of the equine intervertebral disc and their clinical relevance, description of the normal morphology and a practical, biologically credible, grading scheme are needed. The objectives of this study are to describe the gross and histological appearance of the equine intervertebral discs and to propose a grading scheme for macroscopic degeneration. Spinal units from 33 warmblood horses were grossly analyzed and scored. Of the 286 intervertebral discs analyzed, 107 (37%) were assigned grade 1 and grade 2 (considered normal), and were analyzed histologically. A nucleus pulposus and an annulus fibrosus could be identified macroscopically and histologically. Histologically, the nucleus pulposus was composed of a cartilaginous matrix, and the annulus fibrosus of parallel collagenous bands. A transition zone was also histologically visible. Intra- and inter-observer reliability scores were high for all observers. Higher grades were associated with greater age. Gross changes associated with equine intervertebral disc degeneration (grades 3-5)—i.e. yellow discoloration, cleft formation, and changes in consistency of the nucleus pulposus—were largely similar to those in humans and dogs and were most prevalent in the caudal cervical spine. Equine intervertebral disc degeneration was not associated with osteophyte formation. Changes of the vertebral bone were most common in the thoracolumbar spine, but were not correlated with higher grades of intervertebral disc degeneration. Thus changes of the vertebral bone should be excluded from grading for equine intervertebral disc degeneration.

Keywords: horses, intervertebral disc degeneration, grading, gross, histology, nucleus pulposus, annulus fibrosus

INTRODUCTION

Neurological conditions originating from the equine neck are common [57]. Non-infectious, non-traumatic causes have mostly been attributed to space-occupying changes of the facet joints, vertebral dorsal laminae and ligamentum flavum leading to static compression of the spinal cord and nerves or to cervical vertebral instability characterized by dynamic narrowing of the spinal canal during movement of the neck [12, 28, 35]. Although cervical neurological abnormalities in horses have been related to intervertebral discs (IVDs) in case reports [15-17, 24, 30, 32, 33, 38, 44, 45, 48, 55, 56], degeneration of the IVD is thought to be clinically less relevant [7, 26, 33, 36, 53] and a detailed morphological description is missing. However, numerous studies in humans and dogs do show a compelling relationship between IVD degeneration (IVDD) and clinical signs [2, 9, 29, 31, 46] but systematic studies of equine IVD disease seem to be lacking. Moreover, there is absence of consensus amongst authors about the anatomical characteristics of the equine IVD. Some publications claim the lack of a nucleus pulposus (NP) [7,53], while in others a fibrous [33, 36, 52, 53] or fibrocartilaginous [26, 58] NP is acknowledged. Nonetheless, like humans and dogs [5, 8], it is agreed that there is also a peripheral annulus fibrosus (AF) in horses [17, 24, 44, 56, 58] which is composed of collagenous bands [58].

To be able to determine the clinical importance of equine IVDD, a precise definition of the anatomical structures and the morphological characteristics of degeneration is required. Therefore, this study had three objectives. Firstly, to describe the gross and histological appearance of the normal equine IVD, to facilitate the development of a grading scheme for gross changes of the IVDs and the vertebral bone including changes of the subchondral bone (vertebral endplate) and changes of the ventral part of the vertebral body since these anatomical structures are also included in grading of human and canine IVDs [5, 51]. Secondly, to develop a grading scheme of the gross pathological changes of the equine IVD. Thirdly, to evaluate the prevalence of IVDD within different spinal regions.

MATERIALS AND METHODS

Animals

Vertebral columns were harvested post-mortem from 33 warmblood horses that either died unexpectedly or were humanly euthanized for reasons unrelated to the current study and referred for necropsy to the Department of Pathobiology, Faculty

of Veterinary Medicine, Utrecht University (Supplemental Table S1). All but two of the horses used in this study were privately owned. One horse was used for police work. Necropsy was performed with the owner's informed consent to investigate the cause of death or the cause for the clinical signs. One of the horses was owned by the Faculty of Veterinary Medicine, Department of Equine Sciences of the Utrecht University and used for teaching purposes which included obtaining surgical skills with subsequent euthanasia with approval of the local ethics committee (DEC number 2013.III.01.012). Horses were of different ages, varying from 8 months to 21 years (mean age 8.8 +/- 6.1 years), different breeds (28 Royal Dutch Sport horses (RDSH), 2 Zangersheide horses, 1 Trakehner, 1 Holsteiner, 1 Westphalian horse) and different sexes (15 mares, 6 stallions, 12 geldings).

Sampling

The vertebral columns were dissected and cut mid-sagittally using a K430 band saw (Kolbe, Germany; blades Munkfors, Sweden). The cut surfaces of the IVDs were photographed with a Nikon D80 digital single lens reflex camera (Nikon, Japan) and the analysis was based on the spinal unit (subchondral bone-IVD-subchondral bone). Only one IVD was visible per photograph to allow unbiased evaluation. Only pictures of good quality to evaluate subtle changes were used, resulting in a total of 286 spinal units (86% of the number photographed) being analyzed. Four different regions were selected for examination, based on common sites of IVDD and related diseases in humans and in non-chondrodystrophic dogs, the two most commonly studied species affected by IVDD [3, 23]. The IVDs of the cervical spine (C2-T1) were selected because in humans this is the second most common region showing IVDD after the lumbar region [22, 49]. In addition, in non-chondrodystrophic dogs the caudal cervical spine is predisposed to develop IVDD-related diseases [9]. The IVDs of the cervical spine were further subdivided into 2 regions: 1) cranial to mid-cervical region (IVDs between the cervical vertebrae C2 and C5 [10]) and 2) the caudal cervical region (IVDs between C5 and the thoracic vertebra T1 [11, 28]) to identify possible differences in the distribution of IVDD in the equine cervical spine as seen in the dog [9]. In humans and dogs severe IVDD can lead to osteophyte formation (spondylosis)[3, 51]. To investigate whether IVDD is also important in the development of osteophytes (spondylosis) in the horse the intervertebral discs between thoracic vertebrae T11 and T13, the most common region for horses to develop spondylosis[25, 53], were selected. Finally, the lumbosacral region (IVDs between the lumbar vertebrae L4 and the sacral vertebrae S1) was chosen, as this is the most common location for IVDD in humans and for diseases associated with IVDD in non-chondrodystrophic dogs [2, 22, 49]. To make sure not to damage the IVD between C7 and T1 during necropsy, the cervical and thoracic parts of the spine were separated by sawing through vertebra T2.

Consequently, the IVD between T1 and T2 was readily available and therefore also used to develop and validate the grading scheme.

Development of a macroscopic grading scheme for IVDD and the vertebral bone

The photographs of the IVDs were analyzed for morphologic changes of the NP, AF and vertebral bone using a human grading scheme [51], which is also validated for the dog [3] and which was subsequently adjusted for the horse as deemed necessary. In short, for grading of the IVD the annulus fibrosus and the nucleus pulposus were evaluated for its texture, color and the presence of clefs. IVD considered normal showed a gelatinous, semi-translucent nucleus and white shiny lamellae. Degenerated discs were characterized by a fibrillary nucleus pulposus, with yellow (-whitish) discoloration of both the nucleus and the annulus with or without clefs (Table 1, Fig. 1-9). For grading of the vertebral body, both the subchondral bone and the ventral part of the vertebral body were evaluated. With increasing grades the subchondral bone changed from trabecular to more compact. The ventral part of the vertebral bone was being reviewed for the loss of rounded margins and the development of osteophytes (Table 2, Fig 1 and Fig. 10-14).- For human and canine discs, grades 1 and 2 are considered normal, and grade 4 and 5 degenerated, with grade 3 representing a transitional stage [6, 50]. In a preceding pilot study (results not shown), the grading of morphological changes of the subchondral bone as well as osteophyte formation and spondylosis of the ventral part of the vertebral body did not correlate with the grades for changes of the AF and NP, and therefore these morphological aspects were graded in two separate schemes.

Validation of the macroscopic grading schemes

The photographs were assigned a random number using an online randomization program and graded twice each by three independent observers with a time lapse of at least a week between grading sessions of each observer. Inter and intra observer reliabilities were calculated by using a Cohen's weighted Kappa analysis (quadratic weights of 1, 0.9375, 0.75, 0.4375 and 0). A κ -value of less than 0.00 is considered poor, a value between 0.00 and 0.20 as slight, between 0.21 and 0.40 as fair, between 0.41 and 0.60 as moderate, between 0.61 and 0.80 as substantial and a value between 0.81 and 1.00 as almost perfect [3, 27]. The grades assigned during the second round of grading by each observer were added and averaged for a total averaged final grade per spinal unit. If the assigned grade from the second grading differed by more than 1 between the observers, the image was reviewed by the three observers and a consensus grade was allotted.

Statistical analysis

To evaluate the association of the grade for IVDD and the grade for changes of the vertebral bone with age and distribution, the final grades were log-transformed to meet the model assumptions for normality and constant variance. The outcomes were analyzed using a linear mixed model with explanatory continuous variable age and factor variable region and horse was added to the model as random effect to take the correlated observations within horse into account. The Akaike information criterion (AIC) was used to select the best model and Bonferroni correction was applied to correct for multiple comparisons. Residuals were used to investigate the correctness of the model assumptions. A scatterplot showed a linear association between the grades for IVDD and the grades for the changes of the vertebral bone within the same spinal unit only up to grade 3 (Fig. 15). Therefore correlation was determined with a Spearman's rank-order correlation test. All statistical analyses were performed using SPSS version 22 (IBM).

Normal histology

For analysis of the histological characteristics of the normal equine IVD, 107 discs assigned grade 1 and grade 2 (37%) were cut into slices of 0.5 cm thick and fixed in 10% neutral-buffered formalin and then decalcified in 10% ethylene-diamine-tetraacetic acid (EDTA) before routine processing into 4 µm sections that were stained with hematoxylin and eosin (HE) and with alcian blue/ picosirius red (AB/PSR) [4, 18, 37]. Depending on the size of the IVD, 2 to 5 histological sections were necessary to encompass the entire IVD. The data analyzed in this study will be used for further research and are therefore not available as Supplemental Materials in the near future.

RESULTS

Macroscopically the AF and the NP could be identified using mid-sagittal sections in all dissected regions of the vertebral column (Fig. 1-9). The IVD was convex on the cranial aspect and concave at the caudal aspect, and this shape was most prominent in the cervical region. The NP was characterized by a gelatinous, non-lamellar texture compared to the AF, and was placed slightly eccentrically towards the dorsal part of the IVD (Fig. 1). The NP of a normal disc was defined as shiny, blue-white, semi-translucent and pulpy. A firmer more solid NP with a fibrillar texture and often with yellow-white discoloration was interpreted as mild, early degeneration. Cleft formation of the NP was interpreted as severe degeneration occurring in later stages. The normal AF was defined as a lamellar structure with the ventral AF mildly broader and about

twice the height of the dorsal AF. Cleft formation of the lamellae in a dorso-ventral direction, nearly always accompanied by a yellow discoloration, was interpreted as degeneration. Bulging of a few millimeters of the dorsal AF into the spinal canal was seen commonly in all grades (Fig. 1, 2, 8,9). However, in none of the IVDs this was deemed extensive enough to have caused pressure on the spinal cord as visible on mid-sagittal sections of the vertebral column. Herniation of the nucleus pulposus was not seen in any of the IVDs examined.

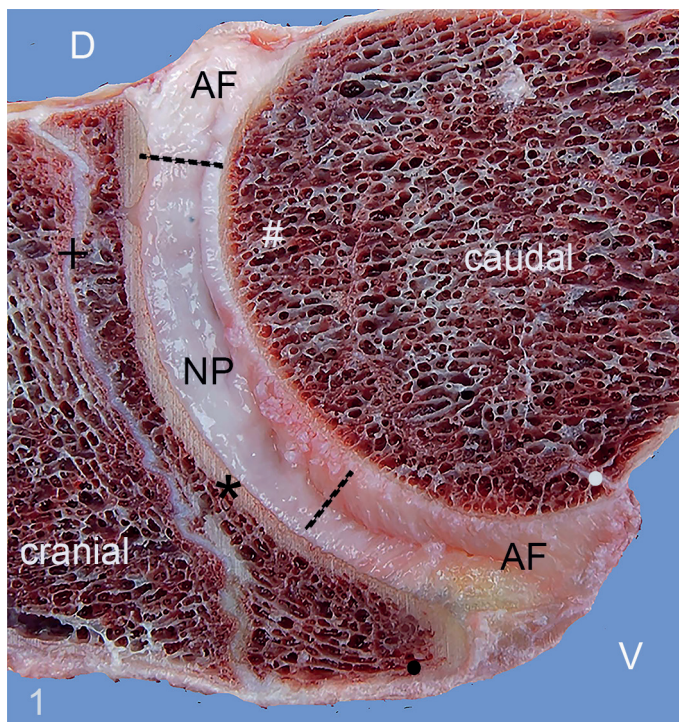


Fig. 1. Normal intervertebral disc, C7T1 (intervertebral disc between cervical vertebra 7 and thoracic vertebra 1), mid-sagittal spinal section, 2-year-old horse. Grade 1 (normal) for intervertebral disc degeneration, and grade 2 for changes of the vertebral bone. The gelatinous, semi-translucent, white and shiny nucleus pulposus (NP) is visible between the dotted lines. The annulus fibrosus (AF) is white and contains horizontal lamellae. The dorsal AF shows minimal dorsal bulging. Cranially there is a rim of subchondral compact bone (*), whereas the caudal subchondral bone is trabecular. The ventral part of the vertebral body (+) is rounded. D, dorsal; V, ventral; +, growth plate; *, compact subchondral bone/ vertebral endplate; #, subchondral trabecular bone/ vertebral endplate; •, ventral part of the vertebral body.

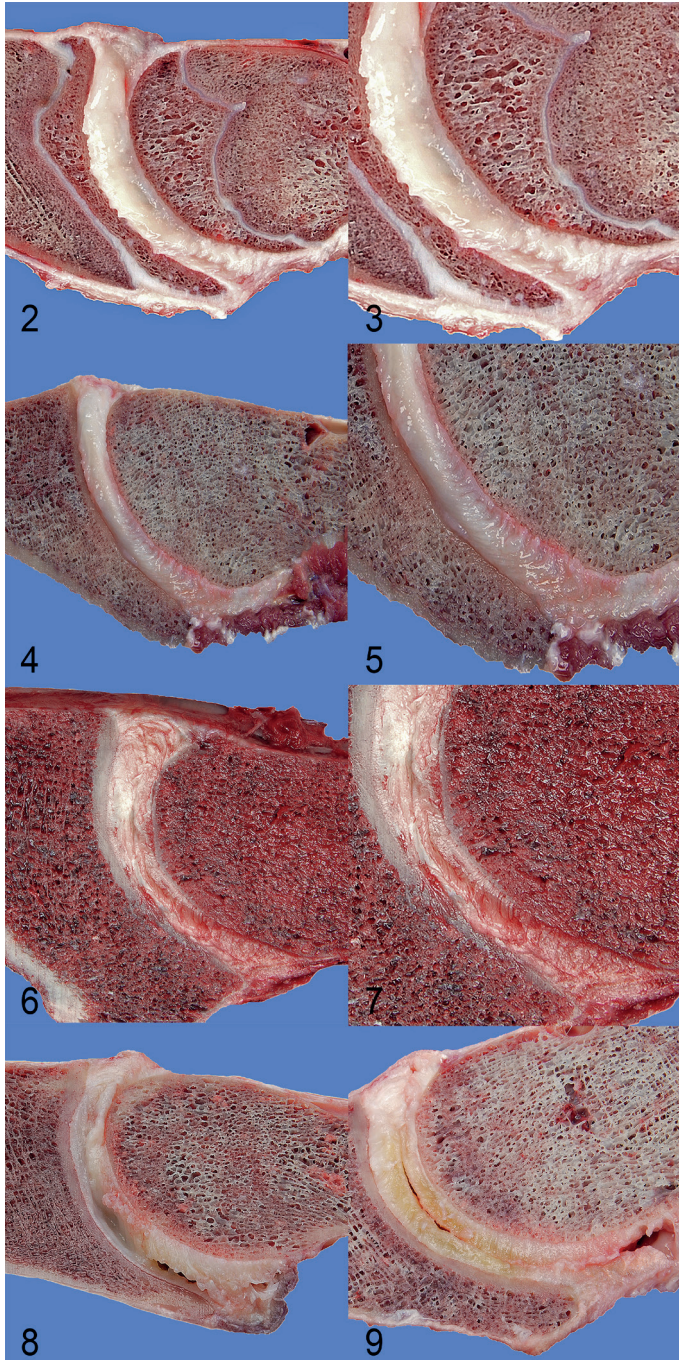


Fig. 2-9. Grade 1-5 for intervertebral disc degeneration, mid-sagittal sections of the spinal column, horse. **Figures 2-3.** Grade 1, C5-C6, 8 months old. The nucleus pulposus (NP) is white, gelatinous and shiny. The dorsal and ventral parts of the AF are white, shiny and ventrally horizontal lamellae are easily visible. The dorsal AF shows minimal dorsal bulging. **Figures 4-5.** Grade 2, C2-C3, 6 years old. The NP is partially gelatinous and partially fibrillar, and has a more condensed consistency than in grade 1. The AFs are white and shiny. The horizontal lamellae of the ventral AF are visible (Fig 5). **Figures 6-7.** Grade 3, C3-C4, 12 years old. The NP is completely fibrillar and has a more condensed consistency than grade 2. The dorsal and ventral parts of the AF are still white with reduced visibility of the lamellae. **Figure 8.** Grade 4, C6-C7, 10 years old. The NP is fibrillar. The ventral AF has a vertical cleft. The dorsal AF shows minimal dorsal bulging. **Figure 9.** Grade 5, C7-T1, 15 years old. The NP and the AF are slightly yellow with clefting through both. The dorsal AF shows minimal dorsal bulging.

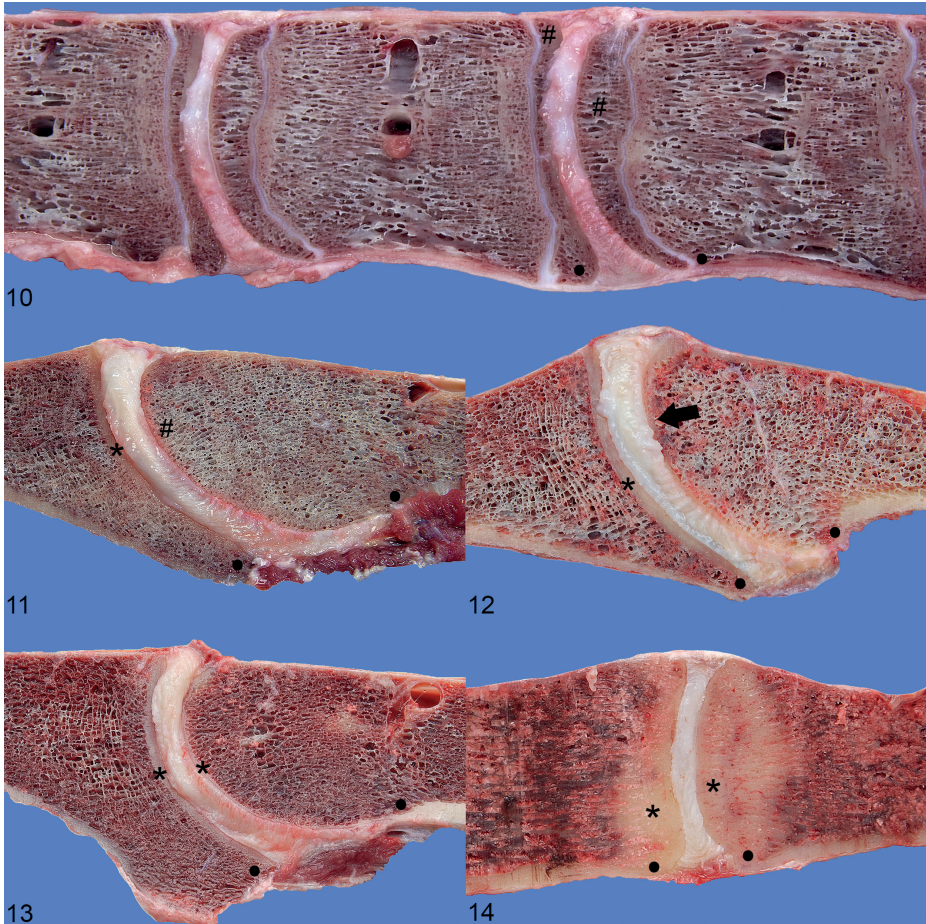


Fig. 10-14. Grade 1-5 for changes in the vertebral bone, mid-sagittal sections of the spinal column, horse. **Figure 10.** Grade 1, T11-T12, 1 year old. The cranial and caudal subchondral bone are composed of trabecular bone (#). The ventral part of the vertebral body has rounded margins (*). **Figure 11.** Grade 2, C2-C3, 6 years old. Cranially there is a rim of subchondral compact bone (*). The caudal subchondral bone is composed of trabecular bone (#). The ventral part of the vertebral body is rounded (*). **Figure 12.** Grade 3, C3-C4, 15 years old. Cranially there is a rim of subchondral compact bone (*). Caudally the subchondral trabecular bone is multifocally more compact (arrow). The ventral part of the vertebral body is rounded (*). **Figure 13.** Grade 4, C4-C5, 10 years old. Cranially there is a rim of subchondral compact bone (*). Caudally there is a smaller rim of compact bone (*). The ventral part of the vertebral body is rounded(*). **Figure 14.** Grade 5, L5-L6, 10 years old. Both cranially and caudally there are thick bands of compact bone (*). The ventral part of the vertebral body is rounded (*).

Histologically the normal IVD was dorsally and ventrally composed of approximately 10 parallel bands that stained brightly red with the AB/PSR stain, consistent with an AF that is rich in collagen type I. The more centrally located part of the IVD consisted of a blue intercellular matrix, compatible with a proteoglycan-rich (mucinous) cartilaginous NP. Between these two parts a rather poorly demarcated transition zone was visible in which there was a gradual transition of the staining characteristics of the intercellular matrix (Fig. 16). This histological difference was co-localized with the grossly visible different morphological characteristics of the peripheral annulus region and the central nucleus region of the equine IVD. At the cranial and caudal margins, the NP and AF were bordered by a rim of hyaline cartilage of approximately 8 chondrocytes thick, compatible with a cartilaginous endplate (Fig. 16 and 17).

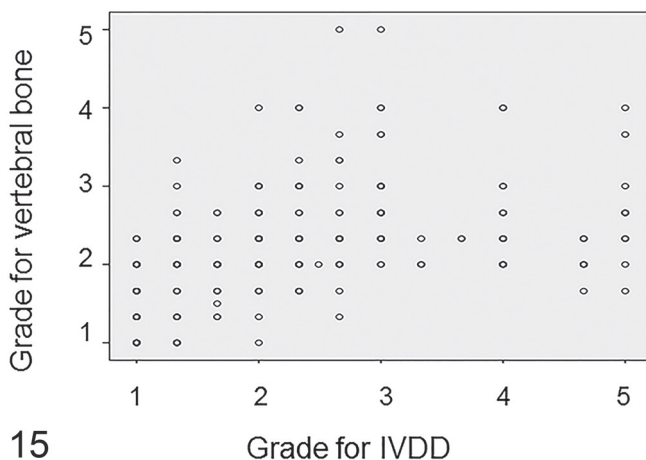


Fig. 15. Correlation between the total averaged final grade for intervertebral disc degeneration (IVDD) and for changes of the vertebral bone. Changes in the vertebral bone are linearly associated with grades 1-3 for IVDD, but are not associated with grades 4-5 for IVDD

IVDD was significantly more severe in the caudal cervical region (C5-T1) with a mean grade of 2.69 +/- 1.64 standard deviation (SD) compared to the cranial cervical region (mean 2.00 +/- 0.89 SD), thoracic (mean 2.02 +/- 0.86 SD) and lumbosacral region (mean 2.08 +/- 0.87 SD) (Fig. 18, Table 3) ($P < 0.05$). The grade for IVDD increased significantly with age: grade 1, 4.12 +/- 4.15 years of age (mean \pm SD); grade 2, 8.10 +/- 4.91 years; grade 3, 11.52 +/- 5.84 years; grade 4, 11.13 +/- 5.35 years; grade 5, 14.20 +/- 3.31 years ($P < 0.05$). The grades for changes of the vertebral bone also increased significantly with age: grade 1, 2.05 +/- 1.99 years of age (mean \pm SD); grade 2, 8.12 +/- 5.2 years; grade 3,

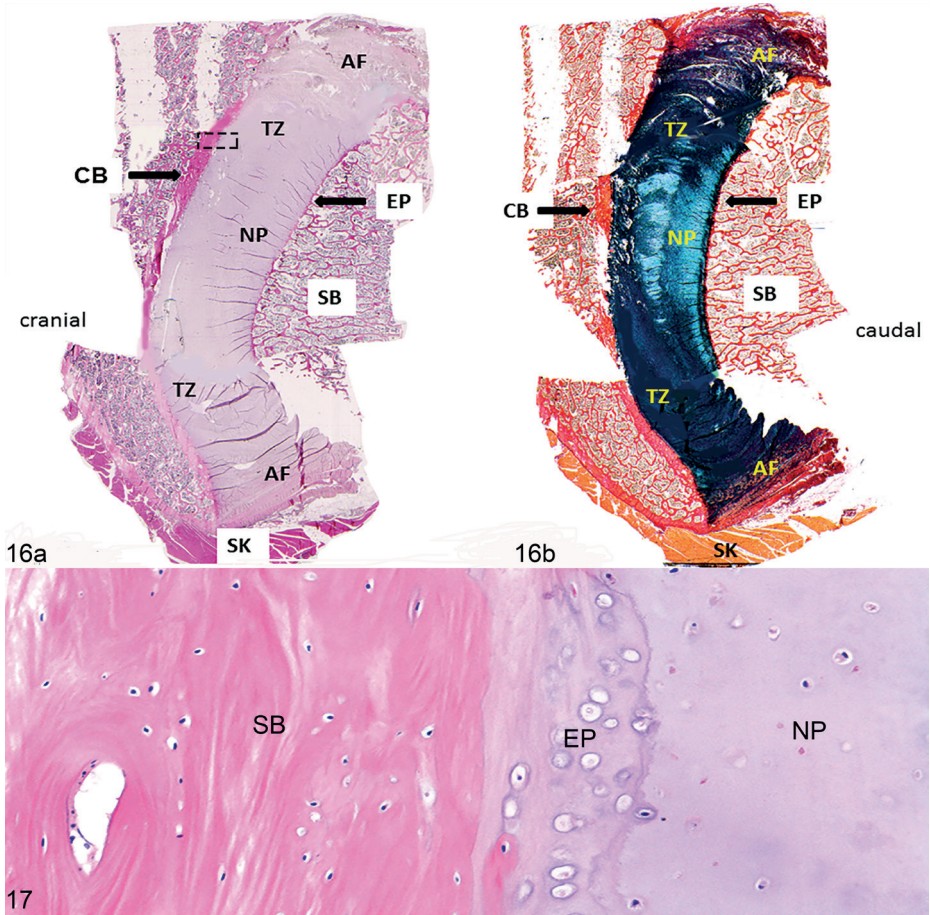
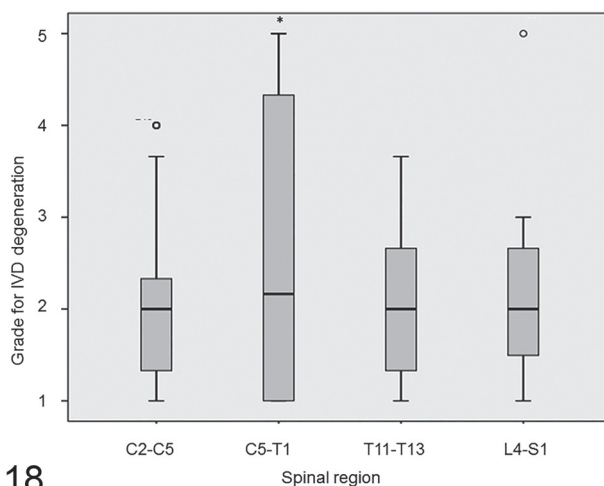


Fig. 16-17. Normal intervertebral disc, C3-C4, 11-year-old horse. Grade 1 for intervertebral disc degeneration, and grade 2 for changes of the vertebral bone. There is no obvious distinction between the annulus fibrosus (AF) and the nucleus pulposus (NP) with the hematoxylin and eosin stain (Fig. 16a). However, the alcian blue/picrosirius red stain (Fig. 16b) does show clear difference between the red collagenous AF, and the blue proteoglycan-rich NP, and these are separated by a transition zone (TZ). On the cranial and caudal margins, the IVD is bordered by a cartilaginous endplate (EP) composed of hyaline cartilage and on the cranial aspect a rim of subchondral compact bone (CB) is visible. SB, subchondral bone; SK, skeletal muscle. The rectangle indicates the area of the intervertebral disc enlarged in Fig. 17. **Figure 17.** The cartilaginous nucleus pulposus (NP) is flanked by an endplate (EP) composed of hyaline cartilage. SB, subchondral bone. Hematoxylin and eosin.

11.79 +/- 6.08 years; grade 4, 14.5 +/- 3.8 years; ($P < 0.05$). The formation of subchondral compact bone was significantly more extensive in the thoracic and lumbosacral regions (mean \pm SD grade of 2.34 +/- 0.75) compared to the cervical segments (2.01

+/- 0.67) (Fig. 19, Table 4) ($P < 0.05$). The cartilaginous endplate was not visible without microscopic magnification in any of the IVDs examined. There was a significant correlation between the grade for IVDD and the grade for changes of the vertebral bone, ($r_s = 0.56$, $P < 0.01$) which was almost exclusively due to the changes of the subchondral bone. Changes of the ventral part of the vertebral body were only present at the two thoracic IVDs of the oldest horse and were characterized by a partially bony, partially fibrous bridge with involvement of the outer layers of the ventral AF between the corresponding vertebrae. These IVDs were both assigned a grade 3.

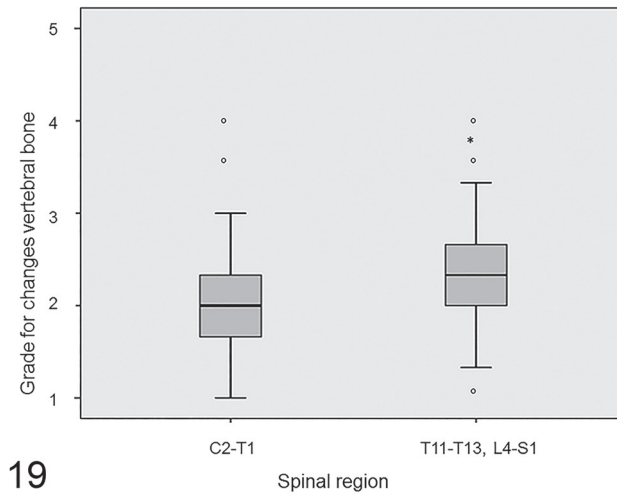


18

Fig. 18. Distribution of grades for intervertebral disc degeneration (IVDD) within the different spinal regions. IVDD was significantly more severe in the caudal cervical region (C5-T1) compared to the cranial cervical, thoracic and lumbosacral region. * $P < 0.05$. The box spans the first to the third quartile (*interquartile range*). The line inside the box represents the median. The whiskers show the minimum and maximum.; o, outliers.

The intra-observer reliability was substantial to almost perfect with mean κ scores of 0.78, 0.87 and 0.87 for the three observers when using the grading scheme for IVDD. The interobserver reliability for this grading scheme was also substantial to almost perfect with κ scores of 0.75 and 0.82.

The intra-observer reliability for the scoring scheme for changes of the vertebral bone was moderate to substantial with mean κ scores of 0.50, 0.70 and 0.77. The interobserver reliability for this grading scheme was fair to moderate with mean κ scores of 0.39 and 0.56.



19

Fig. 19. Distribution of grades for changes of the subchondral bone within the different spinal regions. Increased density of subchondral bone was significantly more extensive in the thoracic and lumbosacral regions compared to the cervical segments. * $P < 0.05$. The box spans the first to the third quartile (*interquartile range*). The line inside the box represents the median. The whiskers show the the minimum and maximum.; o, outliers.

DISCUSSION

In contrast to previous publications[7, 53], this study showed that the equine IVD does have a grossly and histologically discernible proteoglycan-rich NP that is distinct from the lamellar collagenous AF. This is similar to the situation in humans and dogs (Fig. 1) [5, 6, 8, 37, 51]. Furthermore, cranially and caudally located cartilaginous endplates separated the IVD from the bony vertebral endplates, and a transition zone was present between the AF and the NP which is also comparable to the situation in humans and dogs [6, 37]. In literature on the human and canine intervertebral disc, the bony vertebral endplate adjacent to the cartilaginous endplate of the IVD is commonly referred to as subchondral bone. As shown in this study and described previously [44, 58], a rim of cartilage between the IVD and the vertebral bone is also present in the horse. To be consistent with the vast majority of literature the vertebral endplate is called subchondral bone in this study. The distinction between the AF and the NP was much less clear, both macroscopically and histologically (in the HE stain), in horses compared to human and dogs (Fig. 1 and 16). Grossly, in horses of all ages, the NP was never as translucent as in normal human and canine IVDs, making it more difficult to distinguish the NP from the AF. Presumably this is why in previous publications [7, 53]

the equine IVD was said to lack a NP. Nevertheless, the AB/PSR stain clearly showed a morphological and biochemical difference between the AF and NP and this histological difference was co-localized with the different gross morphological characteristics of the peripheral annulus region and the central nucleus region of the equine IVD. Bulging of a few millimeters of the dorsal AF into the spinal canal was commonly seen in all grades and was considered to be too small to have caused pressure on the spinal cord, suggesting that minimal bulging of the dorsal AF occurs in normal horses.

Gross changes that were in accordance with degeneration as described for human and canine IVDs could be identified in all parts of the IVD [1, 5, 6, 51]. The presence of yellow discoloration and cleft formation are the only features previously described for equine IVDD[7, 53], whereas the present study identified additional morphological characteristics like a reduced gelatinous and an increased fibrillary appearance of the NP This interpretation is likely to also apply to horses.

Although the correlation between grades for IVDD and changes of the vertebral bone was statistically significant, this significance seemed to be present for grades 1-3 only (Fig. 15). The more severe grades for IVDD (grade 4 and 5) were not associated with a substantial increase in changes of the vertebral bone suggesting that age is a more dominant factor for these changes than IVDD. Furthermore, grades for IVDD were significantly associated with localization in the caudal cervical spine whereas grades for changes of the vertebral bone were significantly associated with the thoracolumbar spine. Therefore, macroscopic grading of equine IVDD should only include the morphology of the NP and the AF to prevent under or over interpretation of the severity of IVDD.

It has been suggested that osteophyte formation in the horse is not secondary to IVDD [7]. The findings in the present study support this assumption. Of the 39 IVDs assigned a grade 4 or a grade 5, none showed changes of the ventral part of the vertebral body. Additionally, ventral bridging was seen only between three thoracic vertebrae of one horse, and in that case both associated IVDs were assigned a grade 3 for IVDD.

An age-related increase in the bone density of the equine cervical subchondral bone, directly adjacent of the cartilaginous endplate, was found in this and a previous study [58]. The increased density of the subchondral bone is probably a common feature of aging in horses, as we have found no correlation with pronounced IVDD (grades 4 and 5). The density of the subchondral trabecular bone was significantly less in the

cervical than in the thoracic and lumbosacral segments, perhaps because the former trabeculae are oriented less horizontally, possibly leading to less axial compression stress and subsequently lower bone density as dictated by Wolff's law [42].

The equine grading scheme presented here was based on a commonly used human grading scheme that does not include the parameters joint space width (considered to be indicative for IVDD on radiographs in both humans and dogs[40, 46]) or dorsal bulging and herniation of the IVD. These parameters were not included in the human grading scheme because they are considered consequences of, and not part of the degenerative process [20], and therefore these parameters were also not incorporated in the equine scheme.

When investigating the pathogenesis and the clinical relevance of equine IVDD a standardized method for evaluation and grading is necessary to assess the gross characteristics and the severity of degeneration. Such a method will allow reliable comparison of results in future research. A good grading scheme is reproducible, which is reflected in high kappa scores for intra and inter observer reliability [51] as was the case in the adapted grading scheme used in the present publication. A good grading scheme should also be biologically credible [51]. In humans, dogs and also in horses IVDD is correlated with age [1, 7, 36, 54]. The grades for IVDD assigned in the present study were also significantly associated with age, supporting its biological credibility.

In accordance with the existing literature [7, 36], IVDD was significantly more prevalent in the caudal cervical segment compared to the other segments examined. In addition to the age- related component, IVDD in humans and dogs is thought to be influenced by genetic and mechanical factors, and reduced nutrient supply [2, 19, 31, 39]. In humans, IVDs undergo microstructural changes to a similar extent in all regions and age-related degeneration affects the entire spine [1, 49]. A higher prevalence of degeneration in certain regions in both humans and dogs can occur due to locally increased mechanical loading [1, 19, 39, 43, 49]. Also in horses increased mechanical load has been suggested as a cause for the increased prevalence of IVDD in the caudal cervical spine [7]. In addition, dorsoventral mobility may promote IVDD in the horse [53]. According to the literature, the movements in the caudal cervical spinal joints are larger than those in the cranial cervical spine [41], which might explain the observed difference in prevalence of IVDD between these 2 regions. The lower incidence of IVDD in the thoracic spine of humans and dogs has been attributed to the stabilizing effect of the rib cage with resultant reduced mechanical stress on the IVDs [29, 47]. The horse has a comparably rigid thoracolumbar spine that, as in humans and dogs,

might at least partially explain the low incidence of IVDD in this region [26, 34, 52]. An increased prevalence of degeneration in the equine lumbosacral disc has been previously described [36, 53] but this was not confirmed by the present study. In these earlier publications the breeds of horses, if specified, did not belong to the group of warmblood horses. This suggests that the breed or the work the animal is used for might influence which IVD has the highest mechanical loading and subsequently the highest risk for development of degeneration. It might be that the lumbosacral area is more affected in the racing Thoroughbred than in warmblood horses, as the former breed performs exclusively at the gallop. Ventrodorsal flexion-extension is known to be largest at canter or gallop and the lumbosacral junction is known to show by far the largest range of motion [13, 14, 21]. Unfortunately, the type of work the horses were used for was not mentioned in these publications.

In conclusion, the equine IVD had a grossly and histologically discernible proteoglycan-rich NP and a lamellar collagenous AF, which is similar to the situation in humans and dogs. The morphological changes associated with equine IVDD are largely similar to those found in humans and dogs. A grading scheme for equine IVDD, based upon a generally accepted human scheme, was developed which proved useful as was reflected in high κ -values for intra and interobserver reliability. IVDD, as evaluated by the use of this grading scheme, was associated with increasing age, confirming the biological credibility of the scheme. IVDD was most prevalent in the caudal cervical spine (C5-T1). In horses, subchondral bone changes were not correlated with IVDD, and therefore, should be graded separately, in contrast to the case in humans and dogs. We suggest using this grading scheme in further research into the pathogenesis of equine IVDD, possible breed-related differences, its effect on the vertebral column and its relevance for the development of neurological conditions arising from diseases of the spinal column in horses.

Acknowledgements

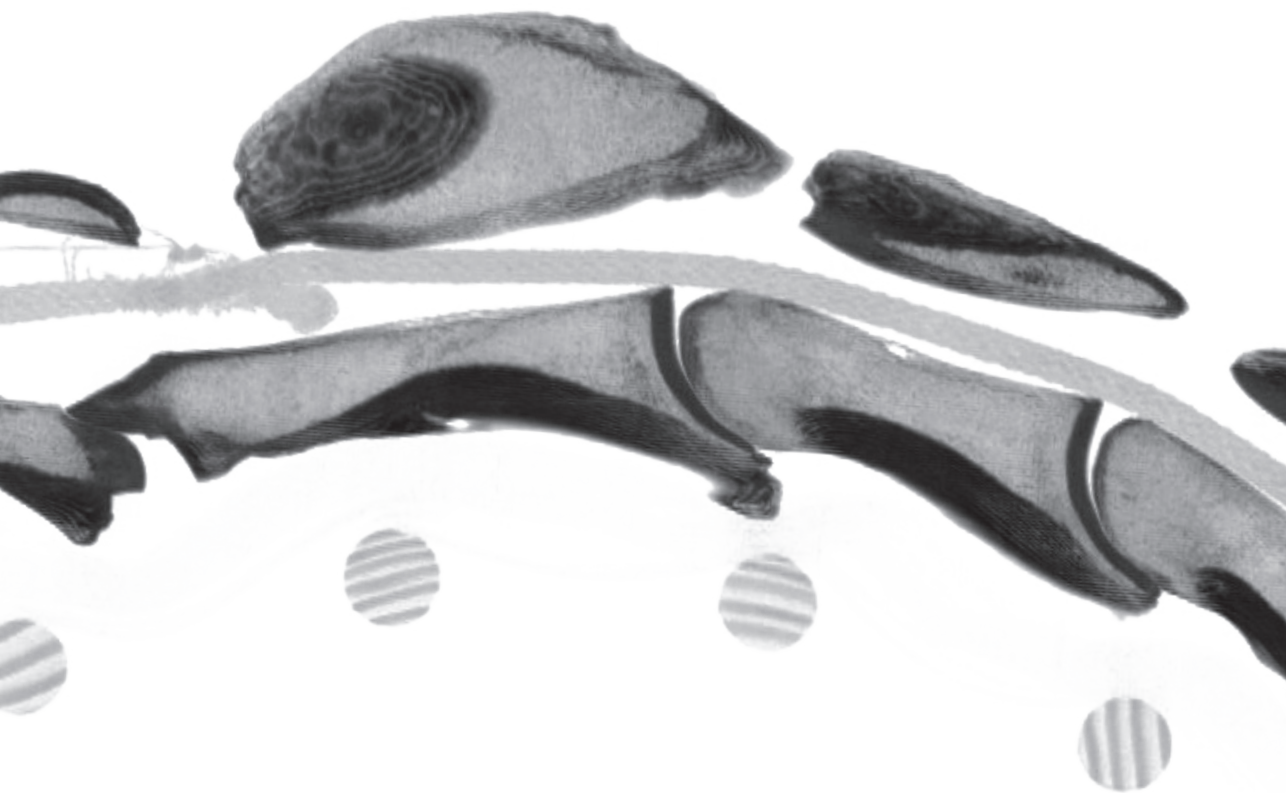
The authors like to thank Rachel E. Thomas for proofreading and Prof. P.R. van Weeren for critically reviewing the manuscript

REFERENCES

1. Adams MA, Roughley PJ. What is intervertebral disc degeneration, and what causes it? *Spine*. 2006;31(18):2151-2161.
2. Bergknut N, Egenvall A, Hagman R, et al. Incidence of intervertebral disk degeneration-related diseases and associated mortality rates in dogs. *J Am Vet Med Assoc*. 2012;240(11):1300-1309.
3. Bergknut N, Grinwis G, Pickee E, et al. Reliability of macroscopic grading of intervertebral disk degeneration in dogs by use of the Thompson system and comparison with low-field magnetic resonance imaging findings. *Am J Vet Res*. 2011;72(7):899-904.
4. Bergknut N, Meij BP, Hagman R, et al. Intervertebral disc disease in dogs - Part 1: A new histological grading scheme for classification of intervertebral disc degeneration in dogs. *Vet J*. 2013;195(2):156-163.
5. Bergknut N, Rutges JPHJ, Kranenburg H-C, et al. The dog as an animal model for intervertebral disc degeneration?. *Spine*. 2012;37(5):351-358.
6. Bergknut N, Smolders LA, Grinwis GC, et al. Intervertebral disc degeneration in the dog. Part 1: Anatomy and physiology of the intervertebral disc and characteristics of intervertebral disc degeneration. *Vet J*. 2013;195(3):282-291.
7. Bollwein A, Hänichen T. Age-related changes in the intervertebral disks of the cervical vertebrae of the horse. *Tierärztl Prax*. 1989;17(1):73-76.
8. Boos N, Weissbach S, Rohrbach H, et al. Classification of age-related changes in lumbar intervertebral discs: 2002 Volvo award in basic science. *Spine*. 2002;27(23):2631-2644.
9. Cherrone KL, Dewey CW, Coastes JR, et al. A retrospective comparison of cervical intervertebral disk disease in nonchondrodystrophic large dogs versus small dogs. *J Am Anim Hosp Assoc*. 2004;40(4):316-320.
10. Clayton HM, Kaiser LJ, Lavagnino M, et al. Dynamic mobilisations in cervical flexion: Effects on intervertebral angulations. *Equine Vet J*. 2010;42(suppl):688-694.
11. Down SS, Henson FMD. Radiographic retrospective study of the caudal cervical articular process joints in the horse. *Equine Vet J*. 2009;41(6):518-524.
12. Dyson SJ. Lesions of the equine neck resulting in lameness or poor performance. *Vet Clin North Am Equine Pract*. 2011;27(3):417-437.
13. Faber M, Johnston C, Schamhardt H, et al. Basic three-dimensional kinematics of the vertebral column of horses trotting on a treadmill. *Am J Vet Res*. 2001;62(5):757-764.
14. Faber M, Johnston C, Schamhardt HC, et al. Three-dimensional kinematics of the equine spine during canter. *Equine Vet J Suppl*. 2001;33(suppl):145-149.
15. Foss RR, Genetzky RM, Riedesel EA, et al. Cervical intervertebral disc protrusion in two horses. *Canadian Veterinary Journal*. 1983;24:188-191.
16. Fuentealba IC, Weeks BR, Martin MT, et al. Spinal cord ischemic necrosis due to fibrocartilaginous embolism in a horse. *J Vet Diag Invest*. 1991;3(2):176-179.
17. Furr MO, Anver M, Wise M. Intervertebral disk prolapse and diskospondylitis in a horse. *J Am Vet Med Assoc*. 1991;198(12):2095-2096.
18. Gruber HE, Ingram J, Hanley Jr. EN. An improved staining method for intervertebral disc tissue. *Biotech Histochem*. 2002;77(2):81-83.
19. Hadjipavlou AG, Tzermianianos MN, Bogduk N, et al. The pathophysiology of disc degeneration: A critical review. *J Bone Joint Surg - Series B*. 2008;90(10):1261-1270.

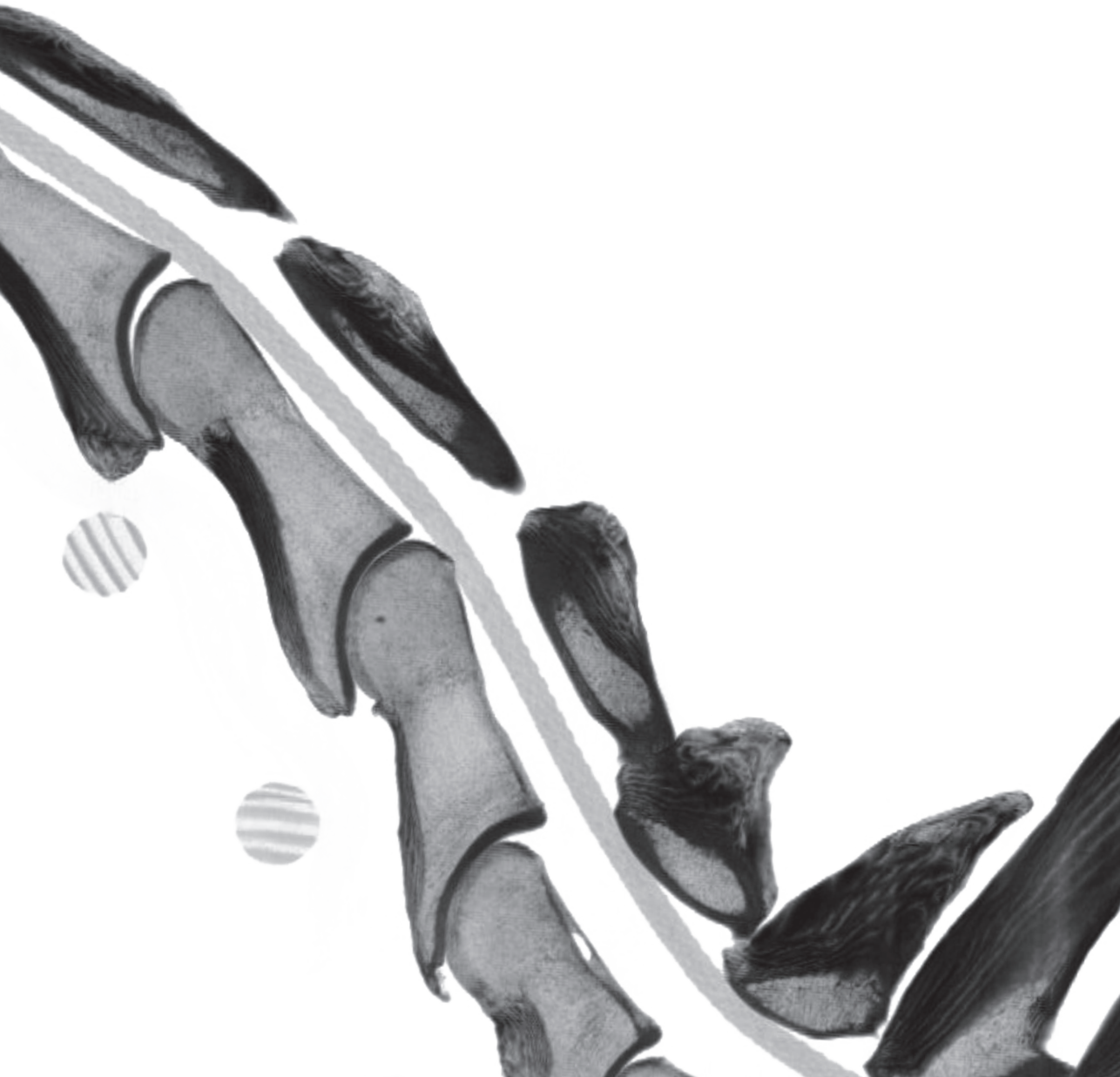
20. Hansen HJ. A pathologic-anatomical study on disc degeneration in dog, with special reference to the so-called enchondrosis intervertebralis. *Acta Orthop Scand*. 1952;11(suppl):1-117.
21. Haussler KK, Bertram JE, Gellman K, et al. Segmental in vivo vertebral kinematics at the walk, trot and canter: a preliminary study. *Equine Vet J*. 2001;33(suppl):160-164.
22. Ho-Pham LT, Lai TQ, Mai LD, et al. Prevalence and Pattern of Radiographic Intervertebral Disc Degeneration in Vietnamese: A Population-Based Study. *Calcif Tissue Int*. 2015;96(6):510-517.
23. Ikegawa S. The genetics of common degenerative skeletal disorders: osteoarthritis and degenerative disc disease. *Annu Rev Genomics Hum Genet*. 2013;14:245-256.
24. Jansson N. What is your diagnosis? Multiple cervical intervertebral disk prolapses. *J Am Vet Med Assoc*. 2001;219(12):1681-1682.
25. Jeffcott LB. Disorders of the thoracolumbar spine of the horse—a survey of 443 cases. *Equine Vet J*. 1980;12(4):197-210.
26. Jeffcott LB, Dalin G. Natural rigidity of the horse's backbone. *Equine Vet J*. 1980;12(3):101-108.
27. Landis JR, Koch GG. The measurement of observer agreement for categorical data. *Biometrics*. 1977;33(1):159-174.
28. Levine JM, Adam E, MacKay RJ, et al. Confirmed and presumptive cervical vertebral compressive myelopathy in older horses: A retrospective study (1992-2004). *J Vet Int Med*. 2007;21(4):812-819.
29. McInerney J, Ball PA. The pathophysiology of thoracic disc disease. *Neurosurg Focus* 2000;9(4).
30. McKelvey WAC, Owen RR. Acquired torticollis in eleven horses. *J Am Vet Med Assoc*. 1979;175(3):295-297.
31. Meij BP, Bergknut N. Degenerative lumbosacral stenosis in dogs. *Vet Clin North Am Small Anim Pract*. 2010;40(5):983-1009.
32. Nappert G, Vrins A, Breton L, et al. A retrospective study of nineteen ataxic horses. *Can Vet J*. 1989;30(10):802-806.
33. Nixon AJ, Stashak TS, Ingram JT, Norrdin RW, Park RD. cervical intervertebral disk protrusion in a horse. *Vet Surg*. 1984;154-158.
34. Pagger H, Schmidburg I, Peham C, et al. Determination of the stiffness of the equine cervical spine. *Vet J* 2010;186(3):338-341.
35. Powers BE, Stashak TS, Nixon AJ, et al. Pathology of the vertebral column of horses with cervical static stenosis. *Vet Pathol*. 1986;23(4):392-399.
36. Rooney JR. The Horse's Back: Biomechanics of lameness. *Vet Clin: Equine Pract*. 1982;4(2):17-27.
37. Rutges JPHJ, Duit RA, Kummer JA, et al. A validated new histological classification for intervertebral disc degeneration. *Osteoarthritis Cartilage*. 2013;21(12):2039-2047.
38. Sebastian MM, Giles RC. Fibrocartilaginous embolic myelopathy in a horse. *J Vet Med Series A* 2004;51(7-8):341-343.
39. Seiler GS, Häni H, Busato AR, et al. Facet joint geometry and intervertebral disk degeneration in the L6-S1 region of the vertebral column in German Shepherd Dogs. *Am J Vet Res*. 2002;63(1):86-90.
40. Sharp NIH, Wheeler SJ, Cofone M. Radiological evaluation of 'wobbler' syndrome -caudal cervical spondylomyelopathy. *J Small Ani Pract*. 1992;33(10):491.
41. Sleutjens J, Voorhout G, Van Der Kolk JH, et al. The effect of ex vivo flexion and extension on intervertebral foramina dimensions in the equine cervical spine. *Equine Vet J Suppl*. 2010;(38):425-30. doi(38):425-430.
42. Smit TH. The use of a quadruped as an in vivo model for the study of the spine - Biomechanical considerations. *Europ Spine J*. 2002;11(2):137-144.

43. Smolders LA, Bergknut N, Grinwis GCM, et al. Intervertebral disc degeneration in the dog. Part 2: Chondrodystrophic and non-chondrodystrophic breeds. *Vet J* 2013;195(3):292-299.
44. Speltz MC, Olson EJ, Hunt LM, et al. Equine intervertebral disk disease: A case report. *J Equine Vet Sci.* 2006;26(9):413-419.
45. Stadler P, van den Berg SS, Tustin RC. Cervical intervertebral disk prolapse in a horse. *J S Afr Vet Assoc.* 1988;59(1):31-32.
46. Taher F, Essig D, Lebl DR, et al. Lumbar degenerative disc disease: current and future concepts of diagnosis and management. *Adv Orthop.* 2012;2012:970752.
47. Takeuchi T, Abumi K, Shono Y, et al. Biomechanical role of the intervertebral disc and costovertebral joint in stability of the thoracic spine: A canine model study. *Spine.* 1999;24(14):1414-1420.
48. Taylor HW, Vandeveld M, Firth EC. Ischemic myelopathy caused by fibrocartilaginous emboli in a horse. *Vet Pathol.* 1977;14(5):479-481.
49. Teraguchi M, Yoshimura N, Hashizume H, et al. Prevalence and distribution of intervertebral disc degeneration over the entire spine in a population-based cohort: The Wakayama Spine Study. *Osteoarthritis Cartilage.* 2014;22(1):104-110.
50. Thompson JP, Pearce RH, Ho B. Correlation of gross morphology and chemical composition with magnetic resonance images of human lumbar intervertebral discs. *Transactions Ann Meeting Orthopaed Res Soc.* 1988(13):276.
51. Thompson JP, Pearce RH, Schechter MT, et al. Preliminary evaluation of a scheme for grading the gross morphology of the human intervertebral disc. *Spine.* 1990;15(5):411-415.
52. Townsend HG, Leach DH. Relationship between intervertebral joint morphology and mobility in the equine thoracolumbar spine. *Equine Vet J.* 1984;16(5):461-465.
53. Townsend HG, Leach DH, Doige CE, et al. Relationship between spinal biomechanics and pathological changes in the equine thoracolumbar spine. *Equine Vet J.* 1986;18(2):107-112.
54. Urban JPG, Roberts S. Degeneration of the intervertebral disc. *Arthritis Res Ther.* 2003;5(3):120-130.
55. Walling BE, Stewart MC, Valli VE. Pathology in practice. *J Am Vet Med Assoc.* 2011;239(2):199-201.
56. Whitwell KE. Causes of ataxia in horses. *Pract Equine Pathol.* 1980;2(4):17-25.
57. Wijnberg D, Bergmann W, Veraa S. Neurological neck problems, diagnostics and prognosis in the horse. *Prakt Tierarzt.* 2015;96(2):150-158.
58. Yovich JV, Powers BE, Stashak TS. Morphologic features of the cervical intervertebral disks and adjacent vertebral bodies of horses. *Am J Vet Res.* 1985;46(11):2372-2377.



8

General Discussion



GENERAL DISCUSSION

The cervical vertebral column is a complex part of the horse's body with its vertebrae, synovial joints, intervertebral discs, nuchal ligament, muscles, and tendons, which all interconnect and contribute to the complex role of balancing the axial motion chain. It conducts and protects the spinal cord, whose exiting nerves play a crucial role in motion of the appendicular skeleton [1-5]. As dysfunction of one or a combination of these cervical elements will affect the biomechanical capabilities of the individual horse, the impact on performance in equestrian sports can be substantial [5]. Against this background, the potential effects of vertebral and muscular morphologic variations on biomechanical functioning, either directly or indirectly via the influence of surrounding structures such as the intervertebral disc, has been an area of research focus during the last decade [6-9].

To evaluate the role that existing and recently available imaging modalities can play in the assessment of the cervical vertebral variations and of disorders of the intervertebral disc, the two aims of this thesis were:

- ☞ To increase the knowledge of cervical vertebral patterning variations in horses and their potential clinical effects.
- ☞ To investigate the development and degeneration of the cervical intervertebral disc in young and adult horses, in relationship to the potential effects of the vertebral variations mentioned in the first aim.

The first part of this thesis (**Chapters 2, 3 and 4**) focuses on imaging features of cervical vertebral variations and their clinical impact. Vertebral patterning variation is a phenomenon that is encountered in many species and in **Chapter 2** the potential translational value for human medicine of the vertebral congenital malformations found in domesticated animals is discussed in the format of a literature review. The embryonic development of the vertebral column and the variation in vertebral conformation in domesticated animals is described, highlighting the importance of somitogenesis and sequential differentiation of the sclerotome in vertebral development and limb position along the cranio-caudal axis. An important aspect in this embryonic development is the *Hox*-code, which is a Homeobox-genes expression gradient along the cranio-caudal axis [10, 11]. The *Hox* genes set the junctions to the vertebral series and deletions or changes in these areas of the genome can cause vertebral malformations. This may result in variations in lateral elements (transverse processes and ribs) morphology, or may lead to positional variations of the limb bud

along the cranio-caudal axis of varying impact [11-13]. The cervicothoracic boundary has been shown to be in part regulated by *Hox-5* and *Hox-6* [13-15] with the latter being affected by transcriptional repressor proteins thymine-guanine interacting factor 1 and 2 (Tgif1 and Tgif2) in mice [16]. This shows the complex basis of the embryological processes that lead to formation of the vertebral column. Identification of the factors impairing these processes may result in unraveling the variation that has been described in the equine cervicothoracic vertebrae C6, C7 and Th1 (**Chapter 3**).

In **Chapter 3** the computed tomographic (CT) features of the morphological variations of C6, C7 and Th1, which consist of the transposition of the caudal tubercle of C6 to C7 in association with rudimentary first ribs, are presented. These variations were found in 33.3% of the 78 horses of different horse breeds that formed the study population. No association with clinical symptoms was identified, which is in line with the outcome of the radiographic case-control study in warmblood horses in **Chapter 4**. In that chapter it is also shown that the odds of having radiographically detectable caudal cervical vertebral variations at C6 and C7 were higher or equal in horses without clinical symptoms than in horses with any of the recorded clinical symptoms. It was therefore suggested that having this vertebral variation might be a favorable condition in warmblood horses. While at first sight perhaps counterintuitive, this finding might possibly be explained by the strong selection on certain performance characteristics in the modern warmblood horse [17]. Lately, the *HoxB*-complex has been indicated as a target region for genetic selection in four German warmblood breeds, which means that this region shows a high degree of similarity between breeds (Trakehner, Holsteiner, Hanoverian, Oldenburger) [18]. Because of the strong connection with these breeds, this could explain the relatively high number of warmbloods in our study affected by this cervico-thoracic vertebral variation. Selection of horses occurs not only by performance but indeed also some cervical conformational exterior characteristics have been described to be preferred [19, 20]. Thicker necks together with a natural head-neck position were chosen more often [20]. Another aspect in breeding selection of the warmblood breeds that needs to be highlighted is the fact that their bloodlines are originating from regionally bred working horses and military horses. The modern warmblood has been created by cross-breeding these horses with Arabian and Thoroughbred horses amongst others. The prevalence of vertebral variations at C6 and C7 in the Thoroughbred is with about 33% similar to that in most warmblood breeds [7]. Although not as common as in warmbloods and Thoroughbreds, vertebral variations at C6 and C7 have also been reported in Quarter horses, Arabian horses, a Friesian horse and a Standardbred trotter [6, 9, 21]. In smaller breeds including Shetland ponies and Konik horses, these vertebral variations at C6 and C7 have not yet been found in an ongoing research project using CT as a diagnostic tool (unpublished data).

The second part of this thesis (**Chapters 5, 6 and 7**) focuses on the intervertebral disc with respect to development, degeneration and related imaging features. As the HoxB-complex has been identified as a target region for genetic selection, it may also influence the prevalence of morphologic vertebral variations in the caudal cervical vertebral column of warmblood horses [18]. The biomechanical effect of these vertebral variations on adjacent structures such as the intervertebral disc deserves further investigation. DeRouen et.al. found elongation of C7, a wider intervertebral disc space and an intravertebral sagittal ratio of less than 0.5 at C6 in a significant number of horses [6]. These findings may indicate that morphological variations at C6 and C7 represent a different form of cervical vertebral malformation [6]. Biomechanical alterations have been proposed secondary to these changes in shape of the vertebra and width of the intervertebral disc space [6, 7]. In companion animals and humans, alterations in biomechanical forces have been identified as causes of adjacent segment disease [22]. Changes in position of the vectors of the tensional and compressive forces along the vertebral body towards the adjacent intervertebral discs cause these alterations [22]. Examples hereof are block vertebrae, or surgical fusion of vertebrae, and adjacent segment disease is known to be a cause of secondary intervertebral disc protrusion [22]. A similar phenomenon could possibly occur in the anatomically altered cervicothoracic region of horses as described in **Chapters 3 and 4** of this thesis. In **Chapters 5 and 7**, intervertebral disc degeneration is shown to be located mainly in the caudal part of the cervical vertebral column. An association of macroscopic intervertebral disc degeneration with MRI-detected annulus protrusion was found in **Chapter 5**. This suggests that also in horses disc degeneration can lead to the clinically relevant condition of disc protrusion/extrusion with secondary compressive myelopathy [23-25]. In one of the horses described in **Chapter 5** the dorsal longitudinal ligament was torn with secondary focal hemorrhage and concurrent intervertebral disc degeneration. Hematomas in the vertebral canal associated with embolism caused by fibrocartilaginous tissue fragments have been described in horses and are generally considered to be a sequel to traumatic insults [26-28]. Because it was unknown whether there had been a previous trauma, the possibility of disc extrusion-related hematoma formation needs to be considered as well, as the ventral vertebral plexus runs at this level. In dogs, this condition is seen regularly in cases of thoracolumbar intervertebral disc extrusion [29].

In horses, the intervertebral disc has long been considered as having no clinical importance [30, 31]. Nevertheless, the long list of case reports describing intervertebral disc herniation, protrusion, fibrocartilaginous embolism and discospondylitis suggests otherwise [23, 25, 32-34, 34-40]. Intervertebral disc disease in humans and dogs has

been evaluated with MRI to study anatomy, biochemical composition and for grading degeneration [41-44]. In this same line, in **Chapter 5** the first imaging study of the equine intervertebral disc with MRI is described. The study presents MRI features of the non-degenerated and degenerated intervertebral disc of the cervical spine. It also investigates the association with factors such as location and intervertebral disc protrusion detected by MRI. An important finding was the fact that the standard T2-weighted images as used in other companion animals and humans did not optimally display intervertebral disc degeneration, but proton density weighted images did. This reflects the fact that the equine intervertebral disc is composed in a slightly different way than in companion animals or humans. Nevertheless, it consists of an annulus fibrosus and nucleus pulposus, as described in **Chapter 7**. Histologically the annulus pulposus consists of parallel collagenous lamellae. The nucleus pulposus has a cartilaginous and proteoglycan-rich matrix and the two are interconnected by a transition zone. Macroscopic disc degeneration is graded from 1 to 5 with the higher grades seen more often in older horses and in the caudal cervical spine. Bollwein et. al. also found that macroscopic degeneration increases with age and is seen more often in the caudal cervical spine. However, the presence of a nucleus pulposus had not been identified in that study [30]. This might be explained by the macroscopic similarity of the annulus fibrosus and the nucleus pulposus. However, this similarity does not apply to histology or MRI. Our studies show that these modalities allow for discriminating between both structures (**Chapters 5 and 7**). Unfortunately, no conclusions could be drawn about the clinical impact of intervertebral disc degeneration in the examined population of horses in these two chapters. Nevertheless, a variety of clinical symptoms related to the neck were present in a subpopulation of these horses indeed and included spinal ataxia, pain on palpation, reduced flexion, abnormal movement, abnormal behavior, hypermetria, thoracic lameness that did not respond to local anesthetics, and muscle atrophy, amongst others. However, clinical symptoms could only be directly related to intervertebral disc disease in some of the cases presented. In these horses, outcome of the clinical examination, MRI results and gross pathological examination together were conclusive for a final diagnosis.

It is known that degeneration of the intervertebral disc can cause intervertebral disc space narrowing in humans, companion animals and research animals (e.g. rabbits and sheep). For this reason, the radiographic width of the intervertebral disc space has been used for evaluating degeneration and regeneration of intervertebral discs, mostly of the lumbar spine [45-51]. This approach uses a disc height index (DHI) to reduce the effect of individual variations in size or length and of variations in radiographic magnification [45-47]. In **Chapter 6** the DHI is used for evaluating the

radiographic development of the cervical intervertebral disc in a population of horses varying from one to 18 months old. An equine DHI was designed as a new parameter for intervertebral disc space width assessment in horses. The outcome of the analysis of inter- and intra-observer agreement for the DHI was satisfactory, indicating that this parameter can indeed be considered an applicable tool for cervical intervertebral disc assessment in horses. Future research is needed on the potential significance of the DHI for the assessment of the severity of intervertebral disc degeneration in the aging horse and the clinical impact.

Concluding considerations and perspectives for future imaging options

In summary, various imaging techniques have been applied in this thesis for the assessment of the equine vertebral column. This provides important new insights, but the exact association of imaging findings with clinical symptoms remains challenging. Pathologic conditions that have not been identified before with radiography or ultrasonography prove to become evident when using advanced imaging techniques like CT and MRI. Together with the use of dynamic imaging (e.g. fluoroscopy on the treadmill) and quantitative gait analysis, the biomechanical effects of cervical pathologies may be further clarified. From a practical point of view, the role of basic imaging techniques such as radiography and ultrasound will remain pivotal for early diagnosis in the foreseeable future. The fact that CT and MRI of the complete equine neck are becoming possible in the anesthetized horse facilitates a more thorough work-up for those animals requiring this. More clinically oriented research is needed to become more familiar with the findings of CT and MRI imaging of the equine neck, as to date only limited knowledge is available. Imaging features of intervertebral disc disease on CT, but perhaps also on radiography, should be further explored and their potential clinical impact assessed. The findings of this thesis may form a basis for the radiographic evaluation of intervertebral disc disease in the adult horse. Further research is also needed to evaluate the possible effects that cervical vertebral variations at C6 and C7 may have in warmblood horses. As about 33% of warmblood and Thoroughbred horses do have this condition, future studies should focus on clarification of the very likely multifaceted impact of these variations on biomechanical forces and performance. Important in this context is the development of integration with earlier mentioned dynamic imaging options and quantitative gait analysis.

The findings in this thesis clearly underline the value of diagnostic imaging in the unravelling of pathologic conditions of the equine cervical spine and their clinical impact.

The key results are:

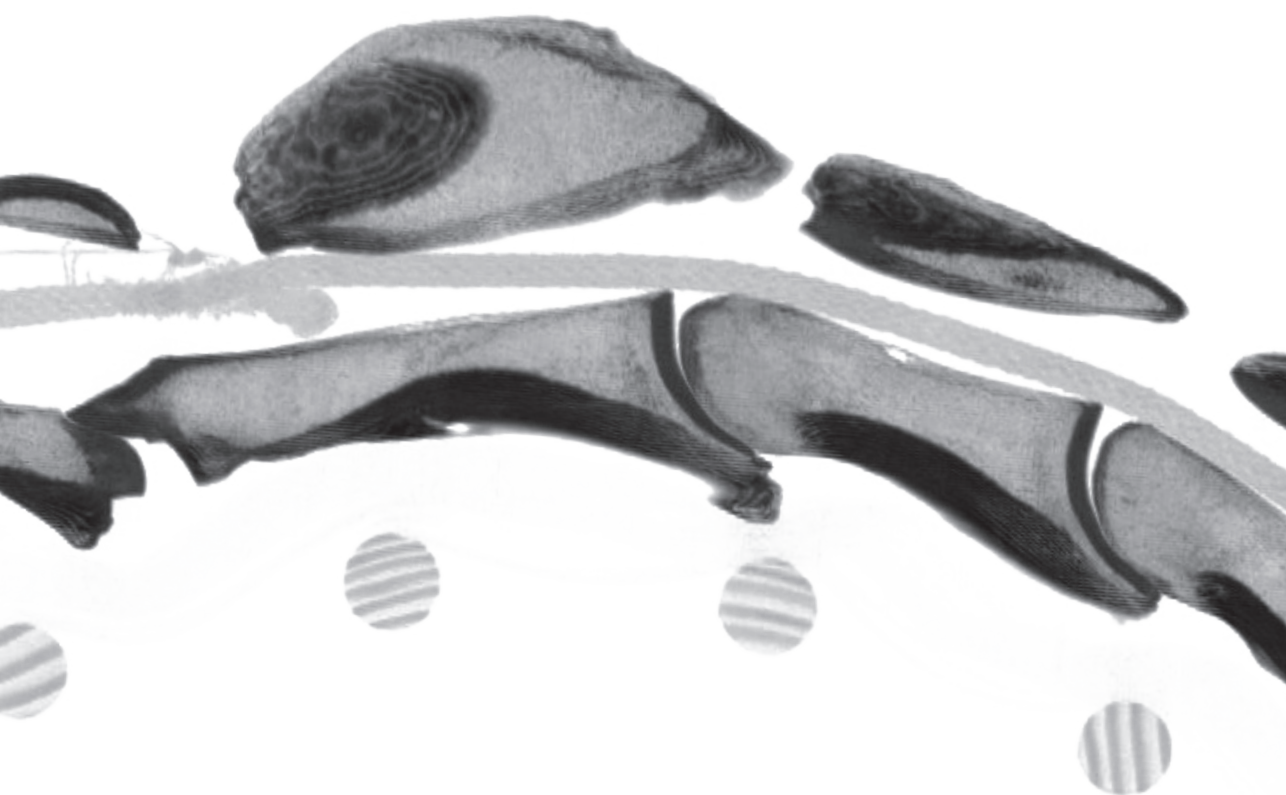
- ☞ Cervical vertebral variations of C6 and C7 in horses represent a homologous variation and occur more often than homeotic variations of the occipito-atlantal or cervicothoracic junctions.
- ☞ Cervical vertebral variations of C6 and C7 occur always together, can be unilateral or bilateral and in some cases together with rudimentary ribs or transverse processes at Th1.
- ☞ Cervical vertebral variations of C6 and C7 are seen in about 33% of Warmblood horses.
- ☞ Cervical vertebral variations of C6 and C7 are not associated with clinical signs in Warmblood horses.
- ☞ The equine intervertebral disc consists of an annulus fibrosus and nucleus pulposus with a short transition zone.
- ☞ The equine cervical intervertebral disc degenerates with age.
- ☞ Degeneration of the equine cervical intervertebral disc is noted most frequently in the caudal cervical spine.
- ☞ Degeneration of the equine cervical intervertebral disc can be detected by MRI.
- ☞ Proton density and gradient echo sequences are better at detecting intervertebral disc degeneration than T2-weighted sequences.
- ☞ Degeneration of the equine intervertebral disc is associated with MRI-detectable disc protrusion
- ☞ Disc height index can be used as a radiographic parameter to assess intervertebral disc space width radiographically in young horses.

REFERENCES

1. Gomez Alvarez, C.B., Rhodin, M., Bobber, M.F., Meyer, H., Weishaupt, M.A., Johnston, C. and Van Weeren, P.R. (2006) The effect of head and neck position on the thoracolumbar kinematics in the unriden horse. *Equine Vet. J. Suppl.* **(36):445-51**. doi, 445-451.
2. Rhodin, M., Gomez Alvarez, C.B., Bystrom, A., Johnston, C., van Weeren, P.R., Roepstorff, L. and Weishaupt, M.A. (2009) The effect of different head and neck positions on the caudal back and hindlimb kinematics in the elite dressage horse at trot. *Equine Vet. J.* **41**, 274-279.
3. Rhodin, M., Johnston, C., Holm, K.R., Wennerstrand, J. and Drevemo, S. (2005) The influence of head and neck position on kinematics of the back in riding horses at the walk and trot. *Equine Vet. J.* **37**, 7-11.
4. Elgersma, A.E., Wijnberg, I.D., Sleutjens, J., van der Kolk, J.H., van Weeren, P.R. and Back, W. (2010) A pilot study on objective quantification and anatomical modelling of in vivo head and neck positions commonly applied in training and competition of sport horses. *Equine Vet. J.* **42 Suppl 38**, 436-443.
5. Zsoldos, R.R. and Licka, T.F. (2015) The equine neck and its function during movement and locomotion. *Zoology (Jena)*. **118**, 364-376.
6. DeRouen, A., Spriet, M. and Aleman, M. (2016) Prevalence of Anatomical Variation of the Sixth Cervical Vertebra and Association with Vertebral Canal Stenosis and Articular Process Osteoarthritis in the Horse. *Vet. Radiol. Ultrasound*. **57**, 253-258.
7. May-Davis, S. and Walker, C. (2015) Variations and Implications of the Gross Morphology in the *Longus colli* Muscle in Thoroughbred and Thoroughbred Derivative Horses Presenting With a Congenital Malformation of the Sixth and Seventh Cervical Vertebrae. *Journal of Equine Veterinary Science*. **35**, 560-568.
8. May-Davis, S. (2014) The Occurrence of a Congenital Malformation in the Sixth and Seventh Cervical Vertebrae Predominantly Observed in Thoroughbred Horses. *Journal of Equine Veterinary Science*. **34**, 1313-1317.
9. Santinelli, I., Beccati, F., Arcelli, R. and Pepe, M. (2014) Anatomical variation of the spinous and transverse processes in the caudal cervical vertebrae and the first thoracic vertebra in horses. *Equine Vet. J.*
10. Burke, A.C. (2000) Hox genes and the global patterning of the somitic mesoderm. *Curr. Top. Dev. Biol.* **47**, 155-181.
11. Nowicki, J.L. and Burke, A.C. (2000) Hox genes and morphological identity: axial versus lateral patterning in the vertebrate mesoderm. *Development*. **127**, 4265-4275.
12. Bordbari, M.H., Penedo, M.C.T., Aleman, M., Valberg, S.J., Mickelson, J. and Finno, C.J. (2017) Deletion of 2.7 kb near HOXD3 in an Arabian horse with occipitoatlantoaxial malformation. *Anim. Genet.* **48**, 287-294.
13. Chen, J.W., Zahid, S., Shilts, M.H., Weaver, S.J., Leskowitz, R.M., Habbsa, S., Aronowitz, D., Rokins, K.P., Chang, Y., Pinnella, Z., Holloway, L. and Mansfield, J.H. (2013) Hoxa-5 acts in segmented somites to regulate cervical vertebral morphology. *Mech. Dev.* **130**, 226-240.
14. Bohmer, C., Amson, E., Arnold, P., van Heteren, A.H. and Nyakatura, J.A. (2018) Homeotic transformations reflect departure from the mammalian 'rule of seven' cervical vertebrae in sloths: inferences on the Hox code and morphological modularity of the mammalian neck. *BMC Evol. Biol.* **18**, 84-018-1202-5.
15. Kappen, C. (2016) Developmental Patterning as a Quantitative Trait: Genetic Modulation of the Hoxb6 Mutant Skeletal Phenotype. *PLoS One*. **11**, e0146019.
16. Melhuish, T.A., Taniguchi, K. and Wotton, D. (2016) Tgif1 and Tgif2 Regulate Axial Patterning in Mouse. *PLoS One*. **11**, e0155837.
17. Asadollahpour Nanaei, H., Ayatollahi Mehrgardi, A. and Esmailzadeh, A. (2019) Comparative population genomics unveils candidate genes for athletic performance in Hanoverians. *Genome*. 1-7.

18. Nolte, W., Thaller, G. and Kuehn, C. (2019) Selection signatures in four German warmblood horse breeds: Tracing breeding history in the modern sport horse. *PLoS One*. **14**, e0215913.
19. van Weeren, P.R. and Crevier-Denoix, N. (2006) Equine conformation: clues to performance and soundness? *Equine Vet. J.* **38**, 591-596.
20. Caspar, G.L., Dhand, N.K. and McGreevy, P.D. (2015) Human Preferences for Conformation Attributes and Head-And-Neck Positions in Horses. *PLoS One*. **10**, e0131880.
21. Veraa, S., Bergmann, W., van den Belt, A.J., Wijnberg, I. and Back, W. (2016) Ex Vivo Computed Tomographic Evaluation of Morphology Variations in Equine Cervical Vertebrae. *Vet. Radiol. Ultrasound*. **57**, 482-488.
22. Crowe, Y.C., Child, G., Lam, R. and McGregor, R. (2019) Congenital block vertebrae and intervertebral disc protrusion in a young cat. *JFMS Open Rep.* **5**, 2055116919868037.
23. Jansson, N. (2001) What is your diagnosis? Multiple cervical intervertebral disk prolapses. *J. Am. Vet. Med. Assoc.* **219**, 1681-1682.
24. Speltz MC, Olson EJ, Hunt LM, Pool RR, Wilson JH, Carlson CS. (2006) Equine intervertebral disk disease: A case report. *Journal of Equine Veterinary Science*. **26 (9)**, 413-419.
25. Stadler, P., van den Berg, S.S. and Tustin, R.C. (1988) Cervical intervertebral disk prolapse in a horse. *J. S. Afr. Vet. Assoc.* **59**, 31-32.
26. Gold, J.R., Divers, T.J., Miller, A.J., Scrivani, P.V., Perkins, G.A., VanBiervliet, J. and de LaHunta, A. (2008) Cervical vertebral spinal hematomas in 4 horses. *J. Vet. Intern. Med.* **22**, 481-485.
27. Bolz, W. (1966) Epidural hematomas in the cervical spinal cord in horses. *Dtsch. Tierarztl. Wochenschr.* **73**, 585-588.
28. Dorner, C., Uzal, F., Carvallo, F. and Palmero, J. (2015) Compressive myelopathy caused by epidural haematoma associated with fibrocartilaginous embolism in a horse. *Equine Vet. Ed.* **8**, 405-409.
29. Gomes, S.A., Volk, H.A., Packer, R.M., Kenny, P.J., Beltran, E. and De Decker, S. (2016) Clinical and Magnetic Resonance Imaging Characteristics of Thoracolumbar Intervertebral Disk Extrusions and Protrusions in Large Breed Dogs. *Vet. Radiol. Ultrasound*. **57**, 417-426.
30. Bollwein, A. and Hanichen, T. (1989) Age-related changes in the intervertebral disks of the cervical vertebrae of the horse. *Tierarztl. Prax.* **17**, 73-76.
31. Yovich, J.V., Powers, B.E. and Stashak, T.S. (1985) Morphologic features of the cervical intervertebral disks and adjacent vertebral bodies of horses. *Am. J. Vet. Res.* **46**, 2372-2377.
32. Allison, N. and Moeller, R.B., Jr. (2000) Spinal ataxia in a horse caused by an arachnoid diverticulum (cyst). *J. Vet. Diagn. Invest.* **12**, 279-281.
33. Foss, R.R., Genetzky, R.M., Riedesel, E.A. and Graham, C. (1983) Cervical intervertebral disc protrusion in two horses. *Can. Vet. J.* **24**, 188-191.
34. Furr, M.O., Anver, M. and Wise, M. (1991) Intervertebral disk prolapse and diskospondylitis in a horse. *J. Am. Vet. Med. Assoc.* **198**, 2095-2096.
35. Nixon, A.J., Stashak, T., S., Ingram J. T., Norrdin R.W. and Park R.D. (1984) Cervical intervertebral disc protrusion in a horse. *Vet. Surg.* **13**, 154-158.
36. Taylor, H.W., Vandevelde, M. and Firth, E.C. (1977) Ischemic myelopathy caused by fibrocartilaginous emboli in a horse. *Vet. Pathol.* **14**, 479-481.
37. Sebastian, M.M. and Giles, R.C. (2004) Fibrocartilaginous embolic myelopathy in a horse. *J. Vet. Med. A Physiol. Pathol. Clin. Med.* **51**, 341-343.
38. Fuentealba, I.C., Weeks, B.R., Martin, M.T., Joyce, J.R. and Wease, G.S. (1991) Spinal cord ischemic necrosis due to fibrocartilaginous embolism in a horse. *J. Vet. Diagn. Invest.* **3**, 176-179.

39. Sweers, L. and Carstens, A. (2006) Imaging features of discospondylitis in two horses. *Vet. Radiol. Ultrasound*. **47**, 159-164.
40. Hillyer, M.H., Innes, J.F., Patteson, M.W. and Barr, A.R. (1996) Discospondylitis in an adult horse. *Vet. Rec.* **139**, 519-521.
41. Bergknut, N., Auriemma, E., Wijsman, S., Voorhout, G., Hagman, R., Lagerstedt, A.S., Hazewinkel, H.A. and Meij, B.P. (2011) Evaluation of intervertebral disk degeneration in chondrodystrophic and nonchondrodystrophic dogs by use of Pfirrmann grading of images obtained with low-field magnetic resonance imaging. *Am. J. Vet. Res.* **72**, 893-898.
42. Pfirrmann, C.W., Metzdorf, A., Zanetti, M., Hodler, J. and Boos, N. (2001) Magnetic resonance classification of lumbar intervertebral disc degeneration. *Spine (Phila Pa. 1976)*. **26**, 1873-1878.
43. Mulligan, K.R., Ferland, C.E., Gawri, R., Borthakur, A., Haglund, L. and Ouellet, J.A. (2015) Axial T1 rho MRI as a diagnostic imaging modality to quantify proteoglycan concentration in degenerative disc disease. *Eur. Spine J.* **24**, 2395-2401.
44. Wada, T., Togao, O., Tokunaga, C., Funatsu, R., Yamashita, Y., Kobayashi, K., Nakamura, Y. and Honda, H. (2016) Glycosaminoglycan chemical exchange saturation transfer in human lumbar intervertebral discs: Effect of saturation pulse and relationship with low back pain. *J. Magn. Reson. Imaging*.
45. Hoogendoorn, R.J., Wuismann, P.I., Smit, T.H., Everts, V.E. and Helder, M.N. (2007) Experimental intervertebral disc degeneration induced by chondroitinase ABC in the goat. *Spine (Phila Pa. 1976)*. **32**, 1816-1825.
46. Lu, D.S., Shono, Y., Oda, I., Abumi, K. and Kaneda, K. (1997) Effects of chondroitinase ABC and chymopapain on spinal motion segment biomechanics. An in vivo biomechanical, radiologic, and histologic canine study. *Spine (Phila Pa. 1976)*. **22**, 1828-34; discussion 1834-5.
47. Masuda, K., Aota, Y., Muehleman, C., Imai, Y., Okuma, M., Thonar, E.J., Andersson, G.B. and An, H.S. (2005) A novel rabbit model of mild, reproducible disc degeneration by an anulus needle puncture: correlation between the degree of disc injury and radiological and histological appearances of disc degeneration. *Spine (Phila Pa. 1976)*. **30**, 5-14.
48. Masuda, K., Imai, Y., Okuma, M., Muehleman, C., Nakagawa, K., Akeda, K., Thonar, E., Andersson, G. and An, H.S. (2006) Osteogenic protein-1 injection into a degenerated disc induces the restoration of disc height and structural changes in the rabbit anular puncture model. *Spine (Phila Pa. 1976)*. **31**, 742-754.
49. Salamat, S., Hutchings, J., Kwong, C., Magnussen, J. and Hancock, M.J. (2016) The relationship between quantitative measures of disc height and disc signal intensity with Pfirrmann score of disc degeneration. *Springerplus*. **5**, 829-016-2542-5. eCollection 2016.
50. Schmidt, H., Dreischarf, M., Strube, P. and Putzier, M. (2016) Preoperative Segmental Disc Geometry as a Possible Predictor for the Clinical Outcome of Lumbosacral Total Disc Replacement. *J. Spine*. **5**,
51. Wei, F., Zhong, R., Wang, L., Zhou, Z., Pan, X., Cui, S., Sun, H., Zou, X., Gao, M., Jiang, B., Chen, W., Zhuang, W., Sun, H. and Liu, S. (2015) Pingyangmycin-induced in vivo lumbar disc degeneration model of rhesus monkeys. *Spine (Phila Pa. 1976)*. **40**, E199-210.





Summary -Samenvatting

Dankwoord

Curriculum Vitae



SUMMARY OF THE THESIS

The equine neck contributes to the balance of the horse, both by its direct biomechanical function as the lever of the head and by transmitting the processed sensory input of the eyes, ears and vestibulocochlear system from the brain to the trunk and limbs. It therefore plays a major function in the total movement pattern of the horse. Modern horse breeds are mostly deployed for equestrian sports. Body conformation and functional characteristics of horses have changed tremendously since domestication started about 6000 years ago. With it a decline in genetic diversity has been recognized, influencing amongst others a part of the genes that is responsible for the embryonic development of the vertebral column, known as the HOX or Homeobox genes. Changes can cause variation in shape and size of the vertebrae. About one third of Thoroughbred and warmblood horses have shape variations of the two last neck vertebrae.

Chapter 1 of this thesis provides an introduction to the embryonic development, anatomy, most common cervical pathologies, and diagnostic approach of the vertebral column. The cervical vertebral column consists of seven vertebrae that form the bony core of the neck and are surrounded by muscles and ligaments that attach at multiple levels to these vertebrae. Articular process joints are connecting these vertebrae dorsally whereas the intervertebral disc forms a shock absorber between vertebrae at the ventral side. The spinal cord is located centrally in the vertebral column and nerves are exiting towards the rest of the body through a space between two adjacent vertebrae (intervertebral foramen). Many pathologic conditions are known to affect the cervical vertebral column and multiple clinical symptoms are associated with these conditions. The key to a correct clinical diagnosis is a thorough clinical examination together with diagnostic imaging.

A complete clinical examination of the neck of a horse consists of many parts, of which the most important are visual inspection in rest, palpation, and assessment of the movement of both the neck and rest of the body. Key findings that may indicate central neck pathology are spinal ataxia with involuntary movement of the limbs, pain, abnormal posture, loss in muscle mass (atrophy), spastic gait or even lameness. Diagnosis of neck pathology can be challenging, as the clinical features might also be present in case of a generalized disease of the nervous system, such as grass sickness or equine motor neuron disease (EMND). To differentiate these generalized diseases from vertebral column pathology, diagnostic imaging can play a crucial role. For this, radiography and ultrasonography have always been most accessible, cost-

effective and easy to use in equine practices around the world. However, superposition of vertebral elements with radiography and inaccessibility of the central spinal soft tissues with ultrasound are increasingly recognized as a set-back in understanding the impact of equine neck pathology on the functioning of the horse. These limitations in current standard diagnostic capabilities have led to an increasing interest in advanced imaging techniques such as computed tomography (CT) and magnetic resonance imaging (MRI). Due to further technological development, CT examination is nowadays more applicable to the neck area of equine patients under general anaesthesia. This technique is very suitable for showing bony changes and secondary narrowing of the vertebral canal or area in between vertebrae (intervertebral foramen) through which the spinal cord and exiting nerves run. The additional value of MRI lies in the possibilities for assessment of the spinal cord and adjacent soft tissue structures, as already well-recognized in humans and companion animals. MRI in horses is for now only possible during post-mortem research as the size of the equine neck size is so large in most cases precluding the application of MRI in the live animal.

The best-known and described pathologic condition of the equine neck is cervical vertebral malformation, of which the changes to the vertebral bodies and joints have been documented extensively. Recently, more insight into the clinical impact that pathology of other parts of the vertebral column than these might have, caused expansion of research towards those other parts and the intervertebral disc. Variation in development of the vertebral column has been recognized in other domesticated animals and humans as a predisposing factor for clinical symptoms such as back pain, as has intervertebral disc disease, *e.g.* herniation.

This thesis consists of two parts in which imaging features and clinical implications of findings are discussed:

- ☞ Anatomical variation in shape of the vertebrae of the neck.
- ☞ Intervertebral disc disease of the neck.

The first part of this thesis starts with a literature review (Chapter 2) highlighting important congenital anatomical variations in the vertebral column of humans and domesticated animals, including companion animals, horses and livestock. Errors in vertebral formation or separation can occur during the first 2 months of fetal development. These lead to abnormalities in shape or number of vertebrae per section. Sections of the vertebral column are the neck or cervical region, the back consisting of a thoracic and lumbar region, and the pelvic area with the sacrum and



the tail. The effect of these variations depends on the severity of the malformation and possible concurrent congenital defects. Therefore, some vertebral malformations are incidentally found in individuals without clinical symptoms. However, death at a young age has also been attributed to some of these vertebral errors and their associated congenital defects.

In horses, variations in vertebral shape of the lower neck region have been noted more often lately and increasingly be associated with clinical symptoms such as neck pain. Radiographic and CT imaging features of these cervical vertebral variations at the sixth and seventh neck vertebrae in a group of predominantly warmblood horses are described in Chapters 3 and 4 of this thesis. These shape variations can be described as a shift of a part of the transverse process of the 6th neck vertebra (C6) to the seventh vertebra (C7) during fetal development. This aberration can be found on one or both sides of the vertebra. The first thoracic rib is abnormally small or absent in some of these horses. The variations at C6 and C7 were seen in around one third of mixed-breed (Chapter 3) or warmblood (Chapter 4) populations. Alterations in motion or biomechanical forces in the lower neck region have been associated with the variation at C6 and C7 due to concomitant local variation in muscle attachment (*m. longus colli*). However, no associations with clinical symptoms were found in either one of these two studies. In contrast, the vertebral variations were seen more often in a control group of horses without clinical symptoms, perhaps indicating that this variation in anatomy may even be favorable.

Adjacent segment syndrome has been described in humans and dogs indicating a higher chance of intervertebral disc disease next to a fused vertebral segment, either on a congenital basis or after surgery. Although fusion and therefore presence of a congenital or surgically created block vertebra is rare in horses, alterations of biomechanical forces due to the congenital vertebral variations mentioned above, might affect the intervertebral discs of this region. In Chapters 5, 6, and 7 of this thesis the development and pathology of the intervertebral discs of the neck in horses are assessed with radiography, MRI and macroscopically during gross pathological examination.

The intervertebral disc of horses differs in composition from those of humans and companion animals. Therefore, an adjusted grading system was developed and used in Chapter 7 for the macroscopic assessment of the intervertebral disc. Degeneration and/or aging of these intervertebral discs were graded in a scale from 1 to 5. The high values were found mostly in the older horses and in the lower neck region.

MRI is considered as the method of choice for assessment of the intervertebral disc and adjacent structures during life in humans and companion animals such as dogs and cats. In Chapter 5 the MRI features of a part of the intervertebral discs of Chapter 7 are described. The chapter describes post-mortem MRI findings of normal and degenerated or aging intervertebral discs and defines the best technique or sequence to assess these changes. In horses, a different sequence (proton density spin echo) than the most common sequence in humans and companion animals (T2-weighted spin echo sequence) was found to be most useful and showed degeneration as hypo-intense or dark areas. The presence of gas or blood products could also be observed (gradient echo sequence), if a cleft was present in the severely degenerated intervertebral disc.

Degeneration has been described to result in a decrease in size of the intervertebral disc due to dehydration, causing a narrowing of the space between two vertebral bodies otherwise referred to as the intervertebral disc space. Collapse of this space can occur in cases of severe degeneration or herniation of the intervertebral disc. Radiography is the most applied technique to assess the intervertebral disc space width and has been used to calculate a parameter called disc height index (DHI) in research animals and human diagnostic imaging. The application of this technique to the neck of horses was evaluated in Chapter 6. In this chapter, young warmblood horses were assessed radiographically from one to 18 months of age and the DHI was measured over time. Sex did not influence the outcome but this was the case with the location and to a certain extent head and neck position. In other words, the values were different when comparing the upper with the lower neck and are therefore not applicable for all intervertebral disc spaces of the neck. Although a small change in DHI was noted in time around 5 months, the DHI values were rather similar for the one and 18-month-old horses. This might indicate a more rapid growth around 5 months but more importantly may also reflect that DHI, of which inter- and intra-observer agreement was good, does not change that much over time. Therefore, the results of this study can be used as preliminary reference values but future research to assess the clinical impact of intervertebral disc degeneration is needed.

In conclusion, this thesis has assessed the anatomic vertebral variations in the equine neck and it has been shown that they occur frequently in warmblood horses. However, no associations with clinical symptoms could be found and it might even be a favorable condition in horses. Concomitant conformational or biomechanical changes might, however, have their influence on intervertebral disc aging or degeneration of the adjacent intervertebral discs. MRI features of intervertebral disc degeneration together with intervertebral disc space width assessment in young horses by means

of measuring the DHI, and postmortem macroscopic grading can show potentially significant changes. With it, a start has been made in the examination of several equine cervical pathologies. Further research is deemed necessary to assess many more of the contributing factors to so far insufficiently understood clinical symptoms and to better understand the biomechanical dynamics of the equine neck in general. Advanced diagnostic imaging techniques will undoubtedly play an important role in this.



SAMENVATTING IN HET NEDERLANDS

De paardenhals vervult meerdere functies bij de balans van het paard door zowel de biomechanische functie als de tegenbalans en hefboom van het hoofd maar ook als weg waarlangs sensorische input van ogen, oren en het evenwichtsapparaat van de hersenen in de vorm van motorische output naar het lichaam en benen plaatsvindt. Hierdoor speelt de hals een belangrijke rol in het totale bewegingsmechanisme van het paard. Moderne paardenrassen worden het meest gebruikt voor de paardensport. Lichaamsbouw en functionele kenmerken van paarden zijn sterk veranderd sinds de domesticatie die ongeveer 6000 jaar geleden plaatsvond. Deze verandering is gepaard gegaan met een sterke afname in genetische diversiteit. Dit had zijn weerslag op onder andere een deel van de genen die verantwoordelijk zijn voor de embryologische ontwikkeling van de wervelkolom, bekend als de HOX of Homeobox genen. Veranderingen in deze genen kunnen variatie in vorm en grootte van de wervels veroorzaken. Vormvariaties komen voor bij ongeveer een derde van de volbloeds en warmbloedpaarden aan de laatste nekwervels.

In Hoofdstuk 1 van dit proefschrift wordt een introductie gegeven in de embryonale ontwikkeling en de anatomie van de hals; ook worden de meest voorkomende halsaandoeningen en diagnostiek hiervan besproken. De halswervelkolom bestaat uit 7 wervels die het benige centrum van de hals vormen, omringd door spieren en ligamenten die op meerdere plaatsen aanhechten aan de wervels. Aan de bovenkant van de wervels vormen de facetgewrichten de verbinding terwijl aan de onderkant van de wervels een tussenwervelschijf zorgt voor de schokdemping tussen twee aanpalende wervels. Centraal in de wervelkolom loopt het ruggenmerg van waaruit zenuwen naar de rest van het lichaam verlopen. Deze uittredende zenuwen lopen door een kleine ruimte tussen twee wervels die het intervertebrale foramen wordt genoemd. Er zijn vele aandoeningen bekend die de functie van de halswervelkolom kunnen beïnvloeden en verschillende klinische symptomen kunnen hiermee in verband gebracht worden. Een goede klinische diagnose is gebaseerd op de combinatie van een gedegen klinisch onderzoek en diagnostische beeldvorming.

Klinisch onderzoek van de paardenhals bestaat uit meerdere stappen; de meest belangrijke zijn visuele inspectie ("adspectie") tijdens rust, palpatie en beoordeling van de hals en de rest van het lichaam tijdens beweging. Symptomen die wijzen op een centrale halsaandoening zijn onder andere die van spinale ataxie waarbij het maken van onvrijwillige bewegingen van de benen kan voorkomen, pijn, afwijkende stand van het lichaam en de hals, verlies van spiermassa (atrofie), spastische gang of

zelfs kreupelheid. Het diagnosticeren van een halsprobleem kan een uitdaging zijn en sommige van de symptomen stemmen erg overeen met de symptomen die bij een meer algemene aandoening van het zenuwstelsel gezien worden, zoals bijvoorbeeld grass sickness of equine motor neuron disease (EMND). Om het onderscheid te kunnen maken tussen deze gegeneraliseerde aandoeningen en halswervelaandoeningen is diagnostische beeldvorming van groot belang. Röntgenonderzoek en echografie zijn hierbij momenteel de modaliteiten die het meest toegankelijk, goedkoop en makkelijk in het gebruik zijn en die in paardenklinieken over de hele wereld routinematig gebruikt worden. Maar superpositie van de verschillende werveldelen op röntgenfoto's en het met echografie niet kunnen bereiken van de diepere weke delen, zoals het ruggenmerg, worden echter steeds meer gezien als belangrijke beperkingen bij dit klinische onderzoek. De effecten die halsaandoeningen op het functioneren van het paard hebben, kunnen met de genoemde modaliteiten dus nog niet volledig genoeg in beeld gebracht worden. Deze limiterende factoren hebben ervoor gezorgd dat er steeds meer interesse is in het gebruik van geavanceerde beeldvormende technieken zoals computertomografie (CT) en magnetic resonance imaging (MRI). Door de verdere technologische ontwikkeling is CT tegenwoordig steeds ruimer beschikbaar voor diagnostiek van de paardenhals, waarbij het paard onder volledige anesthesie moet. Met deze techniek kunnen benige veranderingen en vernauwingen van het wervelkanaal of van de ruimtes tussen de verschillende wervels in (intervertebrale foramina) waar het ruggenmerg en de uittredende zenuwen lopen, in beeld gebracht worden. De meerwaarde van MRI ligt vooral in de beoordeling van de weke delen zoals het ruggenmerg en omliggende weke delen. Dit is de reden dat bij mensen en gezelschapsdieren, zoals honden en katten, deze techniek voor verschillende aandoeningen van de wervelkolom (zoals nekhernia's) de voorkeur heeft. Bij paarden is het maken van een MRI van de hals voornamelijk slechts post-mortaal mogelijk omdat het betrokken gebied te omvangrijk is en dientengevolge niet in de scanner past.

De meest bekende en best beschreven halsaandoening bij het paard is cervicale vertebrale malformatie. Deze aandoening gaat gepaard met veranderingen aan wervellichaam en de gewrichten. Daarnaast is de laatste jaren de klinische impact van aandoeningen aan andere delen van de wervels onderkend en is het onderzoek naar deze aandoeningen uitgebreid. Een voorbeeld daarvan is de variatie in de ontwikkeling van de wervelkolom die bij andere gedomesticeerde dieren en mensen is geïdentificeerd als predisponerende factor voor klinische symptomen zoals nekpijn en voor aandoeningen van de tussenwervelschijf zoals een hernia.

Dit proefschrift bestaat uit twee delen waarin de karakteristieken en bevindingen bij de beeldvorming en klinische implicaties van volgende afwijkingen besproken worden:

- ☞ De anatomische vormvariatie van de halswervels.
- ☞ Tussenwervelschijfaandoeningen van de hals.

Het eerste deel van dit proefschrift begint met een literatuurstudie (Hoofdstuk 2) waarin belangrijke congenitale anatomische veranderingen van de wervelkolom van mensen en gedomesticeerde dieren, waaronder gezelschapsdieren, paarden en vee centraal staan. Fouten in de vorming of separatie van wervels vinden plaats tijdens de eerste twee maanden van de foetale ontwikkeling. Deze leiden tot afwijkingen in vorm of het aantal wervels per wervelkolomsectie. De wervelkolomsecties bestaan uit de hals of cervicale regio, de rug bestaande uit de thoracale (borst-) en lumbale (lenden-) regio, en de bekkenregio bestaande uit het sacrum (heiligbeen) en de staart. Het klinische gevolg van een congenitale variatie is afhankelijk van de ernst van de afwijking en de mogelijke andere afwijkingen in het lichaam die soms gepaard kunnen gaan met variatie in de wervels. Daardoor kan het voorkomen dat wervelafwijkingen niet alleen pas later als toevalsbevinding ontdekt worden, maar ook sterfte op jonge leeftijd het gevolg kan zijn van sommige wervelkolomafwijkingen en (andere) congenitale afwijkingen die hiermee samengaan.

Vormvariaties in de lage halsregio worden bij paarden steeds vaker beschreven en worden daarbij aangemerkt als een reden voor klinische klachten zoals pijn. De röntgenologische en CT-karakteristieken van deze cervicale vormvariaties van de 6^e en 7^e halswervel in een groep van voornamelijk warmbloedpaarden worden in Hoofdstuk 3 en 4 beschreven. Deze vormvariaties kunnen omschreven worden als een overgaan van een deel van het dwarsuitsteeksel (transversaaluitsteeksel) van de 6^e halswervel (C6) naar de 7^e halswervel (C7) tijdens de embryologische ontwikkeling. Dit kan aan een of beide kanten voorkomen. Soms is bij deze paarden ook de eerste rib afwijkend klein of afwezig. De vormvariaties van C6 en C7 zijn gevonden bij ongeveer een derde van de paarden in zowel een gemengde paardenpopulatie (Hoofdstuk 3) als in een populatie warmbloedpaarden (Hoofdstuk 4). De vormvariatie van C6 en C7 wordt geassocieerd met veranderde beweging of biomechanische krachten in de lage halsregio door lokale variatie in de aanhechting van spieren (m. longus colli). Tijdens de twee genoemde studies is er echter geen associatie met klinische symptomen gevonden. Wel zijn er meer vormvariaties gezien in de controlegroep van paarden zonder klinische klachten. Wellicht duidt deze bevinding erop dat deze variatie in anatomie op de een of andere manier gunstig is voor paarden.

“Adjacent segment syndrome” is een aandoening die beschreven is bij mensen en honden waarbij de tussenwervelschijf verouderd of degenerereert naast een gefuseerd wervelsegment, dat congenitaal of door chirurgie kan ontstaan. Alhoewel een fusie van halswervels bij het paard niet veel voorkomt, zou verandering in biomechanische krachten door onder andere de aanwezigheid van de congenitale vormvariaties wel de tussenwervelschijven van deze regio kunnen beïnvloeden. In Hoofdstuk 5, 6, en 7 van dit proefschrift worden de ontwikkeling en aandoeningen van de tussenwervelschijven van de paardenhals onderzocht met behulp van röntgen, MRI en macroscopische inspectie (op zicht) tijdens het pathologische onderzoek.

De tussenwervelschijf van paarden verschilt in samenstelling van die van mensen en gezelschapsdieren. Daarom heeft de macroscopische beoordeling van de tussenwervelschijf in Hoofdstuk 7 plaatsgevonden aan de hand van een aangepast graderings-schema. In dit hoofdstuk wordt degeneratie en/of veroudering van deze tussenwervelschijven gegradeerd in een schaal van 1 tot 5 waarbij de laatste categorie voornamelijk bij oudere paarden werd gevonden en in de lage halsregio.

MRI wordt gezien als de beste keuze voor beoordeling van de tussenwervelschijf en omliggende structuren bij mensen en gezelschapsdieren zoals honden en katten. In Hoofdstuk 5 worden de MRI-karakteristieken van een deel van de tussenwervelschijven van Hoofdstuk 7 beschreven. De postmortale MRI-karakteristieken van normale en gedegenererde en/of verouderde tussenwervelschijven worden beschreven en de beste techniek (sequentie) voor de beoordeling van deze veranderingen wordt geïdentificeerd. Bij paarden zijn de degeneratieve veranderingen zichtbaar als donkere (hypointense) gebieden in een andere sequentie (proton density spin echo) dan bij de voor mensen en gezelschapsdieren gebruikelijke sequentie (T2-gewogen spin echo). De aanwezigheid van gas of bloedelementen kan gezien worden op een specifiek sequentie-type (gradient echo sequentie) als er bijvoorbeeld een scheur in de tussenwervelschijf aanwezig is.

Degeneratie van de tussenwervelschijf kan voor dehydratie zorgen waardoor deze als het ware krimpt en de ruimte tussen twee wervels (tussenwervelruimte) smaller wordt. In geval van zeer forse degeneratie of herniëring van de tussenwervelschijf kan dit leiden tot een collaps van deze ruimte. Röntgenonderzoek is de meest aangewezen techniek om de breedte van de tussenwervelruimte te beoordelen. De beoordeling vindt plaats door de disc height index (DHI) te berekenen. De toepassing van deze techniek voor de halswervels bij het paard wordt geëvalueerd in Hoofdstuk 6. In dit hoofdstuk worden jonge paarden röntgenologisch beoordeeld op leeftijden van 1 tot 18 maanden en

wordt de DHI in de tijd bekeken. Geslacht had geen effect op de DHI, maar de locatie in de hals en tot een bepaalde mate de hoofd-hals houding wel. Het verschillend zijn van de waarden voor het voorste en achterste deel van de hals sluit het gebruik van uniforme DHI-waarden voor de hals uit. Er werd een kleine verandering in DHI gezien rond de 5 maanden, maar de waarden op 1 en 18 maanden zijn vergelijkbaar. Dit wijst mogelijk op een snellere groei rond de 5 maanden leeftijd maar toont ook aan dat de DHI niet veel verandert gedurende de tijd waarbij de overeenkomst van en tussen meerdere beoordelaars goed bleek te zijn. Zodoende kunnen de resultaten van deze studie als eerste voorlopige referentiewaarden gezien worden. Maar verder onderzoek is nog wel nodig om de klinische impact van degeneratie van de tussenwervelschijf bij het paard nauwkeuriger te kunnen beoordelen.

Kort samengevat: in dit proefschrift zijn de anatomische vormvariëaties van de halswervels van de paardenhals onderzocht en deze blijken veel voor te komen bij warmbloedpaarden. Er is echter geen associatie gevonden met klinische klachten en het zou zelfs zo kunnen zijn dat het voorkomen van deze variëaties gunstig kan zijn bij paarden. De ermee samengaande anatomische - of biomechanische veranderingen zouden echter wel van invloed kunnen zijn op de veroudering of degeneratie van de naastgelegen tussenwervelschijf. MRI-beelden, de DHI voor beoordeling van de breedte van de tussenwervelruimte, en de postmortale macroscopische gradering. Dit proefschrift draagt bij aan de kennis van de diverse aandoeningen van de paardenhals en de mogelijkheden die de zich steeds verder ontwikkelende beeldvormende technieken daarbij kunnen bieden. Verder onderzoek is zeker nodig naar de vele factoren die bijdragen aan de talrijke onbegrepen klinische klachten in dit gebied en meer specifiek naar de biomechanische dynamiek van de paardenhals. Geavanceerde diagnostische beeldvormende technieken zullen daar ongetwijfeld een belangrijke rol in gaan vervullen.



LIST OF PUBLICATIONS IN PEER REVIEWED JOURNALS.

Presumed cholesterinic granulomas detected on computed tomography in horses are associated with increased lateral ventricle height and age.

Edwards RA, Willems DS, Beukers M, van den Brom-Spienburg A, JCM Vernooij, **Veraa S**. *Vet Radiol Ultrasound*. 2019 Nov; *accepted*.

Equine cervical intervertebral disc degeneration is associated with location and MRI features.

Veraa S, Bergmann W, Wijnberg ID, Back W, Vernooij H, Nielen M, van den Belt AM. *Vet Radiol Ultrasound*. 2019 Nov;60(6):696-706. doi: 10.1111/vru.12794.

Morphological variations of the infraorbital canal during CT has limited association with headshaking in horses.

Edwards RA, Hermans H, **Veraa S**. *Vet Radiol Ultrasound*. 2019 Sep;60(5):485-492. doi: 10.1111/vru.12773.

Clinical, ultrasonographic, and histopathologic findings in seven horses with Descemet's membrane detachment: A case series.

Slenter IJM, Hermans H, Ensink JM, Willems DS, **Veraa S**, Grinwis GCM, Boevé MH. *Vet Ophthalmol*. 2019 Sep; doi: 10.1111/vop.12710.

Computed tomography angiography of a congenital extrahepatic splenocaval shunt in a foal.

Willems DS, Kranenburg LC, Ensink JM, Kummeling A, Wijnberg ID, **Veraa S**. *Acta Vet Scand*. 2019 Aug; 61(1):39. doi: 10.1186/s13028-019-0474-0.

Caudal cervical vertebral morphological variation is not associated with clinical signs in Warmblood horses.

Veraa S, de Graaf K, Wijnberg ID, Back W, Vernooij H, Nielen M, Belt AJM. *Equine Vet J*. 2019 Jun; doi: 10.1111/evj.13140.

A retrobulbar dermoid cyst with involvement of the sinus in an 18-year old pony.

Visser EMS, Caliskan N, **Veraa S**, Hermans H. *Equine Vet. Ed*. 2019 Sep; 31(9): e47-e52.

Local anaesthetic techniques for the equine head, towards guided techniques and new applications.

Hermans H, **Veraa S**, Wolschrijn CF, van Loon JPAM.

Equine Vet. Ed. 2019 Aug; 31(8):432-440.

A minimally invasive partial condylectomy and temporal bone resection for the treatment of a suspected chronic synovial sepsis of the temporomandibular joint in a 3.5-year-old paint horse gelding.

Frietman SK, van Proosdij ER, **Veraa S**, de Heer N, Ter Braake F.

Vet Q. 2018 Dec;38(1):118-124. doi: 10.1080/01652176.2018.1535216.

Temporary Segmental Distraction in a Dog with Degenerative Lumbosacral Stenosis.

Willems N, Kersten RFMR, van Gaalen SM, Öner FC, Strijkers GJ, **Veraa S**, Beukers M, Tryfonidou MA, Meij BP.

Vet Comp Orthop Traumatol. 2018 Jul;31(4):298-303. doi: 10.1055/s-0038-1639599.

Intervertebral Disc Degeneration in Warmblood Horses: Morphology, Grading, and Distribution of Lesions.

Bergmann W, Bergknut N, **Veraa S**, Gröne A, Vernooij H, Wijnberg ID, Back W, Grinwis GCM.

Vet Pathol. 2018 May;55(3):442-452. doi: 10.1177/0300985817747950.

Ex vivo computed tomographic evaluation of morphology variations in equine cervical vertebrae.

Veraa S, Bergmann W, van den Belt AJ, Wijnberg I, Back W.

Vet Radiol Ultrasound. 2016 Sep;57(5):482-8. doi: 10.1111/vru.12393.

Osteochondral dysplasia of the coxofemoral joints in a Friesian foal: Clinical findings and methods of diagnosis.

Hermans H, **Veraa S**, Ploeg M, Boerma S, Hazewinkel HAW, Back W.

Equine Vet. Ed. 2016 Sept;28(9):486-491

Pulmonary alveolar proteinosis in a cat.

Szatmári V, Teske E, Nikkels PG, Griese M, de Jong PA, Grinwis G, Theegarten D, **Veraa S**, van Steenbeek FG, Drent M, Bonella F.

BMC Vet Res. 2015 Dec 9;11:302. doi: 10.1186/s12917-015-0613-4.



Axial osteitis of the proximal sesamoid bones and desmitis of the intersesamoidean ligament in the hindlimb of Friesian horses: review of 12 cases (2002-2012) and post-mortem analysis of the bone-ligament interface.

Brommer H, Voermans M, **Veraa S**, van den Belt AJ, van der Toorn A, Ploeg M, Gröne A, Back W.

BMC Vet Res. 2014 Nov 19;10:272. doi: 10.1186/s12917-014-0272-x.

The effect of Clostridium botulinum toxin type A injections on motor unit activity of the deep digital flexor muscle in healthy sound Royal Dutch sport horses.

Wijnberg ID, Hardeman LC, van der Meij BR, **Veraa S**, Back W, van der Kolk JH.

Vet J. 2013 Dec;198 Suppl 1:e147-51. doi: 10.1016/j.tvjl.2013.09.050.

Effect of Clostridium botulinum toxin type A injections into the deep digital flexor muscle on the range of motion of the metacarpus and carpus, and the force distribution underneath the hooves, of sound horses at the walk.

Hardeman LC, van der Meij BR, Oosterlinck M, **Veraa S**, van der Kolk JH, Wijnberg ID, Back W.

Vet J. 2013 Dec;198 Suppl 1:e152-6. doi: 10.1016/j.tvjl.2013.09.051.

Pressure plate analysis of toe-heel and medio-lateral hoof balance at the walk and trot in sound sport horses.

Oosterlinck M, Hardeman LC, van der Meij BR, **Veraa S**, van der Kolk JH, Wijnberg ID, Pille F, Back W.

Vet J. 2013 Dec;198 Suppl 1:e9-13. doi: 10.1016/j.tvjl.2013.09.026.

Computed Tomography in the diagnosis of malignant sinonasal tumours in three horses.

Veraa S, Dijkman R, Klein WR, van den Belt AJM.

Equine Vet Ed. 2010 June; 21(6): 284-8.

Comparative imaging of spinal extradural lymphoma in a Bordeaux dog.

Veraa S, Dijkman R, Meij BP, Voorhout G.

Can Vet J. 2010 May;51(5):519-21.

Computed tomography of the upper cheek teeth in horses with infundibular changes and apical infection.

Veraa S, Voorhout G, Klein WR.

Equine Vet J. 2009 Dec;41(9):872-6.



DANKWOORD

In een radiologiewereld vol grijstinten en hier en daar wat zwart, gloort er nu wit licht aan de beeldvormende horizon. De beelden die samen een verhaal vormen over paardenhalzen, diagnostiek, goede collega's, vertrouwen, tijd en uiteindelijk resulteren in het proefschrift dat nu een boek vormt. De pagina's van dit boek hadden niet gevuld kunnen worden zonder een bijdrage van de vele mensen om me heen en daarvoor mijn dank!

Allereerst mijn promotoren Jan-Willem Hesselink en René van Weeren; waardevol was jullie bijdrage toen de artikelen vorm mochten krijgen, jullie ervaring in hoe het verwoord moet worden en de puntjes op de "i" gezet, hoe je editors en reviewers tegemoet komt en een promotie echt vorm geeft. Hartelijk dank voor alle feedback, vooral in die laatste weken!

Beste AJ, beste copromotor; het meest waardevolle dat je me kon geven was tijd. Tijd uit de kliniek en tijd om me op de statistiek te concentreren, tijd om te schrijven maar ook tijd om mijn gedachten eindelijk op een rijtje te krijgen en ze daadwerkelijk op papier te zetten! Ook toen de bladzijden van het proefschrift zich gingen vullen en de eindstreep in zicht was, steunde je me. Dank voor alles in de afgelopen jaren. Nu dit hoofdstuk afgerond is, kun je eindelijk van je welverdiende pensioen genieten...alhoewel iets in me vermoedt dat we je nog vaak op onze afdeling radiologie zullen zien!

Dank aan al mijn medeauteurs, maar in het bijzonder Wim, Inge, Willie, Kim, Carmen, Hans en Mirjam.

Wim Back, zonder jou zou dit proefschrift geen begin gehad hebben. Met je onuitputtelijk enthousiasme heb je mij overtuigd om eens verder te kijken naar de beeldvorming van de paardenhals en daarna zoveel werk verricht om de patiënten, de mensen en de omgeving zover te krijgen dat dit onderzoek mogelijk werd. Je bleef altijd op zoek naar nieuwe mogelijkheden waarvoor mijn grote dank.

Inge Wijnberg, dank voor je altijd kritische en vooral ook klinische blik daar waar ik dreigde te verzanden in de wirwar van onderzoek doen.

Willie Bergmann, wat zou het mooi zijn als ons onderzoek een basis mag zijn in de zoektocht naar halsafwijkingen. Van tussenwervelschijf tot facet...er is nog zoveel te leren!

Kim de Graaf en Carmen Scheffer, wat ontzettend blij ben ik met de samenwerking tussen onze klinieken. Er zijn zoveel vraagstukken om op te lossen en nog zoveel wegen die we samen kunnen bewandelen op weg naar een klein stukje van de waarheid op het gebied van wervelkolomveranderingen. Dank voor al jullie hulp en tijd.

Hans en Mirjam, statistiek was een uitdaging die ik samen met jullie ben aangegaan. Dank voor al jullie geduld, uitleg en begrip. Het eindresultaat mag er zijn!

De hele afdeling radiologie, met in het bijzonder mijn mede-radiologen Martijn, Susanne, Leonie, Irene, Tetyda, Kim, George, Federico, Xander, Mauricio, Ralph, Dorien, Henk en Nienke. Dank voor jullie geduld, mijn verhaal aanhoorden en maar al te goed begrepen dat ook ik niet kliniek en onderzoek tegelijkertijd kon doen. Elise als Photoshop expert...bedankt voor je hulp bij het samenstellen van de prachtige multi-panel figuren. Het hele radiologie-team dat elke keer weer klaar stond om een hals te scannen, op CT of MRI...we hadden die wervelkolombak misschien eerder aan moeten schaffen! Bedankt Joris, Monique, Marjolein, Anke, Chantal, Mascha, Ingrid, Joost, Kim en Sander, Bas, Wendy, Suzan, Marieke, en last but not least Hans die zorgde voor prachtige wervelkolom preparaten zodat die vormveranderingen ook tastbaar werden.

Lieve Susanne, wat hebben we al veel samen meegemaakt! Lofoten, Davis, Bursa, Wroclow, Windsor, organisatie EVDI congres 2014, scientific committee en met als thuisbasis Utrecht zijn we niet alleen goede collega's maar ook vrienden geworden. Wat waardeer ik jou steun, eerlijkheid en kritische blik maar vooral ook de gezelligheid. Altijd heb je in mij geloofd en me gezegd dat het me zou lukken. Je kwam zelfs een jaar terug naar onze geliefde afdeling voor 1 dag in de week en hebt me daarmee dat zetje kunnen geven dat ik nodig had. Onwijs bedankt en tijd voor een feestje...laten we dansen!!!

Kees Dik, het heeft zo moeten zijn en heel even het gevoel dat je vanaf die andere plek meekijkt...mijn promotie op jou verjaardag. Dank voor alles wat je voor me hebt gedaan, de richting die je gaf en het advies om altijd kritisch te blijven op eigen werk... vorm, structuur en belijning.



Lieve vrienden, goede collega's en mijn familie (en een ieder die ik dreig te vergeten...) ook jullie vormen een groot deel van de beeldvorming en het tot stand komen van dit proefschrift. Zonder jullie was het in ieder geval een heel stuk saaier geweest!

My dear Chiara! How we have struggled, cursed but persevered! Woman power....yes we can!

Tetyda, bedankt voor alle leuke momenten op het werk maar vooral ook daarbuiten. Er staat nu een nieuwe uitdaging voor jullie deur waarvan ik zeker weet dat Ludwig en jij het geweldig gaan doen. Tot ziens in Hamburg!

Marieke Voorhorst, wat ben ik blij om jou mijn bijna-buurvrouw te mogen noemen. Even de boel de boel laten en gezellig te kletsen over alles wat we meemaken...en dat is best wat als dierenarts-specialisten en mama's van een paar prachtige kids.

Hille, wat zei je ook alweer over thuis werken? Het wordt tijd voor een etentje!

Mijn Gentse Chickies Eefje, Marijke, Nanne, Kelly en Thea; we hebben in Gent samen hard gevochten voor die dierenartstitel maar wat was de weg daarna op z'n zachtst gezegd gevarieerd voor ons allemaal. Wat ben ik blij dat we na al die jaren nog steeds vriendinnen zijn en ook al zien we elkaar niet zo vaak als we zouden willen, die keren dat we elkaar zien is het als vanouds gezellig. Binnenkort weer high-tea?

Lotte, onze wegen leken te scheiden na Gent maar niks was minder waar. Ook al lijkt het leven soms wat anders in petto te hebben, weet dat onze deuren altijd voor jullie open staan.

Vriendjes en vriendinnetjes uit Roermond, er is post! Denny & Charlie, Ruby & Romeo, Maaïke & Patrick, Sim & San. Ongelofelijk hoe snel de jaren voorbij gaan en wij met z'n allen nog steeds elkaars leven mogen delen. Of het nu een midwinter barbecue, bruiloft, feestje of afscheid is, een eindeloze stroom van foto's of een filmpje via Whatsapp... "Zoals een kip hoort bij een ei en regen hoort bij zonneschijn"...zo hoort het bij mij om vrienden met jullie te zijn;) Friends 4-ever!

Lieve Kim, lieve Marriska! Er zit muziek in onze vriendschap en we hebben in de afgelopen 25 jaar al vele soorten ritmes samen mogen spelen. Van hele lage naar hele hoge noten en samenkomend in het middenregister, waarbij onze vriendschap soms piano is maar op momenten van lekker meiden-date-dagen zeker allegro is. Dat we ons levenslied nog heel lang als ensemble mogen spelen!

Kim & Rogier, Femke & Björn; bedankt voor alle gezellige momenten, barbeques, ski ervaringen en speciaal Kim bedankt voor alle aangedragen verhuismogelijkheden! We hebben dan eindelijk ons eigen paleisje gevonden en dus is een volgend diner of wellicht verjaardagsfeest bij ons. Maar nu eerst een ander feestje.

Burgh-Haamstede...een hele Zeeland-groep aan mensen waar ik binnen kwam en me ondertussen niet meer van kan voorstellen hoe het zonder jullie zou zijn. Oud&nieuw, vakantie, feestjes en weekenden aan de kust. Bedankt voor alle gezelligheid en vriendschap Jarno & Marjo, Cath & Martijn, JP & Jolien, Anke & Mark, Arjen & Maartje, Martine & Marnix, Joost & Mischa, Rutger & Brigitte.

Jarno & Marjo, we hebben eenzelfde tempo in ons leven met vele mooie momenten om op terug te kunnen kijken...Wat ontzettend fijn om jullie vrienden te mogen noemen, onze verhalen en dieptepunten met jullie te kunnen en mogen delen en altijd op jullie te kunnen bouwen. Ook al was "Hell"-endoorn een klein minpuntje... bedankt voor alles!

Leo en Annemiek, samen met Sander mijn tweede schoonfamilie. We hebben erg genoten van Italië en hopen vaker gebruik te mogen maken van jullie gastvrijheid.

Joyce en Tjarco, Noémie wat ben ik blij met jullie als mijn schoonfamilie. Ook al zien we elkaar lang niet genoeg, altijd staan jullie voor ons klaar, heeft Emily de tijd van haar leven tijdens een van haar vele logeerpartijtjes, kunnen we altijd aanschuiven bij jullie aan tafel en zeg ik voor nu heel hartelijk dank. Volgende keer bij ons!;

Lieve Corry, treinreizen vanuit Bilthoven heeft een rare nasmaak na november 2014 maar toch klom je opnieuw in de trein naar Utrecht. Tijd samen is kostbaar, dat realiseren we maar al te goed en de momenten waarop we elkaar zien te kort. De promotie van Maurice in december 2014 kon je met Ambulance Wens gelukkig deels bijwonen...deze keer gewoon van begin tot eind en vanuit een stoel!

Pap en mam, altijd zijn jullie er voor mij en steunen me in al mijn keuzes. Van Bos- en Natuurbeheer in Wageningen, naar diergeneeskunde in Gent met een “Licence to Heal”, via een internship paard in Someren naar dierenarts-specialist diagnostische beeldvorming in Bilthoven. Daar waar ik op m’n plek was en vooral ook dicht bij Simone en nu onze prachtige gezinnetjes. Het was bij tijd en wijlen geen gemakkelijk traject met de nodige ups en downs maar altijd geloofden jullie in mij. Nu deze volgende droom uitkomt, kan ik jullie alleen nogmaals danken voor alles wat jullie altijd voor mij maar ook voor mijn gezinnetje doen en hoop nog heel lang de beelden van ons levensverhaal samen met jullie te mogen maken.

Lieve zus, lieve Simone, Simpie, mijn Mona-toetje; voor altijd begrepen, voor altijd onvoorwaardelijke liefde en voor altijd iemand waar ik op kan bouwen, zonder jou geen leven. Wat ben ik blij dat we zo dicht bij elkaar wonen, dat onze prachtige dochters samen op mogen groeien en: Sander, een leven zonder jou naast Simone kan ik me niet meer voorstellen met altijd de deur wagenwijd open op momenten dat het nodig was. Liefde, steun en toeverlaat, plezier en gewoon zijn. Onwijs bedankt. En als kers op de taart zijn jullie prachtige dochters Isabella en Frederique erbij gekomen; dichtbij en vertrouwd, samen het leven delen en samen spelen. Twee gezinnetjes, verbonden met elkaar.

Mijn liefste eigenwijze, sprankelende en zorgzame Emily.

Rosalie, mijn bloem van vrolijkheid, doorzettingsvermogen en moed.

Relativerend en drijfveren om er iets van te maken. Wat hou ik ontzettend veel van jullie, onvoorwaardelijk, voor altijd...en trots omdat ik jullie mama mag zijn.

Mijn liefste, Maurice, ik hou van je met heel mijn hart en kan geen leven zonder je voorstellen. Met al mijn gekheden, uitstel van keuzes en vooral gedrevenheid om er samen met jou iets van te maken in het leven, ons gezinnetje waar we intens van kunnen genieten. Met jou onuitputtelijke werklust, maar bovenal de 200% liefde en relativering die je dochters je bieden...samen. En na deze lange reis aan het einde van dit verhaal kom ook ik graag bij jou thuis.

Stefanie

Life is not about waiting for the storm to pass, it's about learning to dance in the rain.



CURRICULUM VITAE



Stefanie Veraa was born on the 24th of November 1979 in Krefeld, Germany. After high school in Roermond she certified for the propaedeuse of “Bos- en Natuurbeheer” at Wageningen University and Research (WUR). After this, she started her veterinary studies and graduated cum laude in 2005 as a veterinarian at the Faculty of Veterinary Medicine, Ghent University Belgium. Her love for diagnostic imaging started then and there with the final thesis entailing “Computed tomography of the equine head”. She enjoyed an internship at the Veterinary Centre Someren in 2005-2006 that was followed in 2006 by a residency in Veterinary Diagnostic Imaging at the division of Diagnostic Imaging of the Faculty of Veterinary Medicine of Utrecht University in The Netherlands. Stefanie became a diplomate of the European College of Diagnostic Imaging (ECVDI) in 2010. She has been working as a staff member since and gradually rolled into a PhD-track after becoming aware of the shortage in scientific information about imaging the equine neck. Ever since, she has been expanding the horizon of imaging in this anatomic area and has been a speaker on this and other topic in many national and international conferences. Stefanie lives currently in de Bilt with Maurice and their two beautiful daughters Emily and Rosalie.

Stefanie Veraa is geboren op 24 november 1979 in Krefeld, Duitsland. Na de middelbare school in Roermond heeft ze de propaedeuse van “Bos- en Natuurbeheer” behaald van de Wageningen Universiteit en Research (WUR). Hierna is ze diergeneeskunde gaan studeren en in 2005 met onderscheiding afgestudeerd aan de faculteit Diergeneeskunde van de Universiteit Gent te België. Hier is haar liefde voor diagnostische beeldvorming begonnen met als onderwerp voor haar laatstejaars thesis “ Computertomografie van het Paardenhoofd”. Ze heeft daarna in 2005-2006 een internship afgerond bij het Veterinair Centrum Someren, gevolgd door een opleiding tot specialist in de Veterinaire Diagnostische Beeldvorming bij de afdeling Diagnostische Beeldvorming van de Faculteit Diergeneeskunde, Universiteit Utrecht in Nederland. Stefanie is in 2010 geslaagd voor haar specialisten examen waarna ze veterinaire specialist werd van het European College of Diagnostic Imaging (ECVDI). Vanaf toen heeft ze als staflid bij de afdeling gewerkt en is langzaam in een PhD-trajet gerold nadat haar duidelijk werd dat er een wetenschappelijk tekort aan informatie over beeldvorming van de paardenhals was. Vanaf toen heeft ze grenzen verlegd over beeldvorming van deze anatomische regio en heeft vele malen hierover en over andere onderwerpen gesproken op nationale en internationale congressen. Stefanie woont momenteel met Maurice en hun twee prachtige dochters Emily en Rosalie in de Bilt.





